Vol. 53 • No. 3

March 2010

Microwave Journal

X Parameters,

S-Functions, Poly-harmonic Distortion Models, Waveform Engineering, Hot S-22, NonLin-S, Active Harmonic Load Pull, NVNA, OpenWave Forum.

Nonlinear Device Characterization is heating up and everyone from test equipment manufacturers to software developers are involved. Will their efforts transform the microwave component industry?

MVP

Elektrobit MIMO-OTA Emulation

horizon house

Founded in 1958

mwjournal.com

Boonton's Peak Power Meters...
The Future of Amplifier Testing.

In the past, your options were using one- or two-tone test signals to measure amplifier linearity. Today, Boonton allows you to use your signal to characterize your DUT. No more extrapolating graphs or guessing likely compression points. Our family of peak power meters offers powerful statistical analysis tools, and is joined by the fastest and widest dynamic range sensors in the industry.

If you measure extreme signals with:

- High peak to average ratio
- Ultra-low duty cycle
- Noise-like communication signals

Boonton delivers the fastest and most comprehensive results in the industry.

For more information visit us at boonton.com or call
+1 973-386-9696

Wireless Telecom Group
Boonton Microlab Noisecom Willtek

Boonton


MCL B 744
ADP-2-10

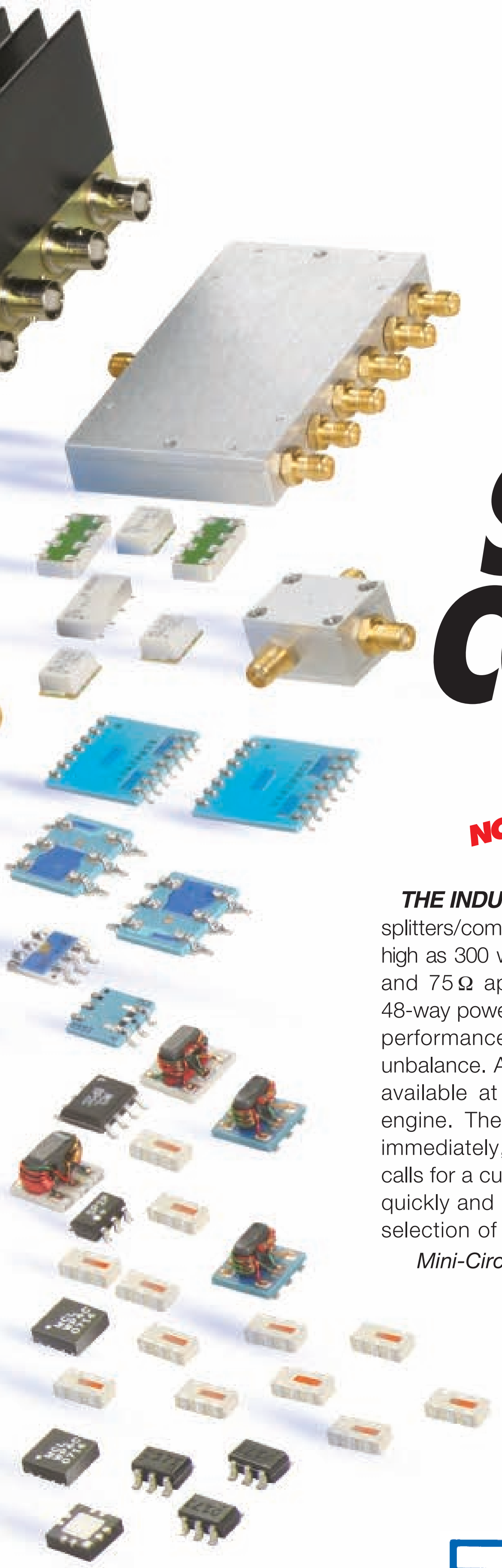

POWER/ SPLITTERS COMBINERS

NOW! from **2 kHz to 18 GHz** as low as **79¢**

THE INDUSTRY'S LARGEST SELECTION Mini-Circuits offers thousands of power splitters/combiners for applications from *2 kHz to 18 GHz* and with power handling as high as 300 watts. Choose from coaxial, flat-pack, and surface-mount housings, for 50 Ω and 75 Ω applications. The industry's largest selection includes 2-way through 48-way power splitters/combiners in 0°, 90°, and 180° configurations, with outstanding performance in terms of insertion loss, VSWR, amplitude unbalance, and phase unbalance. All models are characterized with detailed data and performance curves, available at the touch of a button using Mini-Circuits advanced Yoni2 search engine. These ***low-cost, off-the-shelf power splitters/combiners*** are available immediately, and backed by Mini-Circuits 1year guarantee. But if your application calls for a custom unit, our development team will meet or exceed your requirements quickly and cost-effectively. Contact Mini-Circuits today, for the industry's largest selection of power splitters/combiners.

Mini-Circuits...Your partners for success since 1969

RoHS Compliant
Product availability is listed on our website.

Mini-Circuits®
ISO 9001 ISO 14001 AS9100 CERTIFIED

P.O. Box 350166, Brooklyn, New York 11235-0003 (718) 934-4500 Fax (718) 332-4661

Yoni2™ ***The Design Engineers Search Engine*** *finds the model you need, Instantly* • For detailed performance specs & shopping online see **minicircuits.com**

Patent Pending

IF/RF MICROWAVE COMPONENTS

448 rev D

Visit http://mwj.hotims.com/28487-71 or use RS# 71 at www.mwjournal.com/info

More Noise

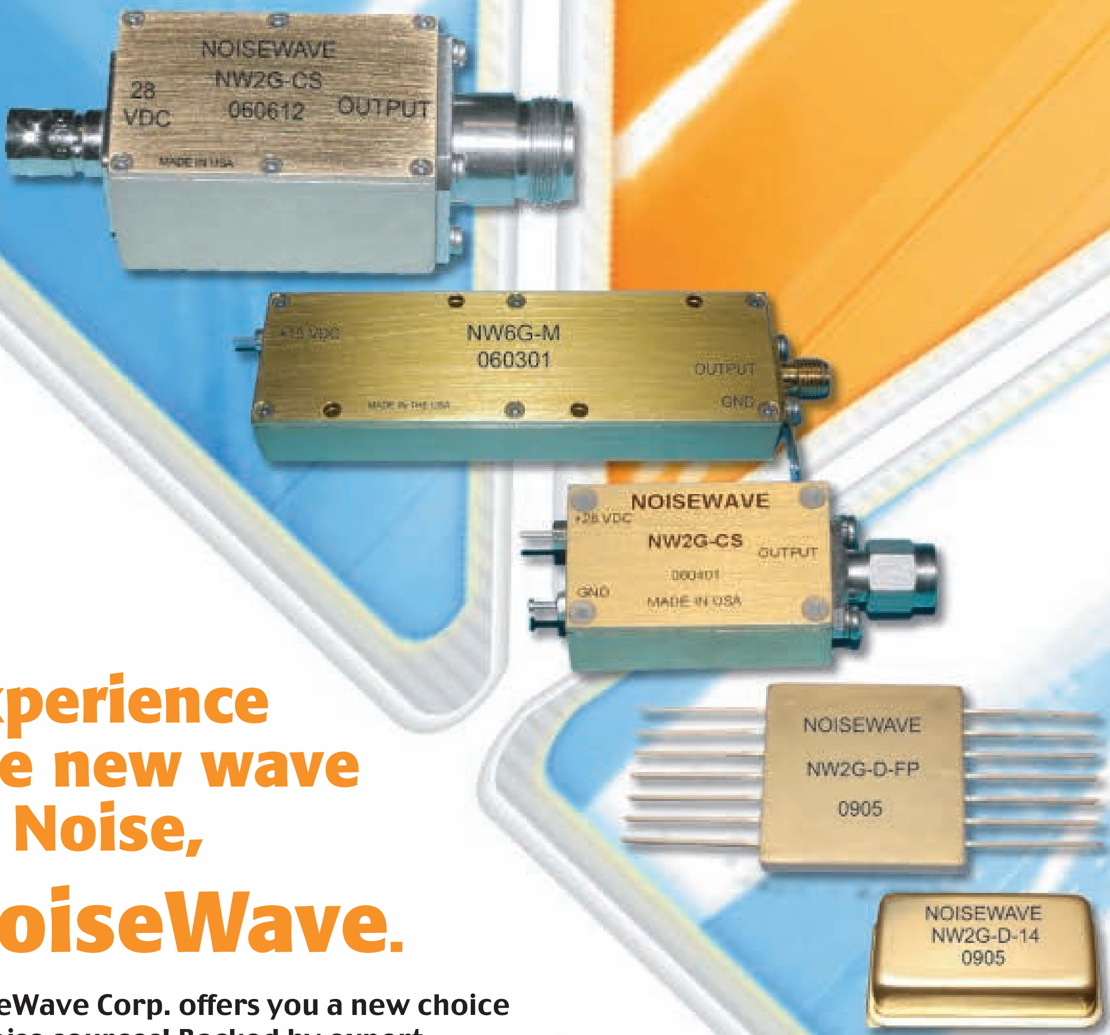

Experience the new wave in Noise,

NoiseWave.

NoiseWave Corp. offers you a new choice in Noise sources! Backed by expert designers in Noise, NoiseWave provides reliable Noise Components, Noise Diodes and Noise Generators for telecommunications.

Our goal is to give you the most reliable, the most advanced and the most cost effective Noise products, while providing unmatched, superior service.

Contact us to order a standard product, always available from stock, or let us design a custom noise source guaranteed with a quick delivery.

Choose NoiseWave, the new wave in Noise!

For more information Contact Ed Garcia at:

NOISEWAVE
The new wave in NOISE

NoiseWave Corp.
Phone (973) 386–1119
Fax (973) 386–1131
egarcia@noisewave.com
www.noisewave.com

Visit http://mwj.hotims.com/28487-90 or use RS# 90 at www.mwjournal.com/info

Microwave Journal

MARCH 2010 VOL. 53 • NO. 3

FEATURES

COVER FEATURE

MVP: MOST VALUABLE PRODUCT

TUTORIAL

TECHNICAL FEATURES

53 Years of Publishing Excellence

Microwave Journal (USPS 396-250) (ISSN 0192-6225) is published MARCHly by Horizon House Publications Inc., 685 Canton St., Norwood, MA 02062. Periodicals postage paid at Norwood, MA 02062 and additional mailing offices.

POSTMASTER: Send address corrections to *Microwave Journal*, PO Box 3256, Northbrook, IL 60065-3256 or e-mail mwj@omeda.com. Subscription information: (847) 291-5216. This journal is issued without charge upon written request to qualified persons working in that part of the electronics industry, including governmental and university installation, that deal with VHF through light frequencies. Other subscriptions are: domestic, $120.00 per year, two-year subscriptions, $185.00; foreign, $200.00 per year, two-year subscriptions, $370.00; back issues (if available) and single copies, $10.00 domestic and $20.00 foreign. Claims for missing issues must be filed within 90 days of date of issue for complimentary replacement.

Posted under Canadian international publicatioans mail agareement #PM40063731

Microwave Journal

FEATURES

PRODUCT FEATURES

DEPARTMENTS

KLEENEX VS. TISSUE

Characterizing nonlinear devices at microwave frequencies has always been a challenge for the designer, the device modeler and the supporting infrastructure (test equipment, CAD libraries, etc.). This month's lead story is an overview of the latest developments in this area. We are at a crossroads; the efforts of years of R&D have come to fruition. Multiple vendors now offer nonlinear microwave measurement systems and measurement-based models. Whether the industry anoints the X-parameter or the format to be defined by the OpenWave forum as the de-facto standard for nonlinear measurement-based models remains to be seen. Either way, the general approach could do for nonlinear devices what EM simulation did for passive devices. We may be witnessing the end of proprietary empirical models and questionable device representation in our design efforts. In their place, designers gain access to well-defined models made possible with links between measurement and simulation. It is now up to these designers and their solution providers to determine (through experience) whether we converge on a common standard for greater interoperability among vendors or diverge as a result of performance differences and/or brand loyalty.

David Vye
Editor

STAFF

Publisher: Carl Sheffres
Editor: David Vye
Managing Editor: Keith W. Moore
Technical Editor: Patrick Hindle
Associate Technical Editor: Dan Massé
Staff Editor: Jennifer DiMarco
Editorial Assistant: Barbara Walsh
Consulting Editor: Harlan Howe, Jr.
Consulting Editor: Frank Bashore
Consulting Editor: Peter Staecker
Consulting Editor: Dan Swanson
Web Editor: Samantha Bookman
Audience Development Manager: Michelle Frazier
Traffic Manager: Edward Kiessling
Marketing and Event Coordinator: Kristen Anderson
Director of Production & Distribution: Robert Bass
Graphic Designer & Production Coordinator: Janice Levenson
Graphic Designer: Sachiko Stiglitz

EUROPE

International Editor: Richard Mumford
Office Manager: Eugenie Hardy

CORPORATE STAFF

CEO: William M. Bazzy
President: Ivar Bazzy
Vice President: Jared Bazzy

Executive Editorial Office:
685 Canton Street, Norwood, MA 02062
Tel: (781) 769-9750
FAX: (781) 769-5037
e-mail: mwj@mwjournal.com

European Editorial Office:
16 Sussex Street, London SW1V 4RW, England
Tel: Editorial: +44 207 596 8730 Sales: +44 207 596 8740
FAX: +44 207 596 8749

www.mwjournal.com

Printed in the USA

Microwave Journal Online

The latest industry news, product updates, resources and web exclusives from the editors of *Microwave Journal*

Go to www.mwjournal.com

Free Webinars

MWJ/Besser Associates Webinar Series: RF & MW Power Amplifiers

This webinar presents an introduction to RF and microwave power amplifier design and characteristics. Included are discussions on basic power amplifier concepts, classes of operation, linearity, and efficiency enhancement techniques. Presented by Besser Associates and *Microwave Journal*.

Sponsored by **AWR Corp.** and **M/A-COM Technology Solutions**

Live webcast: 3/23/2010, 11:00 am (ET)

Online Technical Papers

High Power Amplifier Measurements Using Agilent's NVNA

White Paper, Agilent Technologies Inc.

R&S MATLAB® Toolkit for Signal Generators and Power Sensors

Thomas Roeder and Dr. Carolin Troester, Rohde & Schwarz

New Measurement-based Models Enhance Nonlinear Analysis

White Paper, AWR Corp.

MIMO Over-The-Air Testing

Doug Reed, Spirent Communications

Executive Interview

Peter von Nordheim, Managing Director of **Spectrum Elektrotechnik GmbH**, explains why he founded the company, his personal commitment to driving the company forward, the development of sales worldwide and future plans.

Expert Advice

Wayne Struble, Distinguished Fellow of Technology at **M/A-COM Technology Solutions**, discusses various approaches to modeling RF components including IP encryption, behavioral and X-parameter based models, model extraction, simulation speed, ease of end use, model accuracy, and model limitations.

EDAFocus

Agilent's ADS 2010 recently added support for IBIS-AMI, a modeling standard for SerDes transceivers found in high-speed serial links. The feature will support signal integrity engineers with the design and verification of chip-to-chip multigiga-bit/s serial links.

TestBench

The TM500 Test Mobile from Aeroflex is the first to support multiple-UE emulation for rigorous load testing of the 3GPP W-CDMA Release 8 DC-HSDPA standard, enabling base station and core-network designs to be load-tested, stressed and optimized.

Join Us (direct links at www.mwjournal.com)

LinkedIn Group "RF and Microwave Community"

Facebook *Microwave Journal* Fan Page

Follow us on **Twitter** @mwjournal, @pathindle and @KAatMWJ

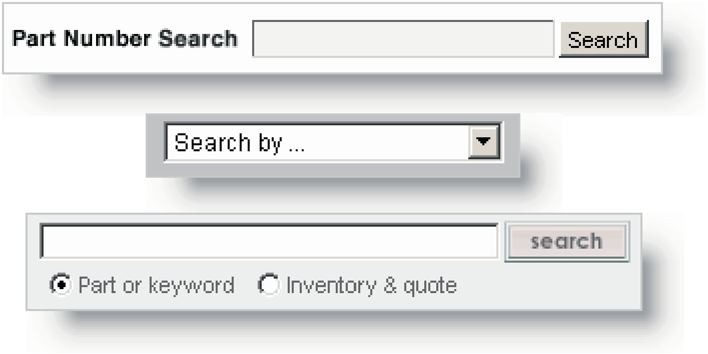

Their sites have search engines. Ours has a find engine.

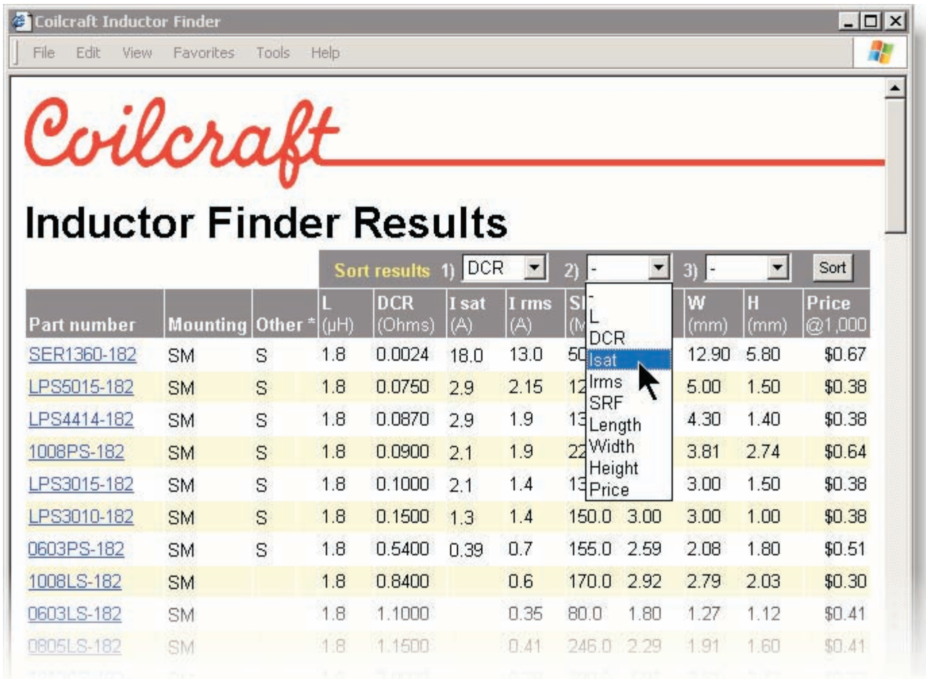

On most inductor web sites, their search engine results in more aggravation than answers.

But Coilcraft's web site is different.

In seconds, our Inductor Finder will show you all the parts that meet your electrical and size requirements. You can sort the results by your most important parameters. Compare pricing. Even analyze the core and winding losses of up to four different power inductors!

You'll find lots of other design tools to help you choose the perfect part. And then request free samples with just a few clicks.

So quit searching for magnetics and start finding them at **www.coilcraft.com**!

ORDER DIRECT
BUY.COILCRAFT.COM
800-322-2645
OVERNIGHT DELIVERY ORDER BY 5
RoHS COMPLIANT

Coilcraft®

www.coilcraft.com 800/322-2645

APRIL 2010

SUNDAY	MONDAY	TUESDAY	WEDNESDAY	THURSDAY	FRIDAY	SATURDAY
28	29	30	31	1	2	3
4	5	6	7 **Ansoft HFSS Product Training** Boston, MA	8	9	10
11	12	13 **MWJ Besser Webinar: RF Components for Aerospace & Defense Markets** Sponsored by ROHDE & SCHWARZ	14	15	16	17
18	19	20	21	22	23	24
25	26	27 **MWJ Webinar: State of Compound Semiconductors** Presented by STRATEGY ANALYTICS	28	29	30	1

Multi-day events:

- April 8–9: **MOS-AK/GSA Workshop** Rome, Italy
- April 5–9: **Reverberation Chamber Theory/Experiment Short Course** Oklahoma State University Stillwater, OK
- April 12–13: **WAMICON** Melbourne, FL
- April 13–15: **ChinaMW 2010 China International Exhibition and Forums on Microwave & RF** Beijing, China
- April 12–16: **APEMC 2010 Asia-Pacific Symposium on Electromagnetic Compatibility** Beijing, China
- April 21–22: **WTW 2010 2010 IEEE Wireless Test Workshop** Santa Cruz, CA
- April 19–20: **ARMMS RF and Microwave Society Conference** Oxfordshire, UK
- April 19–21: **CST European User Group Meeting** Darmstadt, Germany
- April 26–27: **INMMIC 2010** Gothenburg, Sweden

Go to: www.mwjournal.com/events

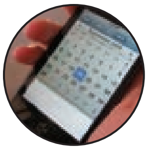

Coming Events

CALL FOR PAPERS

MILCOM 2010
Deadline: March 12, 2010

Asia Pacific Microwave Conference
Deadline: May 31, 2010

ONLINE

MWJ Show Coverage of Satellite 2010
Post Date: March 23, 2010

MWJ Show Coverage of CTIA Wireless
Post Date: March 30, 2010

www.mwjournal.com/events

MARCH

IWCE 2010
March 10–12, 2010 • Las Vegas, NV
www.iwceexpo.com

SATELLITE 2010
March 15–18, 2010 • Washington, DC
www.satellite2010.com

CTIA with RF/Microwave and M2M Zones
March 23–25, 2010 • Las Vegas, NV
www.ctiawireless.com

APRIL

WAMICON 2010
IEEE Wireless and Microwave Technology Conference
April 12–13, 2010 • Melbourne Beach, FL
www.wamicon.org

APEMC 2010
Asia-Pacific Symposium on Electromagnetic Compatibility
April 12–16, 2010 • Beijing, China
www.apemc2010.org

ARMMS RF and Microwave Society Conference
April 19–20, 2010 • Oxfordshire, UK
www.armms.org

MAY

MIE 2010 and ICMMT 2010
2010 Microwave Industry Exhibition in China (MIE 2010)

2010 International Conference on Microwave and Millimeter Wave Technology in China (ICMMT 2010)
May 8–11, 2010 • Chengdu, China
www.cnmw.org

Radar 2010
IEEE International Radar Conference
May 10–14, 2010 • Washington, DC
www.radar2010.com

RFIC 2010
IEEE Radio Frequency Integrated Circuits Symposium
May 23–25, 2010 • Anaheim, CA
www.rfic2010.org

IMS 2010
IEEE MTT-S International Microwave Symposium
May 23–28, 2010 • Anaheim, CA
www.ims2010.org

ARFTG 2010
75th ARFTG Microwave Measurement Conference
May 28, 2010 • Anaheim, CA
www.arftg.org

JULY

EMC 2010
IEEE International Symposium on Electromagnetic Compatibility
July 25–30, 2010 • Fort Lauderdale, FL
www.emc2010.org

SEPTEMBER

EuMW 2010
European Microwave Week
September 26–October 1, 2010 • Paris, France
www.eumweek.com

OCTOBER

AMTA 2010
Antenna Measurement Techniques Association
October 10–15, 2010 • Atlanta, GA
www.amta2010.com

4G World
October 18–21, 2010 • Chicago, IL
https://4gworld.com

MILCOM 2010
October 31–November 3, 2010 • San Jose, CA
www.milcom.org

DECEMBER

Asia Pacific Microwave Conference
December 7–10, 2010 • Yokohama, Japan
www.apmc2010.org

To bring you a superior integrated assembly – we assembled a superior integrated team.

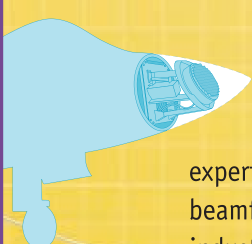

Our expanded S&D Group offers integrated solutions for next-gen systems like tomorrow's AESAs.

For over 40 years, the world's primes have relied on Anaren's deep microwave engineering expertise and innovations like beamforming technology and the industry's first DFDs, DRFMs, and Passive Ranging Subsystems (PRSS).

Now, to help you deliver the multi-function, multimission solutions of the future, we proudly introduce the all-new Anaren Space & Defense Group.

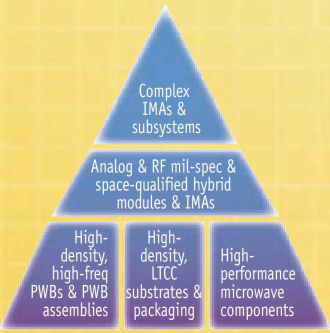

Anaren's vertically integrated capabilities are now affording our customers innovations at all levels of complexity.

Comprised of Anaren Microwave, Anaren Ceramics, MS Kennedy, and Unicircuit – each a longstanding and respected supplier – our team now offers a remarkable talent and technology toolbox in one seamless, highly innovative, and refreshingly accessible organization.

Covering DC to 44GHz, top-level capabilities include:

COVER FEATURE

FUNDAMENTALLY CHANGING NONLINEAR MICROWAVE DESIGN

Nonlinear: "Of or relating to a device whose behavior is described by a set of nonlinear equations and whose output is not proportional to its input."
–The American Heritage® Dictionary of the English Language, Fourth Edition

S-parameters have been used to represent linear networks for simulation and design since the 1960s. Measuring S-parameters was made possible with the introduction of the network analyzer. Designers could then integrate S-parameter "black-boxes" along with other electrical components using linear frequency-domain simulators. The measure, model and simulate triumvirate has proven quite successful for high frequency electronic design of linear devices. Unfortunately, the nonlinear behavior of high-frequency semiconductor devices cannot be represented by S-parameters. Nonlinear device characterization has always been challenging and limited. To better serve designers, test equipment manufacturers, software providers and integrated device manufacturers would like to offer similar black-box characterization for nonlinear devices.

Over the past two decades, developments in nonlinear measurement, modeling and simulation have been introduced in literature. This past year, *Microwave Journal* and others have published numerous articles describing products based on these efforts. In this article, we take a glimpse at the history of development, what is currently available, and how the future of nonlinear characterization/simulation and the microwave electronics industry are intertwined.

WHY CHANGE IS HAPPENING

Nonlinear devices perform critical functions from frequency conversion to signal amplification. Under large-signal drive conditions, they distort waveforms (time domain) or generate harmonics, inter-modulation and spectral regrowth (frequency domain). Sometimes the behavior is exploited, as in the case of a mixer or frequency doubler; sometimes it must be managed, as in the case of a linear amplifier.

Market demands for more bandwidth—driven by the explosive growth of social media and smart phones—along with the desire to reduce telecommunication's carbon footprint is forcing our industry to deliver products that are more linear (to increase capacity) and efficient (to lower power consumption). As these demands become more stringent, the industry faces an inflection point as to how to reach these goals. What is the most efficient way to capture, portray and address nonlinear behavior in the design process?

REPRESENTING NONLINEAR DEVICES

Microwave electronics are developed through a variety of "custom" modeling/design

DAVID VYE
Editor, Microwave Journal

methods. Currently, the more common approaches include:

1. Empirical and Physics-based compact models such as Materka, Curtice Cubic, or Gummel-Poon use physical knowledge of the device and an array of measured data such as S-parameters and current-voltage (I/V) data (DC and pulsed). Model parameters are empirically adjusted to fit this measured data, extracting the model parameter values that replicate the device response to given stimuli. A data file of these parameters is generated by the modeling team and delivered to the designer for use with the appropriate circuit simulation model. The extracted compact model aims to provide a reasonably accurate representation of the device, which is scalable (i.e. transistor size/gate periphery) and applicable for the intended operating range.

New transistor technologies and demand for greater accuracy leads to an increase in device and model complexity, driving the need for enhanced characterization techniques and specialized test equipment. New model development can take years and often requires the skills of PhD level technologists. Their expertise is needed to ensure that the model adequately predicts behavior for the intended application and that the measurement system itself does not introduce errors. Good models are expensive to develop, contain sensitive device information and are often proprietary. Such models do not address larger networks, such as an RFIC functional block. For that, a detailed circuit block or behavioral model is needed.

2. Load-pull measures figures of merits (FOM) such as output power or power-added efficiency versus the load or source impedance. The data is collated into constant performance contours on a Smith chart, providing the impedance target for a matching structure. Since no device model is developed, sensitive device information is protected and parameter extraction is no longer required. While easier to obtain than compact models, load-pull information limits the understanding of device performance to specific metrics, test conditions and device criteria (gate periphery, bias, packaging). A change to any of these invalidates the load-pull information. Fortunately, automation in load-pull systems makes additional tests a viable solution for a reasonable number of operating variables. As a direct design tool, active harmonic load-pull systems can overcome losses between the load and device and provide independent control of impedance values at harmonic frequencies in order to achieve optimum device performance in the lab. Furthermore, load-pull plays an important role in the efforts to develop the measurement-based black-box models described below.

3. Lastly, designers may use a hybrid of S-parameters, load-pull and behavioral models based on nonlinear FOMs such as conversion gain, saturated power, the 1 dB compression point, two-tone third-order intercept point, etc. This method is most common in system development where block integration is the main focus and critical impedance matching will occur at the circuit level using one of the approaches mentioned previously.

Nonlinear behavioral models do have some noteworthy limitations. For instance, they only work in the forward direction, might only assume a single tone input, and may not account for impedance mismatch at the device ports. This leads to unacceptable simulation errors when cascading nonlinear devices, like mixers and amplifiers. In addition, these behavioral models require multiple instruments and configurations to obtain the various FOMs that define them. To streamline the design process, a measurement-based nonlinear behavioral model would have to overcome these FOM behavioral model inaccuracies. It would also need to be easily extracted from a single measurement system developed to generate such a model for the intended software simulation environment.

Due to the complexity, lead time and cost of developing a compact model, the limited information offered by load-pull and FOM black-boxes, technologists have been pursuing an alternative that is easier to implement, sufficiently generalized and provides reliable accuracy. The effort to develop measurement-based nonlinear black-boxes, similar to S-parameters, dates back to the late 1980s and early '90s.

THE CHALLENGE OF NONLINEAR CHARACTERIZATION

A key issue for nonlinear measurements is that they do not simply scale with the stimulus. Unlike the microwave network analyzer, which measures the ratio between the stimulus and the response in order to characterize the linear DUT, a large-signal VNA must measure absolute values in order to fully represent nonlinear DUT behavior. The response is often at a different frequency than the stimulus.

Measured nonlinear behavior can be expressed by a series of equations in time or frequency domain using voltages/currents or waves. The voltage-current or wave combination at all ports define the state of the device in a unique way. If one performed an infinite number of measurements by changing the environment (i.e. power levels, biases, load impedances, etc.), the resulting infinite table of realizations would describe this device completely. Clearly, this is not an option. However, performing a limited set of experiments, which then can be interpolated with confidence, is practical. Such a model would be valid within a well defined set of operating conditions, including the excitation signals.[1] This "measurement based" black-box would offer certain benefits over the compact model, load-pull or FOM behavioral models. Such a model could accurately replicate the signal distortion currently addressed by compact models, without the intensive extraction process. It would only require that the black-box was obtained with a measurement system under similar conditions as the intended application, calling for closer collaboration between characterization and design.

EARLY NONLINEAR EFFORTS

Hewlett-Packard (now Agilent) began research in nonlinear modeling and measurement technology back in the '90s. In 1990, the company started a small research group called the "HP - Network Measurement and Description Group" or HP-NMDG. The group, which included J. Verspecht, E. Van Damme, F. Verbeyst and M. Vanden Bossche (who was finishing his PhD thesis on "Measuring Nonlinear Systems: A Black-box Approach for Instrument Implementation" with sponsorship from HP), was tasked with developing a nonlinear network measurement system (NNMS). Initial efforts were on extending S-pa-


Advanced Technology – It's in our Genes
CST MICROWAVE
STUDIO
2010

rameters to weakly nonlinear devices using Volterra series (VIOMAP). Over the years internal HP prototypes were given different names when presented at conferences or industry tradeshows including the Vector Nonlinear Network Analyzer (VNNA) and the Large-Signal Network Analyzer (LSNA).[2]

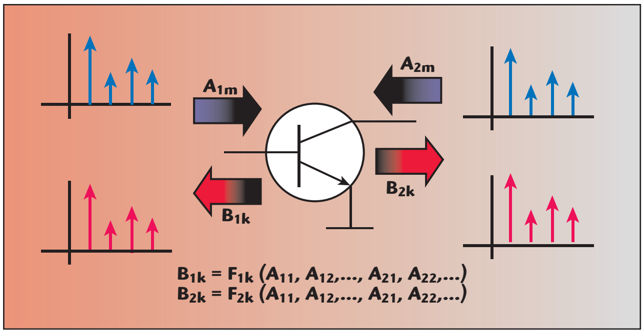

▲ *Fig. 1 The concept of describing functions.*[5]

THE POLY-HARMONIC DISTORTION MODEL

Limitations of the VIOMAP approach led to new modeling efforts by HP through Jan Verspecht and David Root in the early 1990s. HP funded Verspecht's PhD work at the University of Brussels (VUB) on a multi-frequency "Describing Function" concept to address the limitations of the Volterra theory in accurately describing "hard nonlinear" behavior (see ***Figure 1***). Unlike the Volterra theory, this new mathematical framework described very hard nonlinear behavior as encountered in comparators, harmonic mixers, samplers and other hard clipping devices.[3] The DUT could be represented by a spectral mapping function, F_{pm} (1) that correlates all of the relevant input spectral components A_{qn} with the output spectral components B_{pm}, whereby q and p range from one to the number of signal ports and whereby m and n range from zero to the highest harmonic index.[4]

$$B_{pm} = F_{pm}(A_{11}, A_{12}..., A_{21}, A_{22}...) \quad (1)$$

These efforts ultimately led to the Poly-harmonic Distortion (PHD) modeling approach, which is the basis for today's commercial nonlinear measurements, modeling and simulation. In June 2003 Marc Vanden Bossche would leave HP/Agilent and created a separate company, Network Measurement and Description Group (NMDG). NMDG continued developing a software architecture and framework called the Integrated Component Characterization Environment (ICE) and S-function models. Agilent continued its research and investment on PHD modeling. In 2005, Agilent's Loren Betts began research into the nonlinear measurement and modeling problem while pursuing his Agilent-sponsored PhD through the University of Leeds (UK) under Professor Roger Pollard.[6] Bett's PhD research brought him together with Verspecht and Root, whose combined work, along with others at Agilent, led to enhancements to the PHD modeling approach and ultimately the X-parameter model and the Nonlinear Vector Network Analyzer (NVNA) on the Agilent PNA-X platform.

Meanwhile, other companies have also used the PHD modeling approach as a starting point including NMDG's S-functions. Basically the approach defines mappings of the input signal to the spectral components appearing at all the device ports, generated by device nonlinearity. Under nonlinear operating conditions, the superposition principle is not valid. However, in many practical cases, such as a power amplifier stimulated with a narrowband input signal, there is only one dominant large-signal input component present (A_{11}) whereas all other input components (the harmonic frequencies) are relatively small. In that case, the harmonic superposition principle for the relatively small input components can be applied, as illustrated in ***Figure 2***. During the measurement, several small-signal tones that are harmonically related to the fundamental drive are used to perturb the device under test at each large-signal state. These small perturbation

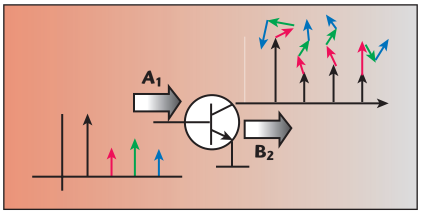

▲ *Fig. 2 The harmonic superposition principle.*

MIMIX POWER AMPLIFIERS & FETs... DRIVING LINEARITY

In today's world, the challenge is moving an ever-increasing amount of information through the same narrow bandwidths. Here at Mimix Broadband, our power amplifiers and FETs drive linearity and minimize distortion, maximizing innovation.

Like our XP1050-QJ Power Amplifier. This PA delivers 15 dB of gain, 34.5 dBm of P1dB and 48 dBm of OIP3 in a standard QFN package, making it an ideal choice for point-to-point radios operating in the ETSI 7 GHz radio band, with modern high-order modulation schemes. The XP1050-QJ is the light at the end of the tunnel!

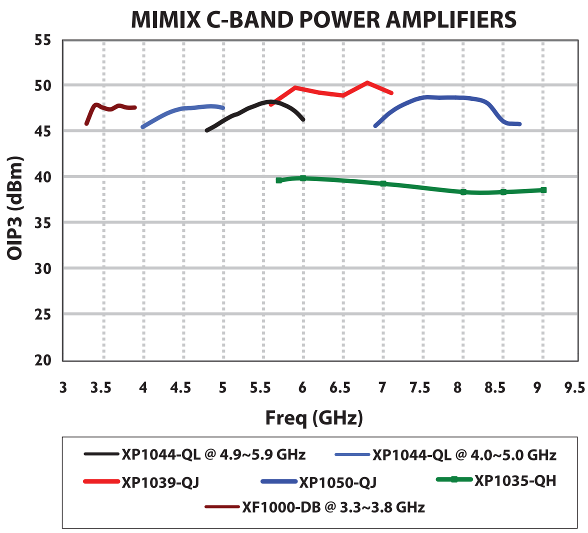

MIMIX BROADBAND IS DRIVING LINEARITY

	Device	Frequency (GHz)	Gain (dB)	P1dB (dBm)	OIP3 (dBm)	Current (mA)	Voltage (V)	Package (mm)
Power Amplifiers	XP1044-QL	3.5-6.0	19.5**	34.0	46.0	850	8.0	7x7
	XP1039-QJ	5.6-7.1	16.6	35.5	49.0	1400	8.0	6x6
	XP1050-QJ	7.0-9.0	15.0	34.5	48.0	1400	8.0	6x6
	XP1035-QH	5.9-9.5	26.0	29.0	39.0	500	6.0	4x4
FETs*	XF1000-DB	DC-6.0	10.0***	34.0	47.0	550	8.0	3x6
	XF1001-SC	DC-6.0	10.0**	30.0	45.0	350	8.0	SOT-89

*FETs Coming Soon | **@ 6.0 GHz | ***@ 4.9 GHz

Explore our wide range of high linearity products and download complete datasheets at www.mimixbroadband.com.

Mimix BROADBAND™
10th Anniversary
providing optimal semiconductor solutions worldwide

Mimix Broadband, Inc., 10795 Rockley Rd., Houston, TX 77099 U.S. 281.988.4600 mimixbroadband.com tones are injected at ALL the terminals of the device in turn and at each harmonic of the fundamental drive. The harmonic superposition principle asserts that the magnitude of the small test signals is such that the perturbation can be viewed as a linear process analogous to mixer theory whereby only the LO signal is large enough to bring a nonlinear device into a time dependent linear operating mode.

By introducing a complex phase reference point (2) set by the phase of the large-signal A_{11}, the spectral mapping function of (1) can be re-written as (3) so that the mapping between input and output is time invariant.

$$P = e^{+j\varphi(A_{11})} \tag{2}$$

Substituting $e^{j\theta}$ by P^{-1} in (4) results in

$$B_{pm} = F_{pm}(|A_{11}|, A_{12}P^{-2}, A_{13}P^{-3}, \ldots \times A_{21}P^{-1}, A_{22}P^{-2}, \ldots)P^{+m} \tag{3}$$

A linearization of this equation results in a PHD model (4).

$$B_{pm} = \sum_{qn} S_{pq,mn}(|A_{11}|)P^{+m-n}A_{qn} + \sum_{qn} T_{pq,mn}(|A_{11}|)P^{+m+n}\mathrm{conj}(A_{qn}) \tag{4}$$

The basic PHD model equation (4) simply describes that the B-waves result from a linear mapping of the A-waves, similar to classic S-parameters. That the right-hand side of (1) contains a contribution associated with the A-waves as well as the conjugate of the A-waves is significantly different from S-parameters, where the conjugate part is not present at all. That is the case since, with S-parameters, the contribution of an A-wave to a particular B-wave is not a function of the phase of that A-wave. Any phase shift in A will just result in the same phase shift of the contribution to the particular B-wave. This is no longer the case, however, when a large fundamental signal (A_{11} wave) is present at the input of a nonlinear DUT. In that case, the large-signal A_{11} wave creates a phase reference point for all other incident A-waves, and the contribution to the B-waves of a particular A-wave depends on the phase relationship between this particular A-wave and the large-signal A_{11} wave.[4]

The PHD modeling approach requires nonlinear measurement systems that can capture the absolute amplitude of signals at the ports of a device as well as the relative phase between frequency components. This information is necessary to study the phase of the distortion and ultimately the nonlinear behavior of the DUT. Therefore, new measurement systems had to be developed to generate the model.

MILESTONES IN NONLINEAR MEASUREMENT DEVELOPMENT

Measuring nonlinearity in the time or frequency domain is driven largely by the state of technology. Measurement systems have used a variety of instruments, including oscilloscopes (both real-time and sampling), vector signal analyzers (VSA), real-time signal analyzers (RTSA), large-signal network analyzers (LSNA) and nonlinear vector network analyzers (NVNA) based on VNAs. Different architectures capture signal distortion through a variety of techniques. Frequency based solutions must maintain or reconstruct the phase relationships between frequency components to achieve faithful waveform representation. If the instrument measures multiple port devices, the phase relationships between signals measured at each port must be maintained as well.

Since a nonlinear DUT creates additional spectral components different from those applied at the input, characterizing a nonlinear device requires an instrument that can measure this complete spectrum in a single measurement take. This is not possible with the "heterodyne" measurements of standard linear network analyzers where the device response is obtained through successive excitation at one single spectral point. A fast way to reuse the "heterodyne" principle was first proposed by Urs Lott.

In 1989, Lott published "Measurement of Magnitude and Phase of Harmonics Generated in Nonlinear Microwave Two-ports."[7] The technique successively measured each harmonic generated by the nonlinear DUT (excited by a pure sine wave) by synchronizing the linear VNA to the corresponding harmonics generated by an auxiliary generator, which was phase coherent with the excitation source (see ***Figure 3***). A known "golden

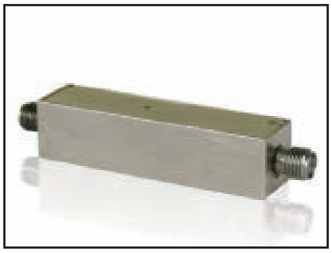

Microstrip and Stripline Filters

Perfect for ground-based and airborne radar systems, airborne vehicle and wing systems, satellites, and radio receivers. Small size, high-performance, and versatile packages make these filters ideal for many applications. Filter topology can be customized to deliver increased rejection on the low side of the passband or symmetric rejection around the passband.

Microstrip & Stripline Filters are ideal for higher frequency requirements because they overcome the difficulties in realizing low values for discrete components. The lack of discrete components coupled with their inherent low mass make them suitable for extremely harsh environments. In addition they are ideal for low cost, high volume manufacturing. Operating frequencies range from 2000 to 25000 MHz.

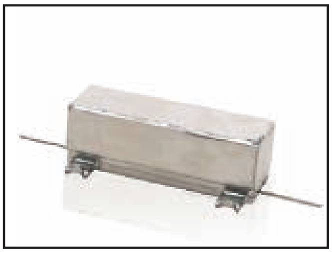

Surface Mount Filters

Small size, high-performance, and versatile packages make these filters ideal for many applications. Operating frequencies range from 5 to 4000 MHz.

PC Mount FIlters

Up to 8 sections can be incorporated, depending on the package style. Operating frequencies range from 0.1 to 4000 MHz.

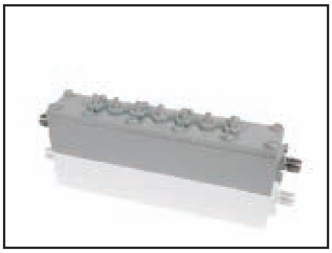

Combline Cavity Filters

The Combline Cavity filter has a usable frequency range of 300 MHz to 20 GHz, percent bandwidths of 0.5 to 60%, and 2 to 14 sections. The variety of customization is nearly limitless.

TRILITHIC
RF & MICROWAVE

With over 50 years of collective experience in engineering and custom manufacturing, Our goal is to anticipate what you'll need tomorrow, and help you stay a step ahead of your competition. In other words, to Think Ahead. It's what drives real innovation at Trilithic.

At Trilithic, innovation is more than engineering and technology. It's about listening to your needs and expectations. So together we can create solutions that work for you today and tomorrow.

www.trilithic.com

standard" diode was used as a phase reference to calibrate phase errors. A major drawback of this initial approach was the assumption that the input signal was a spectrally pure sine wave. This is not often the case since nonlinear microwave systems often distort the input signal through source-pull resulting in the presence of harmonic excitation components on the incident wave of the DUT.[8] Future developments would address this source of error and much of Lott's initial concepts are found in nonlinear network analyzers today.

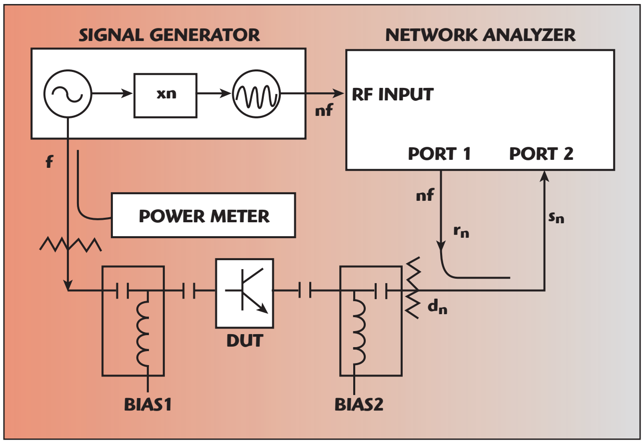

▲ *Fig. 3 Simplified schematic of Lott's VNNA prototype.*

Other early nonlinear measurement systems included that of M. Sipilä, K. Lehtinen, V. Porra[9] in 1988 and G. Kompa and F. van Raay[10] in 1990 (see ***Figure 4***). Both efforts were based on microwave digitizers using digitizing sampling oscilloscopes (DSO) to measure the fast RF time domain waveforms by an equivalent time sampling. Kompa, et al extended the set-up of Sipilä, et al with the use of a VNA to calibrate the test set. Two switches directed the REF and TEST signals to either the broadband sampling oscilloscope (triggered by the fundamental) used to measure the harmonics coherently, or to the network analyzer used to measure the fundamental behavior and calibrate the system. This configuration provided greater accuracy through the VNA calibration and addressed the trigger drift problem. But it was still slow, vulnerable to phase distortion errors introduced by the oscilloscope sampling heads and limited to one port excitation (DUT input).

The calibration procedure used by Kompa, et al and Demmler, et al took into account the phase distortion of the transition analyzer, applying an analog to Lott's approach of using a "reference generator" to precisely obtain the phase relationship between fundamental and harmonic tones.[8] The development of a traceable harmonic phase calibration process was the enabling technology for all subsequent NVNA work. In the mid-'90s, researchers at NIST measuring the phase dispersion of a broadband receiver developed an ingenious electro-optic sampling set-up capable of characterizing harmonic phases up to 100 GHz with a NIST-traceable error of less than one degree.[11] All the harmonic phase standards used in today's NVNAs are traceable to this set-up.

HP built its first LSNA prototype in 1992 based on four couplers to detect the incident and scattered waves at both ports using a 20 GHz bandwidth sampling oscilloscope for the data acquisition. Requiring a few hours to calibrate and about three minutes for each data acquisition, this prototype was much too slow for practical use. It also had trigger drifting problems. A faster solution was found in 1993 by replacing the oscilloscope with a sampler-based

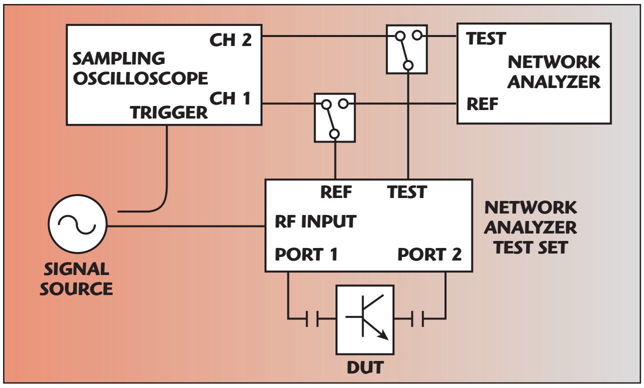

▲ *Fig. 4 Gunther Kompa, et al VNNA prototype.*


DAICO LAUNCHES TRANSMITTER SUBSYSTEMS
Leveraging off a history of superior microwave components, Daico is now delivering TRANSMITTER SUBSYSTEMS with the same quality, reliability and technical innovation.
The DTX09511, designed for a weather monitoring radar system, delivers twelve channels of 1kW pulsed RF energy with ±0.5 dB linearity over a >20 dB dynamic range.
EXPANDING HORIZONS
DAICO Industries
DAICO Industries, Inc.
1070 East 233rd Street
Carson, California 90745
Phone 310 507 3242
Fax 310 507 5701
Daico can show you how to get your design off the ground.
www.daico.com
Visit http://mwj.hotims.com/28487-35 or use RS# 35 at www.mwjournal.com/info

instrument leveraged from two HP Microwave Transition Analyzers, a commercial instrument introduced in 1991. With four fully synchronized RF data acquisition channels, it supported the phase and amplitude measurements of the fundamental and harmonics at both input channels for frequencies up to 40 GHz. Since it was based on the harmonic mixing principle, rather than on equivalent time sampling, the instrument allowed data acquisition about 100 times faster than what was possible with a sampling oscilloscope for the same or even a better dynamic range (typically better than 50 dB).[2]

By 1995, HP used high-precision analog-to-digital convertors to replace the MTA's internal ones, resulting in a somewhat faster instrument with more dynamic range and increased linearity. In 2003, Agilent licensed the LSNA IP to Maury Microwave who continued to offer this sampler-based architecture. Agilent continued nonlinear research with a mixer-based architecture, which resulted in an early nonlinear vector network analyzer (NVNA) prototype based on the Agilent PNA-L in 2005.[6]

Using microwave transition analyzers for signal detection was also being pursued by Demmler, Tasker and Schlechtweg at essentially the same time (1994). Professor Tasker and others at Cardiff University developed the table-based Cardiff model and its associated measurement system. Unlike the PHD modeling approach, which is based on amplitude/phase information of a DUT's spectral response, the Cardiff measurement system captures the current/voltage waveform at the device ports with a test set-up based on a sampling oscilloscope. The resulting model uses four table-based nonlinear functions: Ic, Qc, Vbe and Qb, all defined versus Ib and Vce (based on a non-uniform bias grid) to define device behavior for a given input stimulus, bias and terminating impedance. The system can employ single or multiple-tone large-signal measurements including harmonic load-pull. The look-up table approach forces the designer to stay within the 'measurement space' to avoid extrapolation errors.[12]

COMMERCIAL NONLINEAR MEASUREMENT SYSTEMS

The following is a brief description of the various large-signal or nonlinear vector network analyzers, time-sampling oscilloscope-based systems, and load-/source-pull systems available today.

Agilent Technologies and Partners

Agilent continued nonlinear research with a mixer-based architecture, which resulted in an early nonlinear vector network analyzer (NVNA) prototype based on the Agilent PNA-L in 2005.[6] Today, Agilent's PNA firmware transforms the linear vector network analyzer into an NVNA to measure the vector corrected absolute amplitude and cross-frequency phase stimulus/response of a device. A new Agilent phase reference, based on an active IC, provided the capability to measure the vector corrected cross-frequency phase out to 50 GHz with very narrow grid spacing. Since the amplitude and cross-frequency phase of all the frequency spectra is accurately known, an inverse Fourier transform can be applied to the frequency domain data to generate the time domain waveforms.

These vector corrected stimulus/response measurements lay the foundation for the automated X-parameter measurements. ***Figure 5*** illustrates the PNA-X mixer-based NVNA architecture. Since the X-parameter measurements for a two-port component require two sources, the PNA-X hardware architecture utilizes integrated, "spectrally pure" sources, internal combining network, internal pulse modulators/generators, and flexible signal routing.

The NVNA can be used as a vector corrected time domain scope by measuring the absolute amplitude and cross-frequency phase of the signals with error correction applied. The NVNA with the N5244A PNA-X can sweep from 10 MHz to 50 GHz creating a time domain scope with 50 GHz of detection bandwidth for a discrete point resolution of 1/(50 GHz) ≈ 20 ps. This time domain data can be used to examine the I/V waveforms at the device terminals in order to analyze the linear and nonlinear charac-

Industry's most comprehensive line of LTE design and test products

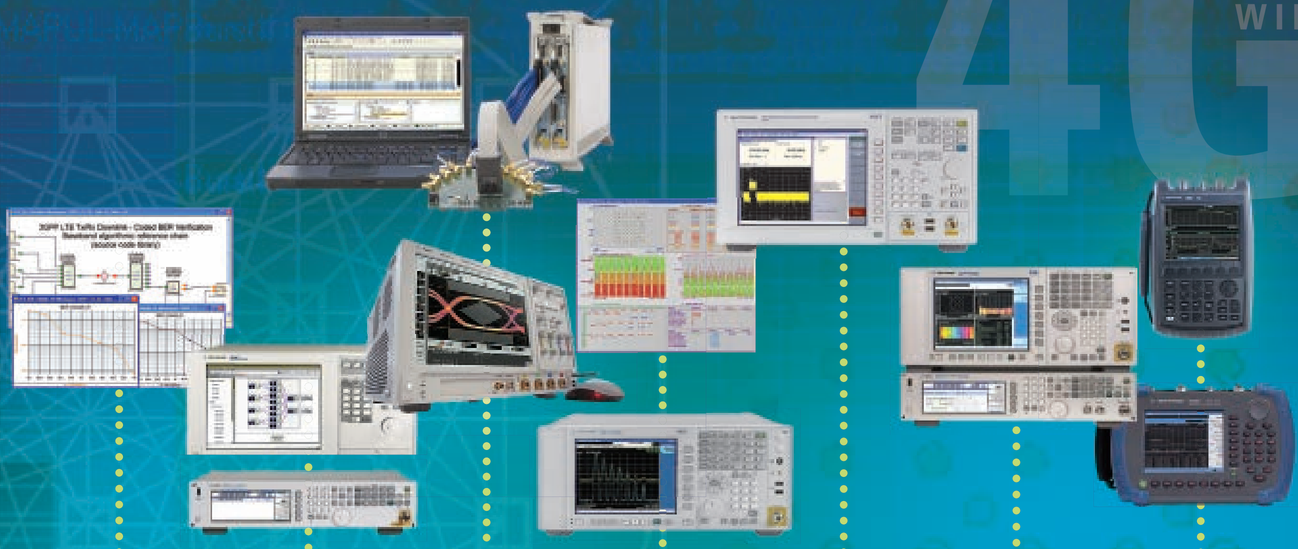

Simulation | Signal Creation | Baseband Analysis | Signal Analysis | UE Development | eNodeB Manufacturing | Network Installation and Maintenance

Agilent gives you the right test equipment at the right time so your products and network meet the latest LTE standards and your project schedule.

"The company's LTE product range spans the entire technology life cycle, from early R&D through manufacturing to network deployment and service assurance."

(Frost and Sullivan, 2009)

www.agilent.com/find/lte

Build your LTE knowledge with our library of FREE resources—authored by LTE experts
www.agilent.com/find/LTEtesting

And, order your copy of Agilent's NEW LTE book
www.agilent.com/find/NewLTEbook

u.s. 1-800-829-4444 canada: 1-877-894-4414

Agilent Technologies

Visit http://mwj.hotims.com/28487-9 or use RS# 9 at www.mwjournal.com/info

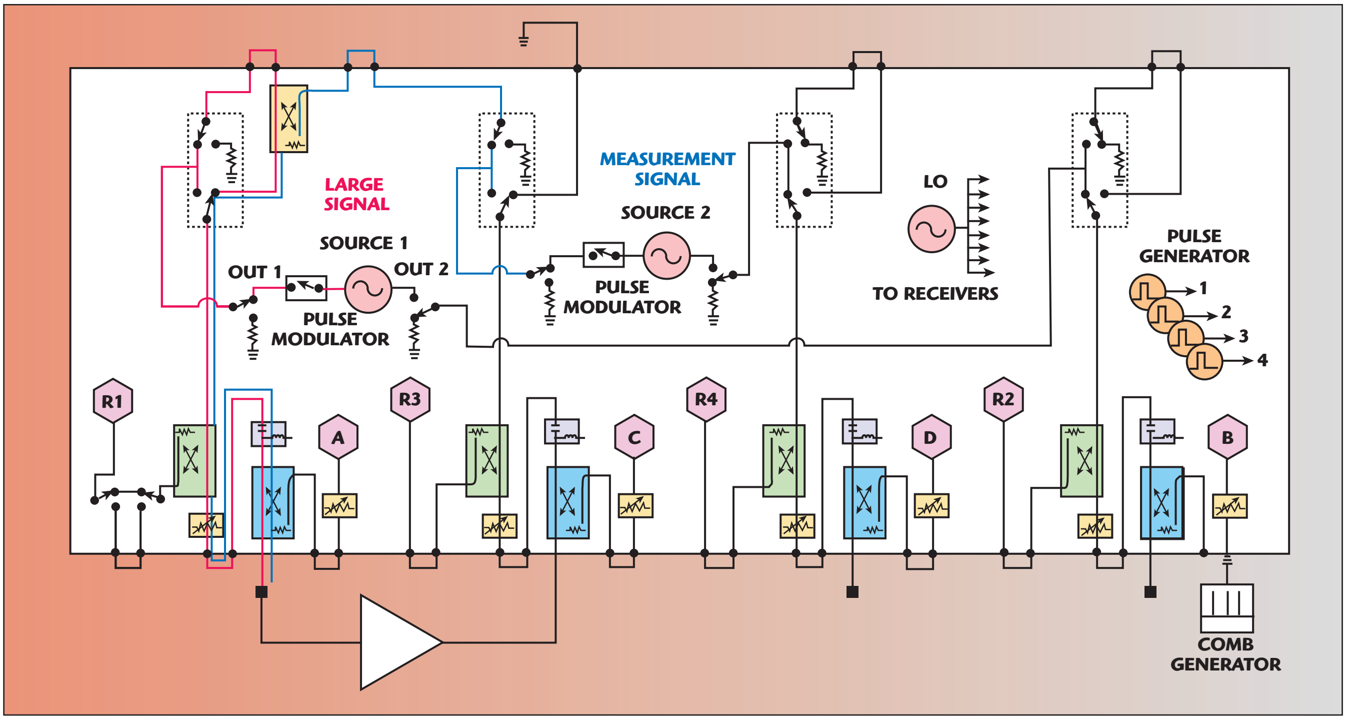

▲ *Fig. 5 Agilent PNA-X NVNA.*

teristics of a component. The RF I/V curves can be superimposed on the DC I/V curves providing the designer important information on the component behavior under various DC bias and RF conditions.

The Agilent instrument can also measure the multi-tone and intermodulation products at the fundamental and harmonic frequencies. The NVNA can be used to analyze complex signals such as those present with a device operating under fast RF and/or DC pulses. To measure and analyze memory effects, a multi-envelope measurement can be performed where the component is stimulated with a pulsed signal (RF and/or DC bias) and the resulting envelope 'a' and 'b' waveforms are measured at the fundamental and harmonics frequencies. The envelope amplitude and phase can be analyzed versus time at each of the spectral components. More recently, the NVNA's measurements were extended to include dynamic envelopes resulting in the new multi-envelope measurement domain.[13] The multi-envelope measurement domain is currently being utilized to measure X-parameters™ with enhanced time-varying dynamics.

Agilent along with Maury Microwave extended the X-parameter measurement capability by adding arbitrary load-dependence X-parameters (fundamental and harmonic frequencies) to the NVNA. This capability has also been extended to the load-pull system from Focus Microwave. The full, complex Gamma dependence of a device under large-signal operating conditions is captured and can be exported into simulation software allowing devices to be accurately represented using X-parameter models in cascaded multi-stage, Doherty or other complex amplifier circuit simulations. Additionally, the load-pull option lets researchers account for arbitrary load mismatches, measure dynamic loadlines and optimize performance. The system does not currently support direct independent control of harmonic impedances; however, the uncontrolled harmonic impedances presented by the load tuner are captured through calibrated measurements and corrected for in the exported X-parameters. Although the system itself does not support optimization through harmonic tuning on the test bench, the information captured in the X-parameters enables performance optimization via harmonic tuning during simulation.

Mesuro/Tektronix

An alternative measurement/modeling approach is offered by Mesuro Ltd., a commercial entity with ties to the longstanding developments taking place at Cardiff University (Tasker, Benedikt, et al). Their "waveform engineering" measurement system includes a test set similar to the VNA and a sampling oscilloscope instead of samplers or mixers. The system (MB20 and MB150) can optimize performance directly on the test bench via active harmonic tuning and generate a measurement-based model.

The measurement solution enables emulation of realistic signal conditions at the DUT. Calibration "removes" the package or test fixture behavior, placing the measurement reference plane directly at the DUT ports. Designers gain direct access to current and voltage waveforms to study their shape and optimize the device performance through control of the harmonic impedances at the device ports. For the case of designing a single-stage amplifier, the benefit to waveform engineering is that real-time visualization and control of I/V waveforms at the device terminals will give the engineer a big advantage in determining what (load) makes the device work best at the time of the measurement rather than by capturing its behavior as a black-box and optimizing the performance during simulation. Independent control of harmonic impedances is critical to optimizing performance through waveform engineering. For design work that goes beyond a single


Mini-Circuits
LAVI

DUT, such as a multi-stage amplifier, a simulation model is still required. For these instances, the Mesuro system can produce the I/V table-based model that was developed at Cardiff University.

The system modules include the following: A wideband receiver based on a Tektronix sampling oscilloscope capable of simultaneously capturing all signal components from DC to 67 GHz with effective 12 bit accuracy and a dynamic range of up to 50 dB; an arbitrary waveform generator (also from Tektronix) that synthesizes fully synchronous waveform shapes for the input and output of the DUT up to 6 GHz, when using both outputs separately, or up to 10 GHz in interleave mode; an RF and baseband test-set that allows for the contactless detection of the current and voltage waveforms and an interface with the active source and load-pull system while providing bias to the DUT; and integrated software tools for calibration, measurement, waveform analysis and control of the system including active harmonic load-pull.

The use of an oscilloscope provides a measurement whose speed is fixed, regardless of the complexity of the signal. These instruments measure over a broad bandwidth and are not limited to acquisition around harmonics of the excitation. There is, however, a corresponding reduction in dynamic range when compared to systems based on harmonic mixing or "sampling downconversion" techniques. The measurement accuracy of the oscilloscope can also be affected by both time-base distortion and jitter, although these can be corrected using methods to compensate for random and systematic timing errors, as described in Reference 11.

NMDG, Rohde & Schwarz, Maury Microwave and Focus Microwave

Starting in 2003, Maury Microwave and NMDG worked together on the first commercially available large-signal network analyzer, the MT4463. This Maury/NMDG LSNA, using technology licensed to Maury by Agilent Technologies, was configured largely from Agilent test equipment and NMDG developed hardware/software. It was released in March 2005 and measured the complete voltage and current or incident/reflected wave behavior under small- (S-parameters) and large-signal conditions.

Since June 2008, NMDG has partnered with Rohde & Schwarz to enable its VNAs with the ability to characterize nonlinear devices in time and frequency domains. NMDG's NM300 ZVxPlus (see ***Figure 6***) is a combination of software and hardware that runs on top of the Rohde & Schwarz ZVA and ZVT series Vector Network Analyzers (VNA), supporting a frequency range from 600 MHz up to 20 GHz. The measurement system can be calibrated to measure the incident and reflected waves or voltages and currents at the ports of a component under test, under realistic conditions using a periodic harmonic-related stimulus and supports analysis of nonlinear harmonic behavior in the frequency domain, harmonic measurements including phase, fundamental and harmonic tuning, time domain

Test, Simulation, RF Distribution Subsystems…
Smart Solutions at Work!

AEROFLEX
WEINSCHEL

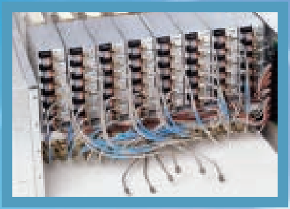
Attenuation Matrices & Multi-Channel Subsystems


RF Distribution Networks


Switch Matrices


RF/Microwave Frequency Translators

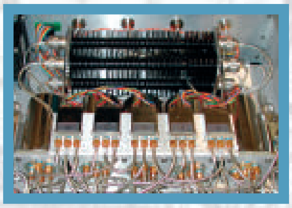
Cellular & Wireless Subsystems with Low IM Performance


Mobile Unit (Radio & WLAN) Fading Simulators


Cable Modem Redundant Switches & Test Systems

Aeroflex / Weinschel offers smart solutions to challenging test, simulation and RF distribution requirements by offering subsystem products that are either off-the-shelf or designed to customer specifications. Our subsystems feature:

- Standard communication interfaces (IEEE-488, RS-232, Ethernet) with proprietary SmartStep® Technology;
- Flexible, high-density mechanical layout & packaging;
- 50 & 75 configurations.

Our subsystems are employed in telecommunications, radar and CNI, satellite and ground communication systems, base station and mobile unit software conformance verification, signal analysis, cable modem and VoIP testing, production test systems and precision microwave related test instruments.

Aeroflex / Weinschel, Inc.
800-638-2048, 301-846-9222
www.aeroflex.com/weinschel
weinschel-sales@aeroflex.com

www.aeroflex.com/microwave

AEROFLEX
A passion for performance.

representation and non 50 ohm measurements.

The R&S VNA features independent synthesizers to support measurements on amplifiers and frequency-converting DUTs such as mixers and front-ends. The high spectral purity of the source signals as well as the high intercept point and high sensitivity of the receivers eliminate the need for external filters in multi-tone measurements and measurements on frequency-converting DUTs. Rhode & Schwarz ZVA can also be used to perform hot-S22 measurements.

NMDG is also partnered with Focus Microwaves, extending their solution to include fundamental and multi-harmonic source- and load-pull systems utilizing computer controlled electro-mechanical wideband and harmonic tuners with VSWR performance ranging from 10:1 to over 200:1.

Anritsu/HFE

Anritsu's VectorStar Nonlinear System stems from collaboration between Anritsu and High Frequency Engineering Sagl of Switzerland (HFE). The system includes an HFE test set, various components for load-pull analysis and the HFE software. Anritsu's MS4640A family of VNAs can control as many as four independent signal sources for multi-tone measurements and direct-access loops for source and receiver monitoring. Applications include built-in programmable power sweeps for gain-compression analysis at multiple frequency points, inter-modulation distortion (IMD) measurements and harmonic measurements.

The Anritsu/HFE nonlinear system inserts a low-loss coupler between the DUT and load-pull tuner, achieving improved measurement accuracy of the source and load impedances at the DUT. This approach makes it possible to monitor the impedance in real time while also monitoring the performance of the DUT. The VNA provides immediate display of the DUT's performance in response to changes in impedance, allowing real-time tuning. Pre-calibrated tuners are not required since the impedance can be monitored while the DUT is being measured. This configuration also eliminates the importance of tuner repeatability. The Anritsu/HFE active loop tuner is capable of providing gamma values to 1.0 at the DUT port. Alternatively, any type of impedance tuner from any vendor can be used in the load-pull system.

Nonlinear data is available directly from the software in a number of formats. This solution can provide nonlinear figures of merit for use in a "system-level" behavioral block or load-pull information for designing an optimum impedance matching network in a separate EDA tool. Anritsu and HFE are exploring exportable nonlinear model formats as members of the OpenWave Forum.

AMCAD/Auriga/Modelithics/VTD/HF Technik

Started in 2004 by researchers from XLIM Laboratory in France, AMCAD provides a modeling tool with pulsed I/V RF characterization and load-pull system. Their associated software platform (IVCAD) controls

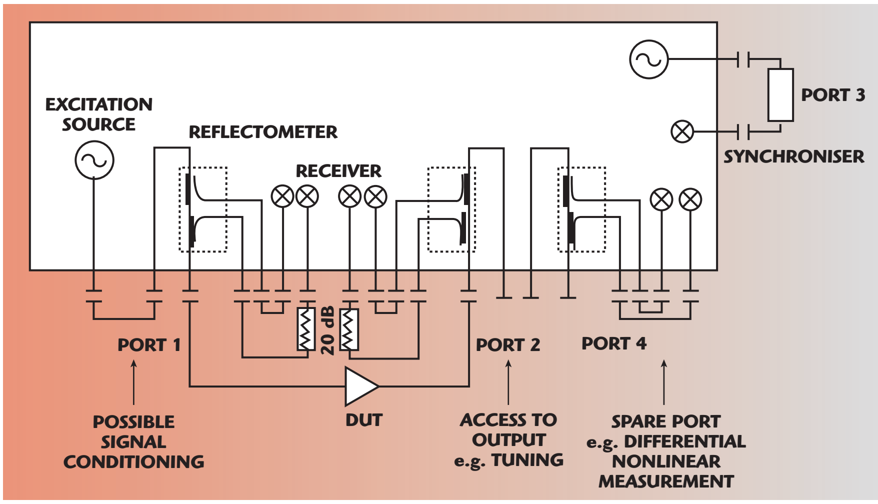

▲ *Fig. 6 Block diagram of standard ZVxPlus configuration.*

these test benches, manages measured data and model extraction with direct links to RF EDA tools (ADS, MWO). They are currently among the few independent companies providing X-parameters characterization and PHD model extraction services.

Other firms offering nonlinear device characterization include Modelithics (DC and pulsed I/V, load-/source-pull, compact model and X-parameter extraction), which was founded in 2001 by Lawrence Dunleavy and Thomas Weller, and Auriga Measurements Systems LLC (DC and pulsed I/V, load-/source-pull, compact model), which was founded in 2004 by Yusuke Tajima. Auriga also manufactures and sells custom Automated Test Equipment (ATE) for device modeling.

In 2008 Jan Verspecht co-founded the company Verspecht-Teyssier-DeGroote SAS. The company, also known as VTD, uses the sampling architecture of the LSNA in order to build the SWAP-X402, an affordable measurement instrument dedicated to the time-domain load-pull characterization of power transistors (not optimized for behavioral modeling). It has the capability to measure the phase and amplitudes of harmonics (and as such the time domain waveforms), even under pulsed operating conditions.

Heuermann HF-Technik GmbH (HHF) is a spin-off of the Aachen University of Applied Sciences. Founded in 2008 by Professor Heuermann, the company's NonLin-S product performs calibrated complex nonlinear measurements with a multi-port-VNA from R&S, Agilent or Anritsu (ZVA, ZVB, ENA, PNA, or Anritsu). The system supports IM measurements, mixer measurements, harmonic measurements, sampling oscilloscope measurements and spectrum analyzer measurements.

DESIGNING WITH NONLINEAR MEASUREMENT MODELS

For further analysis and circuit design, the X-parameters, S-functions, Cardiff models, etc. from the measurement system (Agilent, NMDG/R&S, HFE/Anritsu and/or Tektronix/Mesuro) must operate with a simulator that supports RF/microwave models and analyses, i.e. Agilent EEsof ADS, Genesys or AWR's Microwave Office (MWO). With four different measurement systems extracting models based upon different techniques, there is a need for a common model file format support that reaches across measurement and simulation platforms. This well-recognized need has spawned two approaches.

X-parameters

Since Agilent produces both measurement system and design software, they have developed the capabilities of both simultaneously, leading to the NVNA/X-Parameter solution. The Agilent NVNA firmware allows a user to define the saved data as A and B waves, voltages, currents, or X-parameters. The data is saved in the Microwave Data Interchange Format (MDIF), a file format initially developed for behavioral modeling of nonlinear devices in ADS, which has become a de-facto standard supported by other tools as well. In ADS, the X-parameter simulation component is a native compiled simulation element that directly interfaces with the spectral Jacobian of the nonlinear simulator and can be used with all other ADS components in a circuit design.

Agilent wants to establish X-parameters as an industry standard, publishing the equations (IEEE Explore) and the underlying X-parameter theory. According to Agilent, the files are open, documented, non-encrypted and human readable to "enable broad industry adoption and to encourage others to join in the development of the technology." The company asks for direct collaboration with companies interested in supporting X-parameters in order to provide updates to the standard as it evolves and ensure quality. According to Agilent's website, the company is currently providing additional support to key customers and strategic partners due to the "rapidly developing state of the technology, as well as finite resources."

The OpenWave Forum

Evolving concurrently alongside Agilent's X-parameters approach is the effort spawned by AWR, Anritsu, HFE, Mesuro, NMDG, Rohde & Schwarz and Tektronix last fall to form an industry alliance (www.openwaveforum.org) with the goal of establishing an open standard for exchanging nonlinear behavioral modeling data across multiple vendor tools.

This group, known as the OpenWave Forum (OWF), also wishes to create and promote a unified and transparent data exchange format for large-signal nonlinear simulations, measurements and models. The yet-to-be-finalized open standard will ensure that data from any compliant measurement system would be compatible and transportable to any EDA environment that recognizes the standard. The alliance believes their collective approach is necessary to facilitate an open standard that represents a mutually agreed upon flexible, nonproprietary MDIF data format for nonlinear systems.

Simulation

Microwave nonlinear simulators such as ADS, Genesys, Microwave Office and Ansoft Designer use the Harmonic Balance algorithm, which splits the circuit/system into two sub-circuits, a linear sub-circuit and a nonlinear sub-circuit. This technique, which has been in use for decades, allows the simulator to solve the linear portion in the frequency domain and the nonlinear portion in the time domain. The time domain is required for addressing the time variant signal distortion due to device nonlinearity. The frequency domain provides a speed advantage for solving the linear portions of the network, which may include dispersive elements such as transmission lines. The nonlinear time-domain solution is converted into the frequency-domain via discrete or fast Fourier transform (DFT or FFT) and the spectra of the currents at the linear-nonlinear interface are compared. The spectra used in the algorithm is defined by the RF source (or sources) placed in the schematic to drive the DUT and the simulation setup specified by the user and includes the number of harmonics and intermodulation tones for the simulation engine to solve.

The continuity equation requires that the nonlinear currents equal the linear currents. The technique seeks a solution to this steady-state nonlinear problem by iteratively solving for a set of variables such as the voltages at the linear-nonlinear interface. This iterative process of "balancing" the currents between the linear and nonlinear network nodes can be responsible for lengthy simulation times and in certain cases, a failure to converge. This can occur when the spectral content is high (highly nonlinear conditions) or many nonlinear elements exist.

As a frequency defined device, PHD models are not solved in the time domain, obviating the Fourier transform and iterative solving of the harmonic balance algorithm. Essentially, large-signal VNAs and the PHD modeling approach do in measurements and modeling what Harmonic Balance (and Circuit Envelop) algorithms do in simulation. This results in reduced memory requirements and fast simulation run times.

Model accuracy is ensured by the fact that the PHD model is directly derived from measurements (or models derived directly from circuit simulation). The model's accuracy holds as far as the DUT is stimulated under the conditions for which the assumed harmonic superposition principle holds. The simulation stimuli and load conditions must also reflect those of the measurement. Load dependent PHD models from load-pull measurements (or simulation) are required when the terminal impedances in the simulation are different than those of the measurement system (typically 50 ohm) as would be the case with mismatched cascaded black-boxes (i.e. multi-stage amplifier or front-end module).

Multi-tone Analysis

X-parameters are a complete description of steady-state multi-tone nonlinear component behavior. They scale with number of ports and large-signal tones. The initial X-parameter measurements on the NVNA were supported for a single large tone stimulus on a two-port device. Inferences about component behavior in response to continuous spectrum input envelope signals (digital modulation) can be made by leveraging the AM-AM and AM-PM information in the one-tone X-parameters using circuit envelope analysis. Here the time-varying input envelope is mapped, at each instant in time, into the output envelope value at the same time using the static X-parameters. The results are valid (indicative of the actual device response) provided only that the modulation is narrow-band relative to the carrier. ADS 2009 Update 1 now allows for an arbitrary number of tones and arbitrary number of ports as well as built-in native support for X-parameter simulation.

Prior to this availability there was no direct way to investigate multiple tones around the main drive tone. FDD models are also inherently steady state models, naturally supporting the discrete harmonic tones used in single-tone harmonic balance, and not general or arbitrary waveforms. This limitation can be circumvented by coupling the Harmonic Balance solver with either circuit envelope or complex envelope solvers when more complex drive waveforms are needed for EVM and ACPR analyses. Both methods, Complex Envelope and Circuit Envelope, make use of the AM-AM and AM-PM information in the model and both assume that spectral widening is such that inter-modulation effects are narrow band centered about the carrier.

With the upcoming two-tone X-parameter capability added to Agilent's NVNA, the calibrated nonlinear cross-frequency vector distortion information can be used for designing distortion cancellation circuits and apply other design principles, such as derivative superposition,[9] that previously could be applied only if there was confidence in accurate nonlinear device models. Extending the NVNA to measure three-port devices, such as mixers and converters, is also underway.

At IMS last year, Verspecht, Horns, Betts, Gunyan, Pollard, Gillease and Root reported an extension of the X-parameter model to include dynamics identified from multi-envelope X-parameter measurements on an NVNA with a pulsed stimulus with variable on/off ratios. The model was shown to correctly predict the transient RF response to time varying RF excitations including the asymmetry between off-to-on and on-to-off switched behavior as well as responses to conventional wide-bandwidth communication signals with the high peak-to-average ratios that excite long-term memory effects such as self-heating, dynamic bias effects and trapping phenomena. The approach was applied to an HBT transistor and a commercial PA module that exhibited significant memory effects and experimentally validated by two-tone NVNA measurements us-

ing novel envelope transient measurement techniques.[14]

CONCLUSION

Proprietary empirical models and extraction techniques for nonlinear devices are a costly and time-consuming effort for integrated device manufacturers. Lack of model availability represents a real bottleneck for designers while uncertainty over model quality is a leading cause of design failure. Recent breakthrough innovations in nonlinear characterization (i.e. measurement, modeling and simulation) look to compliment compact models with measurement-based black-box models similar in nature to S-parameters. For nonlinear devices, such models must accurately account for the amplitude/phase information of the DUT's spectral components, which will in turn depend on measurement parameters (i.e. stimuli, load impedances, etc.). Current commercial offerings are based on the Poly-harmonic Distortion model, which takes advantage of the harmonic superposition principle. Such models are derived using a new generation of measurement systems known as large-signal network analyzers or nonlinear vector network analyzer. Model accuracy is assured provided the simulation conditions reflect those of the measurement. Both model and measurement technology are evolving as the industry is adopting this new approach. While less general than a compact model, these measurement-based models and measurement systems are poised to bring relief to what had been a persistent bottleneck in the design process. ■

ACKNOWLEDGMENT

The author gratefully acknowledges the support and contributions of the following individuals: D. Root, L. Betts, C. Plott, J. Civello and J. Smith (Agilent Technologies); S. Reyes and K. Van Diepen (Anritsu); M. Vanden Bossche (NMDG); M. Roth, T. Bednorz, J. Fries and J. Wolf (Rohde & Schwarz); and S. Hess and M. Edwards (AWR). Also, a very special thanks to Jan Verspecht for his impressive contributions to nonlinear device characterization and whose timely and detailed responses to my questions made this article possible.

References

1. http://users.skynet.be/Marc.Vanden_Bossche/nmdgvaria/LSNATechnologyTheory.pdf.
2. J. Verspecht, "Calibration of a Measurement System for High Frequency Nonlinear Devices," Doctoral Dissertation, Vrije Universiteit Brussel, Belgium, November 1995.
3. http://www.janverspecht.com/HTML/profile.htm.
4. J. Verspecht and D. Root, "Poly-harmonic Distortion Modeling," *IEEE Microwave Magazine*, Vol. 7, No. 3, June 2006, pp. 44-57.
5. http://www.home.agilent.com/agilent/redirector.jspx?ckey=1483944&action=ref&lc=eng&cc=US&cname=AGILENT_EDITORIAL.
6. P. Blockley, D. Gunyan and J.B. Scott, "Mixer-based, Vector-corrected, Vector Signal/Network Analyzer Offering 300 kHz to 20 GHz Bandwidth and Traceable Phase Response," *2005 IEEE MTT-S International Microwave Symposium Digest*, June 12-17, 2005.
7. U. Lott, "Measurement of Magnitude and Phase of Harmonics Generated in Nonlinear Microwave Two-ports," *IEEE Transactions*, Vol. 37, No.10, October 1989, pp.1506-1511.
8. A. Barel, "History of Nonlinear Microwave Measurements," Vrije Universiteit Brussel (Dept. ELEC); Pleinlaan 2; B-1050 Brussels, Belgium.
9. M. Sipilä, K. Lethinen and V. Porra. "High-frequency Periodic Time-domain Waveform Measurement System," *IEEE Transactions*, Vol. 36, No 10, October 1988, pp. 1397-1405.
10. G. Kompa and F. Van Raay, "Error-corrected Large-signal Waveform Measurement System Combining Network Analyser and Sampling Oscilloscope Capabilities," *IEEE Transactions*, Vol. 38, No. 4, April 1990, pp. 358-365.
11. D. Williams, P. Hale and K.A. Remley, "The Sampling Oscilloscope as a Microwave Instrument," *IEEE Microwave Magazine*, Vol. 8, No. 4, August 2007, pp. 59-68.
12. M. Demmler, P.J. Tasker and M. Schlechtweg, "On-wafer Large-signal Power, S-Parameter and Waveform Measurement System," Conference Record of INMMC'94-3rd International Workshop on Integrated Nonlinear Microwave and Milimeter-wave Circuits, Duisburg, Germany, October 1994, pp. 153-158.
13. L. Betts, "Vector and Harmonic Amplitude/Phase Corrected Multi-envelope Stimulus Response Measurements of Nonlinear Devices," *2008 IEEE MTT-S Microwave Symposium Digest*, June 2008.
14. J. Verspecht, J. Horn, L. Betts, D. Gunyan, R. Pollard, C. Gillease and D.E. Root, "Extension of X-Parameters to Include Long-term Dynamic Memory Effects," *2009 IEEE MTT-S International Microwave Symposium Digest*, 2009, pp. 741-744.

A MIMO Over-the-Air Emulator for Testing Wireless Terminals

Next generation wireless systems are moving towards ever increasing data rates, higher spectral efficiency and improved quality of service. This development has largely been facilitated by advanced terminals with multiple antennas. However, the use of multiple antennas not only opens up new opportunities, but also presents new testing challenges.

For multi-antenna devices, like cellular phones in LTE and laptops utilizing WLAN, WiMAX and LTE technologies, the traditional approach of testing the antenna characteristics and the signal processing performance separately does not assess the terminal performance realistically.

This is because the conductive testing does not realistically take into account the antenna effects of multi-antenna devices. Because a multiple-input-multiple-output (MIMO) radio channel is a combination of the antenna characteristics and the radio propagation conditions, they need to be tested together in a controlled environment by a MIMO Over-the-Air (OTA) test system consisting of a radio channel emulator and anechoic chamber.

MEETING THE CHALLENGE

That is the challenge and the solution has been developed in the form of the EB Propsim F8 MIMO OTA emulator that utilizes the company's patented file-based emulation approach, which is a pre-requisite to convert the geometry-based stochastic channel models to MIMO OTA models.

The emulator enables evaluation of different mobile terminal designs in a fully repeatable and realistic wireless network environment and makes it possible to test all critical parts of the mobile terminal design at once, including antennas, RF front-end and baseband processing. This eliminates the need for cables and test connectors leaving the mobile device intact, which provides more accurate results of how the device will perform in the real world.

Figure 1 shows the EB MIMO OTA test system in schematic form. The EB MIMO OTA test system consists of a transmitter, EB Propsim F8 MIMO OTA channel emulator, an anechoic

EB (ELEKTROBIT)
Oulu, Finland


COBHAM SENSOR SYSTEMS
WHERE THE POWER OF INTEGRATION IS WORKING FOR YOU
Cobham Sensor Systems is comprised of the following groups: Sensor Electronics, Microwave Electronics, and Microwave Components. For added assurance, all our products, from the smallest MMIC components to the largest antenna subsystems, are designed, manufactured, tested and inspected to meet the most stringent customer specifications.
Count on Cobham for all your product needs -- Electronic Warfare, Homeland Security, Radar, Ground & Mobile Communications, Smart Munitions, Search & Surveillance, Force Protection, Missiles, Space, Satellite Communication, SIGINT, and Overhaul & Repair.
COBHAM
www.cobham.com
ATLANTIC POSITIONING SYSTEMS www.atlanticpositioners.com 727.299.0150 ATLANTIC MICROWAVE www.atlanticmicrowave.com 978.779.6963
CONTINENTAL MICROWAVE www.contmicro.com 603.775.5200 KEVLIN www.kevlin.com 978.557.2400 LANSDALE www.cobhamdes.com 215.996.2000
M/A-COM www.macom.com North America 800.366.2266 Europe +44 0 1908.574200 Asia / Pacific +81.44.844.8296 NURAD www.nurad.com 410.542.1700
REMEC DEFENSE & SPACE www.remecrds.com 858.560.1301 SIVERS LAB AB www.siverslab.se +46 8 477 6811
Visit http://mwj.hotims.com/28487-29 or use RS# 29 at www.mwjournal.com/info

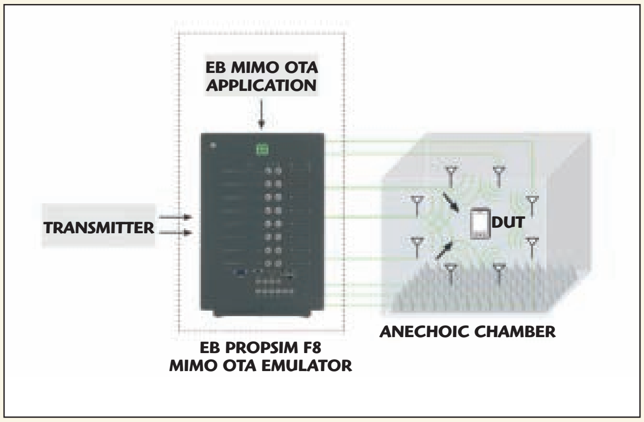

▲ *Fig. 1 The EB MIMO OTA test system in schematic form.*

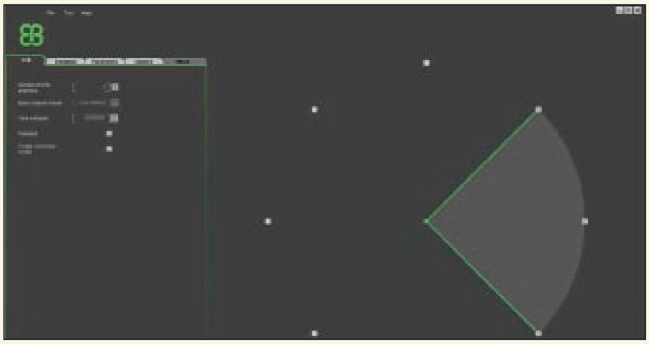

▲ *Fig. 3 The EB MIMO OTA application user interface.*

chamber equipped with OTA antennas (as shown in ***Figure 2***) and a device under test (DUT) with multiple antennas.

The transmitter is connected to the radio channel emulator, which maps the geometry-based channel models to the OTA antennas so that the propagation environment inside the anechoic chamber is realistic. It is possible to create different scenarios such as indoor, urban, micro-cell, urban macro-cell, suburban and rural areas. This way, for instance, the throughput can be verified under various propagation conditions.

A REALISTIC APPROACH

The crucial challenge is to generate realistic angular and polarization behavior within the anechoic chamber to test the antenna performance of the DUT. This geometry-based information, like in 3GPP Spatial Channel Models (SCM), creates the appropriate environment at the DUT antennas. A propagation channel is described by cluster power, delays, nominal arrival and departure angles, and angle spreads of clusters on both arrival and departure ends.

In addition, information about the transmitter antenna arrays, including both array geometry and antenna field patterns, can be used. Also, either the terminal velocity vector or the Doppler frequency components for each cluster(s) are needed and Over-the-Air testing is the only method to analyze the antenna performance. The EB MIMO OTA application user interface is shown in ***Figure 3***.

RADIO CHANNEL PHENOMENA

The most important radio channel phenomena in the geometry-based radio channel model include:

▲ *Fig. 2 The MIMO OTA anechoic chamber.*

- Delay spread: Without realistic modeling of delay spread, the mobile terminal might not be adequately tested. A large delay spread makes it possible to gain from frequency diversity, but too large a delay spread results in inter-symbol-interference.
- Doppler spread: A high Doppler spread causes problems in multi-carrier systems because orthogonal sub-carriers overlap at least partly, which creates inter-carrier interference (ICI). A small Doppler spread is problematic especially in the case of flat fading, since it leads to large average fade duration and lost data packets.
- Angle spread: Angular dispersion reduces correlation between antennas. Low Rx correlation enables a capacity increase with spatial multiplexing and antenna diversity schemes. However, the correlation depends not only on angle spread, but also on antenna characteristics. Therefore, these two items have to be jointly tested.
- Polarization: The cross-polarization ratio (XPR) affects the performance of polarization diversity. Again, the real impact of XPR on DUT performance depends on the radio channel conditions and antenna characteristics.

The EB Propsim F8 MIMO OTA emulator is designed to meet the conformance and beyond-conformance testing requirements of WCDMA, HSPA, 3GPP LTE, WiMAX and IMT-Advanced.

CONCLUSION

The main benefit of MIMO OTA testing is the evaluation capability of the true MIMO performance of the terminal. The commercial benefits of cable-free MIMO OTA testing for mobile terminal manufacturers, wireless operators, and antenna manufacturers can be measured in terms of shorter development and verification time, shorter time-to-market, increased final product quality and savings in quality-related costs.

Operators can increase their end user experience by benchmarking the performance of different terminals in order to choose the most suitable vendor, and terminal manufacturers can optimize their design in a realistic and repeatable test environment. The development times can be shortened due to more realistic test environments, reducing the number of required field tests. From the point of view of certified test houses, MIMO OTA testing will be a totally new business area offering impressive performance measurements.

EB (Elektrobit),
Oulu, Finland,
Tel: +358 40 344 3853,
www.elektrobit.com.

RS No. 303

Defense News

Dan Massé, Associate Technical Editor

ITT Announces Strategic Realignment of Defense Segment

ITT Corp. announced a strategic realignment of its defense segment, a move designed to better align the company with the emerging needs of its expanding global customer base, which is increasingly integrated and network-centric. The realignment will enable better integration of its product portfolio, encouraging a more coordinated market approach and reduced operational redundancies.

"We are positioning ITT to support our customers' emerging technology needs, while also greatly enhancing our ability to stake out new markets," said Steve Loranger, ITT's Chairman, President and Chief Executive Officer. "We believe this move will also allow ITT to achieve greater operating efficiencies and optimize our cost structure, which will help drive successful business strategies for continued top-line growth."

The company's defense segment will be renamed ITT Defense and Information Solutions. Its current organizational structure, comprising seven separate business units, will be consolidated into three larger ones.

- The Electronic Systems and Communications Systems divisions, as well as a portion of the Intelligence & Information Warfare division, will be merged to form a more versatile Electronic Systems division, based in Clifton, NJ. This division will deliver advanced protection measures that work together to help ITT's customers defend their networks and disable enemy networks. It will shift its focus from producing separate, point-of-use products to secure, networked communications systems and powerful sensing, surveillance and reconnaissance technologies that address the entire spectrum of electronic warfare.

> *The company's defense segment will be renamed ITT Defense and Information Solutions.*

- The Space Systems and Night Vision divisions will merge to form Geospatial Systems, based in Rochester, NY. The new center will focus on providing networked sensors, such as next generation imaging, including space and air sensors, image/infrared/digital sensors and air/ground/space systems, which transition the company's capabilities from disparate image acquisition to image processing and distribution across the network.
- The Advanced Engineering & Sciences and Systems divisions will be combined with a portion of the Intelligence & Information Warfare division to form the Information Systems division, based in Herndon, VA. This division will focus on networked decision support solutions through the combination of large system operations and maintenance capabilities with the sophisticated techniques of information integration and protection, such as next-generation air traffic management solutions, national intelligence networks and cyber security. This combination will expand the capabilities that have made ITT a leading systems developer for high-priority needs.

The strategic realignment of ITT's defense segment does not impact the company's previously announced forecast for full-year 2010 earnings per share in the range of $3.85 to $4.05 per share.

Lockheed Martin System Aims Laser Against Ballistic Missile Target

Lockheed Martin announced that the Beam Control/Fire Control system for the US Missile Defense Agency's Airborne Laser Test Bed (ALTB) successfully aimed the High Energy Laser beam in an experiment February 11, in which a boosting ballistic missile target was destroyed. In the lethal demonstration, the directed energy system aboard the modified Boeing 747-400F aircraft engaged and destroyed the threat-representative ballistic missile target shortly after it was launched from a sea-based platform in the Pacific Ocean. The Lockheed Martin-developed Beam Control/Fire Control system focused and directed the beam generated by the Northrop Grumman-developed megawatt-class High Energy Laser, and the Battle Management System developed by Boeing, Airborne Laser Test Bed prime contractor, managed the engagement.

"Shooting down a threat-representative ballistic missile target is the latest in a remarkable series of firsts that the government and industry team has achieved in demonstrating this leading-edge technology," said Doug Graham, Advanced Programs Vice President, Lockheed Martin Space Systems Co. "This successful experiment validates the effectiveness of this revolutionary technology and makes it the most mature directed energy system in the world, opening the door to further new possibilities for the application of this technology."

> *"This successful experiment validates the effectiveness of this revolutionary technology..."*

The Beam Control/Fire Control System tracks the target, determines range to the target, compensates for atmospheric turbulence and focuses and directs the High Energy Laser beam. Lower-energy lasers—the Track Illuminator Laser and the Beacon Illuminator Laser—determine where to point and focus the High Energy Laser. The High Energy Laser beam passes through an optical path before exiting through the conformal window on the nose of the aircraft on its way to the target.

The Missile Defense Agency manages the Airborne Laser Test Bed (formerly known as the Airborne La-

Go to www.mwjournal.com for more defense news items

ser (ABL)), which is executed by the US Air Force from Kirtland Air Force Base, Albuquerque, NM. The Boeing Co. provides the modified aircraft and the Battle Management System and is the overall systems integrator. Boeing's Airborne Laser Test Bed industry partners are Northrop Grumman, which supplies the High Energy Laser and the Beacon Illuminator Laser, and Lockheed Martin Space Systems Co., Sunnyvale, CA, which provides the Beam Control/Fire Control System.

Northrop Grumman Delivers First Production STARLite Radars to US Army

Northrop Grumman Corp. recently delivered the first two production AN/ZPY-1 STARLite radars for the US Army's Extended Range/Multi-Purpose Unmanned Aerial System. Northrop Grumman's STARLite is a small, lightweight radar used for supporting tactical operations. By providing precise battlefield intelligence in all types of weather and in battlefield obscurants, day and night, STARLite significantly improves battlefield situational awareness and optimizes force maneuver and engagement for mission success. Northrop Grumman is working under a 78.5 M dollar contract with the Army's Robotics and Unmanned Sensors Product Office at Aberdeen Proving Grounds, to provide a total of 33 STARLite radar systems between now and April 2011. The radar deliveries followed a compressed 18-month post-contract award schedule that included the successful completion of a rigorous battery of qualification tests of the radar as well as independent performance verification tests conducted by the Army's Test and Evaluation Center at the Yuma Proving Grounds, AZ.

Northrop Grumman is working under a 78.5 M dollar contract

Each STARLite radar features both SAR and GMTI capabilities and comes equipped with a complete software package for interfacing with the US Army One Common Ground Station, enabling easy operator control of the SAR maps and ground moving target detection indication on standard Army maps. The AN/ZPY-1 leverages Northrop Grumman's experience in creating the proven Tactical Endurance Synthetic Aperture Radar and the Tactical Unmanned Aerial Vehicle Radar.

Richard Mumford, International Editor

A New Start for Plessey Semiconductors

A famous name has been resurrected following the bold decision taken by the management teams from Plus Semi in Swindon, UK, and the former X-FAB facility in Roborough, Plymouth, UK, to re-launch Plessey Semiconductors Ltd. The company has been created from the acquisition of the share capital of X-FAB UK Ltd. together with existing key engineering competence within a design and technology centre located in Swindon.

The semiconductor manufacturing facility in Roborough currently produces eight-inch wafers for external customers in a foundry business modelled on 0.35 micron CMOS process technologies. Plessey Semiconductors is transferring its bipolar process technologies on both silicon and silicon-on-insulator substrates to the facility, with the transfer scheduled for completion in 2010.

Plessey Semiconductors' facility in Plymouth.

Both the CMOS and the bipolar process technologies will be used to support a set of existing foundry customers. However, Plessey Semiconductors aims to follow in its namesake's footsteps by developing and supporting a range of high performance analogue and mixed-signal semiconductor products.

"The historical significance of what we are doing is not lost on the management and employees of our new business," said Michael LeGoff, Managing Director of Plessey Semiconductors. "A large proportion of our employees started their careers in Plessey working in the various sites around the UK. We see this announcement as a return to our roots. This is a business model that addresses a market that we know very well—designing and manufacturing a set of high technology semiconductor products that competes with any semiconductor company in the world."

Dr. Paul James, the company's commercial director, added, "We will, of course, continue to support our foundry customers, but Plessey Semiconductors will be a standard products company. Moving into products we will be leveraging our extensive in-house design experience together with our expertise in technology development and optimisation to create innovative products."

Planned new product launches for 2010 include a range of current feedback and voltage feedback high slew rate operational amplifiers and high speed prescalers and dividers operating up to 13 GHz.

Irish Government Backs Bell Labs' Research Expansion

The expansion will generate a greater number of opportunities for Irish academia and industry...

Alcatel-Lucent will expand Bell Labs, the company's research arm, in Ireland, with the backing of the Irish Government, which is offering support through the Industrial Development Agency (IDA) Ireland. The expansion aims to create more than 70 new high-calibre technology positions over the next five years.

Since its establishment in 2005, Bell Labs in Ireland has collaborated closely with both academic and business communities through an Open Innovation programme in strategic areas such as telecommunications, supply chain and the environment. The expansion will generate a greater number of opportunities for Irish academia and industry to benefit from Bell Labs Ireland's unique facilities and technology insight and from exposure to the company's expanding global network.

The extension of this relationship and the increase in the number of technology experts will also enable Bell Labs in Ireland to support Bell Labs' contribution to the recently announced Green Touch Initiative—an open consortium of academic and commercial research institutions from around the world who are creating the technologies needed to reinvent communications networks and make them 1000 times more energy efficient than they are today.

Through its open innovation model, Bell Labs Ireland is a key contributor to successful projects such as the Science Foundation Ireland-supported CSET the Centre for Telecommunications Value-Chain Research (CTVR), a collaborative research centre involving seven Irish universities that has yielded a pool of highly skilled researchers and scientists who are poised to make significant contributions to the Irish knowledge economy.

Roke Service Aids Compliance and Performance Optimisation

In partnership with certification specialist Sulis Consultants, Roke Manor Research Ltd. has launched its *Regulatory Compliance and Performance Optimisation Service* to minimise re-design costs and accelerate product development time. The aim is to deliver accelerated product development by minimising the requirement for re-designs and multiple test cycles.

The service is uniquely scalable, allowing developers of multi-mode mobile products to choose from a range of design consultancy services and pre-compliance testing, through to a complete certification package. The scalability

Go to www.mwjournal.com for more international news items

Mobile handset testing.

element makes the service suitable for both integrated development assistance and inclusion within collaborative partnerships or design ecosystems.

The test facilities available at Roke include a shielded EMC anechoic chamber, with a working distance of 3 m, and CTIA compliant anechoic chamber, both working up to 18 GHz, and suitable for tests including EMC and RF. SAR and ESD facilities are also available.

Access to the company's multi-disciplined on-site engineering team provides an immediate resource for analysis and solutions before the design is complete and the final expensive phase of certification testing starts. For products that have failed compliance testing, a 'Find and Fix' failure analysis service can identify points of failure and resolve them as fast and economically as possible.

Rohde & Schwarz China Open-Lab Starts Operation

Operation has begun at Rohde & Schwarz (R&S) China's first open-lab, in Beijing. The lab will be free-of-charge to existing or potential customers and partners who can apply to the company. After confirmation they can use the R&S open-lab to do experiments or validate their test solutions.

The purpose of the open-lab is to strengthen support to customers...

The purpose of the open-lab is to strengthen support to customers and improve their satisfaction; to help new customers or identify new applications; to promote R&S solutions and equipment; and to create application notes or solution proposals.

The open-lab will provide various test and measurement instruments and accessories, and strong technical support or consultancy. It can help applicants to make full use of R&S test equipment, and create or optimize their test method or solution. Currently, the open-lab covers wireless communication; aerospace and defence; general purpose systems; audio and video and EMC.

Dan Massé, Associate Technical Editor

Mobile Handset Demand Fuels 336.5 Million Shipments

"The year 2009 may have started with a whimper but by 4Q-2009 the global mobile handset market ended with a pretty reasonable bang," says Jake Saunders, Vice President for Forecasting at ABI Research. "We estimate 336.5 million handsets were shipped in 4Q-2009, up 15.1 percent QoQ." Competition continued to squeeze handset ASPs. In 4Q-2009, shipment-based ASPs were down 2 percent to US$117.55.

"Obama's stimulus package certainly helped save the mobile handset industry," Saunders notes. "Renewed consumer confidence in the second half of 2009 meant that shipments for the whole year only shrank 4.5 percent to 1.153 billion. Dire scenarios were mooted in early 2009. There is cautious optimism about 2010 despite the fragile nature of the global recovery. ABI Research forecasts shipments to expand to 1.2 billion handsets in 2010."

Despite Nokia's weakened position in the smartphone segment, it still managed to maintain 37.7 percent of the overall handset market. Samsung, the market-share juggernaut, seems unstoppable. Between June 2008 and December 2009, Samsung increased its market share from 15.2 to 20.5 percent. Samsung has benefited from a strong line-up of feature phones as well as a strong reputation for innovative smartphones. Korea's level of influence over the handset market is further underscored by LG, the third-largest handset vendor (10.1 percent). LG has been counting on its S-Class smartphone series to help it secure a bridgehead in the market.

HTC's market share did not fare well early last year, but its circumstances improved slightly in 4Q, to 1.0 percent share. Notably, HTC announced a revamped handset portfolio strategy, not just targeting high-end smartphones but also launching smartphones that appeal to purchasers with smaller wallets. These low cost "HTC Smart" devices will rely on BREW.

MOBILE HANDSET MARKET SHARE, WORLD MARKETS, 4Q 2009

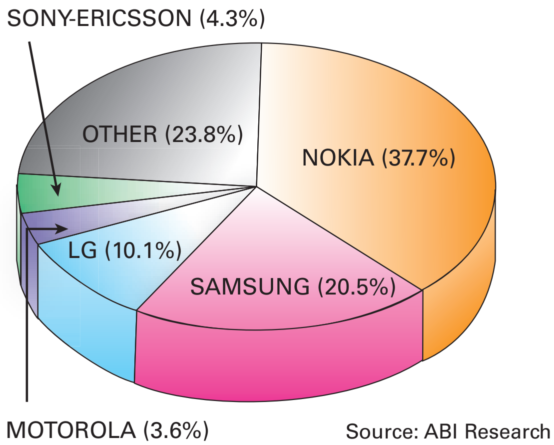

Shipments of Wi-Fi ICs Grew Close to 28 Percent Last Year

In 2009, worldwide shipments of Wi-Fi ICs increased by approximately 28 percent compared to 2008, according to data from ABI Research. Total revenue achieved an estimated compound annual growth rate (CAGR) of 18 percent between 2009 and 2014.

"Despite the uncertain macroeconomic situation, total market demand for Wi-Fi ICs is expected to keep growing," says industry analyst Celia Bo. "The demand for Wi-Fi ICs in mobile devices and consumer electronic devices are the two key engines for Wi-Fi IC's market growth."

In recent years almost all laptops, netbooks, MIDs and smartbooks have shipped with Wi-Fi embedded, a trend that will continue for some time to come. Wi-Fi IC placement in mobile handsets grew by more than 50 percent in 2009 and Wi-Fi-enabled handsets will account for 40 percent of the total of handsets shipped in 2014. Beyond the already established segments, portable media players with Wi-Fi have also seen strong growth, which will continue through 2014.

Wi-Fi IC placement in mobile handsets grew by more than 50 percent in 2009...

More and more consumer electronic devices, such as digital still cameras, digital camcorders, TVs, DVD players, set-top boxes (STB) are adopting Wi-Fi. The total shipments of Wi-Fi-enabled consumer electronic devices increased 33 percent in 2009 compared to 2008; the products with fastest-growing attach rates are digital camcorders, TVs and set-top boxes.

US Broadband Services: Bandwidth Keeps Increasing

Since 2007, In-Stat has conducted an annual broadband "speed test" of broadband Internet subscribers in the United States. The latest survey, conducted in December 2009, shows that both upstream and downstream speeds continue to increase. The 535 survey respondents, who used an online bandwidth measurement tool to measure their bandwidth, reported that their downstream speed had increased by an annual rate of 28 percent. Upstream speed also increased, but by a slightly lower 16 percent.

As in 2008, the access technology with the fastest speeds was fiber to the home, followed by cable modem service. Fixed wireless service leapfrogged DSL service to finish in the third-place position. This seems to have resulted from the increase in the number of fixed wireless broadband subscribers who are using Clearwire's WiMAX-based service. Of all the access technologies reported by the survey

Go to www.mwjournal.com for more commercial market news items

respondents, the access technology with the slowest speed was once again satellite broadband service.

The full results of the broadband bandwidth survey will be published soon in In-Stat's Multimedia Broadband Services research service. For more information about the market for broadband services, check out the recently published "Global Broadband Subs Approach 600 Million."

RFaxis Secures Multiple ZigBee Design Wins from GRT Technology

RFaxis, a fabless semiconductor company focused on innovative, next-generation RF solutions for the wireless and connectivity markets, announced that GRT Technology Co. Ltd. has selected RFaxis' RFX2401 RF Front-end Integrated Circuit (RFeIC) for integration into its family of ZigBee solutions.

Founded in 2005 with headquarters in Taipei, Taiwan, GRT Technology is a solution provider in the rapidly growing ZigBee market. By leveraging Linux-based software with its highly-integrated ZigBee modules, GRT provides plug and play ZigBee solutions for a great variety of global applications that require real-time data delivery and display from remote wireless sensor networks, including 'Smart Energy' (LED streetlight control, power saving devices, etc.); 'Smart Home' (HVAC control, security/alarm systems, RF4CE remote control devices); remote monitoring and care for children and senior citizens; and remote asset tracking and control for agriculture and livestock.

"GRT is a major ZigBee first-mover and has aggressively launched exciting products for the booming ZigBee space," noted Mike Neshat, President and CEO of RFaxis. "We are looking forward to a long and prosperous partnership with GRT, and are excited that our single-chip, single-die RFX2401 RFeIC for ZigBee can enable their mission to deliver global solutions for a better and greener quality of life."

"GRT... has aggressively launched exciting products for the booming ZigBee space."

Di Chiu, GRT General Manager, commented, "To lead the way in the exploding ZigBee market, it is critical for GRT to enhance the reliability and extend the range of our ZigBee solutions. We needed an energy-efficient and cost-effective RF front-end that delivers quality performance and is very easy to implement. After assessing a variety of RF front-end solutions, the RFaxis RFX2401 was the clear winner in terms of rapid integration and superior performance power efficiency over conventional front-end solutions."

Jennifer DiMarco, Staff Editor

INDUSTRY NEWS

EADS North America Test and Services, a division of EADS North America Inc., announced it has acquired **Trig-Tek Inc.**, a Garden Grove, CA-based company, providing precision, dynamic test and measurement instruments for the US aerospace and defense markets. The acquisition of Trig-Tek is consistent with EADS' strategy to provide its customers with the most advanced automatic test solutions. It also supports EADS North America's goal to grow its business in the US and to enhance the company's global test and services offering.

The Microwave Communications Division of **Harris Corp.** and **Stratex Networks Inc.**, **Harris Stratex Networks Inc.**, announced that it has changed its name to **Aviat Networks Inc.** Under its new name the company has pledged its commitment to providing advanced IP wireless network solutions, to continue to make progress in radio access networks and work towards the evolution of wireless technology. The new brand represents a culmination of the company's transformation from that of a specialized microwave backhaul equipment supplier into a world-class provider of advanced IP wireless network solutions, with a comprehensive portfolio of migration solutions and lifecycle services. Today, Aviat Networks is ideally positioned to help operators successfully evolve their existing networks toward an all-IP broadband future, expand into untapped rural and remote markets, and capitalize on the explosive growth of mobile data traffic around the globe.

EMS Technologies Inc. announced the formation of a new business unit, **EMS Aviation**. EMS Aviation will include the company's EMS SATCOM division, a leader in Inmarsat SwiftBroadband systems, and the recently acquired EMS Formation and EMS Sky Connect, providers of air-to-ground connectivity and Iridium-based tracking and messaging, respectively.

Planar Monolithics Industries and **Amplitech** announced the collaboration of its combined product offering, engineering skills and marketing efforts. The companies will independently run the administrative and production facilities, but will share a combined manufacturer's representative sales force, marketing effort and will direct future engineering requirements to the facility best suited to achieve a particular customer's requirement. This collaborative effort takes advantage of the unique skills and offerings of each company independently, culminating in demonstrable best-of-breed microwave system integration and designs for the benefit of the end users and customers.

Mentor Graphics Corp. announced delivery of full-wave 3D electromagnetic (EM) analysis functionality addressing the needs of the industry's most advanced designers of high-performance electronic products. These EM analysis enhancements address the advanced simulation needs of engineers designing PCBs and packages that utilize high-speed interconnect technologies such as SERDES, which operate at multi-gigabit-per-second speeds. The new functionality is a result of Mentor Graphics' recent acquisition of certain assets of **Zeland Software Inc.**, which for 17 years has been a recognized leader in electromagnetic simulation. This new functionality is integrated with the Mentor Graphics HyperLynx® product suites and will analyze, in full electromagnetic detail, 3D structures such as vias, solder bumps, wirebonds and edge connectors.

ITT Corp. announced a strategic realignment of its defense segment, a move designed to better align the company with the emerging needs of its expanding global customer base, which is increasingly integrated and network-centric. The realignment will enable better integration of its product portfolio, encouraging a more coordinated market approach and reduced operational redundancies.

Skyworks Solutions Inc., an innovator of high reliability analog and mixed signal semiconductors enabling a broad range of end markets, announced that Google Inc.'s Nexus One mobile phone is leveraging several of its highly integrated power amplifier modules. These 3G solutions were incorporated in the Google platform as part of HTC Corp.'s reference design.

Remcom announced a new partnership with a market-leading computer supplier to provide custom XFdtd® systems and brand name hardware solutions to customers. Link Computer Corp. has created a hardware solution designed to fully exploit XFdtd's graphics processing unit (GPU) capability. Outfitted with the latest in GPU technology, this system further extends Remcom's efforts to enable customers to deliver products faster and more cost effectively. To offer customers more options, Remcom may add solutions from other vendors as the program grows.

AWR, an innovation leader in high-frequency electronic design automation (EDA), and **NXP Semiconductor** have announced that a small-signal RF design kit is available for NXP's SiGe:C silicon germanium bipolar junction complementary metal oxide semiconductor (BiCMOS) process. The design kit installs easily within AWR's Microwave Office software and functions as an integrated part of the simulation environment.

Accel-RF Corp., a leader in turn-key RF reliability testing systems for compound semiconductor devices, announced the successful shipment and installation of five advanced high power reliability test systems to customers in Europe, in Q4 of 2009. Shipped to both government research and commercial entities, these systems will be instrumental in the development of Gallium Nitride devices in Europe.

For up-to-date news briefs, visit www.mwjournal.com

SYNERGY®
MICROWAVE CORPORATION

MINIATURE FOOTPRINT SYNTHESIZERS

The 1st ever high performance synthesizer on a 0.6" x 0.6" x 0.175" package.

Introducing our **MFSH series** of miniature footprint surface mount synthesizers with on-board microcontroller that allows for self-programmable fixed frequency or wideband signal generation from a **0.6" x 0.6" x 0.175"** package. Several models are available starting with frequencies from **1350 to 8000 MHz** and step size starting from 500 kHz.

Call us for further technical details.

Model #	Frequency (MHz)	Step Size (kHz)	Typical Phase Noise (dBc/Hz)	
			@10 kHz	@100 kHz
MFSH SERIES				
MFSH495550-100	4950 - 5500	1000	-82	-103
MFSH490517-100	4900 - 5170	1000	-83	-104
MFSH480540-100	4800 - 5400	1000	-83	-103
MFSH432493-100	4320 - 4930	1000	-83	-102
MFSH400800-100	4000 - 8000	1000	-75	-93
MFSH615712-100	6150 - 7120	1000	-78	-98
MFSH170340-50	1700 - 3400	500	-85	-108

Features

- Exceptionally Low Phase Noise
- Dimensions: 0.6" x 0.6" x 0.175"
- Standard Programming Interface
- Ultra-wide & Optimized Tuning
- High Immunity To Phase Hits
- Patent Pending Rel-Pro Technology

RoHS COMPLIANT

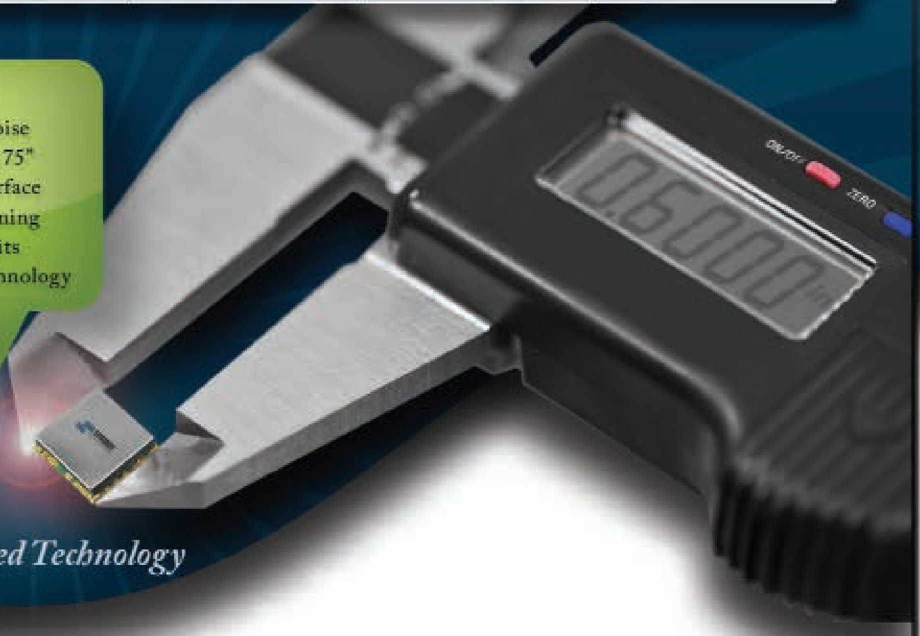

Patented Technology

For additional information, contact Synergy's sales and application team.
Phone: (973) 881-8800 Fax: (973) 881-8361 E-mail: sales@synergymwave.com
201 McLean Boulevard, Paterson, NJ 07504

Visit Our Website At WWW.SYNERGYMWAVE.COM

State of the Art Inc. (SOTA) celebrated its 40th anniversary with an open house December 10, 2009, at the company's headquarters and manufacturing facility in central Pennsylvania. State of the Art Inc. was founded in 1969 as a consulting business specializing in thick film technology seminars as well as other consulting services. Manufacturing began in 1972 and quickly displaced the consulting business. In 1980, SOTA developed the now industry-standard nickel barrier to virtually eliminate solder leaching and inter-metallic formation. In 1987, SOTA became the first MIL-PRF-55342 QPL qualified S-level manufacturer.

SMS Technologies Inc. announced that is has won the 2009 Supplier Excellence Alliance (SEA) Aerospace & Defense Industry Supply Chain Award in the Supply Chain Innovation award category. SMS Technologies is an electronics contract manufacturer providing services from prototyping through volume manufacturing for customers in many industries, including aerospace and defense.

Nitronex, a leader in the design and manufacture of gallium nitride (GaN) based RF solutions for high performance applications in the defense, communications, and industrial & scientific markets, announced that they have shipped over 200,000 custom devices to a major US-based cable television (CATV) amplifier supplier.

OHEL celebrated its 40th year anniversary with an annual dinner on February 21, 2010 at the New York Hilton. The gala event celebrated its agency's milestone and honored Gloria and Harvey Kaylie. Kaylie is the President and CEO of **Mini-Circuits**. Gloria and Harvey are philanthropists who have for many years been generous and devoted members of the OHEL family. They are benefactors of the Marvin Kaylie Center at OHEL, named in honor of Harvey's brother, and of the soon-to-be-dedicated OHEL CAMP. OHEL, founded in 1969, is a pioneering social services agency that delivers a breadth of innovative programs and services for individuals and families at risk, and individuals with developmental or psychiatric disabilities, in both residential and out-patient settings.

CONTRACTS

dB Control, an established manufacturer known for its reliable, high-power microwave amplifiers, radar transmitters and power supplies, has been awarded a five-year contract worth approximately $13.2 M by the US Navy to produce up to 300 amplifiers to be integrated into Electronic Counter Measure (ECM) systems. The contract includes 500 W traveling wave tube (TWT) amplifiers that will be integrated into the entire life cycle of the US Navy's ECM systems.

Cobham has been awarded the Band 5/6 Travelling-wave Tube (TWT) Replacement Module Assembly (TRMA) development contract by the US Navy that could, if all options are exercised, be worth up to US$11.5 M. Cobham was competitively selected for this contract by the US Navy's Naval Surface Warfare Centre in Crane, IN. The primary

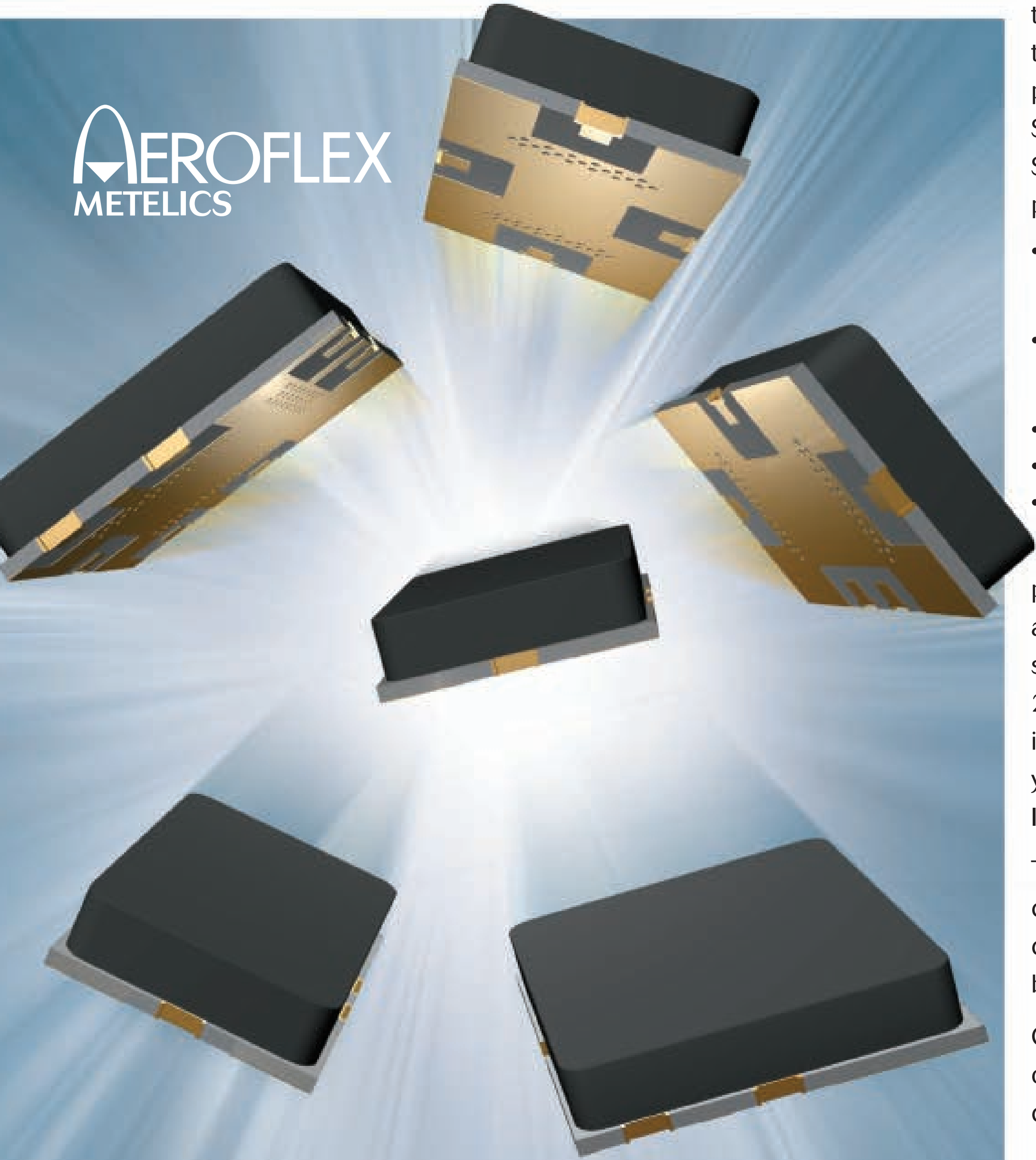

objective is to replace the existing TWT-based RF chain in the ALQ-99 Band 5/6 transmitter with a solid-state amplifier module and DC-DC converter.

SRC, formerly Syracuse Research Corp., announced that it has secured $8.1 M in funding for its Foliage Penetration Reconnaissance, Surveillance, Tracking and Engagement Radar, also known as FORESTER. The revolutionary airborne radar system penetrates through foliage to track people and vehicles on the ground. The funding for the FORESTER program is a combination of two awards to the corporation. The first award of $5.3 M was awarded to SRC as a result of a solicitation by the US Army for an additional FORESTER system to be delivered by June 2011. An additional $2.8 M was secured through the 2009 Consolidated Security, Disaster Assistance and Continuing Appropriations Act for FORESTER technology improvements.

Giga-tronics Inc. announced that it has received three orders valued at $5.1 M for microwave components from a major aircraft manufacturer. The award for high performance specialty filters based upon the company's fast switching YIG technology will be fulfilled by Giga-tronics' Microsource component subsidiary located in Santa Rosa, CA.

Spectrum Control Inc. announced that its Spectrum Microwave Business Unit has been selected by **Thales Communications Inc.**, Clarksburg, MD, as the supplier for the RF power amplifier for the Extended Band Manpack, an accessory to the AN/PRC-148 JTRS Enhanced Multiband Inter/Intra Team Radio. Production of the RF power amplifier will be performed at Spectrum Microwave's Palm Bay, FL operation and is currently expected to commence in early 2010.

Integral Systems Inc. announced that its subsidiary, **RT Logic**, has been awarded a contract by **Iridium Communications Inc.**, to supply two Telemetrix 400XR modulator/receiver (T400XR) modems. The T400XRs will serve as Iridium's next-generation satellite communication modems, handling all Iridium user voice and data between satellite phones and the terrestrial network for their Feeder Link Earth Terminal (FLT) modem upgrade. Based in Bethesda, MD, Iridium Communications operates the Iridium satellite constellation, a system of 66 active satellites used for global voice and data communication.

FINANCIAL NEWS

RF Micro Devices Inc. (RFMD) reported financial results for its fiscal 2010 third quarter ended January 2, 2010. RFMD's December 2009 quarterly revenue increased approximately 24 percent year-over-year to $250.3 M. GAAP gross margin for the quarter increased sequentially from 35.9 to 36.4 percent, and non-GAAP gross margin increased sequentially from 38.1 to 38.4 percent. GAAP operating income was $33.6 M, and non-GAAP operating

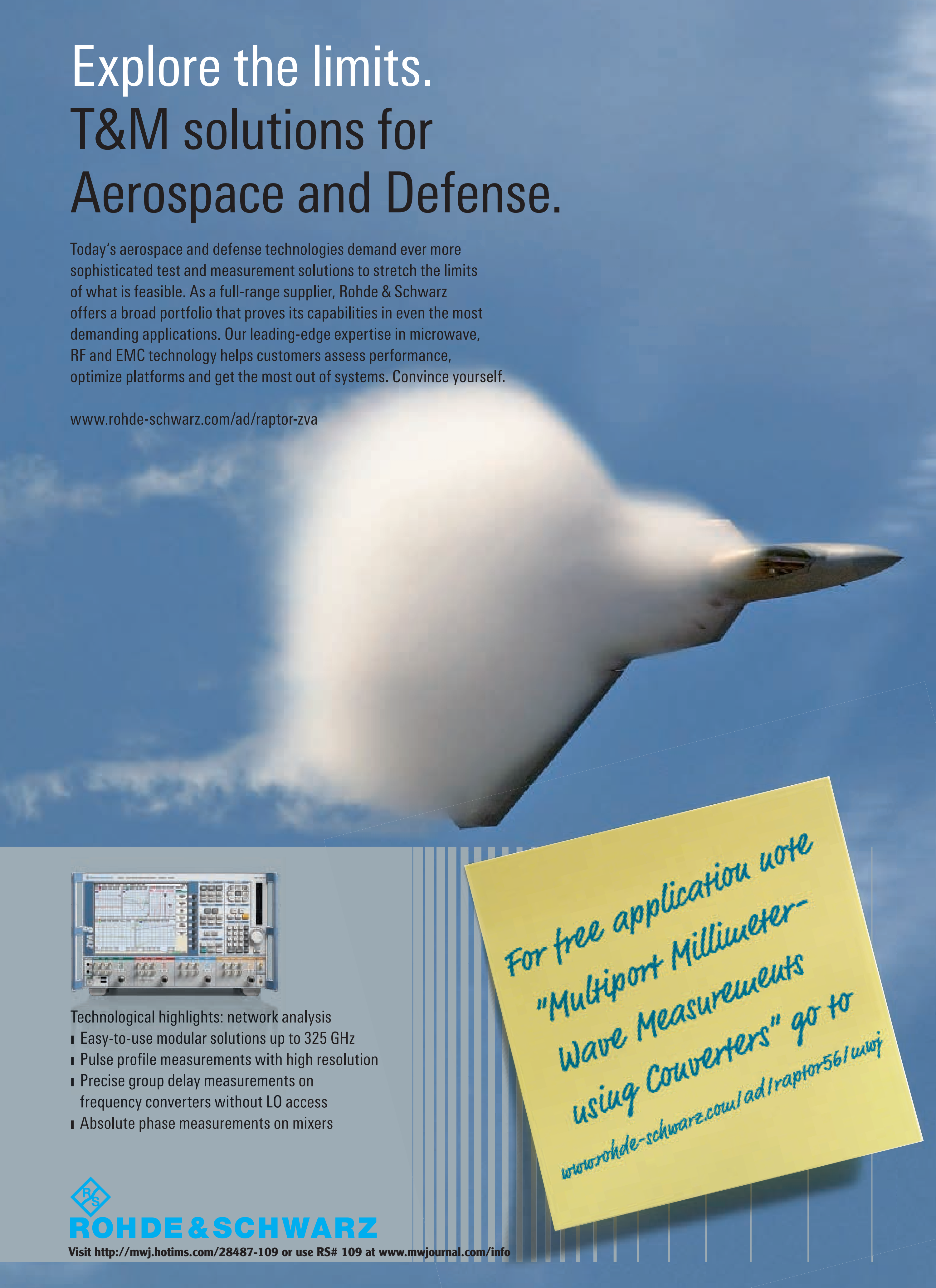
Explore the limits.
T&M solutions for
Aerospace and Defense.
Today's aerospace and defense technologies demand ever more sophisticated test and measurement solutions to stretch the limits of what is feasible. As a full-range supplier, Rohde & Schwarz offers a broad portfolio that proves its capabilities in even the most demanding applications. Our leading-edge expertise in microwave, RF and EMC technology helps customers assess performance, optimize platforms and get the most out of systems. Convince yourself.
www.rohde-schwarz.com/ad/raptor-zva
For free application note "Multiport Millimeter-Wave Measurements using Converters" go to www.rohde-schwarz.com/ad/raptor56/mwj
Technological highlights: network analysis
Easy-to-use modular solutions up to 325 GHz
Pulse profile measurements with high resolution
Precise group delay measurements on frequency converters without LO access
Absolute phase measurements on mixers
ROHDE&SCHWARZ
Visit http://mwj.hotims.com/28487-109 or use RS# 109 at www.mwjournal.com/info

income was a quarterly record $44.6 M. GAAP net income was $24.9 M, or $0.09 per diluted share, and non-GAAP net income was a quarterly record $38.8 M, or $0.14 per diluted share.

PERSONNEL


▲ John Devaney

Cobham plc announced the appointment of **John Devaney** as an independent Non-executive Director and Chairman designate effective immediately. Devaney is currently executive chairman of UK company National Express plc, a position held since April 2009 and Non-executive Chairman of the UK National Air Traffic Services Ltd., a position held since 2005. Devaney will be appointed Non-executive Chairman of Cobham in succession to David Turner at the conclusion of the Annual General Meeting to be held on May 6, 2010, by which time he will have relinquished his executive responsibilities at National Express plc.

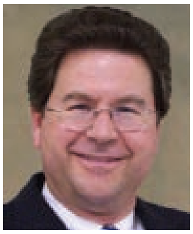
▲ James Rowland

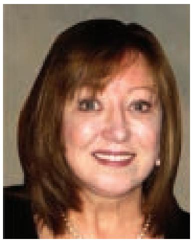
▲ Jan Kendall


▲ Jeff Fordham

MI Technologies announced several recent appointments to its team. MI has appointed **James Rowland** to the role of Vice President of the Customer Support Business Unit. In this role, Rowland will continue to provide the leadership he has shown over the last three years in serving the customer base after the delivery of the company's considerable systems installations and product deliveries. The company announced the appointment of **Jan Kendall** to the role of Vice President, Marketing. Kendall will provide leadership in all aspects of marketing for MI Technologies including product marketing, brand management, marcom and marketing operations. MI Technologies announced the appointment of **Jeff Fordham** to the role of Vice President, Near-Field Systems and Products Business Area. In this role, Fordham will provide increased leadership of the company's continued emphasis in its' expanding near field systems and products market. MI Technologies announced the addition of **Malcolm Warren** to the business development team as an International Sales Director. In this role, Warren will augment the organization's sales and support teams in place in certain international regions and provide leadership of the company's business development efforts in Europe and some select Asian regions.

Aeroflex/Metelics announced the appointment of **Tim Emery** as Vice President of Sales and Marketing for its operations in Sunnyvale, CA, Londonderry, NH, and Lawrence,

2 W & 5 W
DC to 18 GHz ATTENUATORS

from $29.95 ea. (1-49)

Rugged Stainless Steel Construction, High Repeatability, Miniature Size, Low Cost, and Off-The-Shelf Availability are some of the features that make Mini-Circuits "BW" family of precision fixed attenuators stand above the crowd! This extremely broad band DC to 18 GHz series is available in 5 watt Type-N and 2&5 watt SMA coaxial designs, each containing 15 models with nominal attenuation values from 1 to 40 dB. Built tough to handle 125 watts maximum peak power, these high performance attenuators exhibit excellent temperature stability, 1.15:1 VSWR typical, and cover a wealth of applications. So contact Mini-Circuits today, and capture this next generation of performance and value! *Mini-Circuits...Your partners for success since 1969*

***Now Available!* Adapters** (Prices: qty. 1-49)

Type-N to SMA
DC-18 GHz $22.95 ea.

SMA to SMA

QUICK CONNECT SMA
DC-18 GHz from $4.95 ea.

SMA to BNC
DC-2 GHz $3.95 ea.

Type-N to Type-N
DC-6 GHz $9.95 ea.

MODELS (Add Prefix BW-)

2 W SMA	5 W SMA	5 W Type-N	Attenuation (dB)	
$29.95	$44.95	$54.95	Nominal	Accuracy*
S1W2	S1W5	N1W5	1	±0.40
S2W2	S2W5	N2W5	2	±0.40
S3W2	S3W5	N3W5	3	±0.40
S4W2	S4W5	N4W5	4	±0.40
S5W2	S5W5	N5W5	5	±0.40
S6W2	S6W5	N6W5	6	±0.40
S7W2	S7W5	N7W5	7	-0.4, +0.9
S8W2	S8W5	N8W5	8	±0.60
S9W2	S9W5	N9W5	9	-0.4, +0.8
S10W2	S10W5	N10W5	10	±0.60
S12W2	S12W5	N12W5	12	±0.60
S15W2	S15W5	N15W5	15	±0.60

Pb RoHS COMPLIANT

To order Attenuators as RoHS, add + to base model No. *Example: BW-S1W2+*
Adapters available as RoHS, see web site.

Mini-Circuits®
ISO 9001 ISO 14001 AS9100 CERTIFIED
P.O. Box 350166, Brooklyn, New York 11235-0003 (718) 934-4500 Fax (718) 332-4661

YONI2™ Patent Pending ***The Design Engineers Search Engine*** *finds the model you need, Instantly* • For detailed performance specs & shopping online see minicircuits.com

IF/RF MICROWAVE COMPONENTS

331 rev N

MA. Prior to joining Aeroflex, Emery held the position of Vice President of Sales and Marketing for M/A-COM where he worked for 10 years. He has also held executive positions with SMaL Camera, LG Semicon and NEC Electronics.

John Zuk, a marketing and strategy executive with more than 20 years of experience in the high tech and semiconductor industry, has been appointed Vice President of Marketing and Strategy for Tanner EDA, a provider of analog, mixed-signal (A/MS) and MEMS circuit design software. Zuk will lead Tanner EDA's worldwide marketing initiatives as well as strategic foundry relationships. He was formerly the Portfolio & Strategy Executive for IBM's Deep Computing business.

Times Microwave Systems announced that **Bogdan "Bogey" Klobassa** has joined the company. Klobassa has an extensive background and depth of knowledge in grounding and surge protection with several patents to his name. He is a globally recognized authority and speaker in Power Quality, RF System Grounding and EMP protection. Under his leadership, Times will soon be launching its Times-Protect™ lightning and surge protection product line offering superior surge protection solutions for OEMs and system operators to complement the company's RF interconnect products including the industry leading LMR® flexible coaxial cable product line.

▲ Bogdan Klobassa

REP APPOINTMENTS

Vincotech, a supplier of GPS receiver and telematics hardware solutions, and **Atlantik Elektronik**, a full-service electronics distributor and market trend analyst for global technologies, signed a distribution contract solidifying their channel partnership in the European marketplace. With this agreement, Atlantik Elektronik, a successful long-term partner of CSR, and Vincotech being the European GPS module partner of SiRF, a CSR company, will market together the latest GPS modules and telematics solutions. The primary focus of this partnership is on promoting Vincotech's new SiRFstarIV-based technology and telematics product solutions, while at the same time continuing the design-in support of Vincotech's current SiRFstarIII portfolio.

Cree Inc., a market leader in LED lighting and silicon carbide (SiC) semiconductor components, announced a distribution agreement with **Arrow Electronics Inc.** for Cree SiC power products. The agreement gives Arrow's customers ready access to Cree's latest commercially-available SiC Junction Barrier Schottky (JBS) products. Among the Cree products available through Arrow will be the recently released Z-REC™ Series of 600 V Schottky diodes and the 1200 V Schottky diode line.

ADD REALISM TO YOUR TEST SIGNALS WITH RF CHANNEL SIMULATORS

All radio frequency (RF) links are subject to distortion due to the physics of the transmission media, as well as the physical environment in which the link is operating. While designers take these effects into account when developing communication systems, actual testing with these distortions realistically applied to the system under test can be problematic and costly, unless RF channel simulation is utilized.

Margin testing of a transmitter/receiver pair can occur throughout the design phase. Typically, this is done with signal generators substituting for the transmitter portion of the design and spectrum analyzers or vector signal analyzers acting as receivers. However, even with the most sophisticated equipment, this testing is typically performed in static conditions, possibly stressing a few worst, best cases, and nominal operating conditions. For many communication system designs, especially those where one or both of the ends of the communication path are in motion, maintaining realistic RF test conditions offers unique challenges. Static testing can miss communication issues related to the way the signals are impacted by the actual operating environment.

This article discusses how a new category of test tools, called channel simulators, are used in the laboratory and QA areas to create RF signals that match those that occur when communication systems are deployed on platforms in motion. Sometimes channel simulators will be referred to as link emulators, channel emulators or link simulators, depending on region and specific application. Channel simulators provide engineers with an effective and economical way of verifying and optimizing the operation and quality of communication devices, where one or more nodes are in motion.

Channel simulators do exactly what the name implies; they emulate the distortions on an RF signal when receivers and transmitters move with respect to one another. The reasoning behind utilizing a channel simulator in this case is that there are no simple alternatives. The engineering team could finish their design and place the communication system on an aircraft or satellite, thereby putting it into motion and creating realistic conditions. However, the risks of this approach can be disastrous and almost certainly costly. Consider the condition where the link is used for control of the moving platform. It is easy to see where realistic emulation in a controlled environment is a preferred approach, over a possible loss of the communication link and therefore control of the platform. A channel simulator can be utilized throughout the design phase to realistically impair signals, just as if they were in their intended operating environment, whether that environment relates to a drone flying overhead or a mission to the edge of the solar system.

Some may remember the Cassini-Huygens potentially mission-ending communications issues during its undertaking to gather data on Saturn's moon, Titan. The issues were related to the Doppler shift impacts on the communications link, which left uncorrected would have corrupted data received from Huygens as it descended to Titan's surface. The issue was uncov-

MARK LOMBARDI
RT Logic, Colorado Springs, CO

Introducing....
MKR Series

The new standard in high-performance ruggedized test cable assemblies

Only from Micro-Coax®

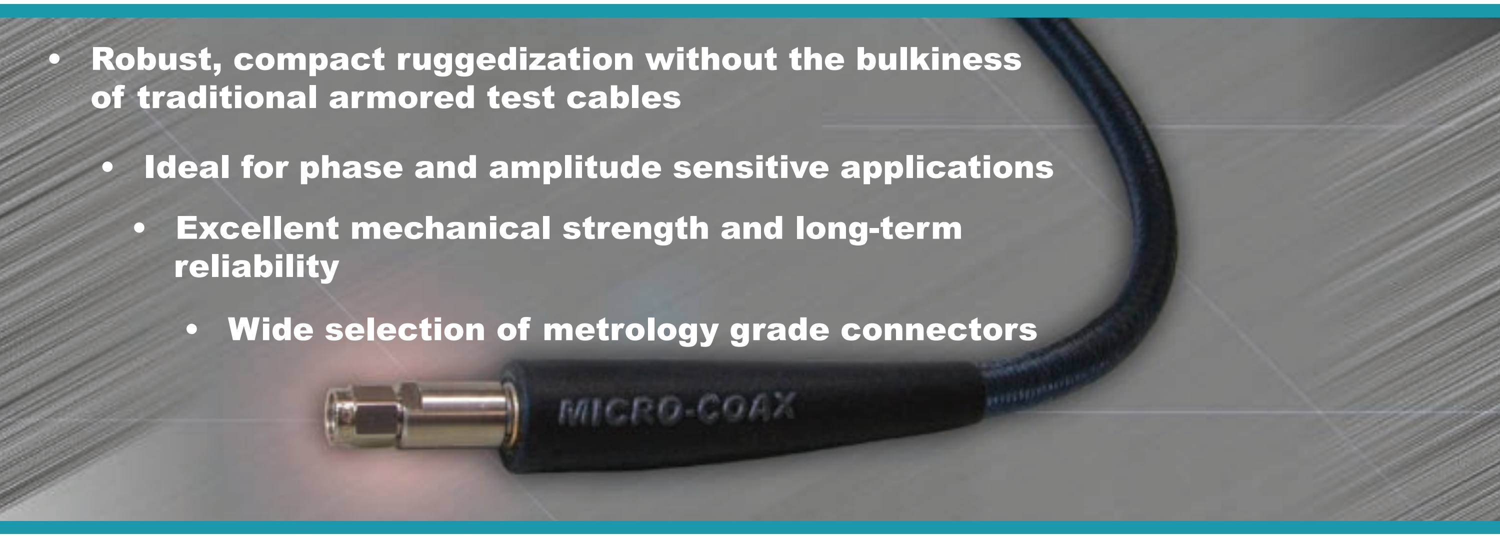

- **Robust, compact ruggedization without the bulkiness of traditional armored test cables**
- **Ideal for phase and amplitude sensitive applications**
- **Excellent mechanical strength and long-term reliability**
- **Wide selection of metrology grade connectors**

Specification	MKR246A	MKR300C
Outer Diameter (in)	0.246	0.300
Static Bend Radius (in)	1.250	1.250
Crush Resistance (lbs/in)	250	250
Frequency (GHz)	DC-40	DC-26.5
Insertion Loss (dB/ft)		
1 GHz	0.11	0.09
5 GHz	0.23	0.20
10 GHz	0.33	0.28
18 GHz	0.45	0.38
26.5 GHz	0.55	0.47
40 GHz	0.68	—

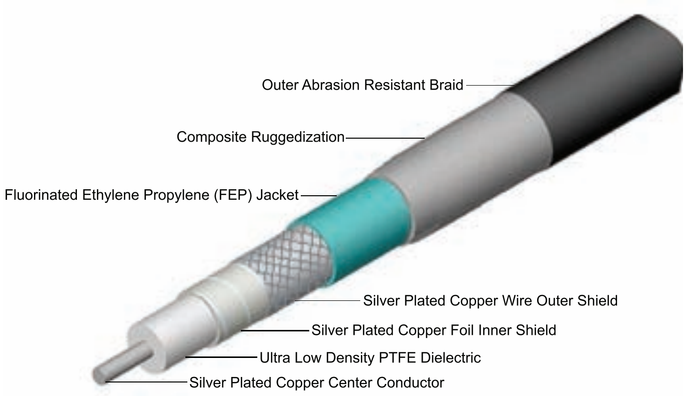

For quick delivery, configure and order online at www.micro-coax.com

MICRO-COAX®

Leading the way in transmission line solutions.

206 Jones Boulevard, Pottstown, PA 19464; P. 610-495-0110 F. 610-495-6656

www.micro-coax.com

ered only after the spacecraft had been launched, making a solution difficult to apply. In the end, the orbital plan of Cassini was altered in order to hold the Doppler shift in the communication channel from the Huygens craft within restricted parameters, thereby preserving most of the mission's goals.

These environmental effects have historically been difficult to simulate in a laboratory, especially in an electrically realistic and physics-compliant way. The channel simulator was created to address exactly this issue. When the channel simulator is placed into the communication link of the system under test, it "passes" (RF or cable connections at RF/IF) the signal from the transmitter on to the receiver, adding impairments that match link conditions that exist in the actual operational environment. This allows every part of the device under test including antennas, amplifiers, converters, transponders, modems, demodulators, and even data recovery and firmware to be tested under realistic RF signal conditions.

Programming of the environmental conditions can be accomplished in multiple ways, from simple point-by-point input of variables to sophisticated modeling of terrain, velocity, antenna locations, interference, weather and background noise to name a few. When this latter methodology is used, the resulting signals can be so realistic that operators would find them indistinguishable from the actual in-motion test. This level of sophistication and realism is achieved by coupling sophisticated motion, terrain, and link budget modeling software to a channel simulator allowing it to add environmental effects to the input signals, as determined by the simulation. The result is a realistic test signal appropriate for detailed parametric transmit- and receive-chain testing. Another aspect of this realistic test signal is that it can also be used for training operators of the equipment being tested.

Figure 1 is an example of an actual flight plan programmed into a modeling software. The simulation can include data such as the aircraft flight characteristics and path, along with the terrestrial features, antenna parameters, link budget parameters, and even antenna placements on the aircraft and ground. This information is then translated into a continuous stream of control parameters, which allows the channel simulator to mimic the RF perturbations en-

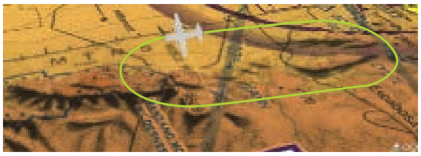

▲ *Fig. 1 Aircraft flight modeled at T = 0 on Analytical Graphics Inc. STK SW.*

countered continuously throughout the flight. For example, if this were the first flight of an experimental aircraft, for which the communication link in question would relay all operating parameters of the first flight, the flight could be flown virtually over and over before any aircraft or personnel were put at risk. By utilizing the actual communication equipment, along with a channel simulator creating realistic waveform impairments, the system can be optimized, insuring reliable communication throughout the actual maiden flight.

The yellow line in the figure represents the communication link between the aircraft and the receiving antenna. As the aircraft proceeds around the flight path (shown in green), the running scenario passes the appropriate programming variables to the channel simulator. The channel simulator in turn adds exact RF perturbations to the signal as the physics of the motion would impart in an actual flight. Some of the communication link variables being modified at the instant the figure was captured include: Doppler (aircraft moving away from the receiving antenna); delay (time for signal to travel the distance between aircraft and receiving antenna); power levels (influenced by distance); and line-of-sight connectivity (terrain and antenna placement on the aircraft are affecting transmission). Other variables to add realism can be included in this scenario, such as radio transmissions, modulation type, data rate, signal-to-noise ratios and radar signals to name a few. It is also important to point out that this can be done with full motion simulation in real-time, accelerated time, or slowed time, not just as a static test. If, for example, the tracking station on the ground was using the time delay of the communication path as a backup measurement of distance from the receiver, the delay imparted by the channel simulator would mimic the delay, even though the test may be running in the lab.

CHANNEL SIMULATOR BLOCK DIAGRAM

One might wonder at this point how

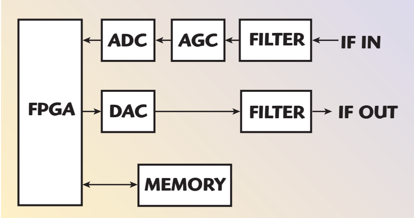

Fig. 2 Channel simulator block diagram.

a channel simulator creates this realistic environment. ***Figure 2*** shows a simplified block diagram. The signal is typically down-converted (not shown) to an IF that is digitized by an ADC, processed through an FPGA with DSP capability, returned to IF with a DAC, and finally up-converted (not shown) back to RF. The key is that the channel simulator must have a real-time RF path, which can then also apply physics-compliant impairments to the signals under test. The end results are test signals that accurately match the real signals when exposed to the actual link environment. A variety of effects outside of the physics-related channel distortions can also be added via signal sources, for example, an intentional or unintentional jamming signal overlapping the link.

Let us now use the example flight plan discussed previously, to highlight the details of how signals are modified due to the physics of a communication system in motion. In this example, the aircraft is in motion with respect to the ground station, creating a Doppler shift. This effect must be considered in order to ensure that the receiver remains locked to the signal while maintaining proper BER performance, even as the received signal's frequency shifts over time due to the relative motion of the transmitter and the receiver. Equation 1 describes the Doppler shift, based on the actual transmitted frequency and the relative velocity between the transmitter and the receiver.

$$F_s = F_a(V/c) \tag{1}$$

where Fs = Doppler shift in Hz

Fa = actual transmitted frequency in Hz

V = relative velocity between transmitter and receiver in km/s

c = speed of light (~300,000 km/s)

The graphical data shown in ***Figure 3*** is calculated using Equation 1. The relative velocity of the aircraft, along with the actual transmitted carrier frequency, serve as input data. This allows the Doppler shift to be graphed at any point along the flight path. You can see the result of the Doppler shift on a 2.4 GHz signal. As the aircraft moves towards the fixed receiving station, the received signal is at a higher frequency than is actually being transmitted. When the aircraft is moving away, the received signal frequency is lower than the transmitted frequency.

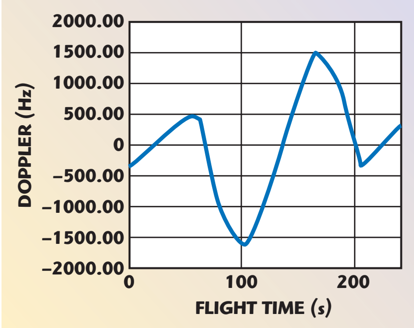

Fig. 3 Doppler shift vs. time for a 2.4 GHz signal observed at the ground station.

TABLE I

TURNS RANGE RATE AT 833 KM/HR CRUISE SPEED

Original Frequency (Fa)	*Approximate Observed Doppler (Fs)*
435 MHz (UHF-band)	± 0.3 kHz
1.2 GHz (L-band)	± 0.9 kHz
2.4 GHz (S-band)	± 1.5 kHz
5.7 GHz (C-band)	± 4 kHz
10.5 GHz (X-band)	± 7 kHz
24.0 GHz (Ku-band)	± 16 kHz

For this aircraft and flight path, the following Doppler shift ranges observed at a fixed ground station are shown in ***Table 1***. Similar data can be constructed for other frequencies, as well as for a number of potential platforms in motion including Middle Earth Orbit (MEO), High Earth Orbit (HEO), and Geostationary Earth Orbit (GEO) satellites, UAVs, and missiles.

On a laboratory bench, a channel simulator used in the configuration shown in ***Figure 4*** can apply the anticipated Doppler shift to the input signal, so that the signal into the receiver system under test is identical to what would actually be received from the transmitter.

Figure 5 shows a similar setup for transmitter system testing. In either test setup, receivers or transmitters under test may be used for flying or ground-based applications. As well, up-converters, down-converters and modems may be necessary in an actual test setup, depending on available equipment and receiver and transmitter characteristics.

Note that these setups allow testing of all receive-chain components, such as antennas, amplifiers, modulators, encryptors, demodulators, decoders, decryptors, bit syncs, etc., because the input signal is completely realistic. Signal connections into and out of channel simulators can be over cables, near-field RF, or long distance RF.

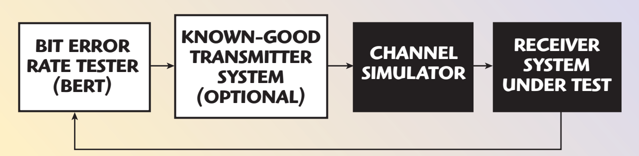

▲ *Fig. 4 Channel simulator configuration for receiver system testing.*

▲ *Fig. 5 Channel simulator configuration for transmitter testing.*

As Equation 1 describes, the Doppler shift is frequency dependent. Since data signals have non-zero bandwidth, various portions of the signal are actually at different frequencies as can be observed with the 120 kbit/sec QPSK signal shown in ***Figure 6***. For precise simulation, the Doppler shift capacity of the channel simulator must apply appropriate and different Doppler shifts across its bandwidth. In Figure 6, for example, the left side of the waveform would receive a slightly lower Doppler shift than the right side, since the left side is at a lower frequency than the right side. This is especially important at high data rates that result in wide bandwidth data signals.

Referring back to Figure 3, it also shows that the Doppler shift rate changes throughout the flight. The flatter, more horizontal areas of the plot are where the Doppler shift remains relatively constant due to comparatively small changes in the closing velocity between the aircraft and the ground station. The steeper portion of the curve is where the aircraft's range from the ground station is changing more rapidly; as the plot crosses the X axis, the velocity changes sign from positive values (aircraft approaching receiver) to negative values (aircraft moving away from receiver). Channel simulators, configured as those shown previously, must apply Doppler shift rates both within and beyond the anticipated ranges for verification of appropriate receiver system margin.

DELAY

All communication systems have some form of inherent delay in propagation between transmitter and receiver. This is true for wire-line systems, optical systems and wireless radio systems, where propagation velocity is related to the dielectric constant of the medium through which the signal passes. Propagation velocity is expressed as a percentage of the speed of light, and in vacuums (dielectric constant = 1) and in air (dielectric constant = 1.00054), propagation velocity can be considered to be 100 percent of the speed of light for most practical purposes.

Therefore, in most wireless communication systems the propagation delay between a transmitter and receiver can be very closely approximated by dividing the straight line distance between the transmitter and the receiver, by the speed of light.

For the specific flight path discussed earlier, the range delay profile of ***Figure 7*** can be expected. Modeling different types of moving platforms and flight paths will produce dramatically different results. When performing one-way tests, where a receiver or transmitter is being tested, the channel simulator must be capable of signal delay ranges dictated by both the closest and farthest expected separation between transmitter and receiver, plus margin. Complete simulations of relay communications scenarios require that the channel simulator be capable of delaying for the full communication

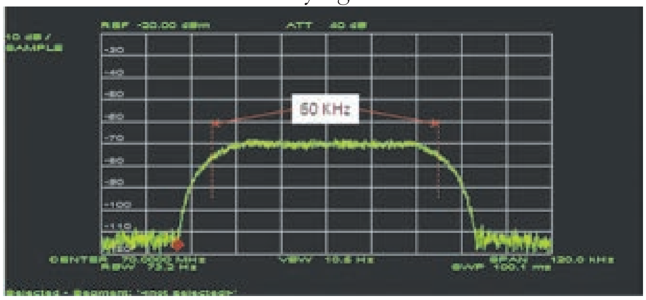

▲ *Fig. 6 Typical 60 kHz bandwidth of a 120 kbit/sec (60 kSymbols/sec) QPSK signal.*

path, both to and from the transmitter/receiver.

For the flight plan illustrated previously, a channel simulator would need a delay capacity of at least 40 μs as given in Equation 2, as well as any other transmitter/receiver delays, plus margin for worst-case system analysis.

$$DT = D/c \qquad (2)$$
$$= (12\ \text{km})/300{,}000\ \text{km/s}$$
$$= 40\ \mu s$$

where DT = total delay in s
D = distance in km
c = speed of light (~300,000 km/s)

Communications systems testing between satellites, space vehicles and ground stations follow the same considerations, except that maximum delays are much larger due to the longer distances between transmitters and receivers.

PATH LOSSES

Receiver system performance also depends on the power level of the received signal. A variety of factors can affect the power levels in the flight example, including terrain, antenna location, weather conditions and orientation. Modeling dynamic signal power levels and validating operation under worst-case conditions are key receiver system tests.

The power level of a received signal is affected by free-space path loss, which can be calculated from Equation 3.

$$L = 32.4 + 20 \log F + 20 \log R \qquad (3)$$

where L = free-space path loss in dB
F = frequency in MHz
R = range in km

A channel simulator must accept a low-level input signal, then further attenuate it according to the attenuation profile of the communications system being tested. Properly simulating communication links to satellites requires much greater attenuation ranges. A LEO satellite requires a channel simulator relative attenuation capacity of 10 to 20 dB. Modeling MEO and HEO satellites having highly elliptical orbits, or where atmospheric, Rician, Rayleigh, or Nakagami fading is to be modeled, the needed relative attenuation range is more on the order of 50 dB.

ADDITIVE WHITE GAUSSIAN NOISE (AWGN)

As with the Doppler, range delay and range attenuation parameters mentioned previously, all communications systems are subject to noise received by the antenna (cosmic noise

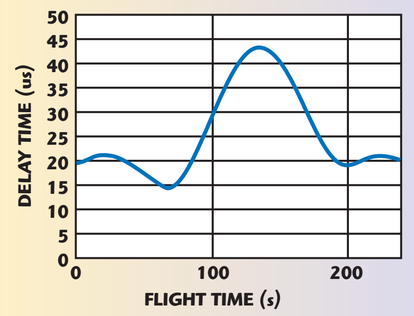

▲ *Fig. 7 Range delay vs. time for a signal from nearly elliptical flight seen at a ground station.*

and radiation from the Earth), as well as other atmospheric and man-made noise. Receiver noise itself is also an important factor. In order for channel simulators to be capable of creating signals truly identical to those that would be received from wireless transmitters, they must contain noise sources capable of generating expected and worst-case noise profiles.

REAL-TIME (CONTINUOUS) SIGNAL PASS THROUGH

Channel simulators must perform their operations in a fully physics-compliant and phase-continuous manner. This ensures that throughout the instrument's capabilities, no data errors are introduced as a result of waveform discontinuities, inappropriate transitions, or glitches. The channel simulator must faithfully model nature in this regard, so that the instrument can be confidently substituted into the communications system for accurate and dependable results. Among other key attributes, this implies sophisticated high-resolution interpolation between commanded Doppler, delay, or attenuation points.

CONCLUSION

While this article used the example of an aircraft circling a ground communication site, the principles and concepts discussed apply similarly to transmitters and receivers that are in motion relative to each other. The understanding of how the environment will modify electrical signals, along with utilization of revolutionary test equipment like the channel simulator, ensure that the system that works on the bench, will also work in motion. In conclusion, while testing of communication systems is a long-standing, well-honed art, the advent of the channel simulator provides engineers with a unique and important test capability that further ensures functionality when it absolutely counts. ■

RF Channel Simulation

When communications really count

DOPPLER • DELAY • PATH LOSS • NOISE • INTERFERENCE

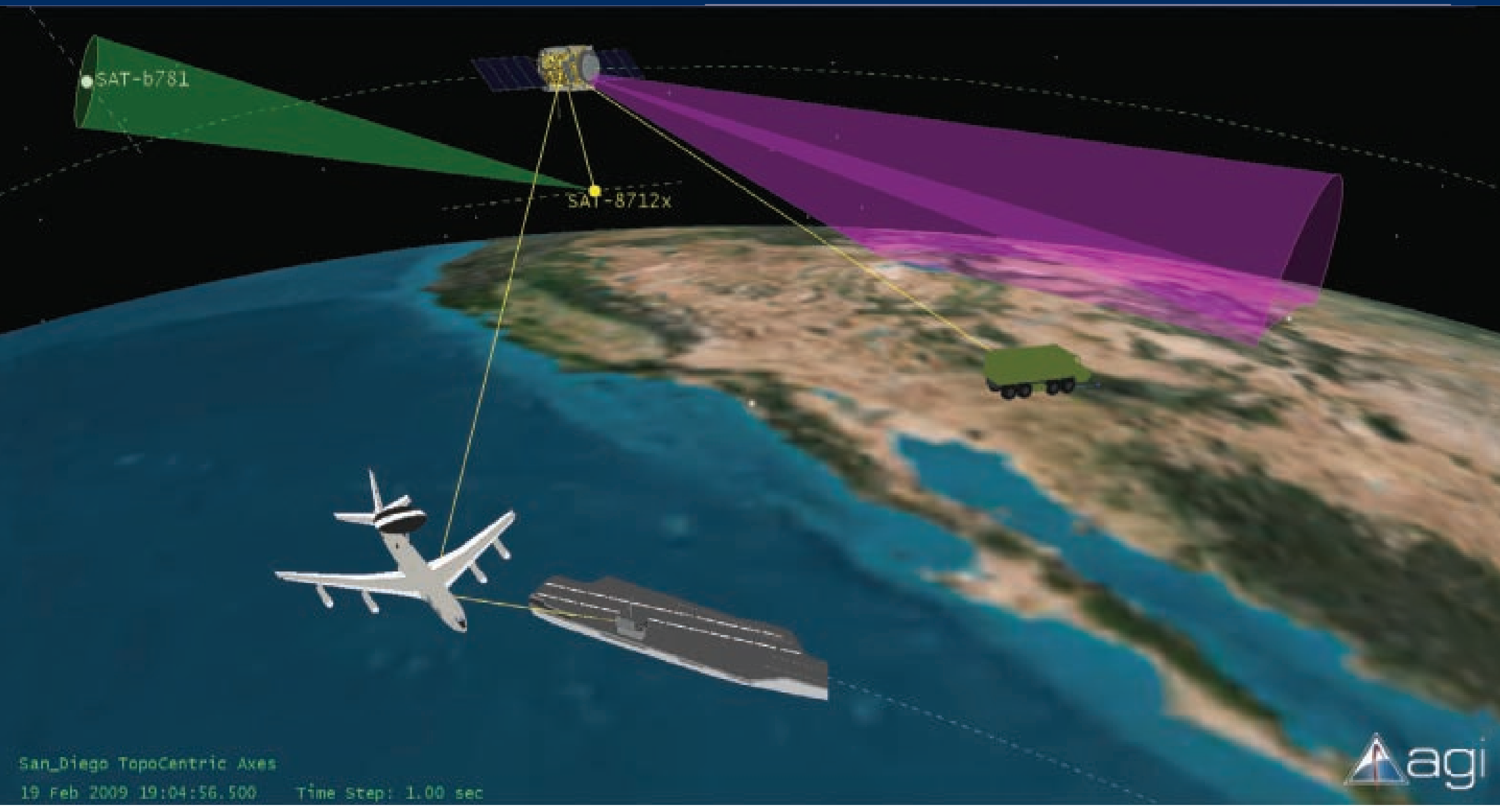

The RT Logic T400CS Channel Simulator adds dynamic, phase-continuous, physics-compliant signal and carrier Doppler shift, delay, path loss, noise and interference to the signals you test with.

Develop and test realistically, thoroughly, quickly and easily, under the most punishing RF and complex motion conditions imaginable - *without ever leaving the lab*.

- Flight and ground system assurance
- Performance and functional verification
- Compliance and regression testing

Visit www.rtlogic.com/cs for demo movies, tech briefs and more.

The Integral Family of Solution Providers.

INTEGRAL SYSTEMS • RT LOGIC • NEWPOINT TECHNOLOGIES, INC. • SAT CORPORATION • LUMISTAR • INTEGRAL SYSTEMS EUROPE

The Integral Difference.

RT LOGIC
an Integral Systems Company

719-598-2801 • sales@rtlogic.com • www.rtlogic.com

MICROWAVE JOURNAL REVIEWED EDITORIAL BOARD

ULTRA-FAST, SIMPLER AND MORE ACCURATE NOISE PARAMETER MEASUREMENTS

Noise parameters are required to design circuits to minimize the effect of noise, but noise parameters have traditionally been very slow and complex to measure. Now a new, ultra-fast method is shown, which is over two orders of magnitude faster, more accurate and simpler, requiring less operator skill to make the measurement.

Electrical noise is created naturally by almost any type of device. In circuits that need to amplify and process very low level signals, noise can interfere with the desired signal, causing degraded or complete loss of reception. This is significant for any wireless receiver, often being the limiting factor on reception quality and range. Much of the interfering noise can be generated by the components in the receiver circuit itself.

There are two approaches that can reduce the effect of noise. The first is to increase the transmitted signal level so that the receiver noise becomes insignificant. However, this is usually not practical because of cost, power, size, weight, safety, or regulatory limitations. The other approach is to reduce the noise generated by the receiver circuitry. This is generally the only cost-effective and practical option available.

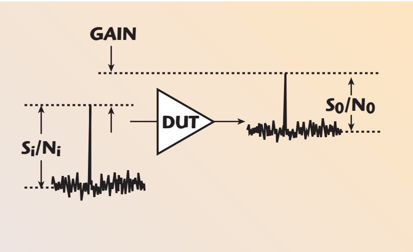

▲ *Fig. 1 Noise figure is defined in terms of input and output signal-to-noise ratios.*

Noise figure is a measure of noise generated by a circuit. It is defined as the output signal-to-noise ratio divided by the input signal-to-noise ratio. It can be expressed as a ratio, sometimes called noise factor, or in dB, as shown in Equation 1 and illustrated in ***Figure 1***. For an ideal, noise-free device, the input and output signal-to-noise ratios would be equal, giving a noise figure ratio of one. In any real device, some noise is added, so the noise figure ratio is always greater than one. One of the objectives for circuit designers is to make the noise figure as low as possible to minimize the adverse effects of noise in the system.

$$F = \frac{S_0 / No}{S_i / N_i} \text{ and } F_{dB} = 10 \log_{10}(F) \qquad (1)$$

GARY SIMPSON
Maury Microwave, Ontario, CA
DAVID BALLO
Agilent Technologies Inc., Santa Rosa, CA

At microwave frequencies, the primary type of noise is thermal noise, which is generated by any resistance in the circuit, or by the active devices used to amplify signals. Resistance is due to discrete resistors or the resistivity of lossy components. The available noise power produced by a resistance is given by Equation 2:

$$P_n = kTB \tag{2}$$

where
P_n = available noise power
k = Boltzmann's constant
T = temperature in Kelvin
B = bandwidth of the system

An active device, such as a transistor, can be modeled as an ideal noise-free two-port network plus two noise sources, as shown in ***Figure 2***. Generally, the two noise sources are partially correlated to one another, so their combined effect either adds or cancels, depending on the value of the source impedance driving the device, expressed in terms of source reflection coefficient, Γ_s. This means that the noise figure of the device will be a function of Γ_s. This function must be understood in order to design circuits for optimum noise performance.

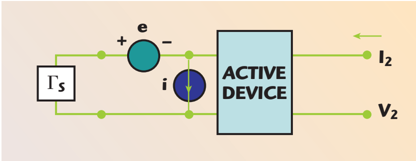

Fig. 2 Basic noise model of an active device.

NOISE PARAMETERS

The variation of noise figure versus Γ_s is described by Equation 3, commonly called the noise figure equation. The parameters F_{min}, r_n and Γ_{opt} are called the noise parameters, and they actually consist of four scalar values, because Γ_{opt} is complex and therefore has a magnitude and a phase component. If the noise parameters are known, then the circuits using the device can be designed to minimize the effects of noise.

$$F = F_{min} + 4r_n \frac{\left|\Gamma_s - \Gamma_{opt}\right|^2}{\left|1+\Gamma_{opt}\right|^2 \left(1-\left|\Gamma_s\right|^2\right)} \tag{3}$$

where
F= noise figure ratio of the device
Γ_s = source reflection coefficient
F_{min}= minimum noise figure
r_n = normalized noise resistance
Γ_{opt}= optimum source reflection coefficient associated with F_{min}

There are other forms of the noise parameters, such as different configurations of the noise correlation matrix, but this set is the most commonly used. If the S-parameters and noise parameters of a device are known, then converting from one form to another is straight forward, similar to converting between S-parameters and Y-parameters, for example.

NOISE PARAMETER MEASUREMENTS

The basic approach for determining the noise parameters is to measure the noise figure of the device-under-test (DUT) with four different known

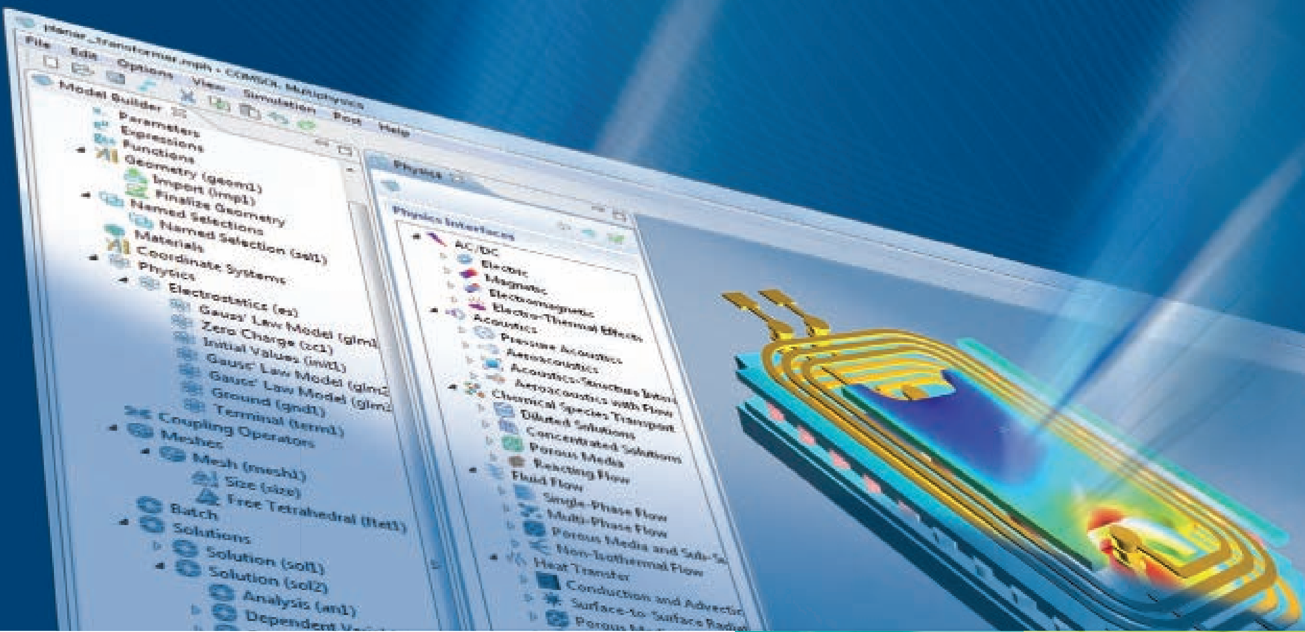

source reflection coefficients, and then use these values to solve four simultaneous noise-figure equations, yielding the values of the four scalar noise parameters. However, noise measurements tend to be sensitive to small errors, so in practice, more than four measurements are made, and then a least-means-squares algorithm is used to reduce the over-determined data.[1,2]

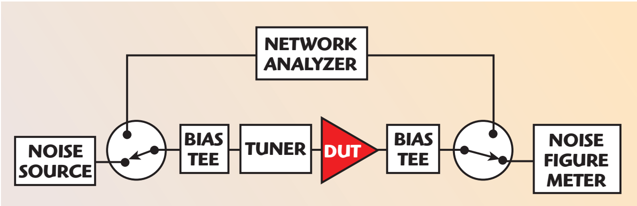

Fig. 3 Traditional noise parameter measurement setup.

Another practical measurement improvement is the use of the noise power formulation shown in Equation 4, instead of the previously shown noise figure equation. This equation allows rigorous accounting of the reflection coefficient difference between the hot and cold states of the noise source. It also allows use of any combination of hot and cold measurements, including the cold-only measurement method commonly used by vector network analyzers.

$$P = kB\left\{\left[t_{ns} + t_0(F_1 - 1)\right]\cdot G_{a1} + t_0(F_2 - 1)\right\}G_{t2} \quad (4)$$

where
P = total measured noise power
k = Boltzmann's constant
B = system bandwidth
t_0 = reference temperature of 290 Kelvin
t_{ns} = temperature of the noise source in Kelvin
F_1 = device noise figure (a function of source reflection coefficient and device noise parameters)
F_2 = measurement receiver noise figure (a function of the DUT output reflection coefficient and receiver noise parameters)
G_{a1} = DUT available gain (a function of the source reflection coefficient and DUT S-parameters)
G_{t2} = measurement receiver transducer gain (a function of the DUT output reflection coefficient, receiver S-parameters and receiver signal-processing gain)

TRADITIONAL NOISE PARAMETER MEASUREMENTS

A traditional noise parameter measurement setup is shown in ***Figure 3***. The RF switches connect the DUT to either the network analyzer or the noise figure meter. The network analyzer is used to measure the S-parameters of the DUT with the tuner set to 50 Ω. The noise figure meter is used to measure noise power for any Γ_s set by the source tuner. When measuring devices that require bias through the RF ports, external bias tees are configured as shown so that the bias is independent of the switch position. An optional load tuner (not shown) is sometimes used with highly reflective devices to reduce sensitivity to error.

The system calibration includes measuring the tuner at many states that cover the whole Smith chart independently at every frequency. This allows the selection of a good set of Γ_s values at every measurement frequency, which is desirable because good measurement accuracy and sensitivity requires the correct selection of tuner impedance states. The reference planes of the tuning block must go from the noise source plane to the DUT input plane.

An in-situ system calibration can be done after doing two network analyzer calibrations. The first is a two-port calibration at the DUT planes. The second is a one-port calibration at the noise source port. By subtracting the error terms of the two calibrations, the two-port S-parameters from the noise source port to the DUT input port can be determined. If an optional load tuner is used, then an additional one-port calibration at the noise receiver plane will be used to get the S-parameters from the DUT output port to the noise receiver port.

To save time in the event that something outside of the tuner changes (a wafer probe, for example), the tuner may be characterized separately. A hybrid in-situ calibration can then be done in the same manner to get a fixed S-parameter block that does not include the tuner.

After the system calibration is complete, the noise receiver is calibrated one frequency at a time; the DUT noise parameters are then measured one frequency at a time.[3,4] This is done because the noise parameter extraction involves complex calculations that are sensitive to small errors, so it is important to select a good pattern of source reflection coefficients to get well-conditioned data.[2] Making the measurements one frequency at time allows an ideal pattern to be selected.

One problem with the traditional approach is that it is very time consuming, due to the large number of tuner states (each requiring physical movement of the probe/carriage assembly), and the large number of single-frequency noise measurements. It is common to sweep 400 or more frequency points in S-parameter measurements, but for measuring noise parameters, that many frequencies would take days. With long measurements, temperature drift can cause significant errors. This is exacerbated by the many lengths of cables required for all the instrument and component connections shown in the measurement setup.

Since traditional noise parameter measurements are slow, they are typically limited to a sparse set of frequencies. But this makes the scatter, outliers and cyclical-frequency errors difficult to interpret. A cyclical error is common with imperfect network analyzer calibrations, where the system errors will add at some frequencies and cancel at others. This can cause an aliasing effect, which can shift the data values up or down. Smoothing techniques can make the data look better, but will not correct for this type of data shift.

NEW ULTRA-FAST NOISE PARAMETER MEASUREMENTS

The new ultra-fast noise parameter measurement method (patent pending) typically speeds up measurements

No matter what your LTE or WiMax applications are, JFW has them covered!

Visit us at CTIA in
Booth #325

If you're looking for reliable RF attenuation products, switches or power dividers that operate up to 6 GHz and beyond, then JFW now has a multitude of products to choose from that cover all WiMax and LTE frequencies.

We also offer a complete line of specialized RF test systems that includes our RF Handover and Fading Simulators, our Transceiver Test Systems and RF Matrix Switches.

JFW specializes in providing custom RF components and sub-systems at catalog prices, so contact us today for an RF solution that's designed with your unique requirement and your budget in mind.

JFW INDUSTRIES, Inc.

Call 317-887-1340 Toll Free 877-887-4JFW (4539)
www.jfwindustries.com E-mail sales@jfwindustries.com

by over two orders of magnitude. This is a major breakthrough for the industry, and makes much larger frequency sets practical.

There are two key features of the new method that contribute to the large speed improvement. The first is that the tuner is characterized with a single set of tuner states (physical tuner positions), each of which is swept versus frequency. The tuner's states are selected to give a good spread on the Smith chart at every frequency within the selected frequency band. The second feature is that the noise power data is swept over frequency, one tuner position at a time. The tuner only has to move to each position once, and the measurements take advantage of the fast sweep times of modern instruments. The fast measurement time virtually eliminates temperature drift as a source of error.

The new method has been implemented with Agilent's PNA-X network

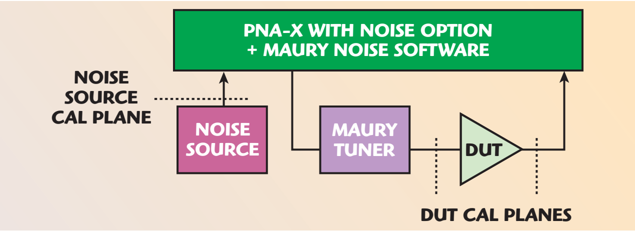

▲ *Fig. 4 New noise parameter measurement setup.*

▲ *Fig. 5 Photograph of the new setup measuring a coaxial DUT.*

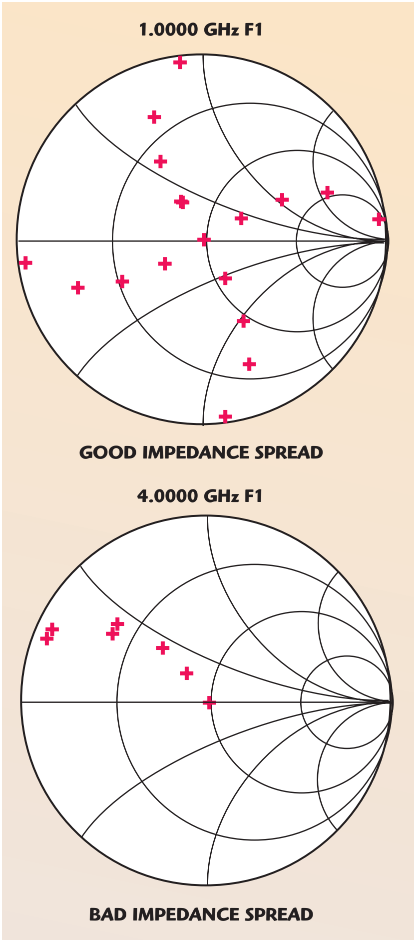

▲ *Fig. 6 Aliasing due to uniform spacing of tuner states results in poor patterns at some frequencies.*

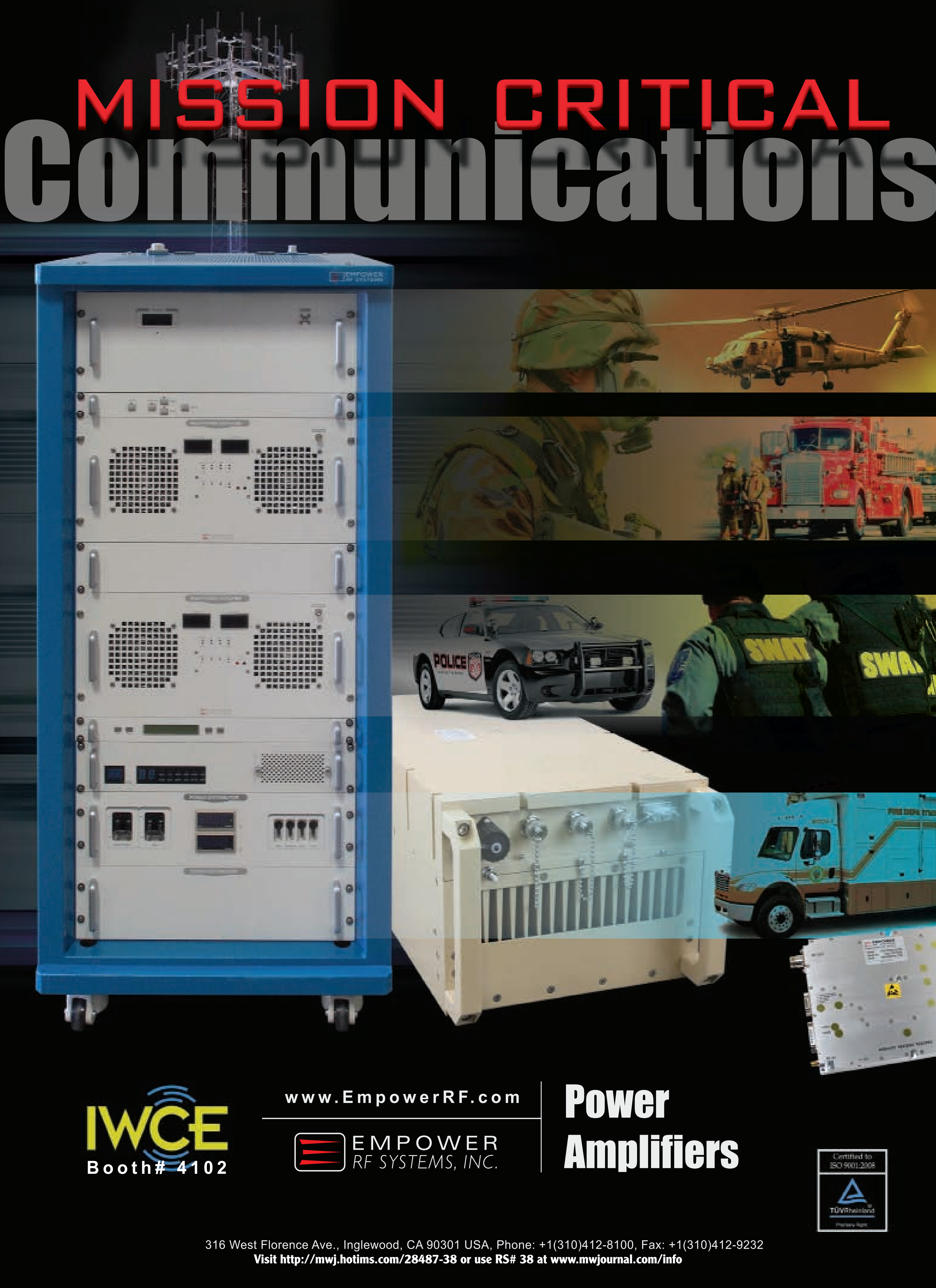
MISSION CRITICAL
Communications
POLICE
SWAT
IWCE
Booth# 4102
www.EmpowerRF.com
EMPOWER
RF SYSTEMS, INC.
Power
Amplifiers
Certified to ISO 9001:2008
TÜVRheinland
316 West Florence Ave., Inglewood, CA 90301 USA, Phone: +1(310)412-8100, Fax: +1(310)412-9232
Visit http://mwj.hotims.com/28487-38 or use RS# 38 at www.mwjournal.com/info

analyzer, which has an optional built-in low-noise receiver and a flexible, switched test set, which greatly simplifies the measurement system, as shown by the block diagram in ***Figure 4***. This reduces the number of cables and connections, helping to stabilize the setup, and offers fewer opportunities for error. A photograph of the setup is shown in ***Figure 5***. The Maury tuner is controlled by a USB cable plugged into the front of the PNA-X.

Since a fixed set of tuner states is used for the entire frequency band, the reflection coefficient pattern may not be as ideal at some frequencies as with the traditional method, depending on how the states are selected. For example, ***Figure 6*** shows the result of selecting uniformly spaced mechanical tuner states. The pattern is fine at one frequency (left chart), but very poor at another frequency (right chart).

A solution to this is to use non-uniform spacing of tuner states. ***Figure 7*** shows the result at the low, middle and high end of the band. As the frequency varies, the points rotate, but a good pattern is maintained at all frequencies. The pattern does use about 50 percent more points than typically used in a traditional noise parameter measurement, but that still allows two orders of magnitude speed improvement.

The new method may be done in multiple frequency bands with tuners that have frequency-banded mismatch probes. For the examples in this article, the data was taken with a Maury tuner model MT982EU30. The low frequency mismatch probe covered 0.8 to 2.8 GHz; the high fre-

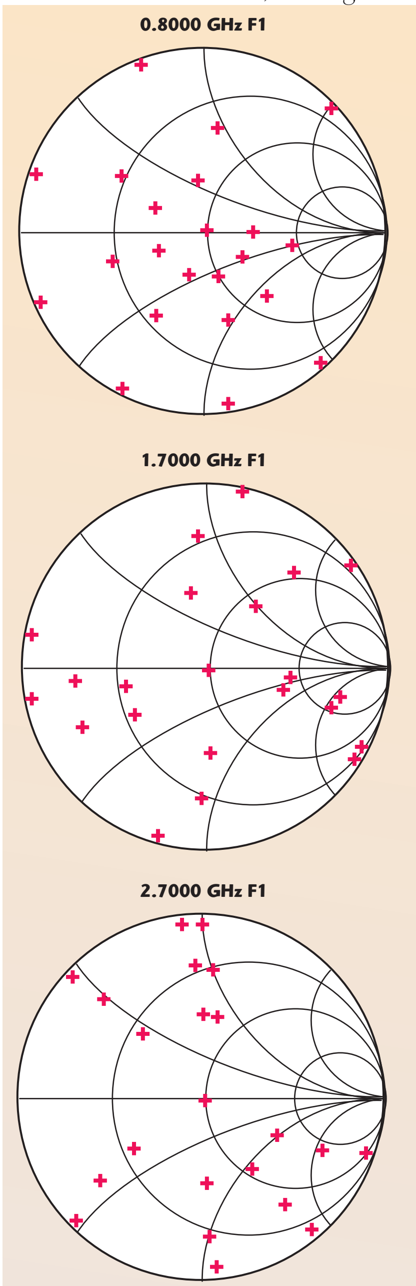

▲ *Fig. 7 Non-uniform spacing of tuner states provides good patterns across frequency.*

S. M. ELECTRONICS L.L.C. DBA

FAIRVIEW MICROWAVE

ATTENUATORS 0-50 GHZ

SA50 $288.00 2.4MM 50GHZ	SA4014 $142.00 2.92MM 1W 40GHZ	SA26B $75.00 SMA 27GHZ	SA18H $30.50 SMA 18 GHZ	SA6H $20.00 SMA 6GHZ	SA6Q $29.00 QMA 6GHZ 2W
SA3011 $12.75 SMA 3GHZ BRASS	SA4017 $500.00 2.92 40GHZ 5W	SA3S5W $36.00 SMA 3GHZ 5W	SA3N10W $70.00 N 3GHZ 10W	SA18S10W $122.00 SMA 18GHZ 10W	SA3T $29.00 TNC 3GHZ 2W
SA18N $47.00 N 18GHZ	SA3NS $26.00 N 3GHZ	SA3N5W $40.00 N 3GHZ 5W	SA18N10W $123.00 N 18GHZ 10W	SA4N-50 $170.00 N 4GHZ 50W	SA18N100 $700.00 N 18GHZ 100W

ADAPTERS 0-65 GHZ

SM3250 $198.00 2.92 M/F 40GHZ	SM3929 $409.00 1.85-1.85 65GHZ	SM3985 $135.00 1.85-3.5 34GHZ	SM8902 $105.00 MINISMP-SMA 26GHZ	SM4216 $25.00 N-M-SMA 6GHZ	SM4742 $39.50 SMA-TNC 18GHZ

DC BLOCKS, EQUALIZERS, TERMINATIONS, DIVIDERS, COUPLERS, CABLES

SD3235 $47.00 DC BLOCK SMA 5KHZ-23GHZ	EQUALIZERS 1-18 GHZ	ST5038 $260.00 2.4MM 1W 50GHZ	SMP0218 $275.00 DIVIDER SMA'S 2-18GHZ	ST3N501 $129 3GHZ 50W	CABLES SMA, N, 2.92 0-65 GHZ

FAIRVIEW MICROWAVE

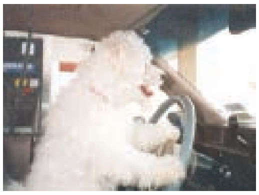

FAST DELIVERY!

WWW.FAIRVIEWMICROWAVE.COM 1-800-715-4396

460 S HIGHWAY 5 FAIRVIEW, TX 75069 1-800-715-4396 FAX: 972-984-1218 EMAIL: SALES@FAIRVIEWMICROWAVE.COM

quency mismatch probe covered 2.8 to 8.0 GHz. The noise software installs and runs inside the PNA-X itself, although it can also be run from a separate computer.

COMPARISON OF THE TWO METHODS

To test and compare the two methods, a microwave FET was permanently mounted in a stripline fixture with 3.5 mm connectors as seen in the photograph of the new system, and the connector planes were the DUT measurement planes. This produced the repeatable connection required for a good comparison. The measurement covered 0.8 to 8.0 GHz, with steps of 0.1 GHz, resulting in 73 frequencies. No smoothing was applied to any of the data shown here.

Figure 8 shows the measured data using the traditional measurement method. F_{min} is approximately 1 dB, and fairly flat versus frequency. F_{min} scatter is about ± 0.2 dB at the lower frequencies, improving to about ± 0.1 dB at the higher frequencies. The scatter is quite uniform, so smoothing would probably be quite effective. But the measurement took 30 hours, 15 minutes, from start to finish.

This scatter is typically not ob-

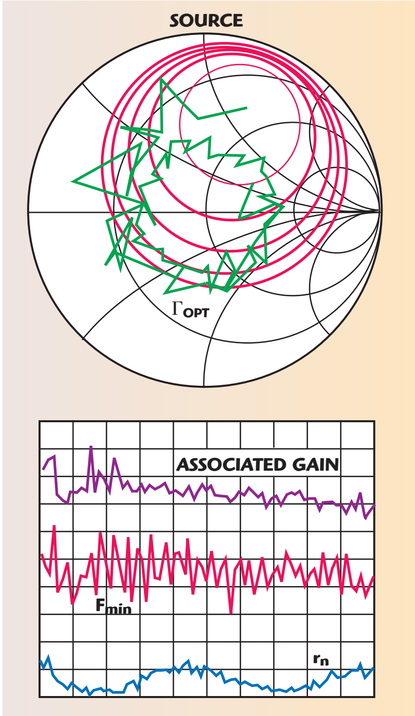

▲ *Fig. 8 Noise parameter data from traditional method with 73 frequencies.*

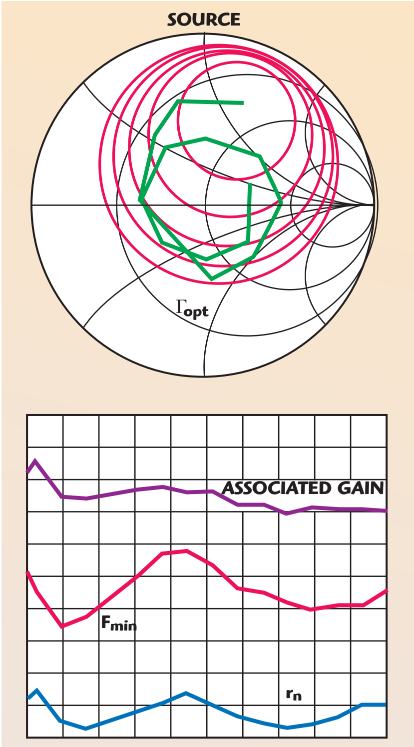

▲ *Fig. 9 Same data as Figure 8 using only 15 frequencies, giving misleading results.*


Military • Aerospace • Electronic Defense
Now AS9100 certified
Innovation and Experience....
Our Legacy
Microphase commitment is to provide the most reliable and advanced engineering solutions our customers demand for today and tomorrows military applications. Always ready to accept the next challenge, we are proud of the important contributions Microphase has made to our nation's defense. Built on Five Decades of experience, true to our founding philosophy, we will continue to bring new cost effective solutions to our customers while maintaining the highest quality standards.
• Multi-Function Assemblies
• Filters
• Multiplexers
• Switch Filter Banks
• Detectors/Limiters
• Detector Log Video Amplifiers
• Agile Filters
MICROPHASE CORPORATION
Microphase Corporation
587 Connecticut Avenue
Norwalk, CT 06854
Phone: 203-866-8000
Fax: 203-866-6727
quote@microphase.com
www.microphase.com
Certified System
AS9100

served by RF designers, since measuring 73 frequencies is actually unrealistic for the traditional method, since it takes too long. Measuring with a step size of 0.5 GHz would be more typical. ***Figure 9*** is exactly the same data, except that all the frequency points in between a 0.5 GHz spacing were deleted, leaving only 15 frequencies, which is typical for the traditional method. The data looks fairly smooth, but there is a very odd hump in the frequency response of F_{min}. It appears that something strange is going on with the DUT with the shifted F_{min} data. But if it is compared to the original data, it is seen that the DUT is normal, and the strange hump is due to aliasing of the data, where low points of the scatter are picked over part of the frequency range, and high points of the scatter are picked over a different part of the band. The dense frequency spacing shows a much more accurate data, and smoothing techniques also become more meaningful with the large number of points.

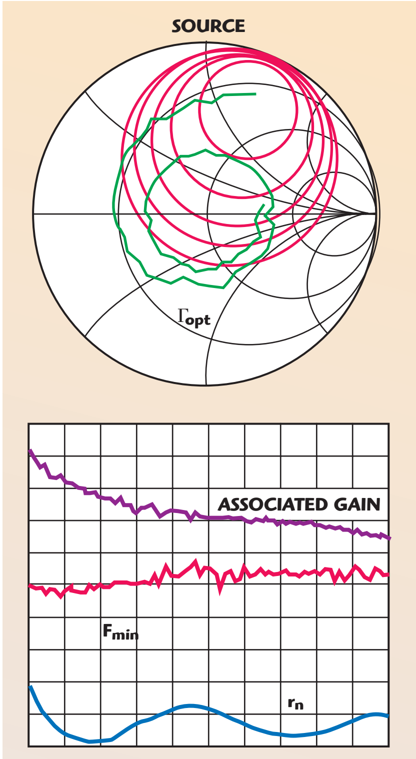

▲ *Fig. 10 Noise parameter data taken by the new method.*

Figure 10 shows the measured data taken with the new method, using the same 73 frequencies. Again, no smoothing is applied to the data, but the scatter is much smaller, so smoothing is not necessary anyway. Using the new method, the measurement took only eight minutes, improving the test time by a factor of 224. A time comparison is shown in ***Table 1*** for 73 and 401 frequencies.

Another significant benefit of the new method is the simplicity of the test setup, calibration and measurement procedure. The connections and calibration process is now similar to that required for S-parameter measurements, so instead of requiring a highly skilled engineer, a technician or other trained operator can easily accomplish the tasks.

IMPROVED ACCURACY

The primary motivation for this work was to speed up and simplify the measurement. But a side benefit is improved accuracy. Some reasons why this makes sense include:

- The new method uses a simpler setup. There are fewer cables and connections, and therefore fewer op-

portunities for problems from cable movement, loose connectors, etc.

- With the new method, a full in-situ calibration is always performed, because it is so fast. This removes the accumulated errors of multiple S-parameter calibrations, and eliminates reconnection errors.
- With the new method, there is minimal drift due to the short calibration and measurement times.
- With the new method, a dense frequency selection is used to eliminate aliasing, because it is fast.
- Smoothing was not shown in any of the data here, but the dense frequency selection would make smoothing more meaningful.

TABLE I

MEASUREMENT TIME COMPARISON OF THE NEW METHOD VERSUS THE TRADITIONAL ONE

	Traditional method measurement time, 73 frequencies	*New method measurement time, 73 frequencies*	*Traditional method measurement time, 401 frequencies**	*New method measurement time, 401 frequencies*
System Cal	25 hrs, 29 min	1 min, 56 seconds	139 hrs, 59 min	3 min, 12 seconds
Noise receiver Cal	2 hrs, 24 min	2 min, 56 seconds	13 hrs, 13 min	10 min, 44 seconds
DUT Measurement	2 hrs, 22 min	3 min, 15 seconds	13 hrs, 2 min	10 min, 54 seconds
Total time excluding connections	30 hrs, 15 min	8 min, 7 seconds	166 hrs, 14 min	24 min, 50 seconds
Time Ratio		224X		400X

* Estimated, based on time to measure per frequency

OPPORTUNITY FOR PRODUCTION TESTING

Production testing of noise parameters has never been an option with the traditional measurement method because of long measurement times. However, the speed and simplicity of the new method opens up new possibilities in manufacturing applications. Production testing of known parts may not require many frequencies, so the measurement time for each device could be less than 30 seconds. Providing noise-parameter specifications or measured data for each part makes products more competitive and more valuable to customers. Circuit designers can use the noise parameters to better predict noise performance of devices in mismatched environments, or to design better matching circuits. In addition, test data allows manufacturers to sort for performance, and to track production runs for continuous process improvement, providing an overall higher level of quality assurance.

CONCLUSION

The new ultra-fast noise parameter measurement method provides more than two orders of magnitude speed improvement, and more accurate data with a simpler setup that does not require a highly skilled operator. The fast measurements virtually eliminate drift, greatly reduce measurement scatter, and allow dense frequency spacing, providing more accurate and more complete data, and better insight into device noise performance. ■

ACKNOWLEDGMENTS

The authors thank Lynn Rhymes of Agilent Technologies Inc., Santa Rosa, CA, for supplying the connectorized test device.

References

1. R.Q. Lane, "The Determination of Device Noise Parameters," *Proceedings of the IEEE*, Vol. 57, No. 8, August 1969, pp. 461-1462.
2. C. Giuseppe and M. Sannino, "Computer-aided Determination of Microwave Two-port Noise Parameters," *IEEE Transactions on Microwave Theory and Techniques*, Vol. 26, No. 9, September 1978, pp. 639-642.
3. "Operating Manual, Automated Tuner System," Maury Microwave Corp., Document number MT993-2.
4. R.Q. Lane, "A 0.5 to 18 GHz Semi-automatic Noise Parameter Measurement Technique," *19th ARFTG Digest*, June 1982, pp. 42-58.
5. G. Simpson, D. Ballo, J. Dunsmore and A. Ganwani, "A New Noise Parameter Measurement Method Results in More than 100x Speed Improvement and Enhanced Measurement Accuracy," *72nd ARFTG Digest*, December 2008.

The Smaller! The Better!

Newer Designed 0.5 Inch Drop-in Circulator

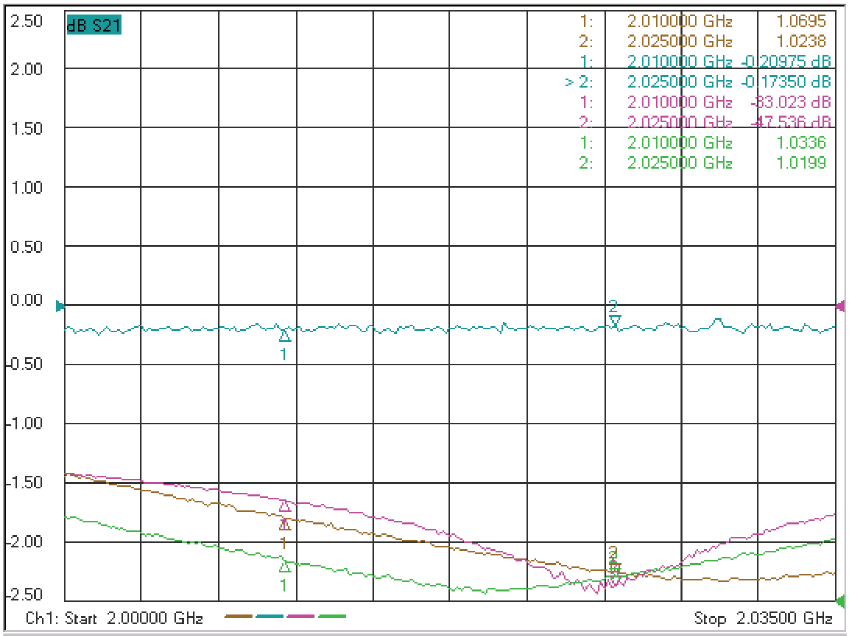

- Insertion Loss: 0.25dB
- Isolation: 25dB
- Application:

2.010~2.025GHz, 3.1~3.5GHz, 5.3~5.9GHz

- Other bands are available

Waveguide Isolators

Surface Mount Circulators

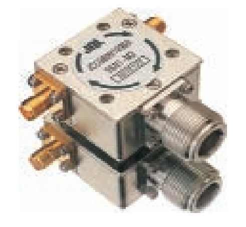

Coaxial Circulators

Cavity Filters

Ceramic Filters

JQL

Tel:1(888)236-9828(US&Canada)
www.jqlelectronics.com sales@jqlelectronics.com

ANALYSIS AND DESIGN OF THE DOHERTY AMPLIFIER BASED ON CLASS F AND INVERSE CLASS F AMPLIFIERS

In this article, a new Doherty amplifier using high-efficiency inverse class F and class F amplifiers is presented. The characteristics of inverse class F and class F amplifiers have been analyzed for their bias conditions and load impedances in order to identify their suitability to be the carrier or peaking amplifier in a Doherty amplifier. An inverse class F amplifier was employed for the carrier amplifier due to its superior linearity and efficiency performance over a wide range of load impedances. The class F amplifier was used for the peaking amplifier by virtue of its larger gain expansion characteristics. The proposed Doherty amplifier was configured using the implemented inverse class F and class F amplifiers for the 1 GHz band and evaluated using two-tone and down-link WCDMA signals. A state-of-the-art efficiency performance was achieved at a given linearity level: A power-added efficiency of 50.9 percent at a third-order intermodulation distortion level of -30 dBc from the two-tone test and 45.2 percent at an adjacent leakage power ratio of -30 dBc from the WCDMA test, respectively.

Wide-band signals with a high peak-to-average ratio (PAR) have been extensively adopted in modern wireless communication systems. For radio-frequency circuit designers, the efficiency versus linearity trade-off turns into one of the most important design considerations. Doherty amplifiers, which employ a load impedance modulation technique, have been adopted for use in base station power amplifiers due to their simple structure, good linearity and high efficiency at average output power levels.[1-6] For high efficiency, various class F and inverse class F (or class F^{-1}) amplifiers have been analyzed and implemented. Most of the previous work regarding class F or class F^{-1} amplifiers has been designed to enhance efficiency.[7-9] However, these amplifiers inherently have poor linearity due to excessive harmonics in the voltage or current waveforms.[10]

XI YAO, S.C. JUNG, M.S. KIM, J.H. VAN, H. CHO, S.W. KWON, J.H. JEONG, K.H. LIM, C.S. PARK AND Y. YANG
Sungkyunkwan University, Suwon, Korea
H.C. PARK
LG Electronics, Seoul, Korea

S. Goto, et al proposed a Doherty amplifier with a combination of class F and inverse class F amplifiers.[11] They reported high efficiency at an output power back-off of 10 dB for two-tone excitation. However, the efficiency and linearity rapidly degraded after the peak point, which can result in significant performance degradation for the signals having much higher peak-to-average power ratio (PAR or PAPR), such as the down-link wide-band code division multiple access (WCDMA) signals. J. Kim, et al proposed a saturated Doherty amplifier using class F amplifiers.[12] They reported very high efficiency but poor linearity. For the WCDMA signal, the reported performance could not come down to an adjacent channel leakage power ratio (ACLR) of -30 dBc. The ACLR performance got even worse for the lower output power level.

In this article, a new Doherty amplifier using class F and F^{-1} amplifiers is proposed. Various possible configurations for the Doherty amplifier were compared with each other, using circuit simulations for a high-power transistor. Based on the simulation and analysis results, it was determined that the performance of the Doherty amplifier can be significantly improved using class F^{-1} as the carrier and class F as the peaking amplifier cell, while the conventional configuration deploys class AB for the carrier and class B for the peaking amplifier. The proposed configuration is exactly opposite to that of S. Goto, et al.[11]

The proposed configuration of the Doherty amplifier was implemented and evaluated for the 1 GHz band using two-tone and down-link WCDMA signals. The measured performance of the proposed Doherty amplifier was compared with a balanced configuration using the same amplifier circuits.

THE CLASS F AND F^{-1} AMPLIFIERS

An ideal class F amplifier is required to have a half-sine current waveform, containing even harmonics, and a square voltage waveform, containing odd harmonics. Meanwhile, an ideal class F^{-1} amplifier is required to have a half-sine voltage waveform and a square current waveform. The efficiency of the class F and F^{-1} amplifiers has been well investigated in many previous research efforts, but the linearity of both amplifiers has not been seriously taken into account. To maximize efficiency, both amplifiers are mostly biased to the class B or C point and terminated with optimized impedances so that the highest power-added efficiency (PAE) can be extracted. However, the highly truncated current waveform, which contains abundant harmonics, ruins the linearity performance of the class F and F^{-1} amplifiers.

The bias point of the class F and F^{-1} amplifiers can be raised from class B or C toward AB so that they have appropriate harmonic current and voltage levels for better linearity. The fundamental impedance should also be tuned not only for efficiency but also for linearity. In order to gain high efficiency and good linearity at the same time, the class F and F^{-1} amplifiers were biased to a class AB and the fundamental impedance was optimized for the best compromised efficiency and linearity.

The output networks of the class F and F^{-1} amplifiers are shown in ***Figure 1***. Because the high-power transistors include significant internal parasitic components, the second and third harmonic control circuits should be located right after the transistor and properly tuned for both amplifiers.[7] A λ/4 short-stub transmission line was used for both the second harmonic control and drain bias feed and a λ/12 open stub transmission line was used for the third harmonic control. Afterward, the low pass fundamental matching network followed and transformed the optimum fundamental load impedance to a 50 Ω load.

For design validation, a harmonic balance simulation was carried out for both amplifiers. The amplifiers were designed using Freescale's MRF281S, a 4 W laterally diffused metal-oxide-semiconductor field effect transistor (LDMOS FET). Since the class F amplifier had the second harmonic impedance shorted and the third harmonic impedance open, the drain current peaking for the second harmonic frequency band and drain voltage peaking for the third harmonic frequency band could be successfully achieved, as shown in ***Figure 2***. For

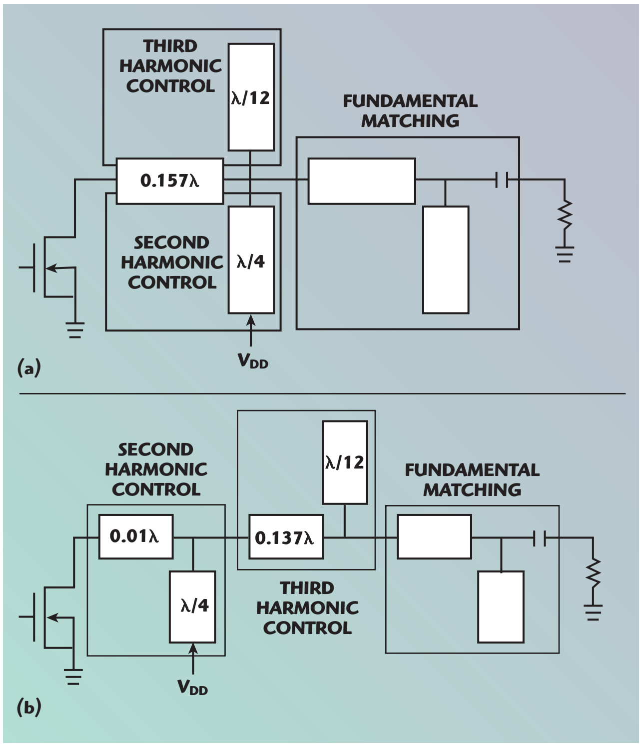

▲ *Fig. 1 Output circuit diagrams including harmonic control networks: (a) class F amplifier and (b) class F^{-1} amplifier.*

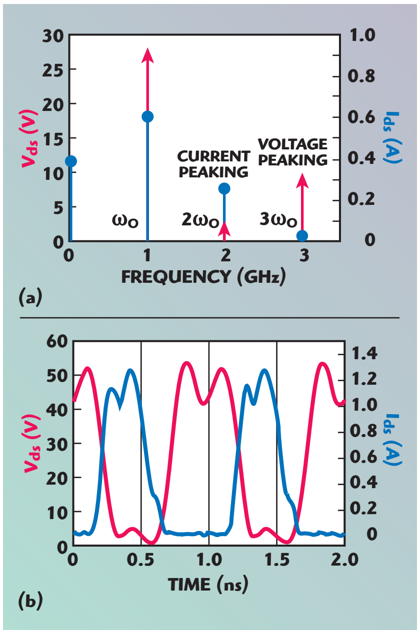

▲ *Fig. 2 Simulated output voltage and current of the class F amplifier at peak power added efficiency: (a) spectra and (b) waveforms.*

TWT Broadband Power Amplifiers

Ideal For: Radar, EW & EMI/EMC Testing

2.5 – 7.5 GHz 500W
2.0 – 8.0 GHz 370W
6.0 – 18.0 GHz 250W
7.5 – 18.0 GHz 250W
18.0 – 26.5 GHz 45W
26.5 – 40.0 GHz 35W
18.0 – 40.0 GHz 45W

Features Include:

- *Compact Size*
- *Forced Air Cooling*
- *Quiet Operation*
- *Extensive Diagnostic With Ethernet Interface*
- *Advanced Thermal Design*

Indoor & Outdoor Applications

For additional information, please contact:
MCL Sales Department at (630) 759-9500 or sales@mcl.com
MITEQ's Component Sales Department at (631) 439-9220 or components@miteq.com

MITEQ

100 Davids Drive
Hauppauge, NY 11788
TEL.: (631) 436-7400 • FAX: (631) 436-7430
www.miteq.com

MCL INC
A MITEQ COMPANY

501 South Woodcreek Drive
Bolingbrook, IL 60440-4999
TEL.: (630) 759-9500 • FAX: (630) 759-5018
www.mcl.com

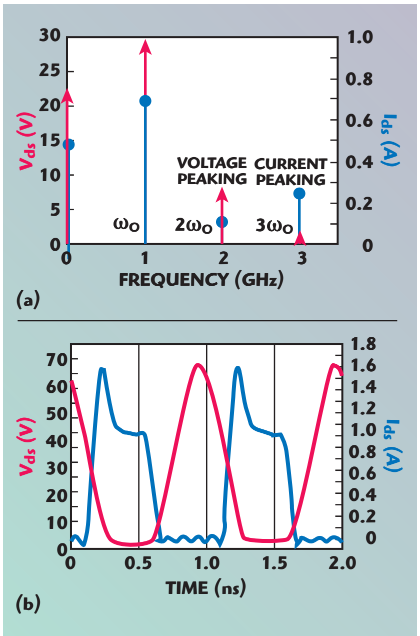

▲ *Fig. 3 The simulated output voltage and current of the class F^{-1} amplifier at the peak PAE point: (a) spectrum and (b) waveform.*

a class F^{-1} amplifier, the second harmonic voltage peaking and the third harmonic current peaking were clearly observed from ***Figure 3***. The resultant time domain current and voltage waveforms are also shown in the figures for class F and F^{-1} amplifiers, respectively.

Table 1 summarizes the simulated and experimental performances of class F and F^{-1} amplifiers, where parantheses indicates a measured value. These amplifiers are all biased at the same class AB point (IDQ = 25 mA). For the two-tone test, the data was extracted at an IMD3 of -30 dBc. The simulated performance of the conventional class AB amplifier is also presented for comparison. For two-tone excitation, the performance of class F and F^{-1} amplifiers exhibit comparable efficiencies and a little higher output power at a given third-order intermodulation distortion (IMD3) requirement of -30 dBc. In addition, the peak PAEs are improved by as much as 4.5 and 8.1 percent for the class F and F^{-1} amplifiers, respectively. Consequently, a comparable linearity and much higher peak PAEs were achieved using class AB biased class F and F^{-1} amplifiers, when compared to the conventional class AB amplifier.

TABLE I

THE SIMULATED AND EXPERIMENTAL RESULTS FOR CLASS F AND F^{-1} AMPLIFIERS COMPARED TO THE SIMULATED CLASS AB AMPLIFIER

	P_{out} (dBm) (Two-tone)	Gain (dB) (Two-tone)	PAE (%) (Two-tone)	Peak PAE (%) (One-tone)
Class AB	33.89	17.89	40.09	57.09
Class F	34.14 (33.32)	17.34 (17.65)	39.12 (43.79)	61.58 (56.80)
Class F^{-1}	34.66 (33.47)	16.86 (17.20)	39.91 (41.74)	65.17 (58.62)

THE CONFIGURATION OF THE NEW DOHERTY AMPLIFIER

The Peaking Amplifier

In the configuration for the Doherty amplifier, the peaking amplifier is generally biased to a class B or C point for two main reasons, while the carrier amplifier is generally biased to a class AB point. First, this low bias could be used

to improve linearity: The third-order intermodulation current of the class B or C amplifier has an opposite phase to the class AB amplifier. Hence, the resultant IMD3 can be improved.

Second, this low bias of the peaking amplifier ensures a correct load modulation in the low power region. Because the peaking amplifier should be turned off in a low power region and supply the same current to the load at a high power level, its gain expansion should be high enough. The sufficiently large gain expansion, which allows it to have a proper ON/OFF transition according to the output power level, is thus a very desirable characteristic for a peaking amplifier.

Therefore, an analysis for the gain expansion of the class F and F^{-1} amplifiers was performed in detail. An output current for the weakly nonlinear current source in general common source amplifiers can be expressed using the Taylor series expansion:

$$i_d(t)=g_{m1}v_g(t)+g_{d1}v_d(t)+g_{m2}v_g(t)^2+g_{md}v_g(t)v_d(t)+g_{d2}v_d(t)^2+g_{m3}v_g(t)^3+\ldots \quad (1)$$

where $v_g(t)$ is an input signal. The g_{mx} and g_{dx} are the xth-order nonlinear expansion coefficients for transconductance and conductance, respectively. If the one-tone signal is excited ($v_g(t) = A\cos\omega_0 t$), the output voltage at the load $Z(\omega)$ can be represented using each harmonic current component:

$$\begin{aligned} v_d(t) &= -i_d(t)Z(\omega) \\ &= -\{i_d(t,\omega_0)Z(\omega_0)+i_d(t,2\omega_0)Z(2\omega_0)+i_d(t,3\omega_0)Z(3\omega_0)+\ldots \end{aligned} \quad (2)$$

where $i_d(t, \omega_0)$ is the n^{th}-order harmonic component of the nonlinear output current and $Z(n\omega_0)$ is the impedance at an n^{th}-order harmonics band.

The output power including harmonic components can be calculated by multiplication of the output current and voltage. The power gain using the dominant terms for the fundamental output power can be expressed:

$$G_P \approx g_{m1}^2 R(\omega_0) R_{in} \cdot \left|1+\frac{3g_{m3}A^2}{4g_{m1}}-\frac{g_{md}g_{m2}A^2Z(2\omega_0)}{4g_{m1}}\right|^2 \quad (3)$$

where $R(\omega_0)$ is the real part of the load impedance for the fundamental frequency band. R_{in} is the input resistance. Since the g_{m3} has a positive value for the class B bias point, the second term in the bracket of Equation 3 contributes to the gain expansion at moderate output levels. However, the third term pulls down the expanded gain by the second term as the real part of the load impedance at the second harmonics band ($Z(2\omega_o)$) becomes larger.

Therefore, the class F amplifier, which has a second harmonic impedance $Z(2\omega_0)$ near 0, gets a larger gain expansion than that of the class F^{-1} amplifier, which has a very large $Z(2\omega_0)$ value. The large-signal simulation results, according to various values of the second harmonic imped-

ance for the gain expansion characteristics, are presented in ***Figure 4***. To clearly see the effect of the second harmonic impedance on the gain expansion, an intrinsic transistor model without any parasitic component was used. As the second harmonic impedance went up, the gain expansion decreased. From the 0 to the 1280 Ω of the second harmonic impedance, more than a 5 dB gain difference was observed.

As a result, the class F^{-1} amplifier is not suitable for the peaking amplifier cell, due to an insufficient gain expansion, even with a class B bias point. On the contrary, the class F amplifier, which has a maximum gain expansion, is expected to deliver a superb performance as the peaking amplifier.

The Carrier Amplifier

The ideal Doherty amplifier can be simply modeled using two correlated current sources for the carrier and peaking amplifiers, a quarter-wave transmission line and the load resistor, as shown in ***Figure 5***. The carrier current source flows through the quarter-wavelength line. The impedance seen from the quarter-wave line toward the load becomes:

$$Z'_1 = \frac{V_0}{I'_1} = \frac{R_0}{2} \cdot \frac{I'_1 + I_2}{I'_1} \qquad (4)$$

where V_0 is the load voltage. The quarter-wave line then transforms the impedance Z'_1 to Z_1:

$$Z_1 = \frac{R_0^2}{Z'_1} = \frac{2R_0}{(1 + I_2/I'_1)} = \frac{2R_0}{1+\alpha} \qquad (5)$$

where $\alpha = I_2/I'_1$. Because the magnitude of I'_1 equals that of I_1, the actual load impedance of the carrier amplifier can be modulated as α varies from 0 ($|I_2| = 0$) to 1 ($|I_2| = |I'_1|$).

$$Z_1 = \begin{cases} R_0, & \text{if } \alpha = 1 \\ 2R_0, & \text{if } \alpha = 0 \end{cases} \qquad (6)$$

At the mid power level, the peaking amplifier works in the transition region between OFF and ON, where the carrier amplifier has a load modulation from $2R_0$ to R_0. Since the carrier amplifier operates under dynamically varying load impedances, according to the output power level, it is generally biased to a class AB point for enough gain even at a very low power level. It should also show good performance while the load impedance varies from $2R_0$ to R_0.

Even for a fixed quiescent current of I_{DQ}, the operational class of the carrier amplifier can also vary according to the load impedance. If the carrier amplifier is intended to have a class AB bias point for the load impedance R_0 at the peak power level, its operation class approaches to a class A as the load impedance is modulated to $2R_0$ (see ***Figure 6***). In other words, the conduction angle for the load impedance $2R_0$ is much larger than that for R_0.

Compared to a class F amplifier, the class F^{-1} amplifier has less degradation

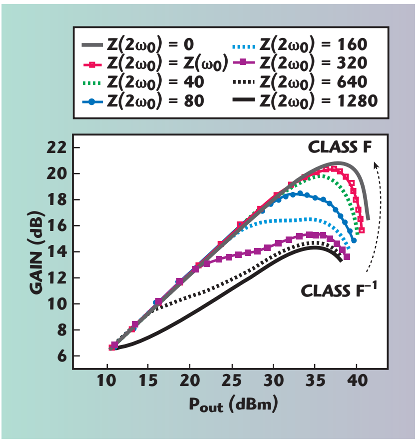

Fig. 4 Simulated gain expansion according to second harmonic impedances.

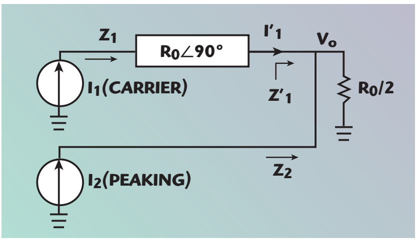

Fig. 5 A simplified operational diagram for the Doherty amplifier.

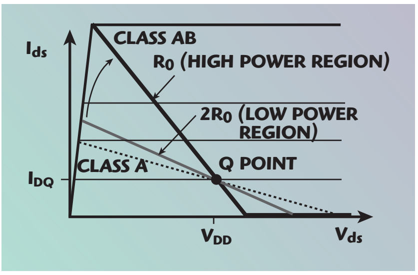

Fig. 6 Operational class variations over the load impedance increase for a fixed quiescent current level.

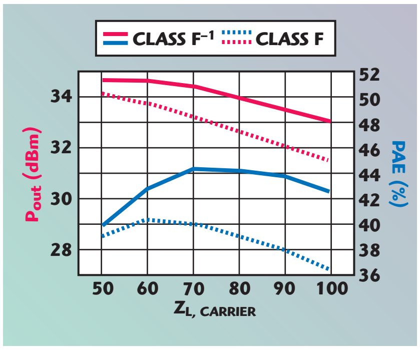

▲ *Fig. 7 Simulated PAE and output power for the class F and F^{-1} amplifiers at an IMD3 level of –30 dBc for various load impedances.*

in PAE at an increased bias condition.[9] Hence, it can be easily surmised that the class F^{-1} amplifier would outperform the class F amplifier at larger load impedance. A two-tone harmonic balance simulation was conducted to verify this hypothesis. The load impedance of the carrier amplifier was swept from 50 Ω (R_0) to 100 Ω ($2R_0$). Both the simulated PAE and output power performance of the class F^{-1} amplifier became better and better than the performance of the class F amplifier at the fixed IMD3 level as the load impedance increased (see **Figure 7**).

Therefore, it can be concluded that the class F^{-1} amplifier should be selected for the carrier amplifier rather than the class F amplifier in spite of their similar performance at the class B bias condition. In the previous subsection, the class F amplifier was already chosen as the peaking amplifier. The new Doherty amplifier configuration, using class F and class F^{-1} amplifiers, is shown in **Figure 8**.

VERIFICATION FOR THE NEW CONFIGURATION

To validate the proposed Doherty amplifier configuration, deploying the class F amplifier for the peaking amplifier and the class F^{-1} amplifier for the carrier amplifier, all four possible configurations for the Doherty amplifier using class F and F^{-1} amplifiers were compared. They are also compared with the conventional Doherty amplifier using a class AB carrier amplifier and class B peaking amplifier.

The class F, F^{-1}, AB and B amplifiers for the 1.0 GHz band were designed for the simulation using a 4 W LDMOS FET. A two-tone harmonic balance simulation was carried out for each possible configuration after optimizing each to have its best performance by tuning the offset lines and the bias condition of the peaking amplifier. The carrier amplifiers have the same fixed I_{DQ} of 25 mA for all of the configurations, while the peaking amplifiers had optimized bias conditions, which were near the class B point and not significantly different from each other. The simulated results for the five configurations are summarized in **Table 2**, where the data for the two-tone test was extracted at an IMD3 of -30 dBc.

As expected, the configuration using the class F^{-1} carrier amplifier and the class F peaking amplifier exhibited the highest output power and PAE at the same time among any other com-

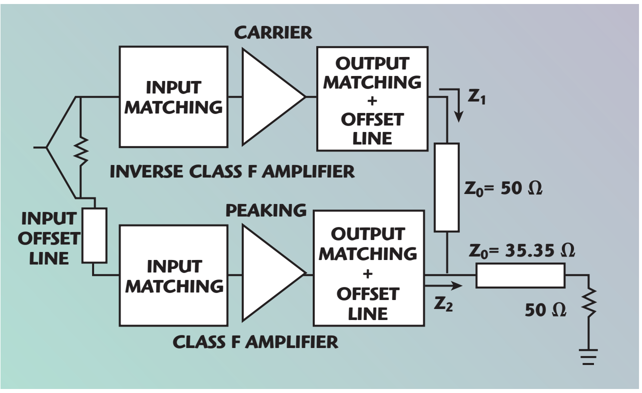

▲ *Fig. 8 Schematic diagram of the designed Doherty amplifier.*

TABLE II
THE SIMULATION RESULTS FOR ALL POSSIBLE CONFIGURATIONS OF THE DOHERTY AMPLIFIER USING THE CLASS F AND F^{-1} AMPLIFIERS

Carrier Amplifier	Peaking Amplifier	P_{out} (dBm) (Two-tone)	PAE (%) (Two-tone)	Peak PAE (%) (One-tone)
Class AB	Class B	36.62	47.85	59.78
Class F	Class F	37.12	48.62	66.82
Class F^{-1}	Class F^{-1}	37.17	51.98	65.94
Class F	Class F^{-1}	35.31	45.05	59.82
Class F^{-1}	Class F	**37.38**	**53.88**	**69.68**

Simple solutions to complex microwave problems

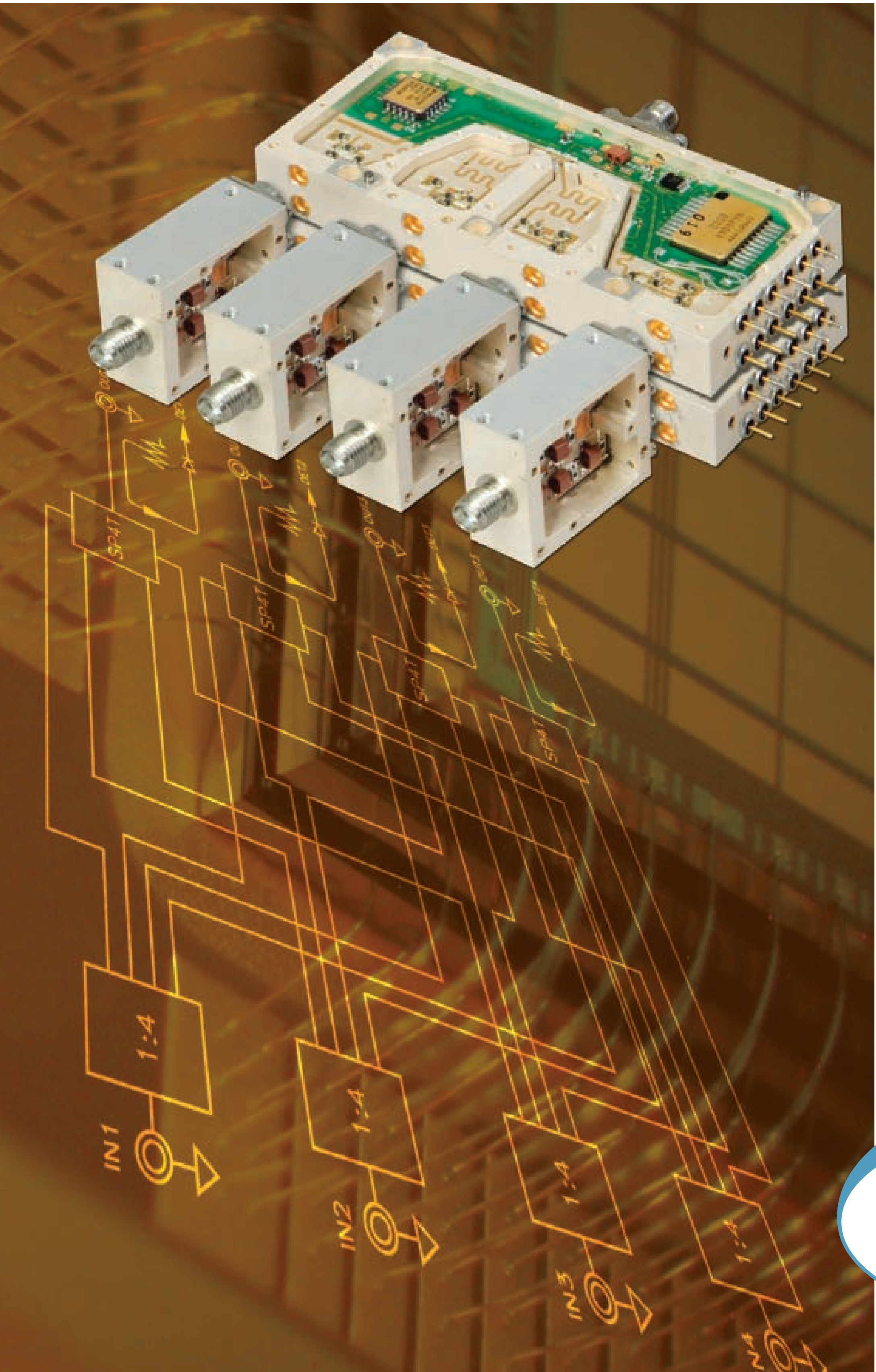

Aeroflex / KDI-Integrated Products has over 50 years of experience in designing and delivering Integrated Microwave Assemblies (IMAs), built to your exact form/fit/function requirements. We can combine attenuators, limiters, switches, phase shifters, detectors, and other digital and/or microwave circuitry to form complex integrated assemblies that save valuable real estate and achieve critical weight restrictions. Examples are:

- Blocking and non-blocking switch matrices
- EW/ECM/ESM assemblies
- Time-delay units
- IFF high-power assemblies

Built with state-of-the-art chip and wire assembly techniques, we utilize our core competencies to provide:

- 0.5 to18.0 GHz frequencies
- 1 W to 4 KW RF power
- Minimization/elimination of interconnections, cross-overs.

Contact us and discover why most of our customers are repeat customers.

SEE US AT MTT-S BOOTH 1310

973-887-5700

www.aeroflex.com/KDI-Integrated

KDI-integrated-sales@aeroflex.com

AEROFLEX
A passion for performance.

Visit http://mwj.hotims.com/28487-6 or use RS# 6 at www.mwjournal.com/info

binations using class F and F^{-1} amplifiers. The opposite configuration using a class F carrier amplifier and class F^{-1} peaking amplifier exhibited the worst. This backed up the analyses and descriptions in the previous subsections.

Compared with the conventional class AB and B based Doherty amplifier, the best configuration delivered more output power, as much as 0.76 dB, and better PAE, as much as 6.03 percent points, at an IMD3 of -30 dBc. Benefiting from harmonic tuning and proper selection for the carrier and peaking amplifiers, these amplifiers can further gain approximately a 10 percent higher peak PAE for a one-tone signal input than that of a conventional Doherty amplifier.

IMPLEMENTATION AND EXPERIMENTAL RESULTS

Because conventional Doherty amplifiers are generally built with identical cells for both carrier and peaking amplifiers, the phase difference of the transmission coefficient between the carrier and peaking amplifier is not significant and can be easily compensated using a tuned input offset line. However, in this case, the difference in the phase response between the class F^{-1} carrier and class F peaking amplifiers should be carefully considered since different amplifiers are employed as the carrier and peaking amplifier cells.

The amplitude modulation to phase modulation (AM to PM) characteristics for the carrier and peaking amplifiers were measured using a network analyzer. ***Figure 9*** shows the measured phase responses of the carrier and peaking amplifiers. As shown, the phase response of the peaking amplifier experienced a huge transition due to a class B bias point while that of the carrier amplifier appeared to be rather flat. The phase difference of about 54.35° was observed around 1 dB gain compression point. It was compensated using an input offset line which was already presented in Figure 8.

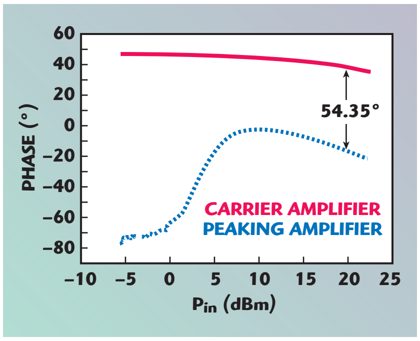

Fig. 9 Measured phase responses of the carrier and peaking amplifiers.

The Doherty amplifier based on class F and F^{-1} amplifiers was implemented using the same device that was used for the design and simulation. ***Figure 10*** shows a photograph of the implemented Doherty amplifier. The fundamental load impedance of (21 + j19) Ω, extracted from the class AB amplifier design, was applied for both the class F and F^{-1} amplifiers. The output offset lines were also added at the end of each amplifier, after the matching networks, to have a proper load impedance modulation. The difference of the output offset lines between the carrier and peaking amplifiers was also compensated in the input offset line. The efficiency and linearity of the Doherty amplifier were simultaneously optimized using a bias adjustment especially for the peaking amplifier. The optimum quiescent current (I_{DQ}) for the peaking amplifier was 1.25 mA, which was almost a class B condition. The quiescent current of the carrier amplifier was 25 mA.

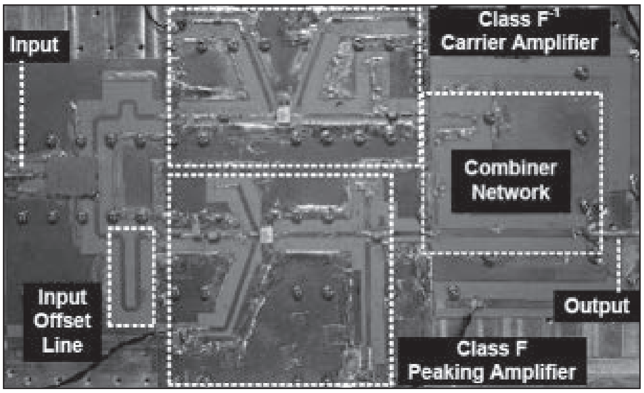

Fig. 10 Photograph of the implemented Doherty amplifier.

The Doherty amplifier was evaluated using the one-tone, two-tone and downlink WCDMA signals. The WCDMA signal has a PAR of 10.5 dB at a complementary cumulative distribution function (CCDF) of 0.01 percent. To see if the load modulation successfully

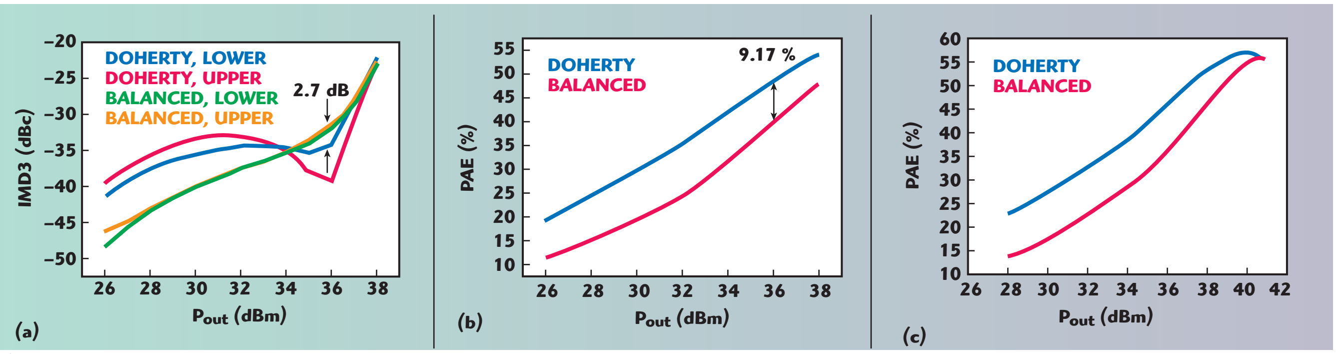

▲ *Fig. 11 Measured performance of the implemented Doherty and balanced amplifiers: (a) IMD3, (b) PAE for a two-tone signal and (c) PAE for a one-tone signal.*

happened, the performance was compared with those of the balanced amplifier with the same amplifier cells. ***Figure 11*** shows the IMD3 and PAE performance for a two-tone excitation at a center frequency of 1 GHz with a tone-spacing of 5 MHz. Compared with a balanced amplifier, improvements in IMD3 of 2.7 dB and PAE of 9.17 percent points were obtained for the Doherty amplifier at an output power of 36 dBm at the same time. Furthermore, a 0.21 dB higher output power and a PAE as high as 50.9 percent were extracted for the Doherty amplifier at an IMD3 level of -30 dBc. The proposed Doherty amplifier presented a peak PAE of 57.4 percent for the one-tone test, as shown also in the figure.

Figure 12 shows the PAE and adjacent channel leakage power ratio (ACLR) performances for the single-carrier down-link WCDMA signal. The proposed Doherty amplifier simultaneously exhibited an improved ACLR by 1.71 dB and a higher PAE by 11.26 percent points at an output power of 34 dBm. More output power, 0.32 dB, and a PAE of 45.2 percent were obtained using the Doherty amplifier at an ACLR of -30 dBc at a 2.5 MHz offset. ***Table 3*** shows a comparison between the measured results in this work with previous works.

CONCLUSION

To improve efficiency under a critical linearity specification for high-power amplifiers, a Doherty amplifier based on class F and F^{-1} amplifiers is proposed. In the new Doherty configuration, class F^{-1} and F amplifiers are used as the carrier and peaking amplifiers, respectively. To determine the Doherty amplifier configuration, the properties of the class F and F^{-1} amplifiers were comprehensively investi-

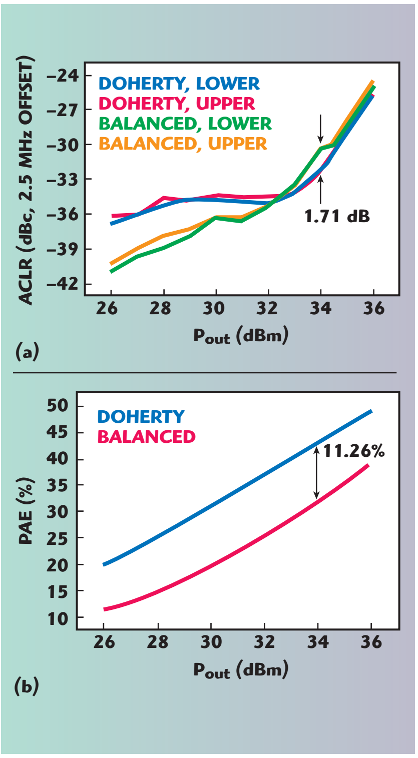

▲ *Fig. 12 Measured performance of the implemented Doherty and balanced amplifiers using a down-link WCDMA signal: (a) ACLR at 2.5 MHz offset and (b) PAE.*

TABLE III

THE PERFORMANCE COMPARISON TO RESULTS FROM PREVIOUSLY PUBLISHED INFORMATION ON DOHERTY AMPLIFIERS

Description	Two-tone (IMD3: -30 dBc)		WCDMA (ACLR: -30 dBc)		Frequency band	Reference
	P_{out} (dBm)	PAE (%)	P_{out} (dBm)	PAE (%)		
Doherty, compact load network	36	43	34.6	41.5	859 MHz	[3]
Doherty, envelope injection	N/A	N/A	46	40	2.14 GHz	[4]
Doherty, optimized linearity	50	40	48	37	2.14 GHz	[5]
Doherty, GaAs HBT	25	40	N/A	N/A	1.88 GHz	[6]
Doherty, GaAs HFET	30	53	N/A	N/A	2.14 GHz	[11]
Doherty, class F^{-1} and F	36.73	**50.9**	34.74	**45.2**	1.0 GHz	This work

gated and compared with each other.

The class F amplifier turned out to be best suited for the peaking amplifier because of the large gain expansion characteristics for operation at a low bias point. On the other hand, the class F^{-1} amplifier was verified to have better performance at higher load impedance, using load line analysis and simulation, which was why it was selected for the carrier amplifier.

The high-efficiency class F and F^{-1} amplifiers were designed and implemented for the 1 GHz band. Their performance was optimized to have the highest possible PAE under a given linearity specification as an IMD3 of -30 dBc. The simulated and measured performances were compared to the simulated conventional class AB amplifier. Using the designed class F, F^{-1}, AB and B amplifiers, various configurations for the Doherty amplifier were synthesized and compared to each other using harmonic balance simulations. As expected, the proposed Doherty configuration significantly outperformed among all the others.

For experimental verification, the proposed Doherty amplifier was implemented as designed using Freescale's MRF281S, a 4 W-PEP LDMOS FET. The measured results include significantly improved performance for the Doherty operation compared to those for the balanced operation. A PAE of 50.9 percent was obtained for the two-tone test at an IMD3 of -30 dBc with a 5 MHz tone spacing. A PAE of 45.2 percent was achieved for the down-link WCDMA signal at an ACLR of -30 dBc at a 2.5 MHz offset using the proposed Doherty amplifier. Both are showing state-of-the-art efficiency performances for the given linearity levels among the previously reported Doherty amplifiers. ■

References

1. Y. Yang, J. Cha, B. Shin and B. Kim, "A Fully Matched N-way Doherty Amplifier with Optimized Linearity," *IEEE Transactions on Microwave Theory and Techniques*, Vol. 51, No. 3, March 2003, pp. 986-993.
2. G. Ahn, M. Kim, H. Park, S. Jung, J. Van, H. Cho, S. Kwon, J. Jeong, K. Lim, J. Kim, S. Song, C. Park and Y. Yang, "Design of a High-efficiency and High-power Inverted Doherty Amplifier," *IEEE Transactions on Microwave Theory and Techniques*, Vol. 55, No. 6, June 2007, pp. 1105-1111.
3. H. Park, J. Van, S. Jung, M. Kim, H. Cho, S. Kwon, J. Jeong, K. Lim, C. Park and Y. Yang, "A New Compact Load Network for Doherty Amplifiers Using an Imperfect Quarter-wave Line," *IEEE Transactions on Microwave Theory and Techniques*, Vol. 55, No. 11, November 2007, pp. 2313-2319.
4. J. Cha, J. Kim, B. Kim, J. Lee and S. Kim, "Highly Efficient Power Amplifier for CDMA Base Stations Using Doherty Configuration," *2004 IEEE MTT-S International Microwave Symposium Digest*, pp. 533-536.
5. K. Cho, I. Hwang, W. Kim, J. Kim and S.P. Stapleton, "Linearity Optimization of a High Power Doherty Amplifier," *2005 IEEE MTT-S International Microwave Symposium Digest*, pp. 1387-1390.
6. Y. Zhao, A.G. Metzger, P.J. Zampardi, M. Iwamoto and P.M. Asbeck, "Linearity Improvement of HBT-based Doherty Power Amplifiers Based on a Simple Analytical Model," *IEEE Transactions on Microwave Theory and Techniques*, Vol. 54, No. 12, December 2006, pp. 4479-4488.
7. H. Park, G. Ahn, S. Jung, C. Park, W. Nah, B. Kim and Y. Yang, "High Efficiency Class-F Amplifier Design in the Presence of Internal Parasitic Components of Transistors," *Proceedings of the 36th European Microwave Conference, September 2006*, pp. 184-187.
8. S. Gao, P. Butterworth, S. Ooi and A. Sambell, "High Efficiency Power Amplifier Design Including Input Harmonic Termination," *IEEE Microwave and Wireless Components Letters*, Vol. 16, No. 2, February 2005, pp. 81-83.
9. S. Goto, T. Kunii, A. Ohta, A. Inoue, Y. Hosokawa, R. Hattori and Y. Mitsui, "Effect of Bias Condition and Input Harmonic Termination on High Efficiency Inverse Class-F Amplifiers," *Proceeding of the 31st European Microwave Conference*, October 2001, pp. 1-4.
10. A. Ohta, A. Inoue, S. Goto, K. Ueda, T. Ishikawa and Y. Matsuda, "Intermodulation Distortion Analysis of Class-F and Inverse Class-F HBT Amplifiers," *IEEE Transactions on Microwave Theory and Techniques*, Vol. 53, No. 6, June 2005, pp. 2121-2128.
11. S. Goto, T. Kunii, A. Inoue, K. Izawa, T. Ishikawa and Y. Matsuda, "Efficiency Enhancement of Doherty Amplifier with Combination of Class-F and Inverse Class-F Schemes for S-band Base Station Application," *2004 IEEE MTT-S International Microwave Symposium Digest*, pp. 839-842.
12. J. Kim, J. Moon, Y.Y. Woo, S. Hong, I. Kim, J. Kim and B. Kim, "Analysis of a Fully Matched Saturated Doherty Amplifier with Excellent Efficiency," *IEEE Transactions on Microwave Theory and Techniques*, Vol. 56, No. 2, February 2008, pp. 328-338.

A Small Printed Ultra-wideband Polygon-like Wide-slot Antenna with a Fork-like Stub

In this article, a novel design of a printed wide-slot antenna with small size, fork-like tuning stub and symmetric structure is presented and experimentally studied, especially for ultra-wideband (UWB) applications. In this design, by embedding three rectangular notches at the edge of the symmetric polygon-like slot below the microstrip-fed line, and by optimizing the feeding structure, new resonant frequencies are generated and the measured impedance bandwidth is increased up to 134.6 percent, from 2.5 to 12.8 GHz, for a VSWR less than 2. This optimized antenna has compact dimensions of 35 × 44 mm with a peak antenna gain of approximately 4.7 dBi.

Printed slot antennas are currently under consideration, especially for use in ultra-wideband (UWB) applications, due to their attractive merits, such as lightweight, ease of fabrication and wide frequency bandwidth.[1] In addition, these antennas are completely planar and are easily integrated with active devices or monolithic microwave integrated circuits (MMIC).[2] On the other hand, these antennas require a large area for the slot and a much larger area for the conductor plane around the slot.[3] Moreover, it can be observed that most broadband designs of a slot antenna are possible, but not with a small size. Therefore, reducing the antenna size, decreasing the cost of manufacturing and also increasing the bandwidth are important goals.[4] Recently, there has also been growing research activity on many other microstrip-line-fed printed slot antennas, especially printed wide-slot antennas[5,6] because of their favorable impedance characteristics. In these designs, the characteristics of printed wide-slot antennas fed by a microstrip line with various tuning stubs have also been studied. A novel printed wide-slot antenna fed by a microstrip line with a fork-like tuning stub has been presented,[6] which is good for bandwidth enhancement but not enough for the UWB applications.

In another design of a wide-slot antenna with a fork-like stub and a square-ring slot,[7] a bandwidth of 114 percent, from 3 to 11 GHz, for a VSWR less than 2.2, has been achieved with dimensions of 100 × 120 mm. A good design of a wide-slot antenna with an octagonal-shaped slot has recently been reported,[8] which has the compact dimensions of 29 × 30 mm and a bandwidth from 2.9 to 12 GHz, for a return loss lower than 10 dB. Two small notches in the bottom edge of the slot are used, but only for fine tuning the im-

Majid Razavi-Rad, Changiz Ghobadi, Javad Nourinia and Reza Zaker
Urmia University, Urmia, Iran

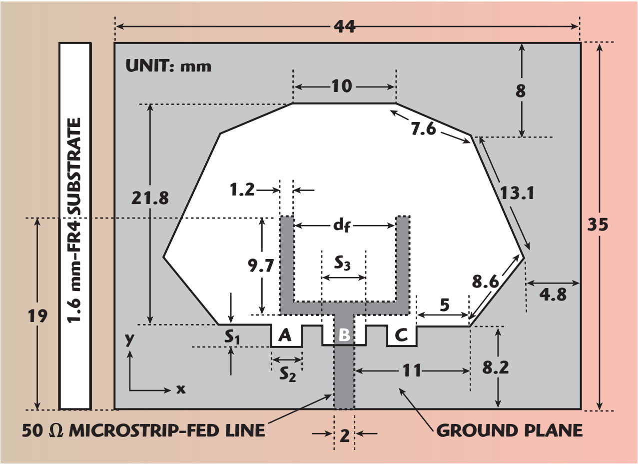

▲ *Fig. 1 Geometry of the proposed polygon-like wide-slot antenna with a microstrip fork-like stub.*

pedance matching characteristics and not for enhancing the total bandwidth.

In this article, a novel design of a printed symmetric wide-slot antenna with small size and good characteristics is proposed and investigated in detail. By using the etched modified octagonal wide slot in the ground plane, three notches in the bottom edge of the slot below the microstrip-fed line and a fork-like tuning stub, an impedance bandwidth from 2.5 to 12.8 GHz with good matching and relatively constant gain can be achieved. In this present deign, small notches are used in order to generate the additional resonant frequencies and also tune the matching simultaneously. Numerical and experimental results for the frequency characteristics, surface currents, radiation patterns, and gain of this proposed slot antenna are also presented and discussed.

ANTENNA CONFIGURATION AND DESIGN

The geometry (with dimensions) of the proposed microstrip-fed wide-slot antenna is illustrated in ***Figure 1***. It shows that the antenna is similar to conventional wide-slot antennas, but with some modifications in the shape of the slot. A modified octagonal wide slot with unequal sides, etched in the ground plane, is used as a radiator, and a microstrip fork-like tuning stub is placed on the other side of the substrate to feed the slot aperture. By using the results obtained by S. Sadat, et al.,[9] and their extensions, it can be said that this octagonal-like slot can excite four different resonant modes with close resonant frequencies. Moreover, this fork-like (U-shaped) tuning stub is introduced to enhance the coupling between the slot and the feed line so as to broaden the operating bandwidth of the antenna, as reported by Li.[1]

Two small notches, denoted by A and C, respectively, with equal dimensions of $S_1 \times S_2$ and another notch (B) between them, with dimensions of $S_1 \times S_3$ are embedded at the bottom edge of the slot in order to generate the additional resonant frequencies and hence improve the total bandwidth and also finely tune the impedance matching characteristic. In this proposed design, the antenna is printed on both sides of an FR4 substrate with dimensions of 35 × 46 mm, thickness of 1.6 mm, relative permittivity ε_r = 4.4 and loss tangent = 0.02. The microstrip feed line of the antenna, with a width of 2 mm, is designed for a 50 Ω impedance and terminated with a standard SMA connector so that it can be connected directly to a measurement system or other standard microwave modules, as shown in ***Figure 2***. All the simulations have been carried out using a finite element method (FEM) software "Ansoft High-Frequency Structure Simulator" HFSS 10.[12]

PARAMETRIC STUDY AND DISCUSSION

The proposed modified octagonal wide-slot antenna without any notches (A, B and C) is considered. In this design, the sizes of the sides of the slot and the dimensions of the fork-like tuning stub are the important parameters that affect the existence and positions of the resonant frequencies and hence the total bandwidth and impedance matching. The optimized values of all sides of this slot, which are not equal to each other, are shown in the figure. Another important parameter (in the feeding structure) to be considered is the distance between two arms of the fork-like stub, d_f. In this study, the other dimensions of the tuning stub, especially the length of the two arms (= 9.7 mm), are fixed.

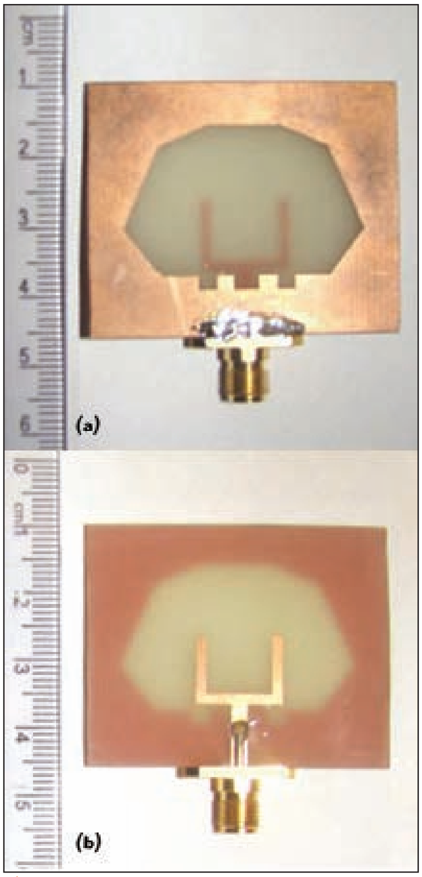

▲ *Fig. 2 Photographs of the fabricated prototype: (a) front and (b) back.*

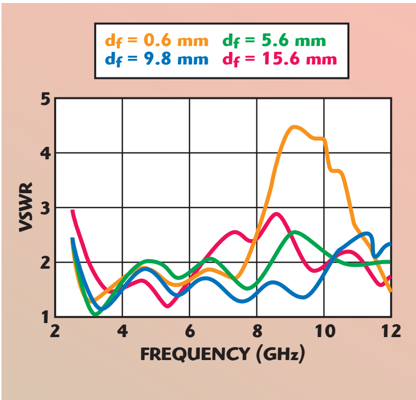

▲ *Fig. 3 VSWR characteristics for different values of d_f.*

Figure 3 shows the full wave VSWR simulation results of this proposed octagonal wide-slot antenna for different values of d_f. From this figure, it is clear that a wide bandwidth with relatively good matching especially in the upper bands is achieved by tuning the distance between the two arms of the fork-like stub, d_f. Moreover, it is seen that by using this form of the octagonal wide slot, four resonances can

TABLE I

THREE ANTENNAS WITH DIFFERENT NUMBER OF NOTCHES

Notch	A	B	C
Antenna I	X	✓	X
Antenna II	✓	X	✓
Antenna III	✓	✓	✓

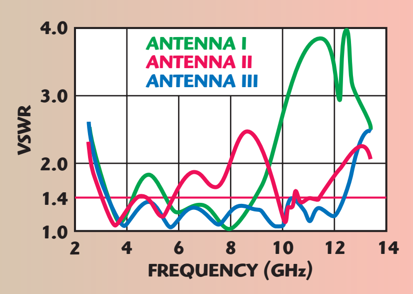

▲ *Fig. 4 Simulated VSWR characteristics with different number of notches.*

be excited. By selecting d_f = 9.8 mm, a wide bandwidth from 2.55 to 10.25 GHz (120.3 percent) for a VSWR less than 2 is obtained. Also note that, by varying the length and width of the two arms of the fork-like stub, the matching is only slightly affected and the bandwidth is about the same. From the geometry of the proposed antenna, it is observed that the internal periphery of this octagonal slot is equal to 92.6 mm (= 10 + (2 × 7.6) + (2 × 13.1) + (2 × 8.6) + 24 mm). This effective length is almost equivalent to 1.05λg, where λg corresponds to the first resonant frequency at 3.4 GHz, for d_f = 9.8 mm. This result shows that the performances of this proposed wide-slot antenna and a magnetic λ/2 dipole are similar.

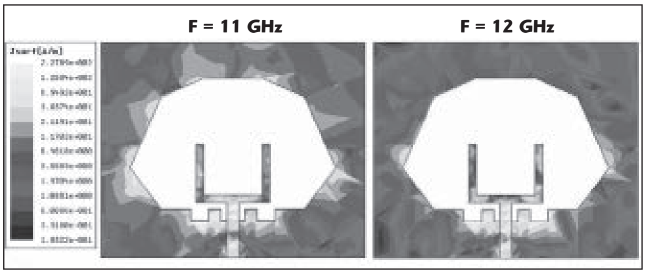

▲ *Fig. 5 Surface current distribution for antenna III.*

In this section, the effects of the three notches (A, B and C), embedded at the bottom edge of the octagonal wide slot on the total bandwidth and impedance matching, are investigated. Also note that these notches are placed below the microstrip-fed line. Therefore, they have a strong effect on the input impedance of the antenna (and hence the impedance matching). From previous discussions, it seems that the important effect of these notches is to generate additional resonances. As a result, by properly adjusting the positions and dimensions of these three notches, with small electrical sizes with respect to the first resonance, at the bottom edge of the slot, new additional resonant frequencies are generated at the higher end of the UWB range, and hence the total bandwidth is increased. Moreover, a very good impedance matching over the whole bandwidth is obtained.

The VSWR characteristics of the proposed modified octagonal wide-slot antenna with different numbers of notches for three various cases (three antennas: I, II and III) listed in ***Table 1***, are shown in ***Figure 4***. The positions of the three proposed notches are shown in the antenna geometry and their optimized dimensions are: S_1 = 2 mm, S_2 = 3 mm and S_3 = 4 mm. Comparing the three antennas (I, II, and III) shows that by using the three notches (A, B and C) simultaneously, a wide bandwidth with very good impedance matching can be achieved. Antenna III shows a simulated wide bandwidth from 2.5 to 12.8 GHz (134.6 percent) for a VSWR less than 2. By employing the three notches simultaneously, a very good impedance matching from 3.2 to 12.3 GHz (117.4 percent) for a VSWR less than 1.4 is also obtained. Therefore, this proposed structure of the wide-slot antenna is very suitable for UWB applications because of its small size, wide bandwidth and very good impedance matching. It is also noted that two new resonances at 11 and 12 GHz are generated, only because of using the three notches at the bottom edge of the slot. Although it is not shown here, it was found that by increasing S_3 (in Antenna I) or S_2 (in Antenna II), the upper edge of the frequency band is decreased. The performances of S_1, S_2 and S_3 are similar.

The simulated current distributions of the proposed octagonal-like wide-slot antenna at the two new resonances of the three notches (A, B & C), 11 and 12 GHz, are shown in ***Figure 5***. On the ground plane, the current is mainly distributed along the edge of the slot for all of the two different frequencies. More current distributions can be seen around the three notches than in any other areas of the ground plane, which implies that these notches resonate at 11 and 12 GHz.

EXPERIMENTAL RESULTS

Based on the optimized parameters of the proposed antenna (Antenna III in Table 1), a prototype antenna was fabricated on a FR4 substrate with dimensions of 35 × 44 × 1.6 mm. The impedance bandwidth was measured using an Agilent 8722ES Vector Network Analyzer, and is shown in ***Figure 6***, with good agreement between the simulated and measured results. The small difference between the positions of the resonances may be caused by the soldering effect of the SMA connector and its mechanical tolerance, which have been neglected in the simulations. It can be seen that

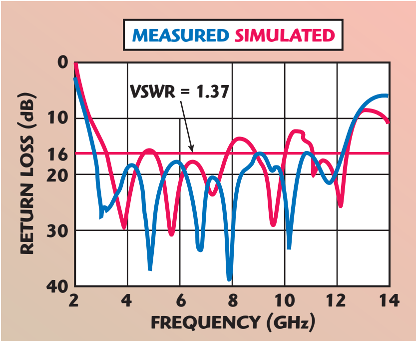

▲ *Fig. 6 Simulated and measured return loss of the optimized wide-slot antenna.*

the measured bandwidth defined by a VSWR less than 2 is from 2.5 to 12.8 GHz and for a VSWR less than 1.37 is from 2.8 to 12.2 GHz. It must be noted that the good performance of this type of printed wide-slot antenna is obtained while the volume of the antenna is approximately 2.46 cm^3, which is smaller than similar wide-slot antennas previously reported.[1-7]

The measured radiation patterns (E- and H-planes) of the proposed wide-slot antenna (Antenna III) are shown in ***Figure 7***. Within its impedance bandwidth from 3 to 10 GHz, the H-plane radiation patterns are almost omni-directional with relatively low cross-polarization level. From an overall view of these radiation patterns, the antenna behavior is quite similar to a typical printed wide-slot antenna.

The measured and simulated peak gains of the three antennas (I, II and III), from 3 to 11.6 GHz, are shown in ***Figure 8***. It is seen that the measured and simulated gains fluctuate within the range from 2.75 to 4.9 dBi and reach their maximum values at 11.6 GHz for the two wide-slot antennas (II and III). The measured antenna gain variation for antenna III is observed to be less than 1.8 dBi, with a peak antenna gain of approximately 4.7 dBi.

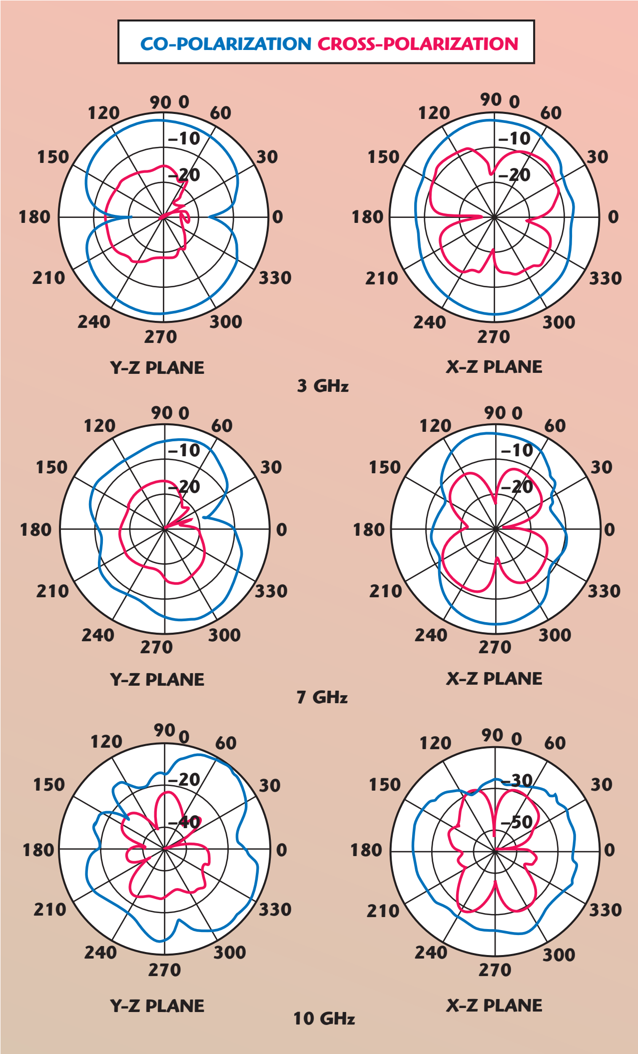

▲ *Fig. 7 Measured radiation patterns.*

CONCLUSION

A novel modified polygon-like wide-slot antenna with small size and fed by a 50 Ω microstrip line has been presented and investigated. Experimental results show that the impedance bandwidth of an octagonal-like slot antenna can be significantly improved by using three small, optimized notches at the bottom edge of the slot. Moreover, by using these three notches at the periphery of the slot and optimizing the octagonal-shaped slot and the fork-like stub dimensions, a very good impedance matching over the whole bandwidth, from 2.8 to 12.2 GHz (125.3 percent) for a VSWR less than 1.37, has been obtained. However, the measured total bandwidth of the fabricated antenna, determined by a 10 dB return loss, is equal to 10.3 GHz, from 2.5 to 12.8 GHz. Within this wide impedance bandwidth, the gain variation is less than 1.8 dBi. These good characteristics, with the compact dimensions of 35 × 44 mm for the proposed wide-slot antenna, make it attractive for future UWB applications. ■

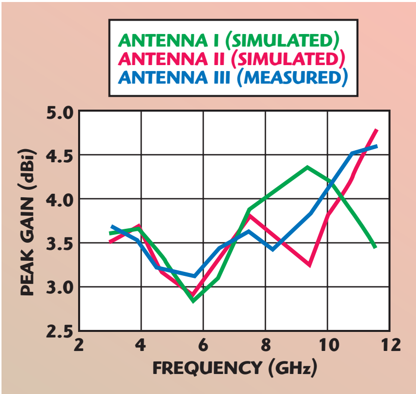

▲ *Fig. 8 Measured and simulated gains of the three antennas.*

ACKNOWLEDGMENT

The authors thank the Iran Telecommunication Research Center (ITRC) for its financial support and its Antenna & Microwave Laboratory, where the proposed antenna was tested.

References

1. P. Li, J. Liang and X. Chen, "Study of Printed Elliptical/Circular Slot Antennas for Ultra-wideband Applications," *IEEE Transactions on Antennas and Propagation*, Vol. 54, No. 6, June 2006, pp. 1670-1675.
2. J.Y. Jan and J.C. Kao, "Novel Printed Wide-band Rhombus-like Slot Antenna with an Offset Microstrip-fed Line," *IEEE Antennas Wireless Propagation Letters*, Vol. 6, 2007, pp. 249-251.
3. N. Behdad and K. Sarabandi, "A Wideband Slot Antenna Design Employing a Fictitious Short Circuit Concept," *IEEE Transactions on Antennas and Propagation*, Vol. 53, No. 1, January 2005, pp. 475-482.
4. W.S. Chen and K.Y. Ku, "Broadband Design of the Non-symmetric Ground $\lambda/4$ Open Slot Antenna with Small Size," *2006 IEEE Antennas and Propagation Society International Symposium Digest*, pp. 2563-2566.
5. M. Kahrizi, T.K. Sarkar and Z.A. Maricevic, "Analysis of a Wide Radiating Slot in the Ground Plane of a Microstrip Line," *IEEE Transactions on Microwave Theory and Techniques*, Vol. 41, No. 1, January 1993, pp. 29-37.
6. J.Y. Sze and K.L. Wong, "Bandwidth Enhancement of a Microstrip-line-fed Printed Wide-slot Antenna," *IEEE Transactions on Antennas and Propagation*, Vol. 49, No. 7, July 2001, pp. 1020-1024.
7. W.S. Chen and F.M. Hsieh, "A Broadband Design for a Printed Isosceles Triangular Slot Antenna for Wireless Communications," *Microwave Journal*, Vol. 48, No. 7, July 2005, pp. 98-112.
8. W.S. Chen and B.H. Kao, "A Triple-band Polygonal Slot Antenna for WiMAX Applications," *Microwave Journal*, Vol. 50, No. 1, January 2007, pp. 134-142.
9. S. Sadat, M. Fardis, F. Geran, G. Dadashzadeh, N. Hojjat and M. Roshandel, "A Compact Microstrip Square-ring Slot Antenna for UWB Applications," *2006 IEEE Antennas and Propagation Society International Symposium Digest*, pp. 4629-4632.
10. W.J. Lui, C.H. Cheng and H.B. Zhu, "Improved Frequency Notched Ultra-wideband Slot Antenna Using a Square Ring Resonator," *IEEE Transactions on Antennas and Propagation*, Vol. 55, No. 9, September 2007, pp. 2445-2450.
11. J.Y. Jan and J.W. Su, "Bandwidth Enhancement of a Printed Wide-slot Antenna with a Rotated Slot," *IEEE Transactions on Antennas and Propagation*, Vol. 53, No. 6, June 2005, pp. 2111-2114.
12. High Frequency Structure Simulator (HFSS), Version 10, Ansoft Corp., 2005.

Majid Razavi-Rad *received his BS degree in physics from Buali Sina University, Hamedan, Iran, in 1990. He is currently working toward his MS degree in electrical and telecommunications engineering at Urmia University, Urmia, Iran. His current research interests include UWB antennas and numerical methods in electromagnetics.*

Changiz Ghobadi *received his BSc degree in electrical engineering-electronics and his MS degree in electrical engineering-telecommunications from the Isfahan University of Technology, Isfahan, Iran, and his PhD degree in electrical-telecommunications from the University of Bath, Bath, UK, in 1998. He is currently an associate professor in the department of electrical engineering at Urmia University, Urmia, Iran. His primary research interests include antenna design, radar and adaptive filters.*

Javad Nourinia *received his BSc degree in electrical and electronic engineering from the Shiraz University, his MS degree in electrical and telecommunication engineering from the Iran University of Science and Technology and his PhD degree in electrical and telecommunications from the University of Science and Technology, Teheran, Iran, in 2000. He is currently an associate professor in the department of electrical engineering at Urmia University, Urmia, Iran. His primary research interests include antenna design, numerical methods in electromagnetism, microwave circuits, filters and signal processing.*

Reza Zaker *received his BSc degree in electrical and electronic engineering from Azad University, Tabriz, Iran, and his MSc degree in electrical and telecommunication engineering from Urmia University, Urmia, Iran, in 2008. His current research interests include printed, ultra-wideband (UWB) antenna design and bandwidth enhancement and miniaturization techniques, mobile small antennas, RFID, microstrip filters and numerical methods in electromagnetics.*

A COMPREHENSIVE BASEBAND GENERATOR AND CHANNEL EMULATOR

Engineers designing, integrating and verifying receiver signal processing components and devices today face a critical challenge. They must keep pace with the rapid design changes imposed by their industry while dealing with the ever-increasing pressure to be first-to-market. Unfortunately, evolving and unclear standards complicate this challenge, leading to design uncertainty and making it more difficult for engineers to meet their schedules. Receiver signal processing test must be performed, but testing to the standard is not enough. Corner cases must also be tested and that testing must take place early in the development cycle, a process that requires either broad or no limits on test parameters. Without such testing, devices can fail under real-world conditions, causing significant rework downstream.

Addressing these challenges is the main goal of the Agilent N5106A PXB baseband generator and channel emulator (see ***Figure 1***). As well suited for engineers working on product development as it is for those conducting advanced research, the PXB can keep pace with rapid design changes and evolving standards by testing receiver signal processing to standards and beyond. It is the only instrument that combines up to 12 DSP blocks—software-defined

▲ *Fig. 1 Agilent N5106A PXB baseband generator and channel emulator.*

AGILENT TECHNOLOGIES INC.
Santa Clara, CA

functional blocks—to construct over 20 calibrated configurations for multi-format baseband generation, real-time fading and signal capture (up to 4x2 MIMO) in a single box. These configurations, along with external instrument connections, can be redefined in seconds using the instrument user interface.

The Windows-based PXB offers up to 120 MHz modulation bandwidth and 512 MSa playback memory, making it ideal for playing back long test scenarios to better approximate real-world signals. It supports standard-based channel models with up to 120 MHz fading bandwidth or 24 paths per fading channel. Additionally, RF and digital I/Q signals can be captured from the engineer's device to the PXB, up to 512 MSa. Captured signals can be monitored using the Agilent 89600 Vector Signal Analysis (VSA) software and post-processed with the engineer's simulator or MATLAB®. Such capabilities enable the PXB to address a number of the issues that complicate receiver signal processing test, including design uncertainty, the time, cost and complexity of system setup and calibration, and rapidly evolving standards.

DESIGN UNCERTAINTY

By letting the engineer customize test cases and validate designs under real-world conditions with the broadest range of test parameters, the PXB effectively tackles the design uncertainty associated with evolving and unclear standards. Fully parameterized signals can be created for established and evolving standards (e.g., LTE, HSPA, W-CDMA, GSM/EDGE, TD-SCDMA, Mobile WiMAX™, WLAN, digital video and GPS) using Agilent Signal Studio software running on the PXB. Agilent's SystemVue software can be used for baseband development or to play back customized MATLAB waveforms. The PXB also allows the engineer to model the signal-propagation environment with fully parameterized, real-time channel emulation. The engineer can use pre-defined standards-based channel models, modify them or configure their own using the PXB's custom correlation table and antenna setup menu.

TIME, COST AND COMPLEXITY OF SYSTEM SETUP AND CALIBRATION

Testing receiver signal processing in multi-format devices is an expensive and time-consuming proposition. To stay on schedule, engineers need simple ways to connect and calibrate their equipment and generate independent, calibrated signals. With less instrumentation to manage—just one box is needed for multi-format, multi-channel baseband signal processing including baseband generation, real-time fading and signal capture—the PXB dramatically simplifies test setup and eliminates the time-consuming work of combining cables, splitters and power meters to connect and calibrate instruments. Additionally, signal routing, summing, sync and calibration are all managed seamlessly inside the PXB.

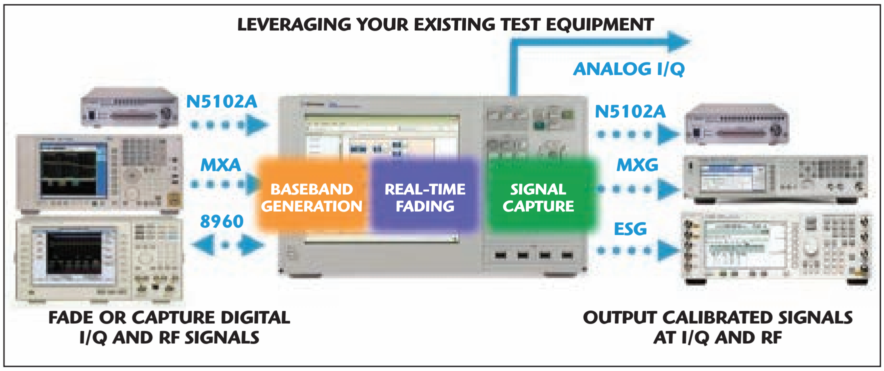

Fig. 2 The PXB allows engineers to maximize their investment value.

Such capabilities significantly reduce the time, cost and complexity associated with system setup and calibration.

RAPIDLY EVOLVING STANDARDS

Testing receiver signal processing today and in the future requires a toolset that can adapt as standards evolve. To get the greatest value from an investment, the instrument used should therefore support multiple functions, future technologies, frequent use and easy upgrades. With the PXB, engineers can leverage one multipurpose diagnostic toolset across the entire R&D lifecycle—from design, integration and verification to pre-conformance—to perform numerous combinations of baseband generation, real-time fading and signal capture (see ***Figure 2***). By providing multiple functions, license-key upgrades and easy on-site upgrades with no calibration required, and performance that can handle future technologies, the PXB also ensures that the user's investment returns ongoing value.

CONCLUSION

Testing receiver signal processing in today's highly-dynamic communications industry can be a challenging and costly proposition. With its ability to minimize design uncertainty, reduce the time, cost and complexity of system setup and calibration, and maximize the user's investment through higher instrument utilization and easy upgrades, the PXB is the ideal solution to this dilemma. Moreover, its flexibility to test beyond standard requirements and to enable numerous combinations of baseband generation, real-time fading and signal capture ensures that engineers—both today and in the future—have the tools they need to get to market on schedule while staying ahead of the competition.

Agilent Technologies Inc.,
Santa Clara, CA
(800) 829-4444,
www.agilent.com/find/PXB.

RS No. 302

NEW DEMODULATION ANALYZERS BRING BENCHTOP PERFORMANCE TO HANDHELD SPECTRUM ANALYZERS

Anritsu introduces demodulation analyzers for LTE, WiMAX, W-CDMA/HSDPA and legacy standards such as GSM, CDMA and EV-DO for use with its Spectrum Master™ MS2712E/MS2713E. The new capabilities make the Spectrum Master MS2712E/MS2713E the first handheld spectrum analyzers in this class to deliver these measurements, and provide field technicians and maintenance engineers with a single handheld instrument to conduct RF measurements, demodulation capabilities and over-the-air tests.

These additional capabilities have been developed to meet today's rapidly changing and fiercely competitive wireless network environment. It is no longer enough for operators and carriers to only test the cable and antenna portion of the system, because many signal quality problems cannot be detected unless the signal is demodulated. When the Spectrum Master MS2712E/MS2713E is configured with these new optional analyzers, technicians and engineers can reduce churn while increasing capacity and improving revenue for carriers.

The newly added AM/FM/PM analyzer provides broadcast and land mobile radio (LMR) technicians/engineers with an alternative to benchtop instruments. Previously, they had to rely on heavier, bulkier and harder-to-use equipment to measure and characterize key parameters for AM/FM signals. With the MS2712E/MS2713E, they can now make all of these measurements with one handheld instrument. Four measurement displays are provided, including the RF spectrum view, audio spectrum display, audio waveform display and summary table display that shows a summary of rate, RMS deviation, RMS depth, SINAD, THD, carrier power, carrier frequency and more.

HIGH ACCURACY MEASUREMENTS

Typically, highly stable reference oscillators were only found in benchtop spectrum analyzers. Anritsu has also developed a GPS option for the Spectrum Master MS2712E/MS2713E that improves the accuracy of the oscillator to ±50 ppb, making the handheld analyzers compliant with 3GPP accuracy requirements. In

ANRITSU CO.
Morgan Hill, CA

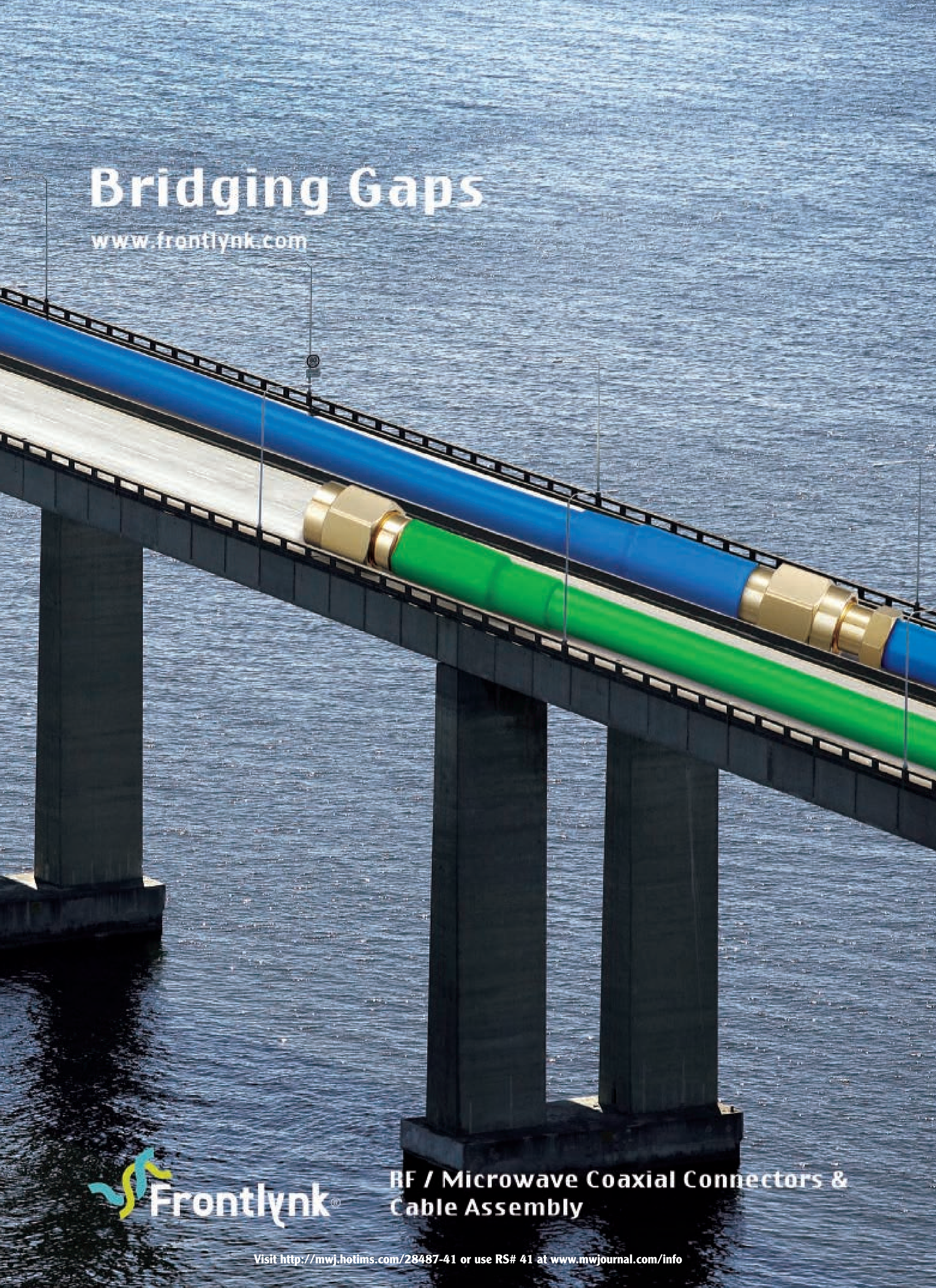
Bridging Gaps
www.frontlynk.com
Frontlynk
RF / Microwave Coaxial Connectors &
Cable Assembly

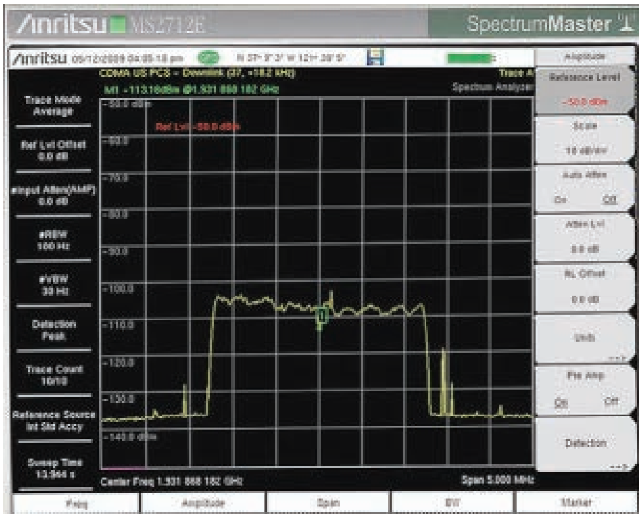

▲ *Fig. 1 MS2712E on screen menus.*

addition, the Spectrum Master MS2712E/MS2713E includes a CW generator option from 2 MHz to 2 GHz with adjustable power between –10 and –90 dBm. The accuracy of the CW generator is also ±50 ppb with the GPS option.

The Spectrum Master MS2712E/MS2713E has dynamic range of >80 dB when conducting transmission measurements. This enables technicians and engineers to quickly tune duplexers in the field, as well as verify antenna isolation and conduct gain measurements on active devices.

In addition, a new interference analyzer option delivers all the necessary tools to monitor, recognize, locate and identify interference. With the interference analyzer, field technicians and engineers can use the Spectrum Master MS2712E/MS2713E to locate intermittent interference signals, as well as find and identify spurs. A 3D spectrogram display enables users to record spectrum events for up to 72 hours and later identify signal events over time and frequency.

SIMPLE OPERATION

Simple to use, the Spectrum Master MS2712E/MS2713E allows most standard measurements to be accessed with a single key stroke. Among the one-button measurements are transmitter power, occupied bandwidth, field strength, ACPR and emission mask compliance. Users can also customize limit lines, and setup limit envelopes and emission masks, which are critical to ensure that excess emissions do not affect other channels and systems.

The traditional high performance associated with the Spectrum Master family is maintained with the MS2712E/MS2713E. The MS2712E has frequency coverage of 100 kHz to 4 GHz, while the MS2713E extends the frequency up to 6 GHz. Dynamic range is better than 95 dB and DANL better than –162 dBm (1 Hz). Menus are easy to navigate via an 8.4" color touch screen display (see ***Figure 1***). All of this performance is available in an instrument that weighs less than 3.45 kg and costs under $10,000.

Anritsu Co.,
800-ANRITSU (800-267-4878),
www.us.anritsu.com/SpectrumMaster.

RS No. 305

AR's Bargain Corner

VENDORVIEW

There is more than one way to get the quality equipment you need. If your budget is tight, the AR Bargain Corner is a good place to find some great values. New with MCB, discontinued and demonstration equipment is available at a fraction of its original price. Visit the company's website, www.ar-worldwide.com, to view AR's Bargain Corner.

AR RF/Microwave Instrumentation,
160 School House Road,
Souderton, PA 18964

www.ar-worldwide.com

High Power Amplifiers

This website offers the company's extensive product line of high power amplifiers for satellite communication. Products are available in rack-mount configurations as well as for outdoor applications. Product offerings span 2 GHz through more than 50 GHz at power levels from 8 W to 3 kW. Xicom's new website is designed to provide ease of use in learning about Xicom's broad offerings of products and services for commercial, military and government users of SATCOM. The website offers quick links to descriptions, features, options and complete data sheets.

Comtech Xicom Technology Inc.,
3550 Bassett Street, Santa Clara, CA 95054

www.xicomtech.com

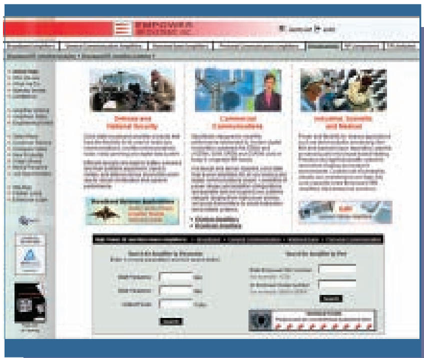

Interactive Product Catalog

This website provides a comprehensive, user-friendly selection of Empower's products and functionality to configure and submit quote requests. The site features a parametric search engine and a collection of RF engineer's applets such as a watts-to-dBm converter, gain calculator and links to contact Empower's sales team. There is also a mobile-friendly version accessible from devices such as a RIM Blackberry.

Empower RF Systems Inc.,
316 West Florence Avenue,
Inglewood, CA 90301

www.empowerrf.com

ICs, Modules, Subsystems and Instrumentation

VENDORVIEW

Hittite's redesigned website includes a dynamic homepage featuring full specifications for over 800 products across 24 product lines, press releases and featured articles. Comprehensive Individual Product "Splash Pages" containing in-depth product information and technical content are located on one easy to navigate page. Engineers will find improved Product Support and streamlined Quality & Reliability pages containing invaluable reference materials.

Hittite Microwave Corp.,
20 Alpha Road, Chelmsford, MA 01824

www.hittite.com

Online Antenna Stock Locator

Laird Technologies announced the launch of its new online antenna stock locator system. The online stock locator provides the company's customers an electronic platform to directly access qualified distributors and its available inventory through the Lairdtech.com website. Laird's online users now have a single destination to search the antenna inventory of several select distributors at the same time.

Laird Technologies Inc.,
16401 Swingley Ridge Road, Suite 700,
Chesterfield, MO 63017

www.lairdtech.com

Filters and Assemblies

VENDORVIEW

Networks International Corp. (NIC) has recently updated its website (www.nickc.com) making it more dynamic and user friendly. The updates include a new spotlight feature highlighting NIC's new products and capabilities and improved search for NIC products. Updates have also been made to NIC's product pages to include links to download .pdf product catalogs and datasheets.

Networks International Corp.,
15237 Broadmoor,
Overland Park, KS 66223

www.nickc.com

New Waves: Test and Measurement

For more new products, visit www.mwjournal.com/buyersguide

Featuring VENDORVIEW Storefronts

GET INFO

General-purpose Test Environment

For high-performance, high-speed testing of RF and microwave devices, Aeroflex introduced the SMART^E™ 5300 general-purpose test environment. The DC to 40 GHz SMART^E 5300 is unique in its ability to test, monitor and control any Device Under Test (DUT) within a single test environment. SMART^E 5300 is designed for parametric and functional testing in the military/aerospace and high-performance commercial markets. The system is ideal for customers with one or more of these demanding RF/microwave test requirements: high throughput production; large number of unique tests per DUT; highly repetitive tests per DUT; product lines requiring rapid software reconfiguration of test systems; and replacement of racks of older or obsolete equipment with a "synthetic" or software-defined test environment.

Aeroflex,
Plainview, NY (703) 629-0331,
www.aeroflex.com.

RS No. 216

Vector Network Analyzer

VENDORVIEW

The N9923A FieldFox RF vector network analyzer (VNA) provides the best measurement stability, 0.01 dB/degree Celsius, and offers integrated QuickCal calibration capability available in a handheld VNA. QuickCal enables consistent measurement results and confidence in the data while eliminating the need to carry a calibration kit into the field. The FieldFox RF VNA expands Agilent's handheld instrument portfolio and is designed for field engineers working in aerospace, defense and network equipment manufacturing, who characterize or troubleshoot RF components for mission-critical communication systems. As a full two-port network analyzer, the FieldFox RF VNA allows operators to simultaneously measure and display all four S-parameters.

Agilent Technologies Inc.,
Santa Clara, CA (800) 829-4444,
www.agilent.com.

RS No. 217

Handheld Spectrum Analyzers

VENDORVIEW

Anritsu Co. announced it has expanded the test capability of its MS2712E and MS2713E Spectrum Master handheld spectrum analyzers to include signal analyzer capabilities. With the new

10 MHz bandwidth demodulation option, the MS2712E/MS2713E can test and verify the RF quality, modulation quality and downlink coverage quality for all the major wireless standards. The new option allows a full suite of RF, demodulation and Over-the-Air (OTA) measurements to be made efficiently and accurately with the MS2712E/MS2713E. Users can conduct these critical tests to improve the Key Performance Indicators (KPI) associated with call drop rates, call block rates and call denial rates. With the Spectrum Master, field technicians can troubleshoot down to the Field Replacement Unit (FRU) in a base station's transmitter chain. The result is fewer costly no trouble faults (NTF) associated with card swapping, and lower inventory of replacement parts.

Anritsu Co.,
Morgan Hill, CA (408) 778-2000,
www.anritsu.com.

RS No. 218

Three-channel Power Meter

VENDORVIEW

AR's model PM2003 is a three-channel power meter with exceptional high-speed measurement capability and a wide dynamic range. Model PM2003 delivers 200 readings per second with one channel and 100 readings per second when two channels are used. Two channels at a time can be simultaneously displayed and recorded; the third channel can be easily switched in to be displayed or recorded.

AR RF/Microwave Instrumentation,
Souderton, PA (215) 723-8181,
www.ar-worldwide.com.

RS No. 256

AWR Design Environment

VENDORVIEW

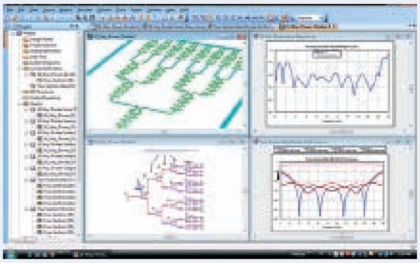

Version 9.01 of the AWRDE is now available for download from www.awrcorp.com. This new release delivers more than 100 enhancements that increase productivity, including key new features to AWR's APLAC® harmonic balance engine, AXIEM™ 3D planar electromagnetic (EM) simulator and new elements. AWRDE Version 9.01 adds a new harmonic balance mode to the APLAC simulator that increases simulation speed for microwave nonlinear circuits, especially when there are an equal number of linear and nonlinear models or more linear than nonlinear models.

AWR Corp.,
El Segundo, CA (310) 726-3000,
www.awrcorp.com.

RS No. 248

Power Conditioning Products

VENDORVIEW

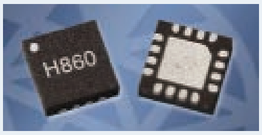

Hittite has introduced its 24th product line, Power Conditioning, ideal for low noise voltage regulation in automotive telematics, cellular/4G, WiMAX/4G, military and test equipment applications. The HMC860LP3E is a low noise, high PSRR (Power Supply Rejection Ratio), quad output linear voltage regulator. It features a low noise band gap reference externally decoupled for best in-close noise performance. high PSRR in the 0.1 to 10 MHz range provides excellent rejection of preceding switching regulator noise. The HMC860LP3E provides four voltage outputs, which are adjustable from 2.5 to 5.2 V, and are ideal for conditioning the DC power supply to many low noise frequency generation subsystems including Hittite's broad line of PLLs with integrated VCOs.

Hittite Microwave Corp.,
Chelmsford, MA (978) 250-3343,
www.hittite.com.

RS No. 220

PXI Programmable Amplifier and Attenuator

NI expanded its automated test product line with two new RF signal conditioning modules that enhance the measurement accuracy and flexibility of PXI-based RF and microwave test systems. In applications such as RF signal path degradation modeling, field strength metering and receiver testing, engineers can combine the new NI PXI-5695 8 GHz programmable RF attenuator with a vector signal generator (VSG) to improve RF signal quality at low power levels. Engineers can integrate the NI PXI-5691 8 GHz programmable RF preamplifier, which also functions as a power amplifier, with VSGs to increase maximum power and with vector signal analyzers (VSA) to measure low-level signals.

National Instruments,
Austin, TX (800) 531-5066,
www.ni.com.

RS No. 221

SPDT Switch

The new PE42556 single-pole double-throw (SPDT) RF switch is designed on Peregrine's UltraCMOS™ silicon-on-sapphire process

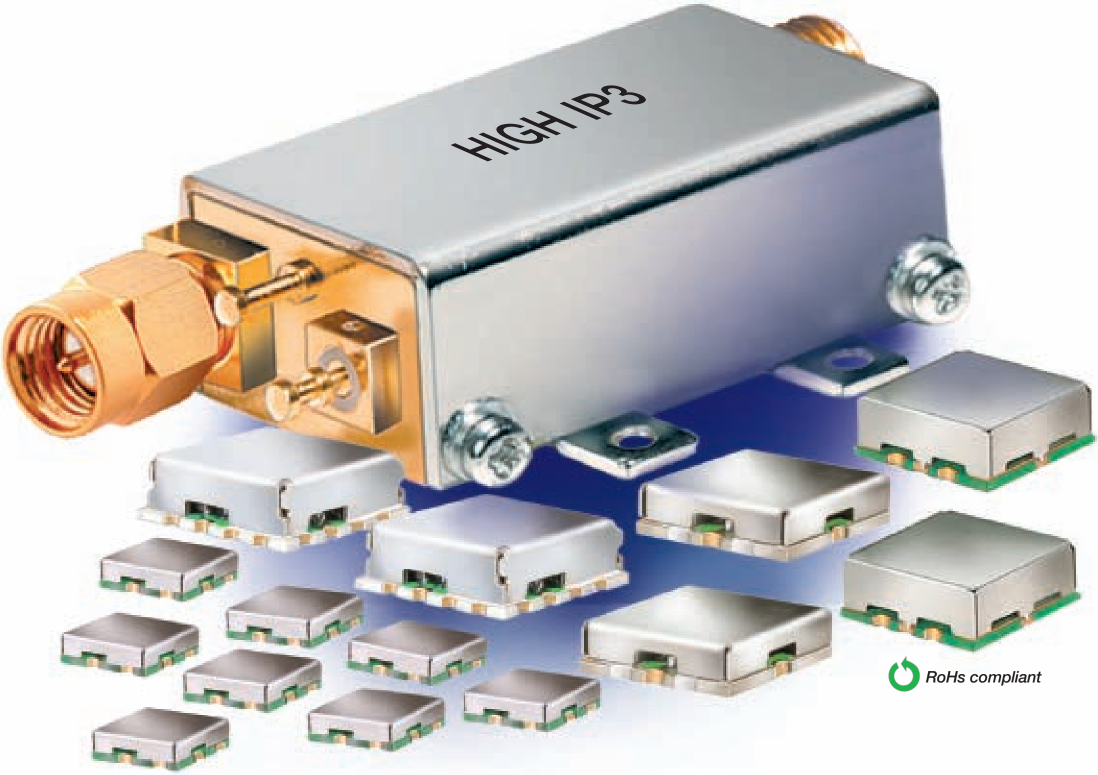

HIGH IP3

New Waves

technology, features excellent broadband RF performance from 9 kHz up to 13.5 GHz without gate or phase lag and insertion loss drift, and ensures fast switch-settling time. The HaRP™-enhanced switch has best-in-class linearity, making it ideal for use in test and measurement applications including Automated Test Equipment (ATE) and general-purpose test and measurement; RF/IF transceiver signal switching; filter bank switching; and discrete DSA stages.

Peregrine Semiconductor Corp., San Diego, CA (858) 731-9400, www.psemi.com.

RS No. 222

Autotest Option

A new 2261 Autotest Option has been developed for the 2201 ProLock, which eliminates the need for an external PC to control the system, making the service test system for 3G mobile phones self-contained. Previously, tests were controlled through test scripts running on a PC utilizing the company's 7310 Lector and Scriptor remote control software. With the new option, the test scripts can reside on the instrument itself and a comprehensive test system for service can be reduced to the company's 2201 ProLock with the 4916 Antenna Coupler and the 4921 RF Shield.

Willtek Communications GmbH, Ismaning, Germany +49 89 99641 132, www.willtek.com.

RS No. 223

Logger with TETRA Protocol

The WiNRADiO PFSL-G3 Portable Field Strength Logging and Surveillance System for mobile signal coverage measurements now features an optional TETRA control protocol decoder. The PFSL-G3 system includes a wide-band HF/VHF/UHF calibrated measuring receiver to measure and log signal strength, combined with an integrated GPS receiver. The signal levels can be measured in µV, dBm or S-units, while field strength can be displayed in µV/m or dBµV/m. Readouts can be shown as instantaneous, peak or average values, calculated over user-definable intervals. It is a ruggedized easily transportable unit, which includes the control computer, the receiver, rechargeable batteries and associated subsystems.

Radixon UK Ltd., Evesham, UK +44 (0)870 446 0449, www.radixon.co.uk.

RS No. 255

Components

Absorptive Switch Matrix

VENDORVIEW

AKON Inc.'s switches and filters division developed a 36-throw absorptive switch matrix measuring 7.3" × 5.4" × 1.2". The model A35-WH183 operates over the 0.3 to 3.3 GHz frequency range, with less than 10 dB insertion loss, less than 0.8 dB peak-to-peak variation between the J0 input port and any output port, less than four degrees phase variation, 70 nanoseconds or less switching speed, and +30 dBm maximum operating import power. The unit is ideal for airborne EW/ECM applications.

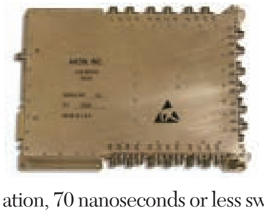

AKON Inc., San Jose, CA (408) 432-8039, www.akoninc.com.

RS No. 224

Ceramic Bandpass Duplexer

VENDORVIEW

The AM1880-1960D268 surface-mount monoblock ceramic duplexer is an excellent choice for use in base station transceivers serving wireless communication applications. The duplexer's center frequency is 1920 MHz and transmit band (1850 to 1910 MHz) insertion loss is less than 3.4 dB. Return loss is at least 11 dB, and rejection is at least 49 dB. Insertion loss in the receive band (1930 to 1990 MHz) is less than 3.7 dB, return loss is greater than 11 dB, and rejection is at least 54.5 dB. The 50 ohm duplexer will handle RF input power of 2 W and measures 4.6 × 23 × 6.5 mm.

Anatech Electronics, Garfield, NJ (201) 772-4242, www.anatechelectronics.com.

RS No. 225

Flexible Cable Assemblies

VENDORVIEW

These low VSWR flexible cable assemblies feature Times Microwave Systems T-Flex® cable. Three-foot long, 0.141" diameter assemblies, terminated with SMA male connectors, exhibit VSWR characteristics of 1.35:1 from 45 MHz to 18 GHz. Suitable for applications through 20 GHz, these 50 ohm flexible cable assemblies meet all MIL-C-17 requirements. EAM's flexible cable assemblies feature excellent corrosion resistance with stable attenuation and phase characteristics over time. Available in standard and custom lengths, these flexible cable assemblies feature PTFE (Teflon®) dielectric with silver plated copper tape and braid shield and fluorinated ethylene propylene (FEP) jacket.

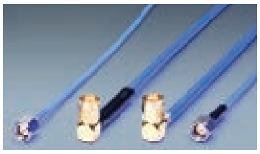

Electronic Assembly Manufacturing Inc., Methuen, MA (978) 374-6840, www.eamcableassemblies.com.

RS No. 227

Resistive Couplers

The compact and easy to use IMK Series resistive couplers function well over a DC to 15 GHz range. Insertion loss is comparable to the more complicated frequency sensitive couplers. This 0.120" × 0.120" device is available with a coupling range from 6 to 30 dB and is rated at 1 W. Samples of the IMK Series resistive coupler are available.

International Manufacturing Services Inc., Portsmouth, RI (401) 683-9700, www.ims-resistors.com.

RS No. 228

75 Ohm Programmable Attenuator

VENDORVIEW

The new 75P-167 is the company's latest solid-state, 75 ohm programmable attenuator. It offers 127 dB of dynamic range with 1 dB resolution. Specifically designed for DOCSIS and MoCA testing, it operates from 800 to 2200 MHz and switches attenuation settings in less than two microseconds. F Female connectors are standard, but other options are available upon request.

JFW Industries, Indianapolis, IN (317) 887-1340, www.jfwindustries.com.

RS No. 229

Tappers

New values for the DN range of tappers are available for outdoor and in-building distributed antenna system applications, where tappers can replace directional couplers at far lower cost and improved performance. The new 20 and 30 dB tappers add to the range of taps that starts at just 3 dB, a 2:1 split. All have much improved VSWR over previous tapper designs and are 50 percent lower in price than the equivalent directional coupler. Each has a bandwidth covering all of the wireless bands from 380 to 2700 MHz, thus including Tetra, SMR/PMR and all cellular bands, including the new 700 MHz and WiMAX 2500 MHz band. Also important, the guaranteed Passive Intermodulation (PIM) performance of all models is <-150 dBc.

Microlab, Parsippany, NJ (973) 386-9696, www.microlab.fxr.com.

RS No. 230

Triple-balanced Mixer

VENDORVIEW

MITEQ's model TBR0058LA3 is a wideband triple-balanced mixer that utilizes a dual quad circuit to provide performance in overlapping RF and IF frequency ranges. This device has an RF and LO of 500 to 8000 MHz and an IF response of 50 to 3000 MHz. This product

is well suited for military and commercial applications and is also available in higher-level diode options for increased 1 dB compression and third-order intercept.
MITEQ Inc.,
Hauppauge, NY (631) 436-7400,
www.miteq.com.

RS No. 231

PIN Diode Switch

VENDORVIEW

Model SS153DHS is a SP5T reflective PIN diode switch that operates from DC to 18 GHz and provides fast switching speed, high isolation, low insertion loss, and is housed in a rugged compact package. Together these features make the switch an excellent choice for applications ranging from electronic warfare systems and simulators to automated test equipment.

The model SS-153DHS has switching speed of 20 ns, insertion loss ranging from 2.6 dB from 2 to 12 GHz and 3.6 dB from 12 to 18 GHz, maximum VSWR of 2:1 and isolation up to 65 dB. It can handle up to 200 mW of RF power and can survive RF power input of 1 W CW and 20 W peak (1 µs pulse width, 5 percent duty cycle).
Narda,
Hauppauge, NY (631) 231-1700,
www.nardamicrowave.com/east.

RS No. 232

Linearized X-band Attenuator

The model AAT-30-479/5S is a linearized X-band atttenuator that operates in a frequency range from 8 to 12.4 GHz. This new 0 to 60 dB linearized attenuator offers a maximum insertion loss of 3 dB and a maximum VSWR of 2:1. Attenuation is accomplished with a transfer function of 10 dB/V; typical DC power required is +15 VDC at 100 mA.
Pulsar Microwave,
Clifton, NJ (973) 779-6262,
www.pulsarmicrowave.com.

RS No. 233

Composite Connectors

The N and 7/16 Composite Connector Series has been expanded with over 20 new variations of plugs, jacks and receptacles. The single-piece design permits the contact pressure to be equally distributed by diverting the entire tightening torque force through pressure on the ground contact junction, which improves the intermodulation level. The electrical performance includes a low operating VSWR, 1.10 maximum up to 7.5 GHz for 7/16 receptacles. Designed to be installed in telecommunications equipment such as remote radio heads, antennas, filters, etc., the connectors are manufactured with corrosion free, composite materials that are UV resistant and meet IEC 68-2-5 and IEC-68-2-9.
Radiall USA Inc.,
Chandler, AZ (480) 682-9400,
www.radiall.com.

RS No. 234

VHF LC Triplexer

VENDORVIEW

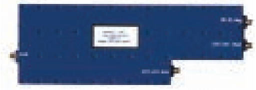

Reactel part number 3TP-90/150-11 is a VHF LC triplexer. This unit exhibits low loss and high isolation as it splits the VHF band into three individual bands. This unit has a high power option and can be outfitted with most any RF connector. Please contact the factory for this or any other filter requirement.
Reactel Inc.,
Gaithersburg, MD (301) 519-3660,
www.reactel.com.

RS No. 236

Circuit Insertion Switch

Relcomm Technologies introduces a cost-effective solution for a circuit insertion type relay. This RRTL-series relay is RoHS compliant and is fitted with type 'N' connectors in a


Amplifier Solutions
Microstrip
Power
Bipolar
Broadband
SATCOM
Surface Mount
High Intercept
Fiber Optic
Waveguide
Dual Output
Cryogenic
Low Noise
Low Noise
Dual Output
Cryogenic
Gated
MITEQ
Low Phase Noise
Desktop
Limiting
Limiting
In Line
In Line
Space Qualified
Space Qualified
3 YEAR WARRANTY
RoHS
ISO 9001
ANAB
For additional information or technical support,
please contact our Sales Department at (631) 439-9220
or e-mail components@miteq.com
MITEQ
100 Davids Drive, Hauppauge, NY 11788
(631) 436-7400 FAX: (631) 436-7430
www.miteq.com

failsafe configuration. The relay is sand and dust proof and has no exposed moving parts for reliable installation. Performance to 4 GHz; maximum characteristics to 2 and 4 GHz in a 50 ohm system; VSWR of 1.15:1 and 1.30:1, insertion loss of 0.15 and 0.25 dB, with isolation greater than -60 dB. Twelve and 24 V operating voltages are available.

RelComm Technologies Inc., Salisbury, MD (410) 749-4488, www.relcommtech.com.

RS No. 237

Drop-in Circulator

Renaissance has recently developed a 700 MHz drop-in circulator with outstanding linear performance for LTE requirements. This device delivers better than -100 dBc IMD for two tone 0.25 W power levels. In addition, Renaissance is offering this circulator with a 13 percent bandwidth in a compact 1.25 inch square cost-effective package. Renaissance continues to provide the cellular infrastructure community with solutions to their most difficult design challenges and has already begun working on new designs for anticipated upcoming requirements at 2.1 GHz to support its customers.

Renaissance Electronics Corp., Harvard, MA (978) 772-7774, www.rec-usa.com.

RS No. 238

Miniature Ultra Flat Schottky Detectors

RLC Electronics' miniature ultra-flat detectors utilize a zero-bias Schottky design. The microwave power is coupled directly to the extremely small components reducing package parasitics and transition mismatches.

This design results in a very low VSWR and a flat, smooth output over a wide bandwidth. Options available include negative or positive output, a choice of three output connectors and operation to 26.5 or 40 GHz.

RLC Electronics Inc., Mount Kisco, NY (914) 241-1334, www.rlcelectronics.com.

RS No. 239

Mixers

Sage Laboratories offers a complete line of standard mixers in various configurations including double balanced, triple balanced, image reject mixers, I/Q Modulators and Single Sideband Modulators. These are available as connectorized, drop-in or surface-mount configurations. Designs conform to MIL-DTL-28837 requirements and are screened to MIL-STD-883. Standard designs offer high isolation between

ports and low conversion loss while offering wide broadband performance. The connectorized mixers are environmentally sealed and include field replaceable SMA connectors. Drop in designs provide an inexpensive alternative for customers installing mixers in sealed housings. Sage Laboratories designs and builds custom mixers to meet demanding requirements.

Sage Laboratories, Hudson, NH (603) 459-1600, www.sagelabs.com.

RS No. 240

Amplifiers

X-band AGC Amplifier

Model AMLSW3011 is a GaAs X-band switched gain selectable amplifier that has

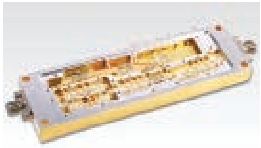

excellent state-to-state gain and phase tracking. The amplifier offers selectable gain steps of 0/10/20 and 30 dB. A minimum OIP3 of +35 dBm is provided in any of the gain states. This amplifier

is also available with an input detector option that limits the output power to +30 dBm maximum under conditions of high input drive. This feature protects components that follow the amplifier in the system cascade. DC voltage is 12 to 18 VDC.
AML Communications Inc.,
Camarillo, CA (805) 388-1345,
www.amlj.com.

RS No. 242

Monolithic IF Amplifier

VENDORVIEW

The Mini-Circuits PSA-0012+ is optimized for use in critical IF amplifier applications having an ideal combination of low gain of 15 dB, low noise of 2.3 dB and high output power of +22 dBm. Operating over a broad frequency range of 50 to 6000 MHz, the PSA-0012+ covers a wide range of typical IF bands making this amplifier ideal for use in a variety of applications. With 12 dB input and 15 dB output return loss, the PSA-0012+ can be integrated into critical circuits with confidence that VSWR interactions with source and load components will not affect performance. In addition, this model is pin-for-pin compatible to the M/A-COM MAALSS0012 IF amplifier and can provide comparable performance making it an ideal replacement part.
Mini-Circuits,
Brooklyn, NY (718) 934-4500,
www.minicircuits.com.

RS No. 243

Power Amplifier

Stealth Microwave, a division of Micronetics Inc., has released the SMTR2224-11G40-RSS, a military grade bi-directional power amplifier (PA) that is capable of up to 10 W of 802.16e and 50 W of 802.11b. Primary applications include WLAN, video and C2 products for UAVs. The unit operates from 2.2 to 2.4 GHz and Tx/Rx gains are 38 and 13 dB, respectively. The PA measures 4.4" × 5.4" × 1.3".
Stealth Microwave Inc.,
Ewing, NJ (888) 772-7791,
www.stealthmicrowave.com.

RS No. 245

Devices

Mixer/Detector Diodes

This family of surface-mount GaAs and Silicon Schottky mixer/detector diodes are designed for high volume pick and place applications.

These control devices are delivered in a plastic SMT package with standard 45 mils W × 75 mils L × 31 mils H dimensions. Their performance and mechanicals allow them to be easily dropped into existing designs. The SMGS family of detectors and mixers includes GaAs model SMGS11, which is ideal for temperature compensation applications. This device operates at > 26.5 GHz and features a minimum breakdown voltage of 5 V, a typical capacitance of 0.10 pF and a maximum resistance of 7 ohms.
Aeroflex/Metelics,
Sunnyvale, CA (888) 641-7364,
www.aeroflex.com/metelics.

RS No. 246

RF Power Transistor Clamping Devices

The TO270WB and TO270WBL clamping devices enhance the connection between a plastic-packaged RF power transistor and the

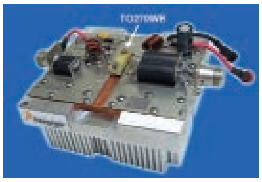

ground plate of an RF amplifier. Often these high-power plastic-packaged devices are just bolted down. The new clamps improve both the electrical ground and the thermal ground, thus increasing P1dB, decreasing IMD3, while improving thermal performance and reliability.
Richardson Electronics,
LaFox, IL (800) 737-6937,
www.rell.com.

RS No. 247

Sources

Voltage-controlled Oscillator

The MW500-1840 1/2" SMT voltage-controlled oscillator (VCO) has a tuning range of 1640 to 1850 MHz from 0.2 to 4.8 V tuning using a 5 V supply. Output power is +8 dBm±1.5 dBm across the band over temperature while using less than 40 mA of current.
Micronetics Inc.,
Hudson, NH (603) 883-2900,
www.micronetics.com.

RS No. 250

5 and 24 GHz FMCW Products

The company has broadened its portfolio of Frequency Modulated Continuous Wave (FMCW) products by adding both the 5 GHz RS3400S/00 FMCW and the 24 GHz RS3400K/00 FMCW versions to the existing 10 GHz RS3400X/00 FMCW model. All three

products are fully synthesized, exhibit low power consumption and offer a wideband sweep for high accuracy. Typical applications include level gauge measurement, collision avoidance in industrial applications, speed measurement, etc. Also, a complete kit for easy evaluation and control of the unit from a PC is available.
Sivers IMA AB,
Kista, Sweden +46-8-703 68 00,
www.siversima.com.

RS No. 251

Direct Synthesizer/Up Converter

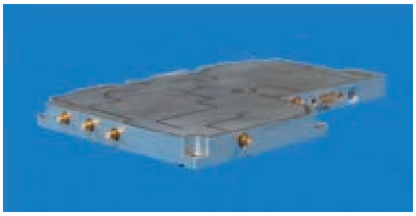

Model SYN152 is an X-band direct synthesizer/up converter that specializes in low residual phase noise ranging from -129 dBc/Hz to -151 dBc/Hz at an X2 L-band Multiplied Output. This unit provides fast LVTTL switching speed between multiplied X-band output and IF supplied output. Additional advanced features of this product include X2, X3, X4 and X17 multiplied output ports while maintaining a compact footprint of 5.46"× 3.74" × 0.41". This model is ideal for airborne applications with its low profile, hermetically-sealed, laser welded package.
TRAK Microwave,
Tampa, FL (813) 901-7200,
www.trak.com.

RS No. 252

Voltage-controlled Oscillator

Z-Communications Inc.'s new RoHS compliant voltage-controlled oscillator (VCO) model CRO2660B-LF in S-band operates at 2660 MHz with a tuning voltage range of 0.5 to 4.5 VDC. This VCO features a typical phase noise of -114 dBc/Hz at 10 kHz offset and a typical tuning sensitivity of 5 MHz/V. The CRO2660B-LF is designed to deliver a typical output power

of 3 dBm at 5 VDC supply while drawing 20 mA (typical) over the temperature range of -20° to 70°C. This VCO features typical second harmonic suppression of -20 dBc and comes in Z-Comm's standard MINI-16 package measuring 0.5" × 0.5" × 0.22". It is available in tape and reel packaging for production requirements.
Z-Communications Inc.,
San Diego, CA (858) 621-2700,
www.zcomm.com.

RS No. 254

MICRO-AD

Visit http://mwj.hotims.com/28487-(RS#)

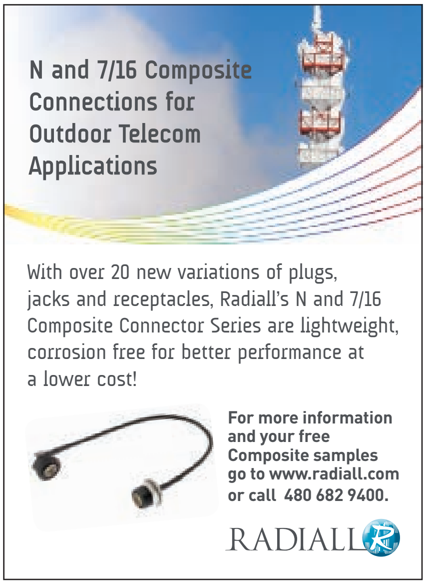

RS 100

RS 104

RS 1

RS 57

RS 18

RS 115

RS 113

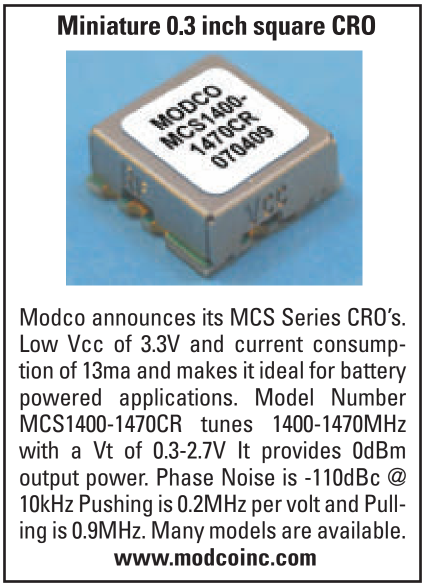

RS 87

RS 32

The Six-port Technique with Microwave and Wireless Applications

Fadhel M. Ghannouchi and Abbas Mohammadi

One of the main issues in microwave and wireless system design is to ensure high performance with low cost techniques. The six-port technique allows for this in critical network design areas. This practical resource offers a thorough overview of the six-port technique, from basic principles of radio frequency measurement-based techniques and multiport design, to coverage of key applications, such as vector network analyzers, software-defined radio and radar.

The first couple of chapters introduce microwave network theory, modeling, network analyzers and the fundamentals of the six-port technique. Design considerations and calibration techniques are then addressed, including the various types of six-port designs and calibration standards and techniques. Six-port network analyzers are covered as are source-pull and load-pull measurements using the six-port technique. The last couple of chapters cover six-port wireless applications, such as receivers, ultra-wideband, software radio and millimeter-wave radios, along with microwave applications such as reflectometer, wave-correlator, direction finders, radar, antenna measurement, material characterization and optical measurement. Each chapter has a list of individual references, which is useful for further research or learning about each area covered.

This book covers a specific focused area of microwave theory and application and is very good for readers who want to learn more about the six-port technique. However, it would not be appropriate for generalists looking to further their knowledge in microwaves unless they are knowledgeable in this area. This book is a practical resource covering the six-port technique and key related applications. To our knowledge, *The Six-port Technique with Microwave and Wireless Applications* is the first book dedicated to six-port applications and principles, and serves as a current, one-stop guide offering cost-effective solutions for challenging projects in the field.

To order this book, contact:

Artech House
685 Canton St., Norwood, MA 02062
(781) 769-9750 ext. 4030;
or
16 Sussex St., London SW1V 4RW, UK
+44 (0) 20 7596-8750

240 pages; $89, £55
ISBN: 978-1-60807-033-6

Advertising Index

RS No.	Advertiser	Page No.	Web Address
1	Advanced Switch Technology	149	http://mwj.hotims.com/28487-1
2	Advanced Test Equipment Rentals	110	http://mwj.hotims.com/28487-2
3,4	Aeroflex	9,139	http://mwj.hotims.com/28487-3
5	Aeroflex / Inmet, Inc.	90	http://mwj.hotims.com/28487-5
6	Aeroflex / KDI-Integrated Products	111	http://mwj.hotims.com/28487-6
7	Aeroflex / Metelics, Inc.	65	http://mwj.hotims.com/28487-7
8	Aeroflex / Weinschel, Inc.	37	http://mwj.hotims.com/28487-8
9,10,11,128	Agilent Technologies, Inc.	33,77,125,151	http://mwj.hotims.com/28487-9
12	AMCAD Engineering	80	http://mwj.hotims.com/28487-12
13	AML Communications Inc.	83	http://mwj.hotims.com/28487-13
	AMTA 2010	130	www.AMTA2010.org
14	AnaPico AG	66	http://mwj.hotims.com/28487-14
15	Anaren Microwave	20-21	http://mwj.hotims.com/28487-15
16	Anatech Electronics, Inc.	98	http://mwj.hotims.com/28487-16
17	Anritsu Company	45	http://mwj.hotims.com/28487-17
18	Applied Radar, Inc.	149	http://mwj.hotims.com/28487-18
19	AR RF/Microwave Instrumentation	87	http://mwj.hotims.com/28487-19
20,21,22	Artech House	68,144,150	http://mwj.hotims.com/28487-20
23	AWR	11	http://mwj.hotims.com/28487-23
24	Boonton Electronics		
	(a Wireless Telecom Group Company)	COV 2	http://mwj.hotims.com/28487-24
25	Carlisle Interconnect Technologies	13	http://mwj.hotims.com/28487-25
26	Cernex, Inc.	28	http://mwj.hotims.com/28487-26
27	Channel Microwave Corporation	18	http://mwj.hotims.com/28487-27
28	Ciao Wireless, Inc.	50	http://mwj.hotims.com/28487-28
29	Cobham Defense Electronic Systems	47	http://mwj.hotims.com/28487-29
30	Coilcraft	15	http://mwj.hotims.com/28487-30
31	COMSOL, Inc.	85	http://mwj.hotims.com/28487-31
32	CPE Italia	149	http://mwj.hotims.com/28487-32
33	CPI Beverly Microwave Division	39	http://mwj.hotims.com/28487-33
34	CST of America, Inc.	25	http://mwj.hotims.com/28487-34
	CTIA Wireless 2010	147	www.ctiashow.com
35	Daico Industries, Inc.	31	http://mwj.hotims.com/28487-35
36	dBm, LLC	96	http://mwj.hotims.com/28487-36
37	Eastern Wireless TeleComm, Inc.	101	http://mwj.hotims.com/28487-37
38	Empower RF Systems, Inc.	91	http://mwj.hotims.com/28487-38
39	ES Microwave, LLC	66	http://mwj.hotims.com/28487-39
40	Fairview Microwave	93	http://mwj.hotims.com/28487-40
41	Frontlynk Technologies Inc.	135	http://mwj.hotims.com/28487-41
42	G.T. Microwave Inc.	94	http://mwj.hotims.com/28487-42
43	Herotek, Inc.	30	http://mwj.hotims.com/28487-43
44	Hirai SK Corporation	124	http://mwj.hotims.com/28487-44
45,46,	Hittite Microwave Corporation	113,114,	http://mwj.hotims.com/28487-45
47,48		115,117	
49	Holzworth Instrumentation	106	http://mwj.hotims.com/28487-49
50	Huber + Suhner AG	75	http://mwj.hotims.com/28487-50
	IEEE WAMICON 2010	70	www.wamicon.org
51	IMST GmbH	68	http://mwj.hotims.com/28487-51
52	ITT Microwave Systems	52	http://mwj.hotims.com/28487-52
53	Jersey Microwave	38	http://mwj.hotims.com/28487-53
54	JFW Industries, Inc.	89	http://mwj.hotims.com/28487 54
55	JQL Electronics Inc.	99	http://mwj.hotims.com/28487-55
56	K&L Microwave, Inc.	7	http://mwj.hotims.com/28487-56
57	KR Electronics, Inc.	149	http://mwj.hotims.com/28487-57
58	Linear Technology Corporation	61	http://mwj.hotims.com/28487-58
59	Lorch Microwave	53	http://mwj.hotims.com/28487-59
60,61	M/A-COM Technology Solutions	42,43	http://mwj.hotims.com/28487 60
62	Maury Microwave Corporation	6	http://mwj.hotims.com/28487-62
63	MECA Electronics, Inc.	86	http://mwj.hotims.com/28487-63
64	MiCIAN GmbH	88	http://mwj.hotims.com/28487-64
65	Micro-Coax	73	http://mwj.hotims.com/28487-65
66	Microphase Corporation	95	http://mwj.hotims.com/28487-66
67	Microsemi	60	http://mwj.hotims.com/28487-67
	Microwave Journal	116,132,136,146	www.mwjournal.com
68	Milmega Limited	137	http://mwj.hotims.com/28487-68
69,70	Mimix Broadband, Inc.	26,27	http://mwj.hotims.com/28487-69
71,72,73,	Mini-Circuits	4-5,16,35,	
74,75,76,		57,58,69,	
77,78,79,		79,97,123,	
80,81,82		127,141,153	http://mwj.hotims.com/28487-71
83,84,85	MITEQ Inc.	3,103,145	http://mwj.hotims.com/28487-83
86,87	Modco, Inc.	148,149	http://mwj.hotims.com/28487-86
88,89	Narda Microwave-East,		
	an L3 Communications Co.	36,126	http://mwj.hotims.com/28487-88
90	NoiseWave Corp.	8	http://mwj.hotims.com/28487-90
91	Norden Millimeter Inc.	32	http://mwj.hotims.com/28487-91
92	OEwaves	105	http://mwj.hotims.com/28487-92
93	OML Inc.	129	http://mwj.hotims.com/28487-93
94	Pascall Electronics Limited	56	http://mwj.hotims.com/28487-94
95	Pole/Zero Corporation	121	http://mwj.hotims.com/28487-95
96	Programmed Test Sources, Inc.	COV 3	http://mwj.hotims.com/28487-96
97	Pulsar Microwave Corporation	104	http://mwj.hotims.com/28487-97
98	Quartzlock	112	http://mwj.hotims.com/28487-98
	QuinStar Technology, Inc.	107	www.quinstar.com
99	R&K Company Limited	122	http://mwj.hotims.com/28487-99
100	Radiall	149	http://mwj.hotims.com/28487-100
101	Radio Waves, Inc.	84	http://mwj.hotims.com/28487-101
102	Reactel, Incorporated	54	http://mwj.hotims.com/28487-102
103	Remcom	119	http://mwj.hotims.com/28487-103
104	RF TEC Mfg., Inc.	149	http://mwj.hotims.com/28487-104
105,106	RFHIC	74,76	http://mwj.hotims.com/28487-105
107	RFMD	109	http://mwj.hotims.com/28487-107
108	RLC Electronics, Inc.	23	http://mwj.hotims.com/28487-108
109	Rohde & Schwarz GmbH	67	http://mwj.hotims.com/28487-109
110	Rohde & Schwarz, Inc.	40-41	http://mwj.hotims.com/28487-110
111	Rosenberger	64	http://mwj.hotims.com/28487-111
112	RT Logic	81	http://mwj.hotims.com/28487-112
113	Sector Microwave Industries, Inc.	149	http://mwj.hotims.com/28487-113
114	Sonnet Software, Inc.	19	http://mwj.hotims.com/28487-114
115	Special Hermetic Products, Inc.	149	http://mwj.hotims.com/28487-115
116	Spectrum Elektrotechnik GmbH	133	http://mwj.hotims.com/28487-116
117,118	Synergy Microwave Corporation	63,143	http://mwj.hotims.com/28487-117
119	Teledyne Storm Products	71	http://mwj.hotims.com/28487-119
120	Trilithic Inc.	29	http://mwj.hotims.com/28487-120
121	Universal Microwave		
	Components Corporation	78	http://mwj.hotims.com/28487-121
122	UTE Microwave Inc.	131	http://mwj.hotims.com/28487-122
123	Waveline Inc.	44	http://mwj.hotims.com/28487-123
124	Weinschel Associates	108	http://mwj.hotims.com/28487-124
125	Wenzel Associates, Inc.	92	http://mwj.hotims.com/28487-125
126	Werlatone, Inc.	COV 4	http://mwj.hotims.com/28487-126
127	Z~Communications, Inc.	49	http://mwj.hotims.com/28487-127

Visit mwjournal.com/info and enter RS# to request information from our advertisers

Sales Representatives

Microwave Journal

Carl Sheffres, Publisher

Eastern and Central Time Zones
Chuck Boyd
Northeast Reg. Sales Mgr.
(New England, Upstate NY, Eastern Canada)
685 Canton Street
Norwood, MA 02062
Tel: (781) 769-9750
FAX: (781) 769-5037
cboyd@mwjournal.com

Michael Hallman
Eastern Reg. Sales Mgr.
(Mid-Atlantic, Southeast, Midwest)
4 Valley View Court
Middletown, MD 21769
Tel: (301) 371-8830
FAX: (301) 371-8832
mhallman@mwjournal.com

Pacific and Mountain Time Zones
Wynn Cook
Western Reg. Sales Mgr.
PO Box 23200
San Jose, CA 95153
Tel: (408) 224-9060
FAX: (408) 224-6106
wcook@mwjournal.com

International Sales
Richard Vaughan
International Sales Manager
16 Sussex Street
London SW1V 4RW, England
Tel: +44 207 596 8742
FAX: +44 207 596 8749
rvaughan@horizonhouse.co.uk

Germany, Austria, and Switzerland (German-speaking)
WMS.Werbe- und Media Service
Brigitte Beranek
Gerhart-Hauptmann-Street 33,
D-72574 Bad Urach
Germany
Tel: +49 7125 407 31 18
FAX: +49 7125 407 31 08
bberanek@horizonhouse.com

Israel
Oreet Ben Yaacov
Oreet International Media
15 Kineret Street
51201 Bene-Berak, Israel
Tel: +972 3 570 6527
FAX: +972 3 570 6526
obenyaacov@horizonhouse.com

Ed Kiessling, Traffic Manager

Korea
Young-Seoh Chinn
JES Media International
2nd Floor, ANA Bldg.
257-1, Myungil-Dong
Kangdong-Gu
Seoul, 134-070 Korea
Tel: +82 2 481-3411
FAX: +82 2 481-3414
yschinn@horizonhouse.com

Japan
Katsuhiro Ishii
Ace Media Service Inc.
12-6, 4-Chome,
Nishiiko, Adachi-Ku
Tokyo 121-0824, Japan
Tel: +81 3 5691 3335
FAX: +81 3 5691 3336
amskatsu@dream.com

China
Michael Tsui
ACT International
Tel: 86-755-25988571
Tel: 86-21-62511200
FAX: 86-10-58607751
michaelT@actintl.com.hk

Hong Kong
Mark Mak
ACT International
Tel: 852-28386298
markm@actintl.com.hk

TEST AND MEASUREMENT

ANSWERS AVAILABLE ONLINE AT WWW.MWJOURNAL.COM

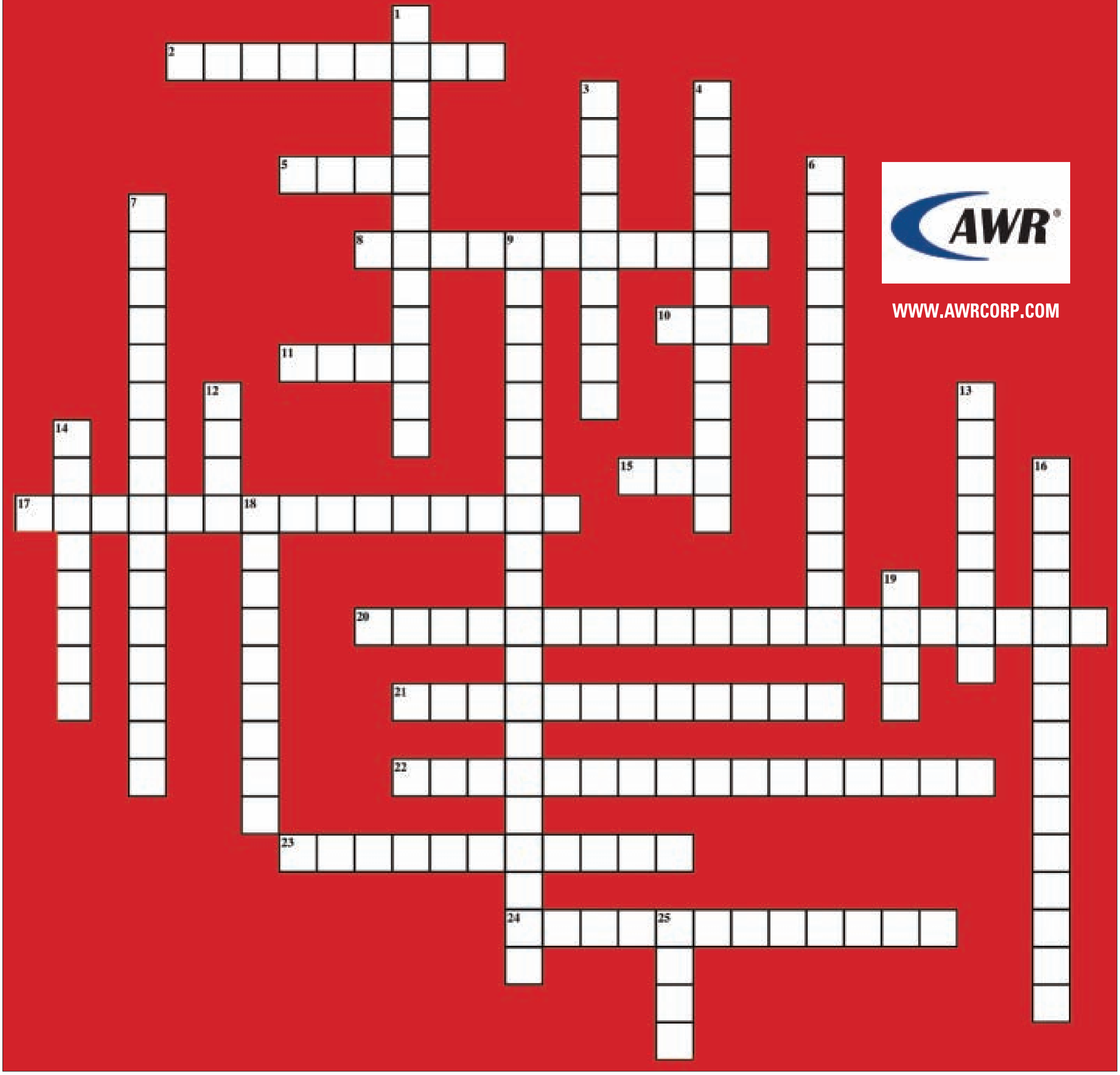

ACROSS

2 Energy at integral multiples of the frequency of the fundamental signal
5 Voltage Standing Wave Ratio
8 The output signal-to-noise ratio divided by the input signal-to-noise ratio (2 words)
10 Intermodulation Distortion
11 Nonlinear Vector Network Analyzer
15 Peak to Average power Ratio
17 A nonlinear, frequency-domain, steady-state simulation (2 words)
20 PAE (3 words)
21 Describes the behavior of linear electrical networks
22 Emulator that produces the distortions on an RF signal when receivers and transmitters move with respect to one another (2 words)
23 Extension of S-parameters for nonlinear behavior
24 Fs = Fa (V/c) (2 words)

DOWN

1 BER (3 words)
3 When the output signal is not proportional to the input signal
4 Mappings of the input signal to the spectral components appearing at all device ports generated by device nonlinearity
6 Amplifier with a half-sine voltage waveform, containing even harmonics, and a square current waveform, containing odd harmonics (3 words)
7 Amplifier that power-combines two amplifiers; one is called the "carrier" amplifier and the second is called the "peaking" amplifier (2 words)
9 EVM (3 words)
12 Short for Additive White Gaussian Noise
13 Short for Poly-Harmonic Distortion model (2 words)
14 Process of altering the impedances at the output of an RF device while measuring the device behavior (2 words)
16 DUT (3 words)
18 The vector ratio of voltage to current
19 Adjacent Channel Power Ratio
25 Large Signal Network Analyzer

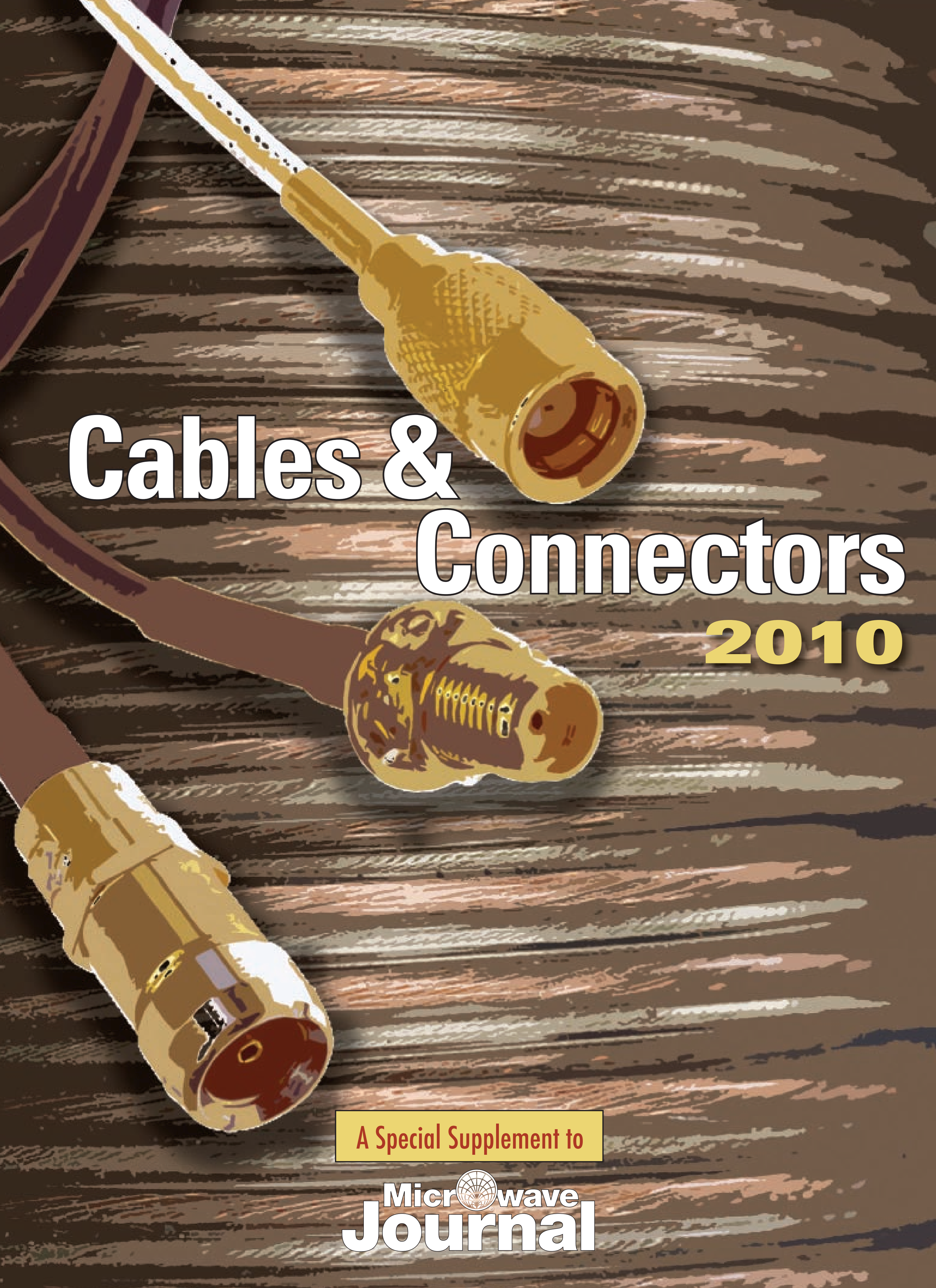

Cables & Connectors

2010

A Special Supplement to

Microwave Journal

New From Maury Microwave

Right Performance
Right Price

TactiCal™ Products

Introducing an entirely new line of ***instrument-grade*** coaxial and waveguide calibration standards which conform to the same high quality and exacting requirements that have made Maury products the ***Gold Standard*** of the industry for over 50 years. Maury's **TactiCal™** Calibration Standards are ideal for applications that don't require metrology-grade components, but still need the level of confidence you only get with Maury products.

Maury's **TactiCal™** line of Calibration Standards are designed to save you money, while providing you with ruggedness and durability for your high-volume, field service and repetitive measurement applications.

Maury's **TactiCal™** Calibration Standards include 50Ω coaxial VNA Calibration Kits, Opens, Fixed Loads and Shorts in 1.85mm, 2.4mm, 3.5mm, and Type N. This new line also includes Waveguide-to-Coax, and Coax-to-Coax (in-series and between series) Adapters. Look for the Maury **TactiCal™** label when you need the best in ***instrument-grade*** calibration standards and you'll always ***Measure With Confidence***.

Call or visit our website for more information about Maury **TactiCal™** and metrology-grade calibration standards, or about any of our full line of Device Characterization Solutions.

MAURY MICROWAVE CORPORATION

2900 Inland Empire Blvd., Ontario, California 91764 • USA
Tel: 909-987-4715 • Fax: 909-987-1112 • Email: maury@maurymw.com
On The Web at MAURYMW.COM

Cables & Connectors Supplement
Table of Contents

FEATURES

Staff

Publisher: Carl Sheffres
Editor: David Vye
Managing Editor: Keith W. Moore
Technical Editor: Patrick Hindle
Associate Technical Editor: Dan Massé
Staff Editor: Jennifer DiMarco
Editorial Assistant: Barbara Walsh
Consulting Editor: Harlan Howe, Jr.
Consulting Editor: Frank Bashore
Consulting Editor: Peter Staecker
Consulting Editor: Dan Swanson
Web Editor: Samantha Bookman
Audience Development Manager: Michelle Frazier
Traffic Manager: Edward Kiessling
Director of Production & Distribution: Robert Bass
Graphic Designer & Production Coordinator: Janice Levenson
Graphic Designer: Sachiko Stiglitz

EUROPE

International Editor: Richard Mumford
Office Manager: Eugenie Hardy

CORPORATE STAFF

CEO: William M. Bazzy
President: Ivar Bazzy
Vice President: Jared Bazzy

Posted under Canadian international publications mail agreement #0738654

CHOOSING THE OPTIMAL HIGH FREQUENCY COAXIAL CABLE

Operating frequencies for coaxial transmission lines have steadily climbed from below 1 to 110 GHz and beyond over the last few decades. This has caused RF/microwave engineers to search for coaxial transmission lines capable of effectively transmitting at these higher frequencies. The coaxial cable market has responded to these substantial leaps in operating frequencies by offering modern cable designs that far exceed the performance specifications contained in the military's most comprehensive coaxial cable standard, MIL-DTL-17. Many leading cable manufacturers now employ production methods, design innovations and material technologies that optimize the transmission of very high frequency microwave signals. However, no perfect design solution exists to fit all possible applications. This article will discuss the pros and cons of different coaxial cable constructions to help engineers and designers choose the optimal solution for their specific design needs.

Coaxial cable derives its name from the spatial relationship shared between the center conductor and the outer conductor. ***Figure 1*** shows this "co-axial" positioning of conductors. A British engineer and mathematician by the name of Oliver Heaviside first patented the basic design of coaxial cable in 1880 (Patent Number: 1407). Then in 1929, almost 50 years later, Lloyd Espenshied and Herman Affel of AT&T's Bell Labs secured a United States patent for the first modern coaxial cable design (US Patent Number: 1,835,031). Soon afterwards, coaxial cable started gaining popularity with radio engineers and became the preferred choice for connecting antennas to transmitters and receivers. As it turns out, coaxial cable is well suited for running up and down metal antenna towers, along gutters, or around any other metal structures since all electrical energy transmits down the interior of the cable and remains isolated from external influences.

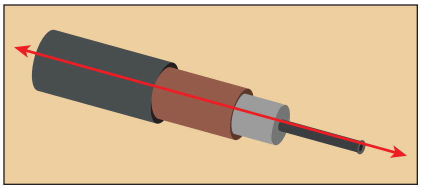

▲ *Fig. 1 Center and outer conductor alignment along a common axis.*

In the late 1920s and early 1930s, Bell Labs set out to determine which coaxial impedance value was optimum. Surprisingly, the optimum impedance changes depending on the primary application. By experimentation Bell Labs found 30 ohms is best for high power, 77 ohms is best for low attenuation, and for high voltage 60 ohms turned out to be the best impedance value. Most modern coaxial cables come in 50, 75 or 93 ohm impedances and 50 ohms is by far

BOB THIELE AND STAN HARDIN
Dynawave Cable Inc., Haverhill, MA

TAILORED SYSTEMS SOLUTONS

For **military/aerospace systems** that require:

- High levels of mechanical and electrical performance under extreme environmental conditions
- Product configured to meet program needs
- Strong support during system development
- Reliable performance over time

HIGH PERFORMANCE CABLE ASSEMBLIES

For **systems and test & measurement applications** that require:

- Rapid product availability and quick-response service
- Durability and reliability over time with use
- Stable microwave performance

BUILD-TO-PRINT MANUFACTURING SERVICES

Serving **defense and select telecom markets** that require:

- 50 Ohm semi-rigid configurations
- High mix, low- to mid-volume production
- Reliable performance as a critical parameter
- Support during customer's product development cycle
- Support for demanding schedules
- Blindmate connector interface expertise

True Blue® • Phase Master® • Storm Flex® • FlexFit™ • Accu-Test® • Maximizer™

Teledyne Storm–Microwave. Where "best fit" means more than just offering you the right product. It also means offering you the right services and technical expertise to support your unique needs. **Call us now to discuss those needs.**

TELEDYNE
STORM PRODUCTS
A Teledyne Technologies Company

Microwave Business Unit
10221 Werch Drive
Woodridge, Illinois 60517

Tel 630.754.3300
Toll Free 888.347.8676
www.teledynestorm.com/mjs0310

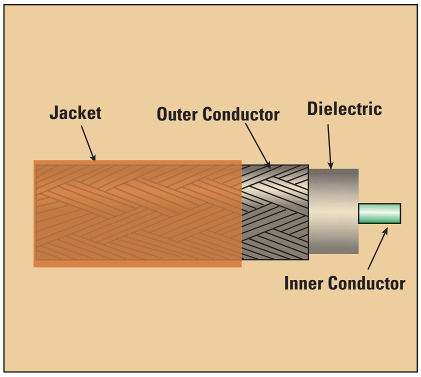

▲ *Fig. 2 Basic coaxial cable construction.*

the most popular impedance choice for high frequency transmission lines.

Although other industry standards have come and gone since the 1930s, MIL-C-17, now called MIL-DTL-17, has become the most comprehensive and most referenced coaxial cable standard. Three examples of how this military standard impacts our daily lives are:

- Cable Television: The National Cable & Telecommunications Association most recent statistics identify 104.7 million CATV subscribers in the United States. The majority of those households receive their video transmissions through a M17/2 - RG6 cable.
- Vital Emergency Services: M17/28 – RG058 remains one of the most widely used 50 ohm radio antenna cables. It is used on most two-way radio communications systems, such as CB radios, police, fire, ambulance and marine radios.
- A recent GOOGLE web search for "MIL-C-17" produced over seven million references.

We see that many times a day our lives benefit from MIL-DTL-17 cables, but when it comes to transmitting frequencies above 12 GHz, designers must turn to modern cable designs that far exceed the performance specifications of M17 cables. When working at higher and higher frequencies the question we have to ask is, "What is the optimal cable choice for my application?" The following discussion seeks to answer this question by looking at various cable constructions.

OPTIMAL COAXIAL CABLE CONSTRUCTIONS

Coaxial cable design choices include physical size, frequency performance, attenuation, power handling, flexibility, strength, environmental conditions and cost. Today's engineers and designers can choose from a wide variety of design and construction choices, each having their own benefits. The common components found in every coaxial cable include the inner conductor, the dielectric, the outer conductor and the jacket. Each of these components can employ production methods, design innovations and material technologies that optimize specific mechanical and electrical properties, but choosing to boost performance in one area often means reducing performance in another. The following discussion will explain this give and take with regard to performance specification, and provide guidance in making the right choices to successfully match a coaxial cable transmission line to an application.

Inner conductor design choices impact the cable's life span when subjected to dynamic flexure. They also largely influence the attenuation performance (see ***Figure 2***). Basic design choices include the number of strands that make up the conductor and the base metal and surface plating. There are other conductor options, but most high frequency cables use these standard wire constructions for inner conductors including single strand (solid), 7 strands, 19 strands and 37 strands. As a general rule of thumb, the more strands a conductor has the more flexible it will be and the longer its dynamic flexure life will extend. However, the down side to increasing the flexibility of the conductor is that the attenuation caused by the conductor also increases. The designer sacrifices attenuation performance for better flexure performance.

Table 1 lists general data pertaining to the dynamic flexure life of copper conductors with various stranding factors. This data was derived experimentally on a MIL-T-81490 flexure test fixture and is offered for reference only since dynamic flexure life depends on bend radius, angular deflection and the rate of flexures per minute.

In addition to the number of strands contained in the center conductor, the base metal or surface plating conductivity can significantly affect the attenuation of high frequency coaxial cables. A phenomenon known as "skin effect" allows cable designers to take advantage of thin surface layers of highly conductive metals such as silver to minimize cable attenuation. Even though silver is expensive, a relatively thin layer of plating provides significant improvement in loss. ***Figure 3*** shows the effective skin depth of electrical energy traveling in on a copper conductor between 10 MHz and 40 GHz. Above 10 GHz the skin depth is less than 1 micron, which demonstrates a 40 micron thickness of silver plating over the copper will carry all of the electrical energy and reduce the overall conductor losses.

Table 2 shows the conductivity of the most common conductor surface plating used in high frequency cables and coaxial connectors, ranked from best to worst. Although silver plating offers better conductivity, it also costs significantly more than copper

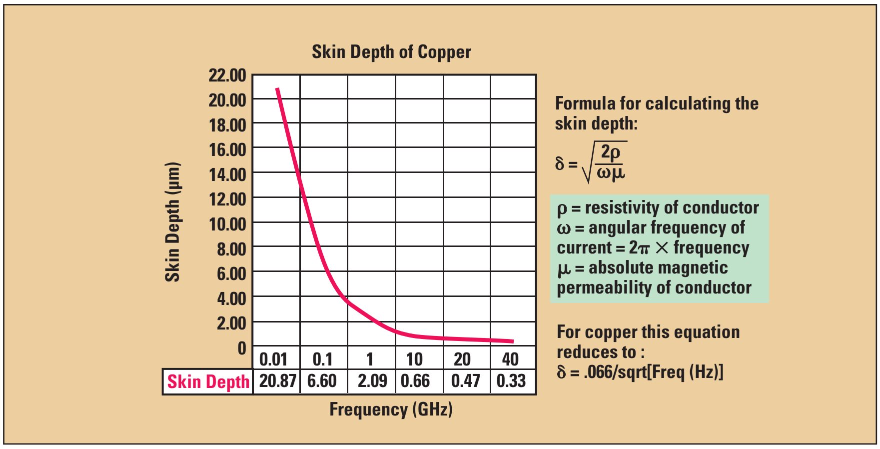

▲ *Fig. 3 Skin depth calculations for a copper conductor.*

Our RF Products Are Ready to Meet Your Toughest Demands

Our RF connectors, cables and cable assemblies are engineered for optimal performance. Whether it's **microminiature**, such as the MMCX and OSMM connectors; **high power**, such as the OSP and OSSP connector series; or the latest in **blind-mate** backplane technology, such as our multiposition SMPM modules designed for VITA 67, our products are made to exacting performance, material and quality standards.

We offer a full range of commercial-off-the-shelf (COTS) and military specified products.

Tyco Electronics has been enabling mission-critical applications for more than 50 years.

To see the full range of solutions, visit **www.tycoelectronics.com/ADM/RF** or talk to your local Tyco Electronic representative.

Visit http://mwj.hotims.com/28486-26 or use RS# 26 at www.mwjournal.com/info

Tyco Electronics
Our commitment. Your advantage.

or aluminum; both cost and attenuation performance must be considered when choosing the optimal conductor finish. Taking advantage of skin effect at microwave frequencies, however, means the plating thickness can be relatively thin, which helps control costs.

To summarize, multi strand center conductors offer much better flexure life, but sacrifice attenuation performance compared with a solid conductor. Consideration must be given as to whether attenuation or flexibility is most important before selecting the best cable construction for any given application. Also, most high frequency coaxial cables employ silver plated conductors because the conductivity of silver is better than aluminum or copper, and the skin effect at high frequencies enables thin layers of silver plating to add substantial performance benefit.

Dielectrics provide an insulating layer between two conductors and, in the case of coaxial cables, also perform an important mechanical function by supporting the outer conductor and keeping both conductors fixed along their common axis. Dielectrics used in manufacturing high frequency coaxial cables have two very important characteristics: low dielectric constants and low dissipation factors.

The dielectric constant (k) of a material is used to determine that material's ability to carry alternating current when compared to air in a vacuum. A vacuum provides the most efficient means of transmitting electrical energy and has a k of 1.000. All other materials have higher values for their respective dielectric constants. Values for the most common coaxial cable dielectrics are shown in ***Table 3***. To minimize power losses it is always desirable to have the lowest possible dielectric constant in high frequency coaxial cables.

Dissipation factor is a measure of the inefficiency of a dielectric material. All dielectrics dissipate electric power in the form of heat because of their inefficiencies and the more inefficient a dielectric is, the higher its dissipation factor will be. Table 3 shows comparable dissipation factors for dielectric materials used in high frequency coaxial cables. To minimize power losses, it is always desirable to use materials with the lowest possible dissipation factors.

As shown in Table 3, air in a vacuum provides the optimal dielectric material for transmitting electrical energy. However, air does not provide the mechanical support required to keep the center conductor and outer conductor of a coaxial cable fixed in place. The next best material, which

TABLE I

COMPARISON OF COMMON STRANDING CONSTRUCTIONS FOR INNER CONDUCTORS

Ranking by Best Attenuation Performance	*Ranking by Best Dynamic Flexure Life*	*Number of Strands*	*Number of Flexures (bend radius = 20x wire diameter)*	*Approximate Attenuation Increase (% of Single Strand Loss)*
1	4	Single Strand	5,000 to 10,000	100
2	3	7 Strand	50,000 to 70,000	107
3	2	19 Strand	150,000 to 200,000	113
4	1	37 Strand	>500,000	122

TABLE II

COMPARISON OF COMMON CONDUCTOR SURFACE FINISHES

Ranking by Best Attenuation Performance	*Surface Material*	*Electrical Conductivity (/ cm Ω)*	*Reduction in Conductivity (% change from Silver)*
1	Silver	$.630 \times 10^6$	100
2	Copper	$.596 \times 10^6$	94
3	Aluminum	$.378 \times 10^6$	60

TABLE III

COMPARISON OF COMMON COAXIAL CABLE DIELECTRICS

Ranking by Dielectric Constant	*Ranking by Dissipation Factor*	*Dielectric Material*	*Dielectric Constant*	*Dissipation Factor*	*Temp. Range (°F)*
1	1	Air in Vacuum (for reference)	1.000000		
2	2	Low Density or Expanded PTFE	1.30	<0.00008	-410 / +500
3	3	(PTFE) Polytetrafluoroethylene	2.05	<0.0002	-410 / +500
4	4	(PFA) Perfluoroalkoxy	2.0	<0.0004	-300 / +500
5	5	(FEP) Fluorinated Ethylene Propylene	2.1	<0.0007	-100 / +400
6	3	(PE) Polyethylene	2.25	<0.0002	-30 / +180
7	6	(PVC) Polyvinyl Chloride	3.18	<.016	-40 / +220


Adapters, Attenuators, Blind Mate Connectors, Cable Assemblies, Connectors, Delay Lines, Duplexers Equalizers, Fine Grain Equalizers, Gain Amplitude Equalizers, Line Stretchers, Machines, Phase Adjusters, Push - On Connectors & Adapters Quick Connections, Terminations (Coax-) Tools, Waveguide to Coax - Adapters & Transmissions, and................
Advanced Designs to your needs!
Spectrum
Elektrotechnik GmbH
when Quality is needed
80905 Munich, Germany
P.O. Box 450533
Telephone: +49-89-3548-040
Facsimile: +49-89-3548-0490
WWW.SPECTRUM-ET.COM * Email: Sales@Spectrum-et.com
Visit http://mwj.hotims.com/28486-20 or use RS# 20 at www.mwjournal.com/info
CableAssembliesE2

TABLE IV

COMPARISON OF VARIOUS OUTER CONDUCTOR SHIELDING CONSTRUCTIONS

Ranking by Best Atten. Perf.	Ranking by Best Shielding Perf.	Ranking by Best Physical Toughness	Ranking by Flexibility	Outer Conductor Style
1	1 >100 dB	4	3	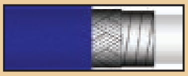 Wrapped Foil + Woven Round Braid
2	2 >90 dB	1	5	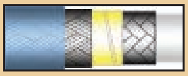 Woven Flat Braid + Wrapped Foil + Woven Round Braid
3	3 >80 dB	2	4	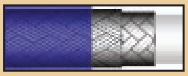 Woven Flat Braid + Woven Round Braid
4	4 >65 dB	3	2	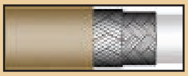 Two Woven Round Braids
5	5 >40 dB	5	1	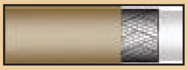 One Single Woven Round Braid

does provide the needed mechanical strength for flexible cables, is a low density Polytetrafluoroethylene (PTFE). Low density PTFE is also referred to as "expanded" or "microporous" PTFE throughout the RF and microwave industry. These terms all describe the same type of material that is standard PTFE with microscopic air spaces distributed throughout. The more air spaces in the material the lower the density and the better the electrical performance of the composite dielectric. This results in a dielectric material, which has a lower dielectric constant and dissipation factor than solid PTFE but still has enough strength to provide a stable mechanical structure to support both conductors.

The top manufacturers of low loss, high performance cables utilize low density PTFE exclusively in their cable constructions for the reasons listed above. GORE™ expanded PTFE and DynaCore™ low density PTFE dielectrics are two examples of how this material technology is applied in coaxial cable products.

MIcable Inc.

ISO9001:2008 CERTIFIED

High performance cable assemblies with stainless steel connectors

USA manufacturing technique
Advanced production & test equipments
Cable & connectors from world's leading RF & Microwave manufacturers

MIcable *is your quality fast and low cost solution !*

Product series	Models *	Inser.Loss Typ.	Return Loss Typ.	Phase Stability vs. Flexure °/GHz	Phase Stability vs. Temp. max. ppm @ +22℃ TO +85℃	FOB Unit Price US$(1-9pcs)
Low Loss Flexible cable assembly with good Phase Stability vs. Flexure	C02-01-01-3FT	1.91dB@18GHz	22dB@18GHz	± 0.05		49.95
Ultra Low Loss Flexible cable assembly with good Phase Stability vs. Flexure & Temperature	A02-01-01-3FT	1.24dB@18GHz	21dB@18GHz	± 0.20	220	69.95
Millimeter Wave Ultra Low Loss Flexible cable assembly with good Phase Stability vs. Flexure & Temperature	B01-40-40-3FT	2.8dB@40GHz	19dB@40GHz	± 0.20	400	134.95

Notes:

* 1. "01"means SMA MALE straight connector, "40"means 2.92mm MALE straight connector,"3FT" means 3 feet long cable.
2. Custom designed assemblies are available.

Seeking world-wide agents

affiliated with SSI

MIcable Inc.
Tel: 86 591-87382856
Email: sales@micable.cn
Website: www.micable.cn

USA Distributor Center:
SSI Cable Corporation
Tel: (360)426-5719
Email: bsmith@ssicable.com

Outer conductor or shield choices impact the attenuation, shielding effectiveness, physical resistance to torque and crushing, and the flexibility of coaxial cables. Basic design choices include braid coverage, application of braid by weaving or wrapping, total number and combination of braid and foil layers, and base metal and surface finish.

There are a variety of ways to design and manufacture shields on coaxial cables. Flexible cables use any combination of braided fine wires and wrapped foils to provide a conductive layer that flexes. ***Table 4*** shows five different variations of outer conductor designs for flexible cables ranked by different design considerations.

Jacket materials serve as a protective covering from the environment. Although cable jackets do not play a role in the electrical performance of a coaxial cable, they are an integral part of the overall cable performance when installed. Some of the environmental conditions cable jackets are designed to protect against include extreme temperature excursions, abrasion, ultra violet radiation, rain, humidity, flame resistance, low smoke and toxicity, resistance to fluids, crushing/bending forces and corrosion. There are various jacket materials offered by manufacturers that are tailored to protect against one or more of these types of environmental conditions. Most manufacturers offer guidance on jacket choices and designers need to consider the service environment their products will experience when choosing the optimal cable for their application.

CONCLUSION

It has been 130 years since Oliver Heaviside first patented the concept of coaxial cable in 1880. Another 80 years have passed since the pioneering work at Bell Labs laid the groundwork for modern coaxial cables to be defined by 50, 75 and 93 ohm impedances and standardized by the military specification, MIL-DTL-17. Today our lives are impacted in many ways by coaxial transmission lines. They are used extensively in two-way communications systems for police and fire departments, rescue personnel, and first responders. The products we consume every day are shipped on carriers who rely on satellite communications systems, GPS tracking and mobile telecommunications technology that all operate with the aid of coaxial cable transmission lines. Our national security is also supported by communication systems, radars, electronic counter measures and target acquisition systems that use coaxial cables.

In the last 30 years a large push to transmit at higher frequencies challenged the manufacturers of high performance coaxial cable to push the technology and introduce new products. These new cables far exceed the performance standards of MIL-DTL-17 and well informed engineers can take advantage of a variety of product designs and innovations to optimize critical performance parameters in their system designs. No single cable offers the best solution for every design application, but by carefully considering the various material and design options related to the inner conductor, dielectric, outer conductor, and jacket and how those options impact the coaxial cable's electrical, mechanical, cost and environmental performance, the optimal product choice can be made. ■

FLEX TEST™ CABLES

DC to 18 GHz from $68^{95} IN STOCK ea. (qty.1-9)

Strength, ruggedness, and reliability…*supercharged!* That's what you get when you choose Mini-Circuits ultra-flexible precision test cables. Engineered to be a workhorse for your day-to-day test operations, these triple shielded cable assemblies are qualified to at least 20,000 bends, employ an advanced strain relief system, and are equipped with passivated stainless steel connectors, *so you can rely on them to* ***flex, connect and disconnect over and over and over again!*** They're so rugged, each test cable is backed by our 6 month guarantee*! With low insertion loss and very good return loss, you can also rely on getting good performance over the wide DC-18 GHz band. Visit our website to choose and view comprehensive performance curves, data sheets, and environmental specifications.

Mini-Circuits...Your partners for success since 1969

New! ***Tough Armored Cables*** *are steel triple shielded and qualified to at least 25,000 bends. They're so rugged they can even pass a crush test of a 600lb. nitrogen tank over the cable 1000 times, without any change in electrical performance.*

RoHS compliant

Frequency Range: DC-18 GHz, Impedance: 50 ohms

Models	Connector Type	Length (Ft.)	Inser. Loss (dB) Midband Typ.	Return Loss (dB) Midband Typ.	Price $ ea. Qty.(1-9)
FLEX TEST CABLES		Male to Male			
CBL-1.5FT-SMSM+	SMA	1.5	0.7	27	68.95
CBL-2FT-SMSM+	SMA	2	1.1	27	69.95
CBL-3FT-SMSM+	SMA	3	1.5	27	72.95
CBL-4FT-SMSM+	SMA	4	1.9	27	75.95
CBL-5FT-SMSM+	SMA	5	2.5	27	77.95
CBL-6FT-SMSM+	SMA	6	3.0	27	79.95
CBL-10FT-SMSM+	SMA	10	4.8	27	87.95
CBL-12FT-SMSM+	SMA	12	5.9	27	91.95
CBL-15FT-SMSM+	SMA	15	7.3	27	100.95
CBL-25FT-SMSM+	SMA	25	11.7	27	139.95
CBL-2FT-SMNM+	SMA to N-Type	2	1.1	27	99.95
CBL-3FT-SMNM+	SMA to N-Type	3	1.5	27	104.95
CBL-4FT-SMNM+	SMA to N-Type	4	1.9	27	112.95
CBL-6FT-SMNM+	SMA to N-Type	6	3.0	27	114.95
CBL-15FT-SMNM+	SMA to N-Type	15	7.3	27	156.95
CBL-2FT-NMNM+	N-Type	2	1.1	27	102.95
CBL-3FT-NMNM+	N-Type	3	1.5	27	105.95
CBL-6FT-NMNM+	N-Type	6	3.0	27	112.95
CBL-10FT-NMNM+	N-Type	10	4.7	27	156.95
CBL-15FT-NMNM+	N-Type	15	7.3	27	164.95
CBL-20FT-NMNM+	N-Type	20	9.4	27	178.95
CBL-25FT-NMNM+	N-Type	25	11.7	27	199.95
		Female to Male			
CBL-3FT-SFSM+	SMA-F to SMA-M	3	1.5	27	93.95
CBL-2FT-SFNM+	SMA-F to N-M	2	1.1	27	119.95
CBL-3FT-SFNM+	SMA-F to N-M	3	1.5	27	124.95
CBL-6FT-SFNM+	SMA-F to N-M	6	3.0	27	146.95
ARMORED CABLES		Male to Male			
APC-6FT-NM-NM+	N-Type	6	3.0	27	181.95
APC-10FT-NM-NM+	N-Type	10	4.8	27	208.95
APC-15FT-NM-NM+	N-Type	15	7.3	27	243.95

Metric Sizes Available On Our Website

6 mo. GUARANTEE

Mini-Circuits will repair or replace your test cable at its option if the connector attachment fails within* ***six* *months of shipment. This guarantee excludes cable or connector interface damage from misuse or abuse.*

Mini-Circuits®
ISO 9001 ISO 14001 AS9100 CERTIFIED

P.O. Box 350166, Brooklyn, New York 11235-0003 (718) 934-4500 Fax (718) 332-4661

YONI2™ Patent Pending ***The Design Engineers Search Engine*** *finds the model you need, Instantly* • For detailed performance specs & shopping online see minicircuits.com

IF/RF MICROWAVE COMPONENTS

403 rev P

COMPARISON OF VNA AND TDR MEASUREMENT UNCERTAINTY USING COAXIAL CABLES

Individuals working in digital applications tend to prefer the Time Domain Reflectometer (TDR), while those involved in traditional RF applications consider the Vector Network Analyzer (VNA) to be a laboratory staple. The push for ever-faster data rates has fueled an analytical re-thinking of high-speed digital signaling. Contemporary wisdom views high-speed digital systems as high-frequency applications, where more traditional microwave analysis techniques apply. Once this concept is embraced, engineers often exploit the strengths of both the TDR and VNA, combining time and frequency domain analysis to accelerate design and development cycles. Both instruments can measure impedance, time delay, phase delay and reflection coefficient so they are often thought of as equals. This begs the question: Is there a quantifiable difference in measurement uncertainty between the TDR and VNA?

Characterizing the time delay of a passive device, such as coaxial cable assembly is a common use for the TDR and VNA. It is therefore an ideal vehicle for a performance comparison. How do the two compare under ideal test conditions, and the less-than-ideal environment of production testing? Do both instruments possess similar levels of measurement precision? This article answers these questions by examining the measurement uncertainty and repeatability of the TDR and VNA.

DESCRIPTION OF EXPERIMENT

To understand the capabilities of any measurement system, it is important to test the system's response to a variety of inputs to avoid erroneous conclusions. For this discussion, the term "input" refers to a "Device Under Test" (DUT), which in this experiment were different cable assemblies from a variety of manufacturers, having a range of insertion loss and VSWR characteristics. In a manner consistent with commonly used production test practices, measurements of the time delay of the cable assemblies described above were measured with a TDR and a VNA. The resulting measurement uncertainty of the two instruments under these conditions was then compared.

A sample of six new cable assemblies were used in the experiment, each equipped with SMA pin connectors. ***Table 1*** details their loss, VSWR and physical length characteristics. The electrical data in Table 1 was acquired through VNA analysis. The experiment consisted of two rounds of testing. Within a round, each sample was connected to the TDR or VNA and measured five consecutive times, without being disconnected or disturbed ("repeat testing"). After five measurements, the sample was

PAUL PINO
W.L. Gore & Associates Inc., Landenberg, PA

Power Dividers

5 Watt power dividers using Wilkinson technology covering 2-6GHz with 18dB of port-port isolation typical. 2, 4 and 8-way configurations are available.

Fixed Attenuators

2 and 5 Watt models with a DC-6GHz range available with SMA or type N connectors

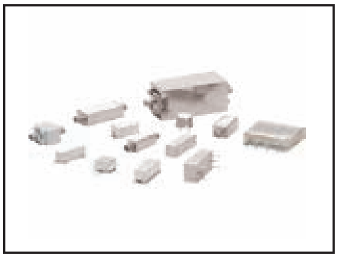

Miniature LC Filters

Lowpass/Highpass and Bandpass filters that are designed to feature high performance in small packages.

Variable Attenuators

Manual with up to 70dB of attenuation in 1dB steps. Solid-state programmable attenuators with a 2-6GHz frequency range and 63dB of attenuation in 1dB steps.

WiMax Test Systems

Trilithic has the capability to integrate various RF components to meet your specific testing & verification requirements. GPIB, Ethernet and other control protocols are available.

TRILITHIC
RF & MICROWAVE

With over 50 years of collective experience in engineering and custom manufacturing, Our goal is to anticipate what you'll need tomorrow, and help you stay a step ahead of your competition. In other words, to Think Ahead. It's what drives real innovation at Trilithic.

At Trilithic, innovation is more than engineering and technology. It's about listening to your needs and expectations. So together we can create solutions that work for you today and tomorrow.

www.trilithic.com

SUBSYSTEMS FOR YOUR SPECIFIC APPLICATION

Trilithic provides test system solutions that are designed to specific requirements.

With as little as a block diagram or a detailed description of your application Trilithic can deliver a custom solution to meet your expectations.

Some of our custom capabilities include the following types of test systems:

Matrix Switching
Blocking and Non-Blocking Configurations
DC–40GHz

Switch Assemblies
1 x 2 up to 1 x 32
Ethernet control available

Preselector Filter Systems
Military Designs
50 and 75 Ohm products
Digital Control Option

Programmable Assemblies
DC–6GHz
Programmable attenuators up to 127 dB per RF path

TRILITHIC
RF & MICROWAVE

think ahead.

(888) 292-2581 www.trilithic.com

TABLE I

ELECTRICAL/PHYSICAL CHARACTERISTICS OF SAMPLE CABLE ASSEMBLY

	Sample 1	Sample 2	Sample 3	Sample 4	Sample 5	Sample 6
Length	39.4 in	96.0 in.	30.0 in.	36.0 in.	120.0 in.	8.0 in.
Max. loss @ 18 GHz	1.13 dB	5.02 dB	2.66 dB	1.32 dB	4.26 dB	0.46 dB
Max. VSWR thru 18 GHz	1.13:1	1.27:1	1.13:1	1.13:1	1.28:1	1.10:1

removed from the instrument and not reconnected until the next round of testing ("round testing"). The sample assemblies were labeled 1 through 6 and their test order within each round was randomized to reduce test bias. Repeat testing reflects instrument uncertainty, while round-to-round testing reflects measurement reproducibility or test uncertainty.

TEST CONFIGURATIONS

During the TDR portion of testing, the sample assemblies were connected directly to the TDR sampling head while the opposite end was terminated with a 3.5 mm precision open standard. This was done to ensure a well-defined and controlled termination. In the VNA portion of testing, the sample assemblies were connected between ports 1 and 2. In both TDR and VNA testing, standard RF cable assembly care and handling practices were exercised. ***Figure 1*** shows the cable sample assemblies.

EQUIPMENT AND TEST CONDITIONS

For the TDR time delay measurement, a sample assembly, fitted with precision open termination, was connected to the TDR and the round-trip time delay value was recorded using the instrument's built-in time delay measurement algorithm. The round trip time delay is taken as the difference in time between the active waveform (T_2), representing the precision open circuit at the end of the sample assembly, and the stored waveform (T_1), representing the open circuit at the TDR head. The time delay was recorded at a 375 mV level. The actual sample assembly time delay is one half the measured round-trip time delay, as shown in ***Figure 2***.

$$\text{Device time delay}_{\text{TDR}} = (T_2 - T_1)/2$$

For the VNA time delay measurement, the sample assembly was connected to VNA ports 1 and 2 and stimulated through a swept frequency range. Using proprietary software, cumulative phase information over the swept frequency range was extracted from the S_{21} data. The time delay was calculated by perform-

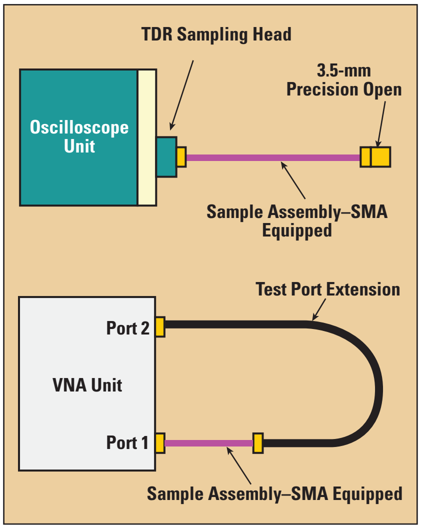

▲ *Fig. 1 Sample assemblies.*

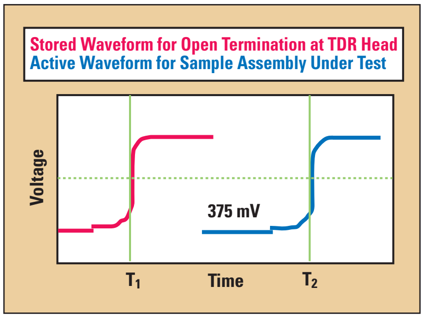

▲ *Fig. 2 TDR waveform display for time delay measurement.*

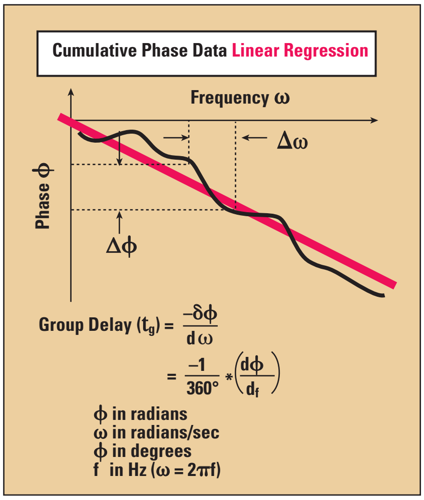

▲ *Fig. 3 Group delay calculation as applied to S-parameter data.*

ing a least-squares curve fit, linear regression of the cumulative phase. The slope of the linear regression is the change in phase with respect to the change in frequency or the group delay (t_g). The group delay value returned from this process is taken as the device time delay (see ***Figure 3***).

RESULTS OF EXPERIMENT

Figure 4 illustrates the ± 3 sigma measurement uncertainty by sample for the TDR and VNA measurements. The following observations were made: measurement uncertainty for both instruments appeared to be device-under-test dependent; the median uncertainty across rounds was considerable; and the overall values for the VNA were significantly lower than those of the TDR. The figure also illustrates the instrument repeatability: the variability associated with measuring the same DUT repeatedly, while not disturbing it or the measurement system. This gives a window into the uncertainty of the instrument itself under the prevailing test conditions. It is predicated on the assumption that the DUT and any related fixtures are stable.

Rounds 1 and 2 were intended to capture the measurement system variability stemming from connect/disconnect cycling of the DUT, referred to as "measurement reproducibility." Connectors can affect measurement reproducibility, but SMA connectors, when new and in good condition, possess sufficient repeatability such that a significant influence on reproducibility was not anticipated. All six sample assemblies were equipped with SMA pin connectors. During the experiment each was thoroughly cleaned before every round and tightened to the appropriate torque value.

In a production test scenario, it is often necessary to re-measure a device for re-classification. ***Figure 5*** shows that between rounds 1 and 2, the measured time delay of a sample differed, on average by 0.3 ps for the VNA and 4.2 ps for the TDR.

ANALYSIS OF BEST-CASE PERFORMANCE

An initial review of the experiment indicated that one sample out of the six performed consistently better than the others in both TDR and VNA testing. The assembly, Sample 6, was identified as a best-case scenario for both instruments and selected to undergo additional analysis. A second experiment, similar to the first, was created to gather information on measurement uncertainty under best-case conditions. With identical instruments, test conditions and configurations, a new experiment consisting of the following was performed:

- Repeat testing consisted of 22 consecutive measurements without disconnecting/disturbing the DUT and test system
- Reproducibility testing consisted of 22 connect/disconnect cycles of the DUT, with measurements taken at each connect/disconnect cycle
- To ensure VNA/TDR test parity, VNA measurements were made using S_{11} reflection techniques as well as the more conventional S_{21} transmission method

The objective was to observe measurement uncertainty under more closely controlled conditions. Towards that end, during TDR testing the 3.5

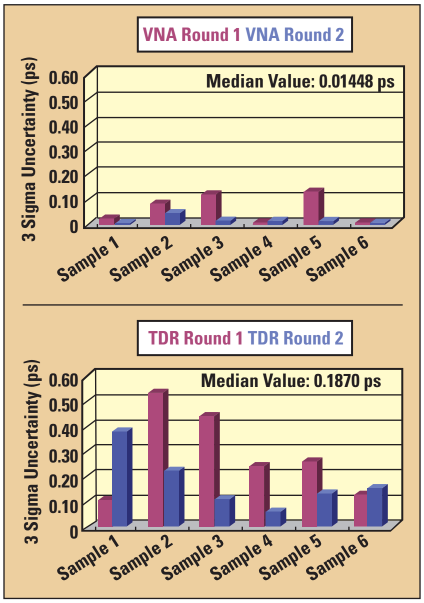

▲ *Fig. 4 "Repeat testing", ±3 sigma uncertainty by test sample.*

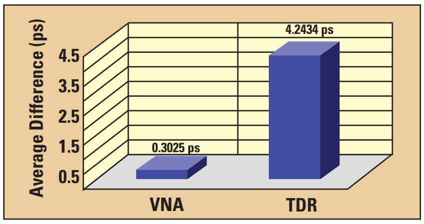

▲ *Fig. 5 Average difference in measured time delay across six test samples from round 1 to round 2.*

mm precision open was left in place during all 22 connect/disconnect measurements; the sample assembly connection was cycled at the TDR sampling head only. Likewise during VNA testing, the sample assembly connection was cycled at port 1 only. This strategy, although not representative of production testing, does introduce a disturbance into the test system such that the outcome can be observed.

The number of measurements (22) was determined through a confidence interval calculation. Twenty-two measurements assure a 98 percent confidence that the sample mean in the experiment will be within ± 0.08 ps of the actual population mean. This is based upon an estimated standard deviation of 0.16 ps.

For this portion of the analysis, TDR and VNA measurement uncertainty was divided into three categories:

- Instrument uncertainty: Uncertainty associated with the instrument platform itself, measured through repeat testing.
- Total uncertainty: Uncertainty resulting from the cumulative effects of instrument characteristics, test fixture, test conditions and operator influences. Measured through connect/disconnect cycling, includes instrument uncertainty.
- Test uncertainty: Resulting from operator error, test fixture influences and prevailing environmental conditions at time of test, measured indirectly.

Figure 6 shows best-case uncertainty for Sample 6. Test uncertainty values were expected to be similar in the TDR and VNA due to similarities in test configurations. With this information, the best-case uncertainty associated with each instrument platform can be assessed.

The pie graphs in ***Figure 7*** reveal that 22 percent of the total measurement uncertainty for the VNA is associated with the instrument itself, as compared to 61 percent for the TDR. This was a repeating theme throughout the experiment. This significant difference means that even under ideal test

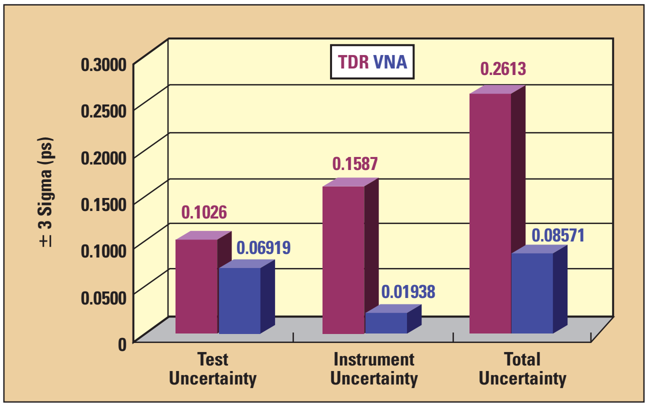

▲ *Fig. 6 ±3 sigma uncertainty analysis based on measurements of Sample 6.*

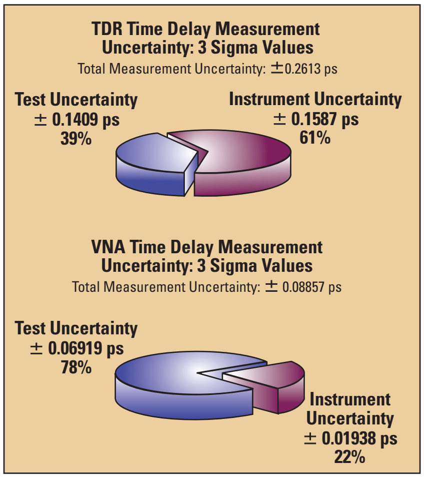

▲ *Fig. 7 Total measurement uncertainty broken down by test and instrument uncertainties.*

conditions, that is minimal test fixture, operator and environmental influences, the gap in TDR/VNA measurement uncertainty will remain, as it is inherent to the instrument performance.

Figure 8 compares the 22 connect/disconnect delta time (T_d) delay measurements of Sample 6 relative to the first measurement using the TDR and VNA. The VNA measurements have a range spanning 0.0983 ps as compared to the TDR's range of 0.275 ps. Both data clearly show a trend downward, that is a progressively shorter device delay. Although the TDR data suggests a repeatability issue with the 3.5 mm connector on the TDR sampling head, it was determined that the variability is associated not with the connector, but the instrument itself.

The downward-trending behavior noted may be attributed to burnishing of the SMA/3.5 mm mated interfaces. A 3.5 mm connector was used as the calibrated reference plane to which the test sample's SMA was mated. Connecting and disconnecting the

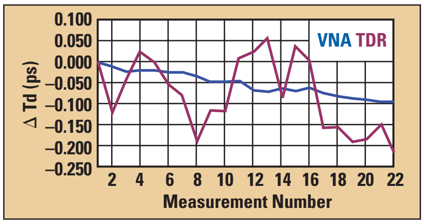

▲ *Fig. 8 Twenty-two connect/disconnect measurements in sequence.*

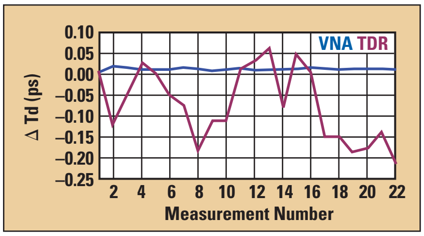

▲ *Fig. 9 Twenty-two connect/disconnect measurements of Sample 6 in sequence.*

SMA interface in succession (without cleaning between cycles, as was done in the experiment) has the potential to burnish the mated connector interface components. It was theorized that over the course of 22 test cycles, the mated interfaces were sufficiently abraded to experience improved electrical contact, as evidenced by a reduction in insertion loss and electrical length.

It is of some interest to compare the absolute time delay values for Sample 6 as measured by the TDR and VNA. An examination of repeat testing produced an average time delay of 0.817364 ns for the VNA and 0.849754 ns for the TDR; a difference of 32.5 ps. This discrepancy was unexpected and an attempt was made to obtain closer agreement between the two instruments.

The average time delay value of 0.849754 ns was referenced to an open circuit at the TDR sampling head, meaning the connection at the head was not terminated. The reflection from the resulting open circuit was stored as a reference waveform. Measurements of Sample 6 were taken with respect to this reference. To improve the agreement between TDR and VNA measurements, the sampling head was fitted with a 3.5 mm pin to 3.5 mm socket precision adapter ("connector saver") from a VNA calibration kit. The adapter provides a precise reference plane and sufficient electrical length to establish a new reference plane well away from the sampling head's 3.5 mm panel connector.

To define a new reference plane, a 3.5 mm (pin) precision open from a VNA calibration kit was used. The open was connected to the sampling head and the resulting waveform was stored as the new reference. TDR measurements of Sample 6 were conducted as described under Equipment and Test Conditions. The above-mentioned method of reference plane calibration was applied to the primary TDR used in this experiment as well as a second TDR of the same manufacturer.

TDR/VNA ONE-PORT MEASUREMENT COMPARISON

To ensure TDR/VNA test parity, the VNA was re-configured from a two-port to a one-port calibration and best-case performance testing was repeated. DUT time delay data was extracted from the resulting S_{11} reflection data. Findings indicate virtually no change in VNA instrument uncertainty, as compared to two-port S_{21} data, and a decrease measurement uncertainty associated with connect/disconnect DUT testing.

Figure 9 compares the 22 connect/disconnect performance of the TDR with that of the VNA, when using S_{11} reflection measurement techniques. As with earlier testing, the VNA's uncertainty is approximately an order of magnitude below that of the TDR under similar measurement conditions.

CONCLUSION

The findings suggest that before making critical production measurements with either a TDR or VNA, an understanding of DUT and measurement system interaction is necessary. Each has its strengths and weaknesses, but in the hands of a properly trained and experienced user, both are formidable tools. Data has been presented indicating that the VNA operates with a significantly lower level of measurement uncertainty under specific conditions. It is left to the reader to decide which best suits his or her needs given the application requirements. ■

ACKNOWLEDGMENT

The author extends his thanks to Jose G. Ramirez, Industrial Statistician, and Harmon Banning, Technologist, and W.L. Gore & Associates Inc. for its guidance and kind assistance in the writing of this technical note.


RF. Microwave Coaxial connector
& Cable Assembly
Frontlynk®
Bridging Gaps
why CAN NOT miss
*Short lead time.
*Accurate cross-examination skills
*High flexibility in manufacture and delivery
*Best Customized Solutions
1.85 mm Connector
DC to 67 GHz; VSWR ≤ 1.2
2.4 mm Connector
DC to 50 GHz; VSWR ≤ 1.2
2.92 mm Connector
DC to 40 GHz; VSWR ≤ 1.2
3.5 mm Connector
DC to 34 GHz; VSWR ≤ 1.2
www.frontlynk.com
E-mail: info@frontlynk.com
Tel: 886-6-356-2626 Fax: 886-6-356-6268
Visit http://mwj.hotims.com/28486-9 or
use RS# 9 at www.mwjournal.com/info

COAXIAL CABLE POWER HANDLING

This application note covers power handling capability of coaxial cables. The matrix of average power over frequency provided for each example cable type is to be used as a guideline.

PEAK AND AVERAGE POWER

There are two potential failure modes in cables used to transmit high peak power. One is voltage breakdown; the other is overheating. The major concern associated with application of peak power is breakdown due to high potential. By themselves, the cable and the connectors may break down under high voltage due to peak power. However, the cable-to-connector junction is the one location on the cable assembly most sensitive to high potential breakdown. Prudent design of overlapping dielectrics and proper selection of connector type, combined with actual high potential or severe requirements testing, ensures that breakdown will not occur. Another consideration in pulsed systems is overheating due to CW power.

TABLE I
CONNECTOR CENTER CONDUCTOR DIAMETERS

Connector	"a" (center conductor diameter)
ETNC	0.085 inch
N	0.120 inch
SC	0.120 inch
SMA	0.050 inch
TNC	0.085 inch

AVERAGE (CW) POWER HANDLING CAPABILITY

The major effect of average power in cable assemblies is the generation of heat from power dissipation and the resultant temperature rise. Many factors are involved in determining this effect for a particular cable assembly, but a short discussion may help distinguish the many facets of the problem.

In all cases, the limit of CW power level is reached when the hottest surface temperature (measured anywhere on the cable assembly) has reached a predetermined temperature, T_{max}. For most high performance high power cable assemblies, T_{max} is on the order of 400°F (204°C). This temperature is chosen based on explosive atmosphere mil spec requirements and also because higher temperature starts to soften the dielectric used in most cables. The temperature T_{max} usually occurs near or on the connector nearest the source. For different types of cables, the tolerance temperature unit that a component within that cable will withstand determines T_{max}. Expressed differently, one may allow T_{max} to increase up to the limit of initial damage to the most sensitive component within the cable.

CONNECTORS AS A LIMITING FACTOR

Heat generation in a connector is analyzed by examining the center conductor diameter "a" of the connector involved (see ***Table 1***). Generally, if the diameter of the center conductor of the cable is approximately the same

RAYMOND SCHWARTZ
AND PETER WALTZ
Cobham Antenna Systems, Microwave Components, Exeter, NH

as the dimension "a" of the connector, the surface temperature at the connector and of the cable next to it will be about the same with power applied. Choice of a small connector for use with a large cable will make the connector hotter than the cable.

The data presented includes a safety margin (SM). This SM will allow operation of cable assemblies at the stated average power levels for the length of time called out in the appropriate mil specs.

Aging is a process dependent on many variables; among them are ambient temperature, mechanical vibration or flexure, and handling. If one could isolate the aging effect due to the application of power only, the following applies (as for all microwave components): there is a time limit, after which continuing the application of CW power will accelerate the aging of the cable assembly. Power application eventually will affect cable performance. These time limits will vary, depending on consideration of all stresses.

HEAT REMOVAL

The following is a discussion of heat removal and experimental results obtained at Cobham. Exact mathematical description of the hot cable assembly in terms of heat flow analysis is almost impossible.

Under steady state conditions (typically achieved after about 20 minutes of continuous CW power application), a cable assembly has a unique temperature distribution. This distribution is heavily influenced by the installed environment. As in all heat transfer problems, the hot cable assembly gets rid of its heat by conduction, convection and radiation. Conduction could be the most effective of the three, especially at high altitude where the air is thin. However, because the geometry of bulkheads and mounting plates in general cannot be predicted, this most effective means of heat removal is not included in the power handling data. In fact, the power handling data relates to a cable that is allowed only convection and radiation for heat removal. While conduction might improve significantly the power handling characteristics of cable assemblies, this note treats any benefit resulting from conduction as an increased safety margin.

Of the two means left for removing heat, convection remains as the more effective, even at high altitude. Cobham has empirical data based on extensive testing of many cable assemblies in the company's temperature-altitude chamber, while varying the chamber's ambient temperature and altitude. These tests were performed on a variety of cable types to generate the power handling and derating the data. The matrix data are a good guide to choosing the right cable for a particular frequency and average power level (see ***Figure 1***).

PRACTICAL CONSIDERATION

A system application may require all cable assemblies to use ETNC connectors. In addition, the cable chosen may have a center conductor considerably larger than that of the connector. When this is true,

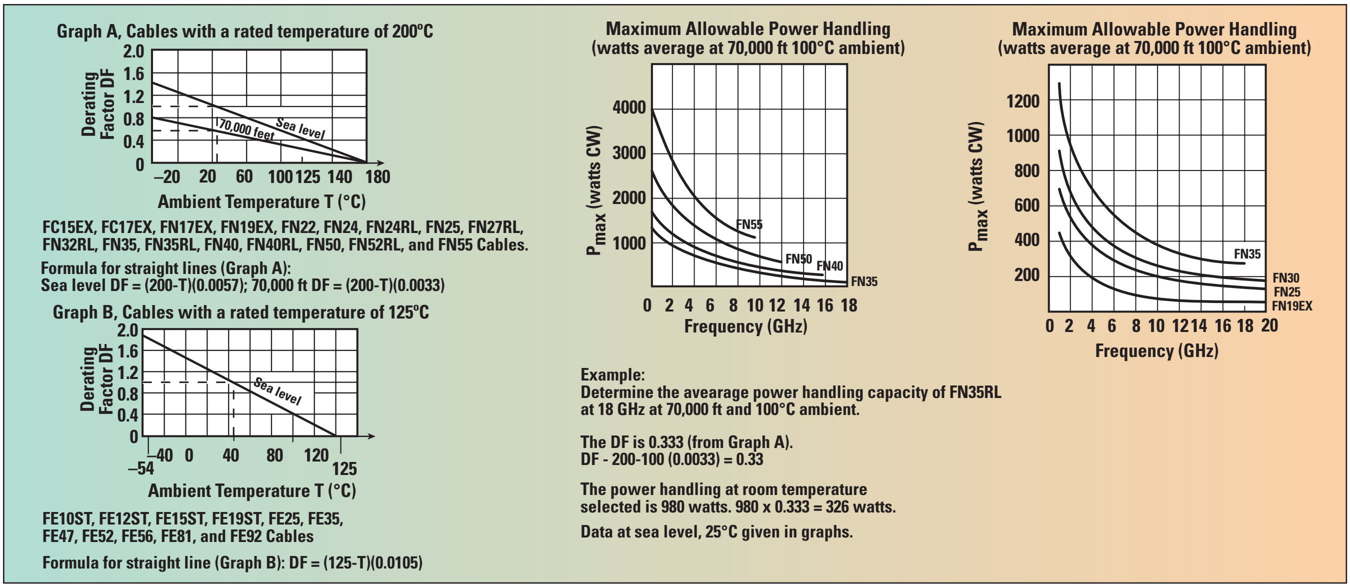

▲ *Fig. 1 Power handling and derating factors for sample cables.*

the connector will be hotter, perhaps considerably hotter, than the cable. Under these conditions, heat sinking of the connector is recommended; bulkhead connectors or finned heat-sunk connectors are examples of such connectors. Usually, heat sinking is sufficient since conduction is very effective at removing heat. However, if power levels and predicted temperatures are very high, tests should be conducted to verify the design.

APPROXIMATE DERATING CURVES

To determine the Derating Factor (DF) at different altitudes or at different ambient temperatures, see Figure 1. Based on the listed groups, select the appropriate derating curve. Multiply the average power handling data at the frequency of interest. The resultant number is the maximum average power handling capability of the selected cable at the selected ambient temperature and altitude (Derated Average Power = DF × Average Power from data section). ■

SEALED FLOATING BLINDMATE CONNECTOR

With modern electronic warfare trending toward the use of portable electronic systems in the field of battle, the environmental sealing qualities of interconnects are under scrutiny now more than ever. Conditions ranging from driving rain to dust storms can wreak havoc on the performance and longevity of electronic components without sufficient sealing. Many component engineers are choosing to use threaded connectors where blindmates would be the preferred choice because they cannot tolerate the possibility of foreign object mitigation into their enclosures. SV Microwave has developed a solution to address this concern.

CURRENT TECHNOLOGIES

SV Microwave currently carries a line of waterproof, threaded, rigid mounted connectors (SMA, TNC among others) that provide environmental sealing using a series of o-rings. As shown in ***Figure 1***, the dielectric is sealed to the connector body by an internal silicone rubber o-ring; the connector body is sealed against the enclosure by a panel o-ring. This design is effectively used to seal connectors in the mated and un-mated condition to IP67 standards, including full immersion in water. This is a field-tested, standard product for SV Microwave.

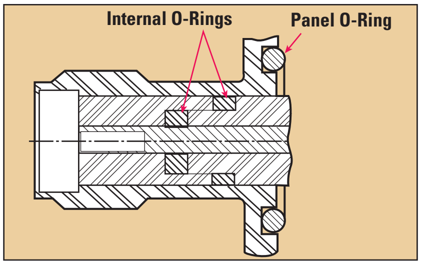

▲ *Fig. 1 Waterproof RF connector sealed with o-rings.*

SV Microwave also offers a full product suite of floating blindmate connectors (BMA, BMMA, BZ, BMZ, ZMA) that are ideal for box to box mating where axial and radial misalignment must be compensated for without sacrificing RF performance. Blindmate connectors are useful when simultaneously mating multiple RF connections because of their low engagement forces. A spring mechanism is used to provide the radial and axial float, as shown in the BMA connector in ***Figure 2***. This is standard technology and has been used extensively on airborne, ground-based and maritime platforms.

The floating mechanism used in the blindmate connector separates the connector line from the enclosure, thus allowing the connector to pivot in the axial and radial directions. While an effective method of generating float, this design does not protect the enclosure from the environment.

NEED FOR A BETTER SOLUTION

SV Microwave customers asked for a connector that has the float of a blindmate and the sealing capabilities of a rigid mounted connector. This product simply does not exist in the high performance RF connector market. RF designers need a connector that can be used in

SV MICROWAVE
West Palm Beach, FL

applications where box to box mating is required outside a sealed enclosure such as in Line Replaceable Units. Radial and axial float are critical in these applications in order to ensure that any misalignment generated during manufacturing or install can be compensated for by the interconnect. Given the high cost and complexity of inside the box electronic components, introducing the potential for water damage or electrical failure caused by foreign object mitigation is not an option.

SV Microwave's goal was to design a connector that provides a solution to this problem by offering a high performance interconnect that is both sealed against the environment and has the floating characteristics of a blindmate connector. SV Microwave now offers the Sealed Floating Blindmate connector (SFB connector).

ELECTRICAL/MECHANICAL SPECIFICATIONS OF THE SFB CONNECTOR

The SFB connector utilizes the physical dimensions and electrical/mechanical performance characteristics of SV's BMZ connector line. These are defined as:

- VSWR less than 1.3:1 at 18 GHz
- Insertion Loss less than 0.3 dB at 18 GHz
- Dielectric Withstanding Voltage = 1000 V RMS
- Axial Float = 0.06"
- Radial Float = 0.02"
- Engage/disengage forces = 12 oz (max)/2 oz (min)

The BMZ interface offers a few distinct advantages over conventional BMA (OSP) and BMMA (OSSP) connector interfaces. The first advantage is the use of splayed fingers and a recessed contact to ensure that the connector is fully grounded before the male and female contacts are mated. This is clearly shown in the cross sectional image of the BMZ connector in ***Figure 3***.

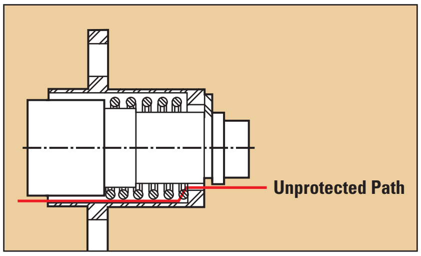

▲ *Fig. 2 Floating blindmate connector (not sealed).*

Another advantage is the tapered dielectric, which allows higher peak power handling than the similarly sized BMMA connector by reducing the air gap between the dielectrics when mated. This design allows the BMZ connector to operate with the highest power to line size ratio in its class.

The SV Microwave SFB connector is ideal in situations where a threaded connector is unacceptable. These situations include field deployed electronic units where a quick disconnect is necessary and applications where tensile ability is restricted by protective gloves or other equipment. The blindmate connector also eliminates the potential for over-torquing the connector and damaging the interface or conversely under-torquing the connector, which could result in sub-optimal mating and decreased electrical performance.

ENVIRONMENTAL SEALING OF THE SFB CONNECTOR

The SFB environment utilizes a sealing method similar

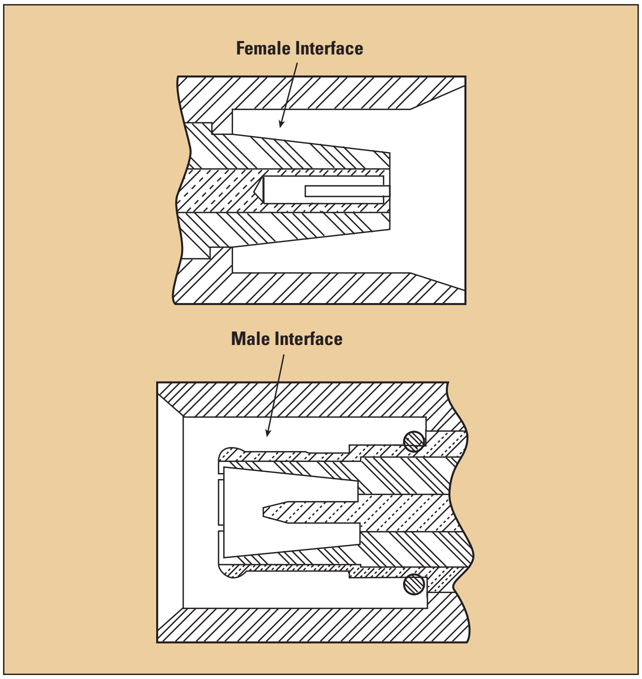

▲ *Fig. 3 BMZ male and female interfaces.*

to the internal and external o-ring seals discussed earlier, but with an additional proprietary mechanism that allows the connector to be fully sealed against the panel while permitting radial and axial float to the levels previously defined. The SFB connector was designed to be compliant with the International Standard for Ingress Protection per IEC 60529. This standard requires the connector to withstand ingress of foreign materials (solid particles) and the harmful effects of water.

SV's target IP requirement for the first iteration of the SFB is IP56. The first digit in IP56 (5) determines the ability of the interconnect (when sealed to an enclosure) to withstand the harmful effects of solid object ingress. Level 5 is the protection level at which the connector is guaranteed to seal against dust such that dust shall not penetrate in a quantity that interferes with satisfactory operation of the connector. This standard applies to the enclosure both in a static un-mated condition and in a dynamic field operation environment.

The second digit in the IP56 rating (6) defines the ability of the interconnect to protect against the harmful effects of powerful water jets projected against the enclosure from any direction. This product is also compliant to this specification in static and dynamic environments. This specification is designed to simulate the exposure of the interconnect to marine and intensely humid and wet environments.

SAMPLE APPLICATION OF THE SFB CONNECTOR

The initial design of the SFB connector consisted of a multiport block incorporating three connector lines. The footprint of this block was designed to minimize the center-to-center spacing of the connectors and the overall dimensions of the multiport block. Schematics of the male and female 3 port block are shown below in ***Figures 4*** and ***5***.

The female multiport block consists of a panel mounted bracket sealed against the panel by a silicon o-ring and

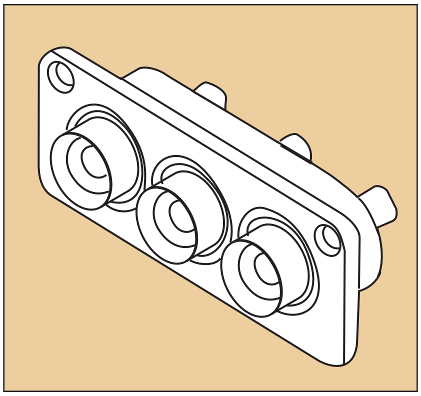

▲ *Fig. 4 Multiport male block.*

three press-in SFB connectors. These SFB connectors are cabled on the inside of the enclosure. The female connector, having no float, is fully sealed to the IP67 standard in the unmated condition making this an ideal interconnect for applications where the outside of the enclosure experiences extreme environmental conditions.

The male multiport block consists of a panel mounted bracket and three snap-in SFB connectors. These connectors are also cabled on the inside of the enclosure. The SFB male connectors contain the radial and axial float and are sealed to the IP56 standard in the unmated and mated conditions.

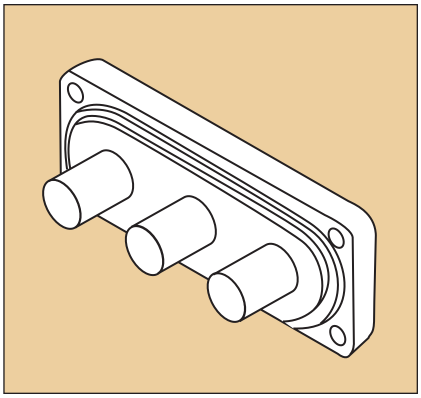

▲ *Fig. 5 Multiport female block.*

This is just one example of how this connector line can be tailored to a specific requirement. These connectors can be custom made to fit any application including:

- Multiport blocks in various configurations
- Termination to standard and non-standard cables
- Individual panel mounted connectors

In the case shown in Figures 4 and 5, the cable on the inside of the enclosure (for the male connector) must be flexible cable in order to accommodate the radial and axial float of the connector. The female connector can be terminated to semi-rigid cable as this connector is rigidly mounted.

The SFB connector offers a unique solution to a common problem encountered in field applications. With the electrical and mechanical performance of a floating blindmate connector and the sealing performance of a rigid mounted connector, RF design engineers now have a suitable alternative when float is required in environmentally sensitive design applications.

SV Microwave,
West Palm Beach, FL
(561) 840-1800 x152,
www.svmicrowave.com.

RS No. 301

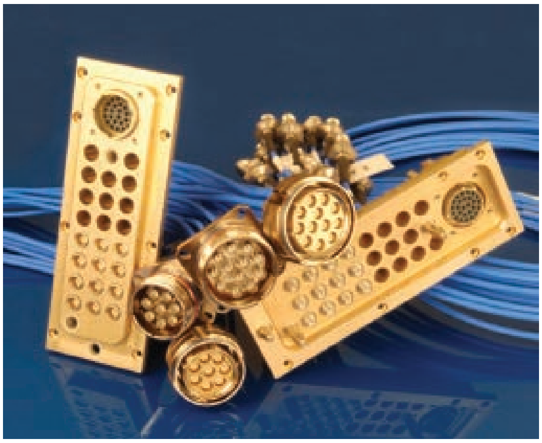

Multipin Connectors for a Wide Variety of Environments

Peter von Nordheim,
Managing Director of Spectrum Elektrotechnik GmbH.
Visit www.mwjournal.com to read this in-depth interview.

In microwave systems coaxial microwave links often have to be regularly connected and disconnected, which means threading and unthreading, torquing and untorquing. As a result, it is not possible to densely pack regular connectors as room is needed for threading and for the use of a torque wrench. Also, in helicopters, airplanes and vehicles, connectors usually have to be safely secured, normally using safety wire through the wire holes in the coupling nuts of the connectors, which is time-consuming.

An alternative is to use multipin connectors to connect microwave signals between two parts of a system. Standard circular blind mate series MIL-DTL-38999 connectors are designed and approved by the military and aerospace industry to meet the most stringent requirements in severe environments and are used for cable-to-panel applications in military, aerospace and other demanding situations.

Originally these connectors were designed to connect up to 128 wires for electronic equipment, but the necessity arose to incorporate coaxial cable contacts for high frequency or microwave applications and the requirement to combine simple electronic wire contacts and microwave coaxial contacts. The disadvantage is the dependence on the contact layouts offered for size 8, size 12 or other coaxial contacts. There is often the need to package numerous microwave links in a connector and to use different coaxial cables, e.g. a fairly thin and flexible cable for higher frequency applications or shorter leads, or a thicker cable for low loss applications and longer assemblies. Size 8, size 12 or other contacts are only available for some coaxial cables and might not be ideal for the application it is intended for. In addition, most standard coaxial contacts are not designed for higher frequency applications.

To address this issue, Spectrum Elektrotechnik has introduced multipin connectors beginning with the SQ-8 (shown in ***Figure 1***), which uses a 4.3 mm high performance low loss coaxial cable and is supplied with eight coaxial inserts for applications up to 24 GHz, using the size 21 MIL-DTL-38999 series III shell. For applications in harsh environments the assem-

Peter von Nordheim
Spectrum Elektrotechnik GmbH
Munich, Germany

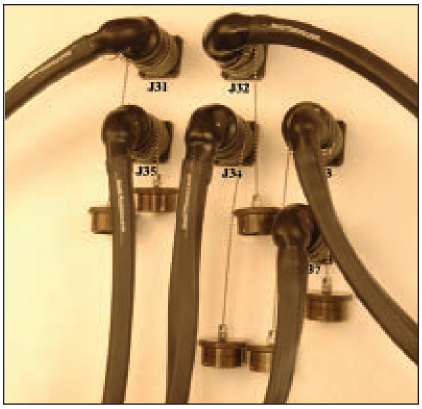

Fig. 1 *SQ-8 multipin connectors can be fitted in compact areas.*

Fig. 2 *The SQ-8 has eight RF contacts.*

blies are supplied armored and water protected.

The need for circular connectors using more coaxial assemblies in a connector and different cables has resulted in Spectrum designing a whole family of multipin connectors that are fully compliant with the MIL-DTL-38999 standard, Series I with a bayonet coupling and Series III with a threaded coupling. Both series are rugged, designed to operate in harsh environments and are available in five different keyed versions, ensuring proper and fool-proof connection.

The original SQ-series uses eight RF contacts (an example is shown in ***Figure 2***) in a size 21 shell; the cable assemblies terminated with spring loaded bayonet catch connector inserts. The TQ-Series and IQ-Series offer size 21 and size 25 shells, with threaded coupling and 4, 7, 8 or 12 (shown in ***Figure 3***) coaxial inserts, and are available for four different cables: spring loaded, limited spring loaded, fixed and pressurized. They are available for DC to 24 GHz and DC to 40 GHz frequency ranges, although the cable used may limit the

▲ *Fig. 3 The TQ-12 has 12 coaxial inserts.*

frequency range. For example, if Spectrum's Type 141 cable is favored, a low loss high performance cable with a jacket diameter of 7.8 mm and an insertion loss of 0.64 dB/m, the frequency range is limited to 18 GHz.

The outer conductors of the cable assemblies in the TQ-Series use the common ground of the MIL-DTL-38999-shell, while the assemblies of the IQ-Series are isolated from each other and also from the ground of the MIL-DTL-38999-shell. Both the BQ-Series and the CQ-Series are identical to the TQ-Series with the exception that they employ the MIL-DTL-38999 standard, Series I with bayonet coupling. They differ from each other because the assemblies of the CQ-Series do not use the same ground, but are isolated from each other and from the ground of the MIL-DTL-38999-shell.

Also, all circular designs, the SQ, TQ, IQ, BQ and CQ-Series are available in pressurized versions, meeting the EIA364_02C test specifications, replacing MIL-STD 1344 and with the capacity to withstand 0.6 bar (8 PSIG) for 35 minutes. These connectors, which are usually bulkhead feed-through or are four-hole flanged versions, are required in airplanes where cable assemblies are installed in walls separating pressurized and unpressurized areas.

Alternatively, multipin adapters (shown in ***Figure 4***) are designed for applications where bulkhead multipin connectors cannot be installed in the wall separating pressurized and unpressurized areas, as male multipin connections need to be used on both sides for disconnection purposes. These adapters are also available in pressurized versions to meet the EIA364_02C test specifications. In addition, hermetically sealed connectors and adapters are designed to be installed in the walls of vacuum test chambers.

The RQ-Series has been developed to address the need for even more cable assemblies to be packaged into one shell, taking up as little room as possible. They are designed for those applications where many more microwave coaxial connections are needed than circular designs can accommodate (where limited space is available) and where many DC and driver signals using AWG wire also have to be connected.

For example, the RQ23-DC26 (shown in ***Figure 5***) connects and disconnects 23 coaxial RF lines and 26 signal and supply lines at once and in seconds, while being as small as possible for such a complex design. When connecting such a high number of assemblies the insertion and withdrawal force is particularly significant. For the RQ23-DC26 a maximum of 150 N is specified for the insertion and withdrawal of all 23 coaxial lines plus the 26 signal and supply lines. The 23 coax inserts use the standard Type 11 or Type 43 high performance cable and are grouped in four to eight assemblies, secured by mounting bolts for easy replacement in the shortest time. Its maximum operating frequency is specified as 25 GHz, but higher frequency designs are available on request.

For applications where even more connections are needed, the newest design, the RQ80-DC120 (see ***Figure 6***), features 80 coaxial connectors operating to 40 GHz and 120 signal lines, all in a unit measuring 107 × 304 mm. Designs are also available that operate up to 65 GHz.

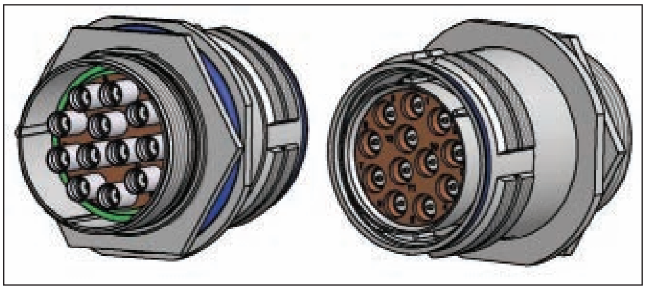

▲ *Fig. 4 Drawing of the 8TQB-Z2ID-29 multipin adapter.*

Modern systems also require accurate phase matching of the cable assemblies in multipin harnesses and Spectrum achieves phase matching through the latest cable manufacturing processes, interface cutting techniques and advanced adjustable connector designs. Also, the adjustable matching mechanism can meet the most serious shock and vibration requirements.

▲ *Fig. 5 The RQ23-DC26 connector.*

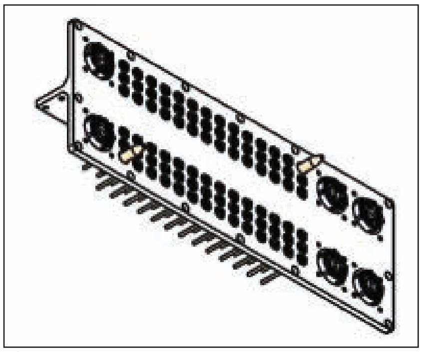

▲ *Fig. 6 Drawing of the RQ80-DC120 connector.*

Selecting the proper materials and aging techniques is important as well as ensuring that the cable assemblies and harnesses operate effectively in the standard temperature range of -54° to +115°C or the extended temperature range of -72° to +200°C. All the Spectrum connectors are RoHS compliant and meet the conditions and corrosion requirements of MIL-STD- 202, method 101, condition B. The multipin connectors are compliant with thermal shock to MIL-STD-202, method 107, condition B, vibration to MIL-STD-202, method 204, condition D, and shock to MIL-STD-202, method 213.

Spectrum Elektrotechnik GmbH,
Munich, Germany,
Tel: +49 89 3548 040,
info@spectrum-et.com,
www.spectrum-et.com.

RS No. 304

Phase Matched Microwave Cable

One thing that the test and measurement, sensors, radar and wireless markets all have in common is the need for robust, high performance microwave cable assemblies. A major attribute of such cables is electrical stability, which has been achieved through the development and advancement of cable technology over many years of manufacturing and applications experience.

The ability of a cable to deliver a signal in good condition with the minimum of loss and delay is the essence of microwave cable design. This is a specific attribute of the new Teledyne Storm 190E Phase Master microwave cable, which is an enhanced version of the 190 Phase Master that has been a standard in the engineers' tool kit for many years. The 190E provides enhanced performance in a number of areas that are becoming increasingly important as signal frequencies increase and the performance requirements, both mechanical and electrical, are becoming more demanding.

In particular it addresses the need for a high level of phase stability versus temperature and cable flexure, reduced insertion loss, increased amplitude stability, improved shielding effectiveness, greater connector retention, and additional mechanical durability focusing on torsion resistance. The result is an amalgamation of Teledyne Reynolds' cable design technology and experience, taking into account customer demands, to bring higher performance cables to the market. The 190E is specified up to 26.5 GHz, dependant on the connector used, the industry standard SMA connector is specified to 18 GHz and the 3.5 mm connector is specified up to 26.5 GHz.

CABLE CONSTRUCTION

The cable construction (shown in ***Figure 1***) is a proprietary combination of a silver plated copper (OFHC) centre conductor [A], a MicroForm™ PTFE tape wrapped dielectric [B], four screening layers, alternate helically wrapped silver plated copper foil [C and E] and silver plated copper braid [D and F], with a blue FEP unarmored jacket (5.05 mm diameter) [G] as standard.

Additional armored jackets to enhance the robustness of the cable include:

Ruggedized - Polyurethane Jacket (see ***Figure 2***), which is for applications where weight, flexibility and abrasion resistance are critical, and moderate compression resistance

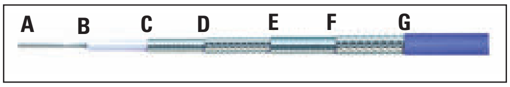

▲ *Fig. 1 Construction of the 190E Phase Master microwave cable.*

Teledyne Reynolds
Newbury, UK

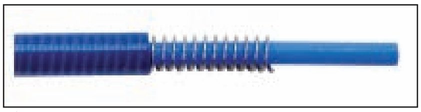

▲ *Fig. 2 Cable with ruggedized, polyurethane jacket.*

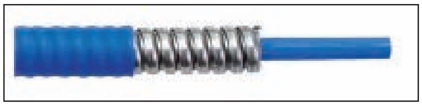

▲ *Fig. 3 Hard armored cable.*

is required (300 lbs/in). The cable is covered with a flexible wound helix of passivated stainless steel wire and an extruded polyurethane jacket. Its temperature range is -54° to +100°C.

Hard Armored (see ***Figure 3***) is suitable for both inside and outside environments where the application requires the ultimate in cut and crush resistance (500 lbs/in), and flexibility and weight are not as critical. The cable is covered with stainless steel interlocked armor and its temperature range is -54° to +135°C.

The complete cable specifications for the 190E Phase Master Cable are shown in ***Table 1***. The exceptional shielding effectiveness, high levels of phase stability with temperature and flexure, and the much improved cable retention capabilities are all products of engineering development driven by market demands.

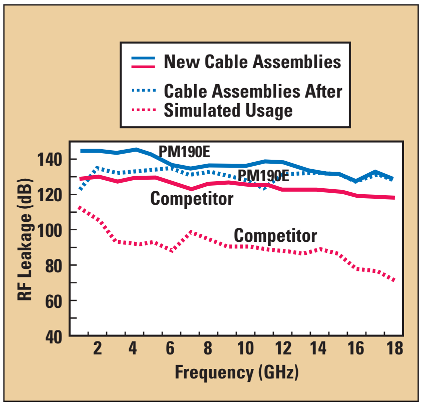

▲ *Fig. 4 Graph of shielding effectiveness.*

The shielding effectiveness is a capability that enables cables to be located in close proximity to other cables and equipment. ***Figure 4*** shows the shielding effectiveness by comparison with a competitor's cable in both new and used conditions. Although there is some reduction in shielding effectiveness with use, the 190E shield construction effectively minimizes that reduction. The effect is a more stable, longer lived cable.

Phase stability performance is affected by both temperature and flexure during use. The 190E is designed to minimize phase shift for both temperature and flexure. ***Figure 5*** demonstrates the minimal effects of both those environmental conditions. The temperature range is -55° to +125°C with a <800 ppm phase shift at the maximum temperature. ***Figure 6*** demonstrates the phase shift due to flexure. The phase shift with the cable in a 90° bend around a 4.0 in (100 mm) mandrel is nominally 1° at 18 GHz.

TABLE I

190E PHASE MASTER CABLE SPECIFICATIONS

Diameter (in/mm)	0.199/5.05
Operating Frequency (Max, GHz)	26.5
Attenuation-Nom @ 2 GHz (dB/ft)	0.112
Attenuation-Nom @ 10 GHz (dB/ft)	0.261
Attenuation-Nom @ 18 GHz (dB/ft)	0.36
Power Handling Average Power in Watts @ 1 GHz	700
Phase Stability vs. Temperature (ppm, nom, °C)	<500 from -55 to +85*
Phase Stability vs. Flexure† (degrees @ 18 GHz, nom)	1
Shielding Effectiveness-Minimum‡ (dB @ 1 GHz)	-120
Typical VSWR (2 straight connectors)	1.35 @ 18 GHz 1.40 @ 26.5 GHz
Min Bend Radius (in/mm)	1/25.4 static 2/50.8 dynamic
Connector Retention up to 18 GHz, straight pull (lbs/kg)	40/18.14
Weight (grams/ft)	21
Velocity of Propagation (%)	82.4
Operating Temperature Range (°C)	-55 to +125

*<800 up to +125
† ±90 degree bends around a 4" mandrel
‡ Subject to connector choice

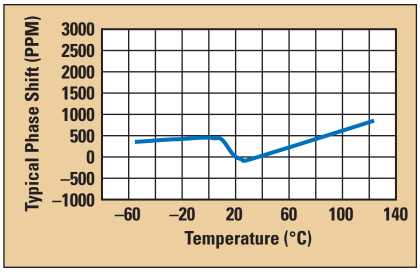

▲ *Fig. 5 Phase Master 190E phase vs. temperature.*

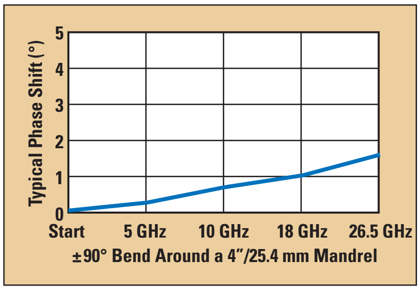

▲ *Fig. 6 Phase Master 190E phase vs. flexure.*

CONCLUSION

The 190E Phase Master microwave cable is aimed at test and measurement, radar, wireless communications, electronic warfare and antenna systems applications. The overall cable stability and specifically the phase stability, leakage shielding and rugged construction are ideally suited to applications in semiconductor test and measurement where repeated use of the test equipment and the high throughput of the device under test require the performance repeatability and environmental ruggedness to work and survive over long periods of use.

For applications in military markets, the ruggedness of the cable is as important as the repeatability of the electrical specification of the cable. For all RF applications the need for insertion loss repeatability and VSWR stability are a given, but the addition of phase stability, especially where the cable is used in harsh environments, becomes a matter of paramount importance. The combination of the design features and the interlocking electrical and environmental performance capabilities delivered by the design provide the robust, high performance cables required to meet today's customer demands.

Teledyne Reynolds,
Newbury, UK
Tel: +44 (0)1635 262200,
www.teledyne-europe.com.

RS No. 300

Cables & Connectors Supplement

Literature Showcase

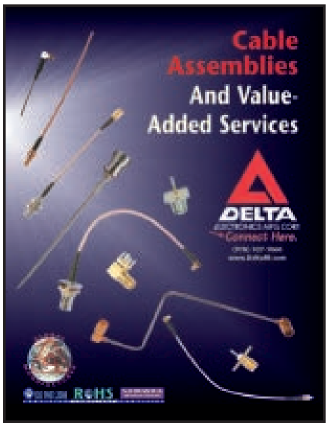

Product Brochure

To assist customers who have a need to streamline their supply chain and logistics, Delta Electronics Manufacturing now offers a broad range of coaxial cable assemblies and other connector-related, value-added component subassemblies. Delta's cable assemblies, incorporating flexible, semi-rigid and hand-formable cables, range in size from micro-miniature to large, high-power types. They cover the spectrum of market needs from high-volume, low-cost assemblies to high-performance, low-volume categories.

Delta Electronics Manufacturing Corp.,
Beverly, MA (978) 927-1060, www.deltarf.com.

RS No. 310

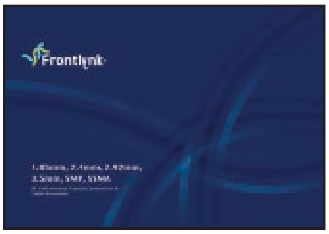

RF/Microwave Connectors

As well as giving details and in-depth specifications of the company's extensive range of 1.85 mm, 2.4 mm, 2.92 mm, 3.5 mm, SMP and SSMA RF/microwave coaxial connectors and cable assemblies, this 50-page catalog also offers an introduction to Frontlynk and explains its capabilities. It explains that the products are developed as the result of extensive research involving critical factors: operating frequency, characteristic impedance, skin effect, cut-off frequency, intermodulation, voltage and power rating, leakage, etc. and emphasizes the company's commitment to quality, testing and supply.

Frontlynk Technologies Inc.,
Tainan, Taiwan +886-6-3562626, www.frontlynk.com.

RS No. 311

Defence Connections

Promoting 'Excellent Connection', this brochure takes the approach that whether in the air, on land or at sea, quality in modern defence technology solutions permits no compromise. The 2010 issue of the defence brochure features solutions for cables, connectors, antennas, and connection-ready cable systems that comply with international standards such as MIL, IEC and Lloyds Register.

HUBER+SUHNER AG,
Herisau, Switzerland, +41 71 353 4111, www.hubersuhner.com.

RS No. 319

Product Catalog

MIcable Inc. produces a wide variety of high quality coaxial cable assemblies with flexible, conformable, and semi-rigid cable and customer specified connectors. The company offers prototypes or volume quantities, all fully tested up to 40 GHz and delivered on time. The product brochure highlights a few of the company's products along with providing performance data. For more information, call 86-591-87382855 or e-mail: sales@micable.cn.

MIcable Inc.,
Fuzhou, Fujian, China +86-591-8738 2855, www.micable.cn.

RS No. 312

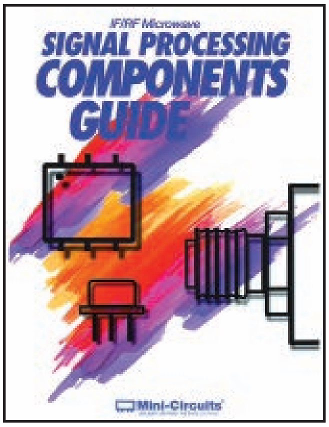

IF/RF Microwave Signal Processing Components Guide

Mini-Circuits' new 164-page catalog includes over 750 new products and is the industry's most comprehensive listing of RF/IF and microwave components and subsystems with more than 4100 products and over 25 product lines, including state-of-the-art amplifiers, mixers, VCOs, synthesizers, filters, test accessories and USB Power Sensors. Mini-Circuits' website provides additional data, application notes, design tools and its powerful YONI search engine, which searches actual test data on over thousands of units.

Mini-Circuits,
Brooklyn, NY (718) 934-4500, www.minicircuits.com.

RS No. 313

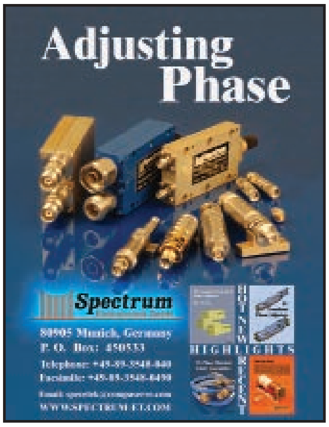

Adjusting Phase

This 52-page catalog focuses on precision phase shifters or phase adjusters that enable the adjustment of the electrical separation between components. It outlines how a precision mechanical movement provides for smooth and accurate adjustment over the frequency ranges from DC to 2 GHz, DC to 3 GHz, DC to 12.4 GHz, DC to 18 GHz, DC to 26.5 GHz, DC to 40 GHz, DC to 50 GHz and DC to 65 GHz, with a secure locking mechanism furnished with every unit. The publication shows the wide selection of components available.

Spectrum E.T. GmbH,
Munich, Germany +49 89 3548 040, www.spectrum-et.com.

RS No. 314

Cables & Connectors Supplement
Literature Showcase

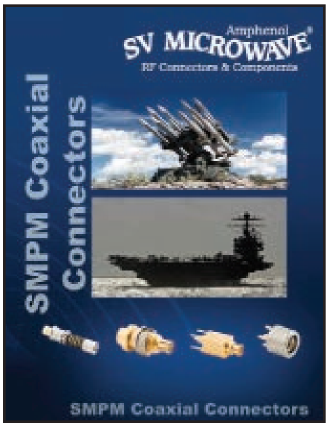

SMPM Catalog

SV Microwave released its new SMPM catalog. The revised catalog features detailed information on SV's entire collection of SMPM coaxial connectors, including technical specifications, applications, drawings and part numbers. SV Microwave SMPM connectors, a push-on design, provide microwave performance through 65 GHz.

SV Microwave,
West Palm Beach, FL (561) 840-1800, www.svmicrowave.com.
RS No. 315

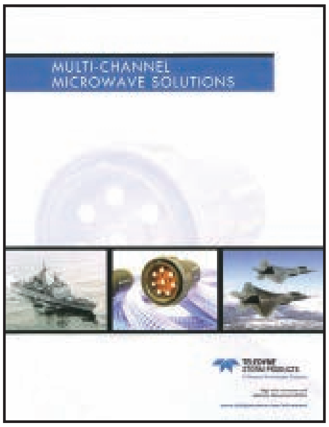

Capabilities Brochure

Teledyne Storm Products' new Multi-channel Microwave Solutions brochure details the company's capabilities in the design and manufacture of both standard and custom multi-channel microwave harness assemblies. The harnesses, found in a wide range of airborne, ground and sea-based military and commercial applications, are backed by Teledyne Storm's more than 30 years of microwave cable design and manufacturing expertise. Includes a case study.

Teledyne Storm Products,
Woodridge, IL (630) 754-3300, www.teledynestorm.com.
RS No. 316

Product Brochure

PhaseTrack II™ is a significant breakthrough in coaxial cable technology. PhaseTrack II is based on the unique, thermally stable Times Microwave Systems' proprietary TF5™ dielectric material. A proprietary engineered material and process combine to make TF5 dielectric the most stable dielectric material available, virtually eliminating the changes of phase with temperature characteristic of other high performance expanded PTFE dielectric flexible RF and microwave coaxial cable assemblies.

Times Microwave Systems,
Wallingford, CT (203) 949-8400, www.timesmicrowave.com.
RS No. 317

Interactive Product Catalog

Trilithic's interactive flip-book catalog is now available online. From custom filters and passive components to subsystems design, this new easy-to-use catalog features an overview of the company's complete line of attenuators, terminations, switches, custom-designed filters, diplexers and subsystems.

Trilithic,
Indianapolis, IN (317) 895-3600, www.trilithic.com.
RS No. 318

Cables & Connectors Supplement

Advertiser Index

Sales Representatives

Carl Sheffres, Publisher

Ed Kiessling, Traffic Manager

Eastern and Central Time Zones
Chuck Boyd
Northeast Reg. Sales Mgr.
(New England, Upstate NY, Eastern Canada)
685 Canton Street
Norwood, MA 02062
Tel: (781) 769-9750
FAX: (781) 769-5037
cboyd@mwjournal.com

Michael Hallman
Eastern Reg. Sales Mgr.
(Mid-Atlantic, Southeast, Midwest)
4 Valley View Court
Middletown, MD 21769
Tel: (301) 371-8830
FAX: (301) 371-8832
mhallman@mwjournal.com

Pacific and Mountain Time Zones
Wynn Cook
Western Reg. Sales Mgr.
PO Box 23200
San Jose, CA 95153
Tel: (408) 224-9060
FAX: (408) 224-6106
wcook@mwjournal.com

International Sales
Richard Vaughan
International Sales Manager
16 Sussex Street
London SW1V 4RW, England
Tel: +44 207 596 8742
FAX: +44 207 596 8749
rvaughan@horizonhouse.co.uk

Germany, Austria, and Switzerland (German-speaking)
WMS.Werbe- und Media Service
Brigitte Beranek
Gerhart-Hauptmann-Street 33,
D-72574 Bad Urach
Germany
Tel: +49 7125 407 31 18
FAX: +49 7125 407 31 08
bberanek@horizonhouse.com

Israel
Oreet Ben Yaacov
Oreet International Media
15 Kineret Street
51201 Bene-Berak, Israel
Tel: +972 3 570 6527
FAX: +972 3 570 6526
obenyaacov@horizonhouse.com

Korea
Young-Seoh Chinn
JES Media International
2nd Floor, ANA Bldg.
257-1, Myungil-Dong
Kangdong-Gu
Seoul, 134-070 Korea
Tel: +82 2 481-3411
FAX: +82 2 481-3414
yschinn@horizonhouse.com

Japan
Katsuhiro Ishii
Ace Media Service Inc.
12-6, 4-Chome,
Nishiiko, Adachi-Ku
Tokyo 121-0824, Japan
Tel: +81 3 5691 3335
FAX: +81 3 5691 3336
amskatsu@dream.com

China
Michael Tsui
ACT International
Tel: 86-755-25988571
Tel: 86-21-62511200
FAX: 86-10-58607751
michaelT@actintl.com.hk

Hong Kong
Mark Mak
ACT International
Tel: 852-28386298
markm@actintl.com.hk